

Optimisation and Mechanistic Insights of Dyskinesia in Rodent Models of Parkinson's Disease

This thesis is submitted for the degree of Doctor of
Philosophy at Cardiff University

Gaynor A. Smith


Supervisors:
Dr Emma L. Lane
Prof. Stephen B. Dunnett

September 2011




Declaration

This work has not previously been accepted in substance for any degree and is not concurrently submitted in candidature for any degree.

Signed  Date 09/2011

STATEMENT 1


This thesis is being submitted in partial fulfillment of the requirements for the degree of PhD.

Signed  Date 09/2011

STATEMENT 2

This thesis is the result of my own independent work/investigation, except where otherwise stated.

Other sources are acknowledged by explicit references.

Signed  Date 09/2011

STATEMENT 3

I hereby give consent for my thesis, if accepted, to be available for photocopying and for inter-library loan, and for the title and summary to be made available to outside organisations.

Signed  Date 09/2011

Summary

The work presented in herein focuses on the optimisation and use of established animal models to study behavioural, pharmacological, histological and molecular correlates of the debilitating motor side effects of current and future treatments for Parkinson's disease, namely L-DOPA induced dyskinesia (LID) and graft induced dyskinesia (GID).

Chapter 3 optimises the 6-OHDA lesion model in mice, from surgical approaches to behavioural assessment of motor function. The neurotoxin was injected at three different regions along the nigrostriatal tract to produce unique patterns of dopaminergic cell death in the midbrain. The resulting cell loss was correlated to behavioural deficits identified through an extensive battery of motor hand tests.

Fully lesioned mice from each of the three models were chosen for chronic L-DOPA treatment, described in **Chapter 4**, where doses were increased every 1-2 weeks. Behaviour was assessed and correlated to deficits on motor hand tests prior to L-DOPA treatment, cell loss within sub regions of the midbrain, serotonergic density levels and upregulations in Δ FosB and striatal TH cell populations.

Chapter 5 uses knowledge gained in previous chapters to use the most appropriate 6-OHDA mouse model of LID for the examination of changes in the Regulators of G-protein Signalling (RGS) following an acute and chronic L-DOPA treatment. RGS2 was the only one to increase significantly following either treatment regime.

In **Chapter 6** a well established rat model of GID (the induction of dyskinesia in the transplanted 6-OHDA lesioned rat through the administration of amphetamine) was used to assess the use of pharmacological agents known to reduce LID. Changes in locomotor function and abnormal inhibitory movements (AIMs) could be assessed giving an insight into the mechanism and receptors involved.

To further the understanding of GID, **Chapter 7** examines dopamine receptor levels, *RGS* transcript expression, and the proportions of dopamine and serotonin cells in the transplanted, 6-OHDA lesioned rodent brain. The aim was to determine any correlation between these parameters and amphetamine induced dyskinesia. Only the number of dopaminergic and serotonin cells could be correlated to dyskinesia and not the proportion of serotonin cells.

As no previous mouse model of GID has been established, **Chapter 8** demonstrates that transplantation of E12 ventral mesencephalon (VM) grafts can be optimised in the lesioned mouse of C57/Bl6 and CD1 strains to give functional recovery, and amphetamine induced dyskinesia. Both strains were also used to demonstrate that transplants were also able to reduce LID.

Acknowledgements

First and foremost I would like to thank my two supervisors Dr Emma Lane and Prof. Steve Dunnett (Em and Steve) for all their help, continued advice and encouragement during my PhD. Your inputs have been invaluable. I have really appreciated them and cannot thank you both enough. I would also like to thank Prof. Anne Rosser for her support throughout. Em good luck with the new ELL group in the years ahead.

Steve you're going to hate me saying this but you're like a dad to some of us! I greatly admire both your open scientific and political style. I couldn't recommend a better place to study than the Brain Repair Group (BRG), I have thoroughly enjoyed my time in lab and hope to always be associated with the BRG family. I don't think there is another place in the world where it is possible to discuss neuroscience, astro-physics, politics, rugby, Eastenders and Lord Sugar under one roof!

I would like to thank Ngoc Nga Vinh for her expertise and teaching me all the molecular techniques I know and Gemma Higgs, Anna Fuller and Nari Janghra for their help with animals and teaching me behavioural techniques at the start of my PhD. Jane Heath i'm sorry the radio always goes rubbish when I enter histology. Thanks also to Ali Baird and Anne-Marie McGorrian for help with organising various things and with licensing issues. Very special thanks also to 'East wing' and 'West wing' post docs, for helping me with various things and for endless discussions (scientific and um.... otherwise): Alex Klein, Andrew Hollins, Claire Kelly, Eduardo Torres, Hanna Lingdren, Mariah Lelos, Rebecca Trueman, Rike Zietlow and Simon Brooks.

Special thanks also to Prof. Angela Cenci for taking the time to listen to presentations/ look at my posters and for your hospitality in Lund. Your input on the pharmacology and mouse aspects of the GID work was much appreciated and our discussions highly motivating. Prof. Buchman and Dr Ninkina (Vlad and Natalia) thanks for the amazing Russian BBQs!

Many thanks to my office mates over last year's: Ulrike Weyrauch (esp for her tea pot), Steve Fielding (Dr Steve), Sophie Precious, Zubeyde Bayram-Weston, Andreas Heuer, Narawadee Chompoo and Amy Evans. Steve fielding thank you for making me laugh so much, you're fixing of the tea maker deciding app is forgiven!...Im ready to start the working class revolution whenever you are! Sophie thank you so much for all the helpful PhD tips, they were invaluable and I wish you every success in the future. Zubeyde I think you're amazing finishing your PhD and having baby Sami! Thanks for everything. Heuer it has been an absolute pleasure working with you. I am not looking forward to the end of GANDY, although im sure it will only be temporary... after all we have set up the first BAND meeting 2025 (thought of after many a rum and coke in a hot tub). I won't miss however the German punk during our long surgery sessions... only kidding! Amy, Ellen, Harry, Lu, Nan, and Susannah good luck in your studies, it's hard to go too far astray in the BRG. Lu thanks for letting me

help out with your exciting projects; I have enjoyed it scientifically and personally. Alex I can't think of a better person to start in the group with and I guess we are going at the same time too, very sad, thanks for all your advice.

I would also like to thank my parents Alan and Mair Smith for letting me choose my own weird path, putting up with me in my youth and for their encouragement throughout my studies.... I will get a proper job soon. Dad your fondness of nature has no doubt fuelled my love of science. Big thanks also to my Grandparents and Sian for all your support over the last few years.

Owen what can I say, there's no better boyfriend than a scientist for understanding the long hours, things not working etc, and you have been incredibly patient and supportive. I'm submitted too now!

Original publications during the course of this PhD studentship

- Heuer A., **Smith G.A.**, Lelos M.J., Lane E.L. & Dunnett S.B. Comprehensive Behavioural Evaluation of Striatal, MFB and Nigral Unilateral 6-ohda Lesioned Mice (Part I). 226(1):281-92.
- **Smith G.A.**, Heuer A., Dunnett S.B. & Lane E.L. Unilateral 6-ohda lesions of the Striatum, MFB and Nigra in Mice (Part II). Analysis of the Behavioural and Histological Hallmarks of L-dopa Induced Dyskinesia. (E Pub ahead of print).
- **Smith G.A.**, Breger L., Dunnett S.B. & Lane E.L. The Pharmacological Modulation of Amphetamine-Induced Dyskinesia in the Grafted Hemi-Parkinsonian Model. (Currently in preparation for *Neuropharmacology*).
- Lane E.L. & **Smith G.A.** (2010). Understanding Graft Induced Dyskinesia. *Regen. Med.* 5(5):787-97.
- **Smith G.A.**, Murphy E., Dunnett S.B. & Lane E.L. Toxin-based Models of Parkinson's disease. *Handbook of Laboratory Animal Science (Volume II)* 3rd Ed. CRC Press U.S.A. (2011).
- **Smith G.A.** & Heuer A. The 6-OHDA Lesioned Mouse Model of Parkinson's Disease. *Contemporary Models of Movement Disorders (Volume I)*. Editors: Lane & Dunnett. Springer/Humana Press. London (2011).

Abbreviations

AADC	Amino acid decarboxylase
AIM	Abnormal inhibitory movement
AMPA	2-amino-3-(5-methyl-3-oxo-1,2-oxazol-4-yl) propanoic acid
AP ¹	Alkaline phosphatase
AP ²	Anterior posterior axis
BBB	Blood brain barrier
DAT	Dopamine transporter
DBS	Deep brain stimulation
DV	Dorsal ventral axis
ERK	Extracellular-signal-regulated kinase
GABA	γ -Aminobutyric acid
GID	Graft induced dyskinesia
GP	Globus pallidus
GPe	Globus pallidus <i>externa</i>
GPi	Globus pallidus <i>interna</i>
GPCR	G-protein coupled receptor
GIRK	G-protein-coupled inwardly-rectifying potassium channel
HPSS	Hanks balanced saline solution
IEG	Immediate early gene
i.p	Intraperitoneal
L-DOPA	L-3,4-dihydroxyphenylalanine
LID	L-DOPA induced dyskinesia
LTP	Long term potentiation
MFB	Median forebrain bundle
ML	Medial lateral axis
MPTP	1-methyl-4-phenyl-1,2,3,6-tetrahydropyridine
MSN	Medium spiny neuron
NA	Noradrenaline
NAcc	Nucleus accumbens
NIH	National Institute of Health
NMDA	<i>N</i> -methyl <i>D</i> -aspartate
<i>ns</i>	Non-significant

PARK-7	Parkinson disease (autosomal recessive, early onset) 7
PBS	Phosphate buffered saline
PCR	Polymerase chain reaction
PD	Parkinson's disease
PDyn	Prodynorphin
PFA	Paraformaldehyde
PINK-1	PTEN-induced putative kinase 1
O.D.	Optical density
LRRK2	Leucine-rich repeat kinase 2
PET	Positron emission tomography
PPE	Preproenkephalin
RGS	Regulators of G-protein signalling
s.c	Subcutaneous
SD	<i>Sprague-Dawley</i>
STN	Subthalamic nucleus
SN	Substantia nigra
SNc	Substantia nigra <i>pars compacta</i>
SNr	Substantia nigra <i>pars reticulata</i>
SSC	Sodium chloride- sodium citrate
TBS	TRIS buffered saline
TH	Tyrosine hydroxylase
TNS	TRIS non-saline
VM	Ventral mesencephalon
VTA	Ventral tegmental area
5-HT	5-Hydroxytryptamine
6-OHDA	6-hydroxydopamine

Contents

1. Introduction.....	13
1.1 Parkinson’s Disease (PD).....	13
1.2. The Basal Ganglia.....	15
1.2.1. The normal brain.....	15
1.2.2. PD Neuropathology.....	20
1.3. Treatment Strategies in PD	24
1.3.1. Historical Surgical Interventions	24
1.3.2. Pharmacological Treatments	25
1.3.4. Deep Brain Stimulation.....	27
1.3.3. Future Cell Replacement Strategies.....	28
1.3.5. Future Gene Therapy.....	30
1.4. L-DOPA Induced Dyskinesia (LID).....	31
1.4.1. Development and Causes	31
1.4.2. Treatment Strategies for LID.....	34
1.5. Graft Induced Dyskinesia (GID)	37
1.5.1. Development and Possible Causes.....	37
1.5.2. Strategies for GID	38
1.6. Animal models of PD.....	39
1.6.1. Pharmacological.....	39
1.6.2. MPTP	40
1.6.3. 6-OHDA	41
1.6.4. Transgenic	46
1.7. Dyskinesia Models.....	47
1.7.1. LID and GID in Primates	47
1.7.1. LID in Rodents.....	48
1.7.2. GID in Rodents	49
1.8. Mechanisms of LID	51
1.8.1. Circuitry and receptor Changes	51
1.8.2. Regulators of G-protein Signalling (RGS) Dysfunction.....	54
1.8.3. Intracellular Signalling.....	57
1.9. Mechanisms of GID.....	59
1.9.1. Causes of GID.....	59
1.9.2. Circuitry and receptor changes	61
1.9.3. Transcriptional Changes.....	62
1.10. Aims of this Thesis	63
2. Methods.....	64
2.1 Animal Husbandry and Legislation.....	64
2.2 Surgery Techniques	64
2.2.1 General Surgery considerations.....	64
2.2.2 6-OHDA Lesions in Rats	65
2.2.3 6-OHDA lesions in mice	65
2.2.4 Grafting of primary dopamine tissue in Rats	66
2.2.5 Grafting of primary dopamine tissue in mice.....	67

2.3 Behavioural Techniques.....	68
2.3.1 General Behavioural Considerations	68
2.3.2 Drug Induced Rotation in the Rat	68
2.3.3 Spontaneous and Drug Induced Rotation in the Mouse.....	69
2.3.4 Automated Locomotor Activity.....	69
2.3.5 Cylinder.....	70
2.3.6 Elevated Beam Test	70
2.3.7. Corridor Test.....	71
2.3.8. Staircase test	71
2.3.9. Rotarod.....	72
2.3.10. Stepping test.....	72
2.3.11. Gait analysis.....	73
2.3.12. Inverted Grid test	73
2.4 Dyskinesia Assessment.....	73
2.5 Molecular and Histological Techniques	74
2.5.1 General Technical Considerations	74
2.5.2 Perfusion.....	74
2.5.3 Snap freezing	75
2.5.4 Immunohistochemistry.....	75
2.5.5 In-situ hybridisation - Probe synthesis.....	76
2.5.6 In situ hybridisation - Optimising.....	78
2.5.7 In-situ hybridisation - Procedure	78
2.5.8 qPCR	79
2.5.9 Western Blotting- Protein Extraction.....	81
2.5.10 Western Blotting- Procedure	81
2.5.11 Tritiated Ligand binding Assays.....	82
2.7 Quantification and Microscopy	83
2.7.1 General quantification and statistics	83
2.7.2 Determining Statistical Power.....	84
2.7.3 Quantification and Density Analysis with ImageJ	84
2.7.4 Analysis of Dopaminergic Grafts	85
3. A Comprehensive Behavioural Assessment of the 6-OHDA lesioned mouse model of Parkinson's disease	86
Summary	86
3.1. Introduction	87
3.2. Experimental Design.....	89
3.3. Results.....	89
3.3.1. Mortality Rates and Weight.....	89
3.3.2. Histological analysis of the lesions.....	91
3.3.3. Group effects on motor deficits	93
3.3.4. Correlation of Motor Deficits and Lesion Extent in the SNc.....	95
3.3.5. Correlation of Motor Deficits and Lesion Extent in the VTA.....	98
3.4. Discussion	100
3.4.1. 6-OHDA Lesion Efficiency.....	100
3.4.2. Mortality Rate Improvement	101
3.4.3. Deficits on Behavioural Tests.....	101
3.4.3. Correlations between Midbrain Cell Loss and Behavioural Deficits.	103
3.4.4. Conclusions	104

4. Assessment of L-DOPA induced dyskinesia in the 6-OHDA-lesioned mouse	107
Summary	107
4.1 Introduction	108
4.2 Experimental design	110
4.3 Results.....	112
4.3.1. Behavioural deficits in mice with 6-OHDA lesions of the Striatum, MFB or SN	112
4.3.2 Histological comparison of mice with 6-OHDA lesions of the Striatum, MFB or SN	114
4.3.3 L-DOPA-induced AIMs, activity and rotation.	117
4.3.4 Correlation of dyskinesia with behavioural hand test scores.	119
4.3.5 Correlating AIMs with histological measures	121
4.3.6 Quantification of TH positive cells in the striatum of 6-OHDA lesioned mice	124
4.4 Discussion	128
4.4.1. Histological characterisation of the lesions.....	128
4.4.2. Lesion effects on L-DOPA dyskinesia.....	130
4.4.3. Behavioural prediction of susceptibility to dyskinesia	131
4.4.4. TH expression in striatal neurons	132
4.4.5. Conclusions	133
5. Regulators of G-Protein Signalling as a Hallmark of Dyskinesia?	134
Summary	134
5.1. Introduction	135
5.2. Experimental Design.....	138
5.3. Results.....	140
5.3.1. Localisation of RGS2, RGS4, RGS8 and RGS9-2 in the Rodent Brain.	140
5.3.2. Dyskinesia and Rotational Assessment.....	142
5.3.2. Striatal RGS mRNA Expression by qPCR.....	143
5.3.3. Regional mRNA Expression of RGS by In situ Hybridisation	145
5.3.4. Correlations of RGS Expression with LID and Rotation.....	149
5.3.5. Changes in RGS protein Expression.....	149
5.4. Discussion	151
5.4.1 RGS expression is not differently modulated by the 6-OHDA lesion.....	151
5.4.2. Lesion and Intact Differences in RGS2 Expression by L-DOPA.....	152
5.4.3. RGS2 Dysregulation	152
5.4.4. RGS2 Dysregulation ‘Off’ and ‘On’ L-DOPA.....	153
5.4.5. Methodological Considerations	154
5.4.6. Conclusions	155
6. The Pharmacological Modulation of Experimental Graft-Induced Dyskinesia	156
Summary	156
6.1 Introduction	157
6.2 Experimental Design.....	160
6.3 Results.....	163
6.3.1. Methamphetamine Dose Response	163
6.3.2. Dopamine Receptor Antagonism.....	165
6.3.3. Opioid Receptor Antagonism	169
6.3.4. Cannabinoid Receptor Agonism.....	169
6.3.5. Adrenergic Receptor Antagonism.....	169
6.3.6. 5-HT Receptor Agonism	173
6.3.7. Glutamate Receptor Antagonism.....	177

6.3.8. Results Summary	184
6.4 Discussion	185
6.4.1. Methamphetamine Dose Response	185
6.4.2. Dopamine Receptor Antagonism.....	185
6.4.3. Opioid Receptor Antagonism	186
6.4.4. Cannabinoid Receptor Agonism.....	186
6.4.5. Adrenergic Receptor Antagonism.....	187
6.4.6. 5-HT Receptor Agonism	187
6.4.7. Glutamate Receptor Antagonism.....	189
6.4.8. Conclusions	191
7. Neural Correlates of Amphetamine Induced Dyskinesia in the Grafted Rat Model	192
Summary	192
7.1. Introduction	193
7.2. Experimental Design.....	194
7.3. Results.....	195
7.3.1. 5-HT and TH Cell Analysis in the Graft.....	195
7.3.2. Dopamine Receptor Levels	198
7.3.3. RGS Transcript Levels	200
7.4. Discussion	204
7.4.1. Graft Correlates of GID.....	204
7.4.2. Efficiency of Graft to Normalise Lesion and L-DOPA Induced Changes.....	206
7.4.3. Conclusions	207
8. A Mouse Model of GID.....	209
Summary	209
8.1. Introduction	210
8.2. Experimental Design.....	212
8.3. Results.....	214
8.3.1. Basal weight of CD1 and C57/Bl6 mice	214
8.3.2. Amphetamine Mediated Rotation in CD1 and C57/Bl6 mice.....	215
8.3.2. L-DOPA-induced rotation and AIMs in C57/Bl6 and CD1 strains.....	216
8.3.2. Amphetamine-Induced AIMs in the Transplanted Mouse	218
8.4. Discussion	223
8.4.1 Optimisation of the Mouse GID model.....	223
8.4.2 Future directions	225
8.4.3 Conclusions	226
9. General Discussion	227
9.1. Animal Models of LID and GID- Pre-Clinical Efficiency.....	227
9.1.1 Dyskinetic Phenotype.....	227
9.1.2 Underlying mechanisms of Dyskinesia.....	228
9.1.3 Dyskinesia Biomarkers	230
9.2. The Future of L-DOPA and Transplantation Strategies.	232
9.2.1 Dopamine Replacement	232
9.2.2. Cell Therapies.....	233
9.3. Is there a Single Treatment for Parkinson's Disease?	235
9.4. Final Summary	237
10. References	238

11. Supplementary Data	i
12. Appendix	ii

1. Introduction

1.1 Parkinson's Disease (PD)

Parkinson's disease (PD) is a progressive neurodegenerative movement disorder that was first characterised in 1817, by George Parkinson in his 'Essay on the Shaking Palsy' (Parkinson, 1817). PD is recognised clinically by characteristic motor abnormalities which include tremor, rigidity, changes in gait, akinesia (absence of movement), bradykinesia (slowness of movement), hypokinesia (reduced amplitude of movement), postural instability, dysphagia and micrographia (reviewed in Yanagisawa et al., 1989, Lichter et al., 1988). Patients typically have different profiles of parkinsonian symptoms that may depend on age of onset (Wickremaratchi et al., 2011). Changes in rapid eye movement (REM) sleep, procedural memory loss, delayed reactions, hallucination and changes in autonomic responses and perception have also been reported, (reviewed in Lichter et al., 1988). It affects up to 1% of individuals over the age of 70 in Europe and a smaller proportion develop a young onset form of the disease which is commonly defined as being when the patient is still of working age. Individuals that have a younger PD onset have an overall worse quality of life than those with late stage development (Knipe et al., 2011). Following diagnosis approximately 80% of patients die within 10 years (von Campenhausen et al., 2005, Ishihara et al., 2007). In the U.K. alone it is estimated that 120,000 people are currently living with PD (Parkinsons.org.uk), resulting in a significant socioeconomic burden, that is predicted to increase in future years. A cross-sectional analysis of over 300 late stage PD patients has shown that each person requires approximately £25,000 - £62,000 worth of medical help per annum, the majority of which is spent on health care professionals (Findley et al., 2011) and only 7% spent on direct medical intervention. As well as the emotional hardship suffered by the individual and family members, an appropriate treatment of PD is much needed to relieve the economic burden in the U.K.

The most effective anti-parkinsonian treatment to date is oral L-3,4-dihydroxyphenylalanine (L-DOPA) medication, used for its efficiency to treat bradykinetic and akinetic motor side effects at relatively low cost. However, long-term use of this treatment usually gives rise to

debilitating abnormal movements, termed dyskinesia (Encarnacion and Hauser, 2008). Interventions that can be used to treat dyskinesia by correcting electrophysiological dysregulation (deep brain stimulation) are costly (Shan et al., 2011), and other transplantation and gene therapy approaches are only at pre-clinical and early clinical trial phases of development (Lindvall and Bjorklund, 2004, Manfredsson et al., 2009). Promising transplantation approaches are hindered, in part, by the development of dyskinetic side effects in some patients that are directly related to the grafted tissue (Freed et al., 2001) and (reviewed in Lane and Smith, 2010).

The defining pathological features of PD are the specific cell death of dopaminergic neurons within the substantia nigra *pars compacta* (SNc), accompanied by the accumulation of the protein α -synuclein into large spheroid inclusions named Lewy bodies (Bethlem and den, 1960, Bethlem and Den Hartog Jager, 1960, Spillantini et al., 1997). Dystrophic Lewy neurites can also be found within the same region post-mortem (Bethlem and den, 1960, Bethlem and Den Hartog Jager, 1960, Spillantini et al., 1997). The Braak hypothesis is sometimes referred to in PD and proposes that Lewy body pathology might spread from one region to another (Braak and Braak, 1990, Braak et al., 2003, Steiner et al., 2011). Although protein aggregation and neuropathology can be correlated (reviewed in Hawkes et al., 2010), it remains unclear whether aggregates cause cell death, are a consequence of cellular dysfunction, or have a protective role. Much has been learnt from the genetic variants of the disease. Mutations in the genes encoding alpha-synuclein, ubiquitin carboxyl-terminal esterase L1 (UCHL1), PTEN-induced putative kinase 1 (PINK1) and Parkin have been linked to familial PD (reviewed in Morris, 2005) and it is thought that genes such as Leucine-rich repeat kinase 2 (LRRK2) and others, may predispose a subsection of the population to an increased risk of idiopathic disease development (Paisan-Ruiz et al., 2005, Shiba et al., 2009) and (reviewed in Morris, 2007).

PD is commonly idiopathic, although there are also genetic variants that contribute to approximately 5% of cases. The idiopathic form is thought to originate from exposure to environmental risk factors such as 1-methyl-4-phenyl-1,2,3,6-tetrahydropyridine (MPTP) -like chemicals, heavy metals and pesticides through farming (Berger, 2000, Richardson et al., 2005), although no single cause has been identified. Explanations for dopamine neuron loss suggest that alternative shifts in energy metabolism within the mitochondria following exposure to substances which inhibit mitochondrial function may cause apoptosis. Chemicals such as MPTP or paraquat reduce nicotinamide adenine dinucleotide dehydrogenase (NADH)

and co-enzyme Q1 reductase activity (Richardson et al., 2005), which points to environmental influences in the disease process. Furthermore, changes in dopamine production have also been found to increase free radical production and oxidative stress. However, elevated scavenger activity has also been noted and these changes may occur following the induction of apoptotic signals by another mechanism (Miyazaki et al., 2007). There is evidence to support each of these mechanisms but which is the leading factor remains undetermined. A significant lack of understanding of the pathogenesis of PD is in part due to uncertainty as to the cause, and without a defined trigger, identifying mechanism is difficult.

1.2. The Basal Ganglia

1.2.1. The normal brain

Parkinsonian symptoms in PD arise through dysregulation of the basal ganglia, resulting in altered signalling to the cortex and hence disadvantageous execution of motor function. Under normal conditions the SNc projects to the caudate nucleus and putamen (collectively known as the striatum), where dopamine mediated signals are relayed to the other output nuclei of the basal ganglia. Striatal neurons are electrically quiescent under normal circumstances, with activity generated by cortical stimulation (Gerfen, 1992). The two main outputs of the striatum are GABAergic and make up the direct and indirect pathways, controlling other output nuclei, namely the substantia nigra *pars reticulata* (SNr), the internal globus pallidus (GPi,) and the subthalamic nucleus (STN). Specifically neurons within the direct monosynaptic pathway project to the GPi and SNr and cause an inhibitory effect on postsynaptic signals to the thalamus. This results in the disinhibition (enhancement) of thalamo-cortical networks and movement (Mink and Thach 1991a,b,c, Boraud et al., 2000). Cells within the indirect pathway project to the GPi and SNr, via polysynaptic connections in the GPe and STN, causing an excitatory action on the thalamus. The balance of direct and indirect signalling, as shown in Fig. 1.1, allows for the excitation of the thalamus and the blockade of irrelevant motor commands for normal motor function through the cortex (DeLong et al., 1986, Alexander et al., 1986). Once movements are initiated in the cortex, signals are fed back to the thalamus, where they are relayed back to premotor and motor areas to control fine movements (Obeso et al., 2000a). In addition to the STN, the glutamatergic cortico-striatal pathway provides another major input to the striatum. The bi-directional modulation of the spiking rates of the GPi and the SNr by GABAergic neurons is only possible because of the autonomous

pacemaker properties of the GPe, GPi, STN and SNr (reviewed in Gerfen and Surmeier, 2011).

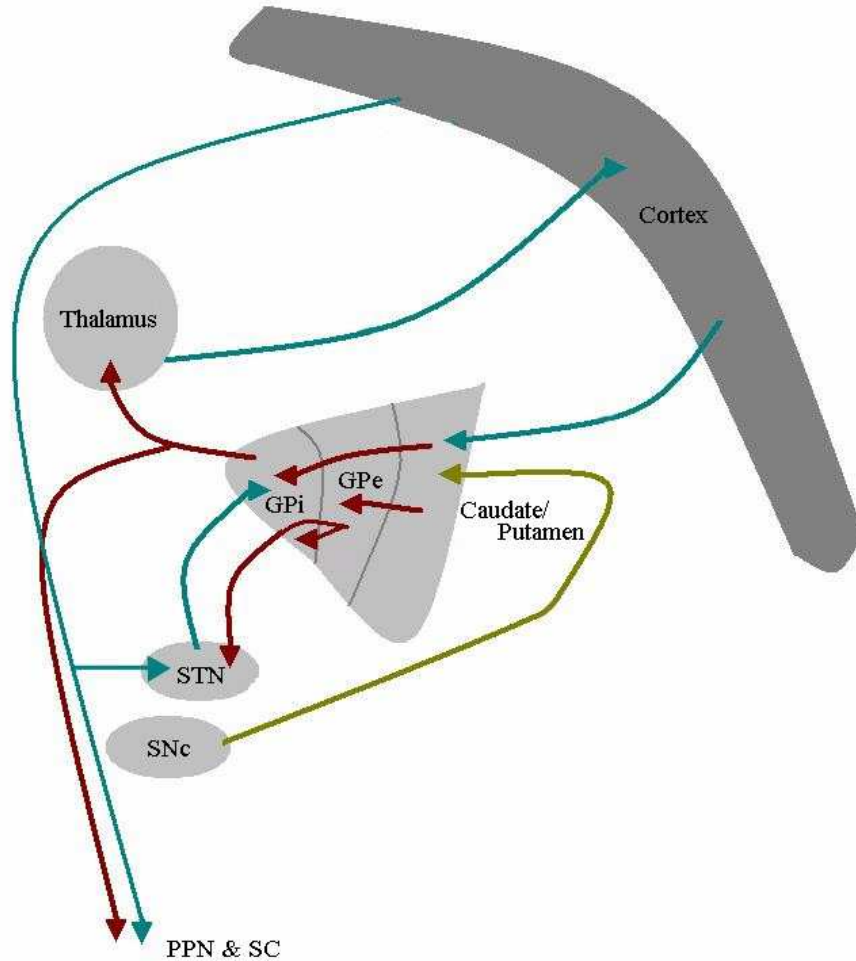


Fig. 1.1. A depiction of the circuitry within the basal ganglia of a healthy human. Dopamine projections (yellow) run from the SN to the caudate nucleus and putamen. GABA neurons (red) in the indirect pathway connect to the GPe and STN while the direct pathway exerts an effect on the GPi. The pedunculo-pontine nucleus (PPN), spinal cord (SC) and thalamus also receive an excitatory glutamatergic input. Glutamatergic signals (blue) connect the thalamus to the cortex, cortex to the STN and the cortex to the GP.

The model of motor function in the basal ganglia, although largely accurate can be seen as over-simplistic as there are other factors influencing this tightly regulated system. The importance of the pedunculo-pontine nucleus (PPN) is often not considered, yet receives inputs from output nuclei and influencing pallidal outputs and subthalamic inputs. Further, afferents from the PPN provide glutamatergic regulation of various nuclei and a cholinergic feedback loop provides input to and from the spinal cord (Pahapill and Lozano, 2000). Serotonergic and noradrenergic projections originating from the dorsal raphé and locus coeruleus (LC) respectively, influence striatal outputs (Moore and Bloom, 1979). L-DOPA induced dyskinesia (LID: a set of uncontrolled inhibitory movements) reflects a second neuropathological state of the basal ganglia (See 1.4.1).

The γ -Aminobutyric acid (GABA) releasing medium spiny neurons (MSNs) of the striatum, controlling direct (striatonigral) and indirect (striatopallidal) pathway, express D₁ or D₂ dopamine receptors respectively and are often distinguished by specific biomarkers other than the receptors themselves (see Table 1.1). 90-95% of the neuronal population in the striatum consists of the projection MSNs, whereas the remaining 5-10% of cells comprised a mixed population of interneurons (DiFiglia et al., 1976). Interneurons can be subclassified into 4 types (Table 1.2). Broadly, interneurons intergrate and modulate feedbackward and feedforward information, between the SNc, thalamus, cortex and GPe and the MSNs of the striatum (Kawaguchi, 1993) and (reviewed in Kawaguchi et al., 1995).

Table 1.1. The distinction between two populations of MSNs in the striatum.

	<i>Subtypes of medium spiny neurons²</i>	
Pathway	Direct	Indirect
Markers	PDyn ¹	PPE ¹
	Substance P	A2a
Receptors	D1	D2
Neuro-anatomy	Rat/mouse – entopeduncular nucleus	Rat/mouse – Globus Pallidus
	Monkey / human – GPi	Monkey/ human – GPe
Size (nuclus)	10–11 µm	10–11 µm

¹ Prodynorphin (PDyn), Preproenkephalin (PPE)

²Table based off information in (Matamales et al., 2009).

Table 1.2. Types of interneurons in the striatum.

	<i>Subtypes of interneurons²</i>			
Type	GABAergic 1	GABAergic 2	GABAergic 2	Cholinergic
Markers	Parvalbumin	Calretinin	Samatostatin	ChAT
			Neuropeptide Y	DARPP-32 ¹
			NOS ¹	
			NADPH ¹	
Receptors	D2		D1	D1 & D2

¹Nitric oxide synthase (NOS), nicotinamide adenine dinucleotide phosphate diaphorase. Dopamine and cAMP-regulated phosphoprotien.

²Table based off information in (Kawaguchi, 1993) and (reviewed in Kawaguchi et al., 1995).

In addition to the basic control of movement by the projection definitions above, neurons of the striatum can be compartmentalised into patch (or ‘striosome’) and matrix neuro-anatomical arrangements that differently control output nuclei. The patch/striosomes division in the striatum are defined by μ -opiate receptor binding and low acetylcholinesterase staining (present in cats and monkeys, but not apparent in the adult rodent) and matrix regions that additionally stain for calbindin and samatostatin. The matrix occupies the majority of the space and receives inputs predominantly from the neocortical and sensorimotor cortex, whereas the striosomes occupy labyrinths within the matrix and receive more limbic allocortical inputs (Gerfen et al., 1985, Gerfen, 1985). This is not exclusive, however, with functional connections from either cortical areas in the patch/ matrix (Gerfen, 1989). There are also discrepancies with the regional cortical connections, as the patch/ matrix are uniform throughout the dorsal and ventral tiers. However, the limbic cortex projects to the ventral area and the neocortex to the dorsal area (Haber and McFarland, 1999). Therefore, although this model has proved invaluable for evaluating connectivity in the basal ganglia, it may be perceived as over-simplified. In addition, striatal outputs from both patch and matrix compartments connect to the GPi and SNr, but only those of the patch project to the SNc.

It is important to note that the SNc can also be compartmentalised into regions of patch and matrix, defined by calbindin staining of neuropil, showing calbindin-poor ‘nigrosomes’ within a calbindin-rich matrix (Gerfen, 1992) of which approximately 60% of the SNc cell bodies reside (Damier et al., 1999a). Cell bodies that in the ventral tier of the SNc project to the striatal patch compartment, however cell bodies originating in medial SNc, project to the matrix (Gerfen, 1992). The ventral tier of the SNc further receives inputs from the patch compartment of the striatum.

1.2.2. PD Neuropathology

Dopamine neuron loss and the presence of Lewy bodies reflect the two main pathophysiological hallmarks of PD. Thus, patients with idiopathic PD exhibit deficits in striatal dopamine signalling and dopamine terminal loss within the striatum accompanied by loss of cells within the SNc (Mitchell et al., 1989, Crossman, 1989); which underlies the characteristic akinetic and bradykinetic motor symptoms characteristic of PD. These cannot be

detected until cell losses have been reached 50 - 60%, with even higher losses needed in dopaminergic fibres, as the result of their extensive branching in the striatum (Bernheimer et al., 1973). In terms of patch/matrix compartmentalisation it is evident that projections from the dorsal SNc are largely spared, with the majority of cell loss in the ventrolateral area (Damier et al., 1999b) and hence denervation of terminals within the putamen. A reduction of tyrosine hydroxylase (TH) and L-aromatic amino acid decarboxylase (AADC) provide pathological markers of dopamine cell loss (Hornykiewicz, 1982). By contrast, other dopaminergic nigro-pallidal and nigro-subthalamic projections are less affected in PD (Lavoie et al., 1989, Whone et al., 2003), although dopamine levels in the GP have been found to be reduced in PD (Fahn et al., 1971). In the dopamine-depleted striatum a subset of interneurons also appear to be dopaminergic, co-expressing TH, the dopamine transporter (DAT), and glutamic acid decarboxylase (GAD) needed for the synthesis of GABA (Huot and Parent, 2007). Their functions in PD remain unclear.

Cell loss in the SNc is a major contributing factor to loss of motor function. However, degeneration is not restricted to this region, with cell loss also evident in the ventral tegmental area (VTA) and corresponding mesocorticolimbic projection areas in the nucleus accumbens (NAcc), the prefrontal cortex and the amygdala. These components form part of the limbic system which is responsible for emotion, memory and reward-based behaviour, such that neuropathological changes in this system are likely to contribute to the non-motor symptoms of PD (Fahn et al., 1971, Jellinger, 1991). There is also evidence that the disease originates in the brainstem, affecting dorsal motor nuclei before the pathological spreading of the disease to the forebrain regions, which can be used to characterise disease stage (Backlund et al., 1985, Braak et al., 2003). Neuropathological changes also occur in the LC and raphé nucleus, reducing noradrenergic and serotonin (5-HT) input, respectively, to the striatum and cortex (Braak and Braak, 2000, Braak et al., 2000).

The presence of Lewy bodies has provided a pathological hallmark of PD since the early years of the 20th century, long before the discovery of dopamine as a transmitter in the late 1950s. Lewy bodies are spherical cytoplasmic inclusions located in cell bodies, although filamentous proteins in the perikaryal cytoplasm termed 'Lewy neurites' are also present and located largely in dopaminergic axons. Lewy bodies are now known to be composed of aggregated α -synuclein, but also contain ubiquitinated proteins and various cytoskeleton components (Spillantini et al., 1997, Kuzuhara et al., 1988). In PD, Lewy bodies are located predominantly

in the ventral tier of the SNc, also the main site of degeneration (Wakabayashi et al., 1990, Wakabayashi, 1989). Degeneration in this region causes electrophysiological circuitry changes (Bardinet et al., 2009), resulting from the lack of dopamine signalling in the striatum.

There is a defined set of circuitry changes (Fig. 1.2) that contribute to the cardinal motor symptoms of PD (Albin et al., 1989). However, as stated above, neuropathology is not restricted to these primary areas. Activation of the D₁ receptors is largely attenuated and there is a reduction in D₂ activation, causing a reduction in the inhibitory control of the GPi and SNr and that of the indirect pathway, to cause an increasing in firing of the STN. Therefore the fine balance of signalling is disrupted by the lack of dopamine signal and excessive glutamate signal causes an over-inhibition of thalamo-cortical projections, resulting in less movement (reviewed in Calabresi et al., 2000b, Sealfon and Olanow, 2000).

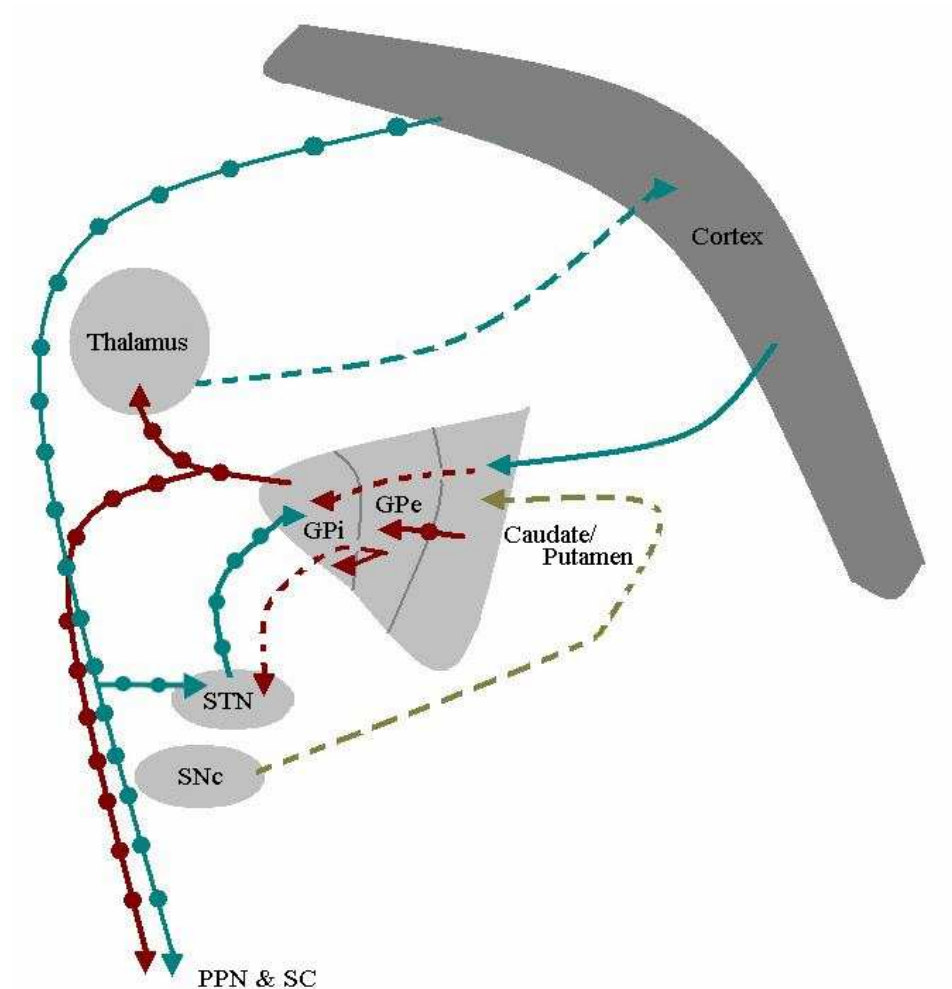


Fig. 1.2. A depiction of the neuropathological changes to the circuitry of the basal ganglia of a PD patient. Dopamine projections (yellow) run from the SNc to the putamen. GABA neurons (red) in the indirect pathway connect to the GPe and STN, while the direct pathway exerts an effect on the GPi. The pedunculo-pontine nucleus (PPN), spinal cord (SC) and thalamus also receive excitatory glutamatergic input. Glutamatergic signals (blue) connect the thalamus to the cortex, cortex to the STN and the cortex to the GP. A reduction in input is signified by the dashed line and an enhancement of signal signified by the dotted line. (Based on (Albin et al., 1989).

The degeneration of dopaminergic neurons causes profound changes in the neuro-peptide markers used to distinguish between direct and indirect signalling pathways. Late stage PD patients have decreases in intra-cellular protein levels of substance P and enkephalin in the putamen (Tenovuo et al., 1984, Sivam, 1991), yet levels of preprotachykinin are maintained (Nisbet et al., 1995). In contrast the precursors to enkephalin and dynorphin, (preproenkephalin and prodynorphin) were found to be increased (Levy et al., 1995). Caution should be taken when analysing the results from post-mortem, as variations in disease stage, tissue fixation processes, time of fixation from death, and prior treatment with dopamine agonists or L-DOPA may all confound results. The MPTP-treated primate model of PD has therefore been used to determine further pathological mechanisms. In accordance MPTP treated primates, that were mildly symptomatic, have an up-regulation of TH and DAT transporter levels whereas those of a severe phenotype show losses similar to that of the PD patient (reviewed in Jenner, 2009, Jenner, 2003). Dopamine and 5-HT turnover is likely increased in the model, following the observation of increased TH and 5-HT fibre thickness in the caudate and putamen, as the result of enlarged neurotransmitter carrying varicosities (Zeng et al., 2010, Song and Haber, 2000). Specific in-depth investigation has been carried out in rodent models of PD concerning receptor and/or intra-cellular changes in relation to experimental dopamine depletion and L-DOPA treatment (discussed in sections 1.6 and 1.7).

1.3. Treatment Strategies in PD

Surgical, pharmacological, and deep brain stimulation (DBS) interventions provide a high degree of symptomatic relief to many PD patients, however none of these strategies prevent or slow disease progression. Given that the main drug treatment for PD causes dyskinetic side effects, as well as the emergence of ‘on’ and ‘off’ phases throughout the day, there is an urgent need for alternative approaches. Consequently, restorative and neuroprotective interventions by cell transplantation and other gene therapeutic approaches for the treatment of PD are being keenly explored.

1.3.1. Historical Surgical Interventions

There are a number of surgical strategies involving the ablation of areas within the basal ganglia that have been used historically for the treatment of PD. Initial procedures involved

the obliteration of the caudate nucleus, this caused some elevation of tremor and rigidity (Meyers, 1951, Meyers, 1942). The stereotaxic pedunculotomy and encephalotomy can elevate tremor and thalamotomy has had positive effects on bradykinesia and resting tremor (Narabayashi et al., 1997, Narabayashi et al., 1987, Walker, 1952). Pallidotomy and subthalamotomy can also be used to alleviate bradykinesia and rigidity (reviewed in Zesiewicz and Hauser, 2001). These crude surgical strategies have mainly been used to treat motor abnormalities up until the introduction of L-DOPA in the 1960's and thereafter open neuro-surgery largely went out of favour as the preferred choice because of complications such as haemorrhage and infection, until the modern era of more selective, targeted and rationally based stereotaxic techniques (see 1.3.5).

1.3.2. Pharmacological Treatments

There are a number of pharmacological treatment strategies for patients displaying parkinsonian motor symptoms. Historically anticholinergics were used as the primary treatment for PD (Kapp, 1992). These are useful as the neurodegeneration associated with PD causes the depletion of acetylcholine as well as dopamine, and were found to be partially useful for treating tremor (Marjama-Lyons and Koller, 2000). Anticholinergics are no-longer preferred as they have been associated with cognitive impairments, and give a number of side effects such as dry mouth, gut problems and blurred vision (Perry et al., 2003). The first dopamine based therapy for the treatment of PD was L-3,4-dihydroxyphenylalanine (L-DOPA). Indeed the discovery of dopamine as a neurotransmitter and its role in Parkinson's disease was integrally tied up with the pharmacological reversal of motor symptoms by L-DOPA in Carlsson's classic studies using reserpine model to deplete brain catecholamines (Carlsson, 1959, Carlsson and Hillarp, 1958, Carlsson et al., 1957).

Currently L-DOPA therapy is the most widely used treatment of PD (reviewed in Espay, 2010, Tan, 2003, Poewe et al., 2010), and is a derivative found naturally in *Mucuna Pruriens* (velvet bean). It exerts a therapeutic effect by ameliorating the pathological decreases in dopamine levels, enhancing dopamine synthesis, stimulating dopamine receptors and thus restoring postsynaptic activity in striatal neurons. L-DOPA is a precursor to dopamine that can cross the blood brain barrier (BBB) where it is converted into dopamine. Oral L-DOPA medication is absorbed in the gut by specific amino acid transporters, where an excess of 99% is metabolised, before entering the blood (Sasahara et al., 1981). The biosynthesis of dopamine from this precursor and biodegradation routes is illustrated in Fig. 1.3. Early clinical

trials with L-DOPA failed, due both to peripherally induced side effects and limited central action, until it was recognised that it had to be administered with a peripheral amino acid decarboxylase (AADC) inhibitor to prevent the conversion to dopamine before entering the brain (Nutt et al., 1987), thus increasing the ‘therapeutic window’ of L-DOPA, causing a greater time in ‘on’ (Brooks and Sagar, 2003).

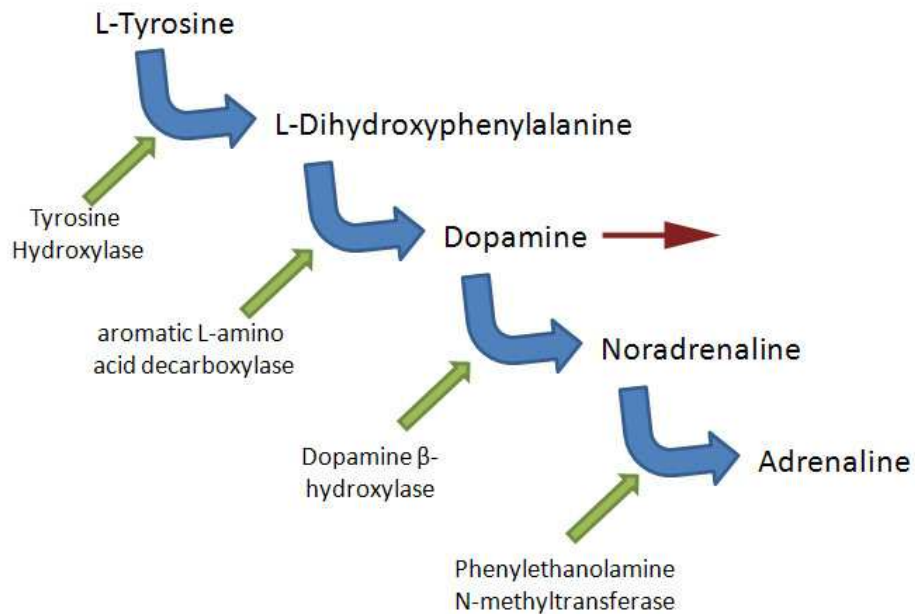


Fig. 1.3. The biosynthesis of dopamine from its precursor L-DOPA from the conversion of L-tyrosine (from the diet) by TH and its subsequent conversion into noradrenaline (NA) and adrenaline catecholamines (in the presence of Dopamine β-hydroxylase and Phenylethanolamine N-methyltransferase). Conversely, these catecholamines can be degraded to non active forms 3,4-Dihydroxyphenylacetic acid (DOPAC) and homovanillic acid (HVA) by the degradation enzymes: monoamine oxidase (MAO) and catechol-o-methyl transferase (COMT), indicated by the red arrow.

Once in the brain, L-DOPA is further metabolised in dopaminergic neuron terminals, interneurons and epithelial tissue, resulting in a short plasma half life of 4 hours. Limiting the metabolism of dopamine in pre-synaptic terminals to HVA and DOPAC may therefore be advantageous to maintain extracellular dopamine levels of the caudate-putamen. Monoamine oxidase B (MAO-B) inhibitors such as rasagiline have been found have to positive clinical effects disease progression and on motor complications when given in the early stage, reducing the degradation of dopamine (Schapira, 2010). Catechol-o-methyl transferase (COMT) inhibitors such as entacapone can also be used in combination with L-DOPA to increase the plasma half life (Nissinen et al., 2009).

Appropriate dopamine agonist treatments are the current focus to manage early stage PD; the most commonly used are D₂ receptor agonists including: pramipexole, bromocriptine, piribedil and cabergoline (Espay, 2010, Tan, 2003, Poewe et al., 2010). Investigators involved in the CALM-PD study found the use of pramipexole in early PD gives an additional neuroprotective effect and a means to control bradykinetic/akinetic movements without dyskinesia, in contrast to L-DOPA (CALM-investigators, 2009). Clinicians currently also favour the use of dopamine agonist drugs to prolong the time before L-DOPA needs to be given for approximately 5 years (Adler et al., 1997). The dopamine agonist action of apomorphine is also exploited in some instances, although usually only in patients with other complications, as it requires daily injection (Stocchi et al., 2001).

The use of D₁ mediated agonism is not currently used in the treatment of PD. However, administration of either SKF-82958 or A-77636 in the MPTP primate model of PD has been found to have anti-parkinsonian actions, although long term use may cause debilitating involuntary side effects (Blanchet et al., 1996).

1.3.4. Deep Brain Stimulation

Deep brain stimulation (DBS) has emerged in the last 15 years for the treatment of PD, and is now an established technique to control movement. DBS involves the control of the electrical output of the basal ganglia by the implantation and fine adjustment of electrodes within specific output nuclei. The technology was developed from early electrical activity modulating

experiments in the 1980s (Benabid et al., 1987). Currently the main target for DBS to eliminate bradykinesia, postural instability and tremor is the STN, where stimulation is often bilateral and targeted to the dorsolateral motor regions (Herzog et al., 2004). Long-term improvements for tremor and bradykinesia have also been noted with GPi-DBS and ventral nucleus of the thalamus-DBS (Zahodne et al., 2009b). Alternative STN and GPi-DBS targets have been compared in randomised double blind clinical trials, but as yet no clear differences between target sites have been observed, with significant improvement of parkinsonian symptoms based on the unified Parkinson's disease rating scale (UPDRS) using both (Follett et al., 2010).

Outcome measures of DBS on symptoms such as gait, speech and cognition are often difficult to interpret (reviewed in Bronstein et al., 2011). However an improvement of depression has been noted with GPi-DBS in contrast to STN-DBS where a worsening was observed (Follett et al., 2010). The latter target has also been associated with cognitive decline one year post-procedure (Mikos et al., 2010, Zahodne et al., 2009a). Although clearly effective, DBS has significant long term costs, not only in the cost of the stimulators themselves and their maintenance, but also the cost of specialist physiologists (Shan et al., 2011) and (reviewed in Groiss et al., 2009).

1.3.3. Future Cell Replacement Strategies

Current strategies only treat motor symptoms and do not stop disease progression or reverse the damage, which are the two main goals of future cell therapies for PD. As so many cells have been lost in advanced stages of PD, resulting in long-term changes in the circuitry of the basal ganglia, one approach has been to directly replace the lost dopamine neurons by the implantation of replacement dopaminergic neurons. In the 1980's the transplantation of adrenal cells into the denervated striatum in animal models of PD produced a degree of motor function recovery mediated by the release of catecholamines (Freed et al., 1983, Freed et al., 1981, Backlund et al., 1985). This led to the first implantation of autologous adrenal medulla cells in PD patients in the early 1980s (Backlund et al., 1985, Lindvall et al., 1988, Lindvall et al., 1989, Madrazo et al., 1988). In spite of initial claims of dramatic alleviation of symptoms by an open surgical approach in two patients (Madrazo et al 1987), this could not be replicated and a series of more careful studies, in particular in the USA, led to the recognition of poor survival of adult medullary cells, limited acute and no sustained functional benefits, and the

surgery itself was associated with significant complications in elderly frail patients, with unacceptable levels of morbidity and occasional mortality (Quinn, 1990). This adrenal medulla approach rapidly fell out of favour. However, animal studies suggested more reliable results in experimental animals by transplantation of allogenic dopaminergic cells from the embryonic ventral mesencephalon (VM) (Freed, 1983, Dunnett et al., 1981, Bjorklund et al., 1981, Brundin et al., 1986). The first transplants of VM of 6-9 week human embryos donated from elective surgical terminations into PD patients yielded good graft survival as visualised by F-dopa PET imaging, and clearcut functional benefits (Lindvall 1990). Long term follow up studies of these first patients continues to show good clinical benefit in at least some patients, sustained over 10-15 years (reviewed in Dunnett et al., 2001). Typically 1.5- 4.9 embryos were used per putamen. Initial preclinical studies used solid tissue pieces that were subsequently demonstrated to have functional effects on the behaviour of animal models when implanted into cortex and ventricles (Bjorklund and Stenevi, 1979, Stenevi et al., 1976). However it was quickly shown that increased improvement of the motor phenotype in models, could be achieved using single cell suspensions with topographic placement in the striatum (Dunnett et al., 1983b, Dunnett et al., 1983a, Schmidt et al., 1981), used for all subsequent clinical trials.

The positive outcome from both the small trials of the 1980's and pre-clinical research enabled the implementation of two large National Institutes of Health (NIH) double-blind, placebo controlled studies (Freed et al., 1990, Olanow et al., 2003). The result of these however was more disappointing than expected (Freed et al., 2001, Olanow et al., 2009a, Olanow et al., 2009b). Ongoing open label trials of 26 patients however has lead to symptomatic improvements based on the UPDRS, 6-24 months post-transplantation (Hagell et al., 1999) and (reviewed in Dunnett et al., 2001). In some patients transplantation enabled a reduction in medication, a reduced time in 'off' and in others L-DOPA could be removed altogether (Freed et al., 2001, Hagell et al., 1999). Evidence from position emission topography (PET) scans in patients has shown the transplanted tissue is able to survive over time and reinnervate the dopamine-depleted striatum, leading to an improvement in clinical tests such as the UPDRS (Cohen et al., 2003, Freeman et al., 1995). Long-term follow up studies have shown that symptomatic improvement goes beyond dopamine replacement and transplantation causes a degree of functional integration, demonstrated by task-driven cortical activation 18 months post-surgery (Piccini et al., 2000). The high variability between individuals (Olanow et al., 2003, Freed et al., 2001) and a large placebo effect in some individuals under controlled

conditions (Goetz et al., 2008), produced some concern regarding the reliability of the technique.

Grafts have also had mixed success in altering abnormal movements caused by L-DOPA. Whilst it has been reported in some trials that the grafts can reduce time in 'on' dyskinesia, in others only marginal improvements or even a worsening effect was seen in patients (Freed et al., 2001, Freed, 2004, Olanow et al., 2003, Olanow et al., 2009b). A number of studies also reported the occurrence of 'runaway dyskinesia', i.e. abnormal movement profile that continues even with the withdrawal of L-DOPA treatment (Freed et al., 2001, Hagell et al., 2002), and which has subsequently been termed graft induced dyskinesia (GID), as detailed in section 1.5.

1.3.5. Future Gene Therapy

An emerging novel surgical treatment for the cardinal symptoms of PD is the delivery of genomic transcripts or recombinant proteins into dopamine-depleted areas. infusion of Glial cell-derived neurotrophic factor (GDNF) into the putamen by low basal and pulsed delivery in 10 PD patients caused initial motor improvements, although the benefits appeared to be lost 9 months after treatment withdrawal (Slevin et al., 2006). However, it has been proposed that the significance levels in this study were based on misleading power calculations, even though re-evaluation of the statistics has justified the beneficial outcome (Matcham et al., 2007). Nevertheless the delivery system by chronic infusion is not ideal, and is associated by significant technical complications and side effects. Therefore the use of viral vectors has been explored as an alternative technology for sustained bio-delivery. An adeno-associated viral (AAV) mediated gene transfer of neurturin (CERE-120), a structural and functional homolog of GDNF, can cause the partial tyrosine hydroxylase (TH)-induction in patients and can reach approximately 15% of putamen (Marks et al., 2008). However, the neuroprotective outcome was not as successful as previous primate studies (Herzog et al., 2007), most likely due to there being less retrograde transport to the SN in the human studies (Marks et al., 2008) and (reviewed in Bartus et al., 2011).

Pre-clinical evidence suggests that growth factor expression in the SN can significantly save a proportion of dying cells (Choi-Lundberg et al., 1997), reflecting new surgical targets that could be exploited in the clinic. Although deemed suitable in for use in humans by a safety

study, the clinical outcome has so far been disappointing (reviewed in Manfredsson et al., 2009). The AAV mediated GAD over-expression into the STN has proved to be safe and efficacious in a double-blind, randomised, sham-controlled clinical trial, causing improvements on the UPDRS 6-months post injection (LeWitt et al., 2011). The use of tyrosine hydroxylase (TH) and GTP cyclohydrolase-1 viral vectors can cause a reversal in certain sensory-motor problems in rodent models of PD, negating bradykinesia and akinesia like deficits (Bjorklund et al., 2010, Kirik et al., 2002) and is now very close to being tested at clinical trial.

A third gene therapy approach that is likely to be exploited in the future is combined TH, AADC and GCH1 transfer to enhance dopamine synthesis in striatal neurons themselves, although ratios will need to be carefully controlled *in vivo* (Duan et al., 2005). Moreover the mechanism by which dopamine synthesised within striatal neurons (which do not have the machinery for vesicular packaging, storage and release of the transmitter) can provide a regulated action at receptors located on the outside of the cells, remains to be explained.

In summary, the invasive nature of gene therapy, along with the significant regulatory concerns surrounding gene manipulation and therapy will mean that it will not be suitable for everyone. Moreover, significant technical advances are also required to optimise the surgical technique and to deduce appropriate concentrations for stable diffusion of the transcripts throughout the caudate-putamen and/or SN.

1.4. L-DOPA Induced Dyskinesia (LID)

1.4.1. Development and Causes

At later stages of the disease, fluctuations in extracellular dopamine concentration from oral L-DOPA treatment give rise to debilitating dyskinesia (a set of abnormal involuntary movements (AIMs) present in the limbs, trunk and face). This is the result of a short L-DOPA half life and hence shorter duration of action, causing the wearing off of the beneficial motor effect before the next dose is given. Adequate symptomatic control may last approximately 10 hours after reaching the brain in the early stage of the disease, but may last as little as two in advanced PD (reviewed in Schapira et al., 2009). It is usual for dyskinetic symptoms to manifest 5-10 years following initiation of L-DOPA therapy (reviewed in Encarnacion and Hauser, 2008), this form of dyskinesia is commonly biphasic or may only occur at times of peak dose ('on' phase) or as a wearing off affect ('off' phase) as the result of fluctuations in circulating plasma L-

DOPA levels (Cubo et al., 2001). Under normal circumstances extracellular dopamine levels are stable, causing the low level continuous stimulation of dopamine receptors in the caudate and putamen, this balance is disrupted by L-DOPA in PD patients and post synaptic receptors are under stimulated when L-DOPA has been utilised and overstimulated at peak dose (reviewed in Stocchi et al., 2009). However if this is controlled adequately dyskinesia can be much reduced, clinicians often favour the use of apomorphine or duodermum pumps so that dyskinesias may be managed (see section 1.4.2). The pulsate nature of L-DOPA treatment leads to permanent post-synaptic changes that sensitise receptors and lead to signalling abnormalities, discussed in section 1.8.

Dopamine level fluctuations and post-synaptic changes result in a second pathological state of the basal ganglia circuitry (Fig. 1.3). It is generally accepted that excess dopamine produced by the action of L-DOPA causes an abnormal decrease in the firing of neurons within the GPi and an excessive dis-inhibition of thalamo-cortical signalling, resulting an increased cortical output (Obeso et al., 2000b). In short, there is a disproportionate signalling of the D₁ mediated direct pathway. The changes to the direct pathway caused by L-DOPA are fundamental to the development of dyskinesia. Lesions of the STN and pharmacological reduction of signalling by GABA receptor agonists can both induce dyskinesia in the absence of L-DOPA (Burbaud et al., 1998, Hamada and DeLong, 1992). In agreement, the agonist action of apomorphine on D₁ and D₂ receptors decreases the activity in the STN and increases firing in the GPe (reviewed in Lozano et al., 2000). This general model of dyskinesia however is often considered to be over-simplified as indicated by other experiments (reviewed in Obeso et al., 2000a). Unexpectedly, dyskinesia is enhanced by GPe lesions and reduced by GPi lesions (Blanchet et al., 1994, Marsden and Obeso, 1994). Thus, evidence suggests that following L-DOPA the basal ganglia undergoes a number of neuro-plastic changes over time, resulting in an alteration of neuronal firing (reviewed in Cenci and Konradi, 2010).

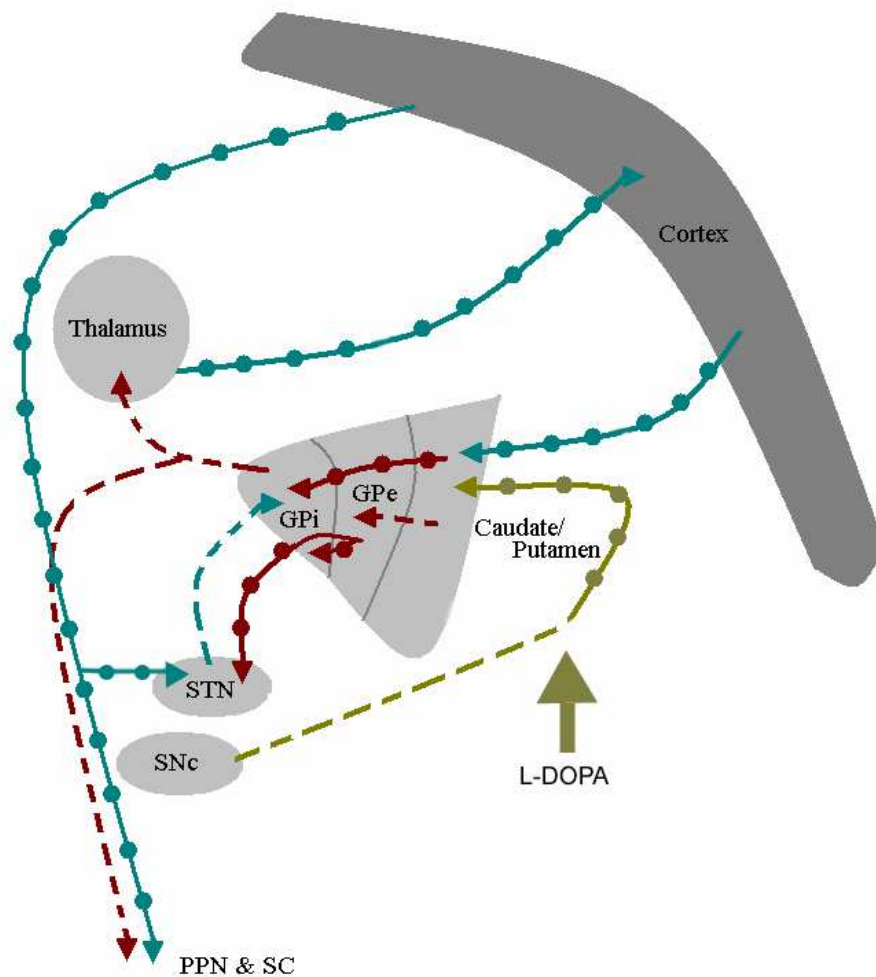


Fig. 1.3. A representative diagram showing the circuitry of the basal ganglia in Parkinson's disease patients, following L-DOPA treatment. Dopaminergic neurons (yellow) project from the SN to the putamen. GABA neurons (red) in the indirect pathway connect to the GPe and STN while the direct pathway exerts an effect on the GPi. The pedunculo-pontine nucleus (PPN), spinal cord (SC) and thalamus also receive an excitatory glutamatergic input. Glutamatergic signals (blue) connect the thalamus to the cortex, cortex to the STN and the cortex to the GP. A reduction in input is signified by the dashed line and an enhancement of signal signified by the dotted line.

It is emerging that dyskinesia in PD is not solely the result of continued dopamine denervation, long term post-synaptic changes and consequent firing patterns of the basal ganglia, but may also be dependent on the interplay of the glutamatergic and serotonergic systems (Cenci and Konradi, 2010). The change in the glutamate controlled cortico-striatal pathway is now found to be critically important in emergence of LID. Dyskinetic PD animal models lack the ability to reverse experimentally-induced long term potentiation (LTP) and have synaptic storage information deficits within the cortex (Cenci and Konradi, 2010, Dunnett, 2003, Picconi et al., 2003, Calabresi et al., 2000a). The manifestation of LID arises though the inability to erase unneeded motor information, termed synaptic depotentiation. In addition, 5-HT neurons have the ability to convert L-DOPA into dopamine and may also contribute to dyskinesia; sufficient autoregulation of dopamine release is prohibited, as 5-HT terminals lack D₂ receptors, thereby providing dysregulated dopamine release into the denervated striatum (reviewed in Carta et al., 2010a, Carta et al., 2008c). Although the relationship between the 5-HT fibres and dyskinetic movements has been established in animal models, there is a lack of post mortem data to confirm this in PD patients.

1.4.2. Treatment Strategies for LID

There are currently no effective treatments for the prevention or amelioration of dyskinesia in response to L-DOPA therapy that do not compromise lifestyle and anti-parkinsonian effects in humans and non-human primates. Historically, pallidotomies were used for their anti-hyperkinetic effect on highly dyskinetic patients (Meyers et al., 1959). However, open brain surgery is no longer preferred. There has been a drive to achieve constant levels of L-DOPA within the striatum, thereby avoiding dopamine fluctuations and dyskinesia and this has been demonstrated by slow infusion into the gastrointestinal tract (Odin et al., 2008). This is not ideal, however, and requires a permanent attachment of an often cumbersome bag to the abdomen, and requires careful monitoring of the dietary habits of the individual. The bag may also present a potential source of infection (Devos, 2009). Therefore an alternative co-treatment strategy using compounds that alter signalling within the basal ganglia are often adopted by clinicians. Subcutaneous apomorphine pumps can also be used to control LID and

where the drug is administered continuously over 6 months, both a reduction in AIMs and ‘off’ phase could be observed (Katzenschlager et al., 2005).

Dopamine receptor antagonists are not used for the treatment of LID, as therapeutic doses will simply result in the worsening of parkinsonism. Similarly reducing L-DOPA without replacing it alleviates LID, but the consequence is a worsening of the bradykinetic symptoms. Amantadine has NMDA antagonistic and anticholinergic properties and has shown to be the most effective for reducing AIMs in L-DOPA treated PD patients; however only 50% of patients have shown an improvement with this combination approach, and severity is only mildly reduced for a short period of time (da Silva-Junior et al., 2005, Godwin-Austen et al., 1970).

Several other compounds have been trialled but are not available as ‘on-label’ drugs for the treatment of dyskinesia. Furthermore, there are new putative compounds but many fail to go beyond the clinical trial stage. The D₂ and α -adrenergic receptor antagonistic and partial 5-HT_{1A} agonist properties of buspirone are able to reduce severe dyskinesia in some patients (Bonifati et al., 1994). Of late, an open labelled clinical trial testing low doses of aripiprazole on LID has shown that even in patients that were not responsive to amantadine, a reduction in the severity and frequency of dyskinesia resulted although in some cases may have also worsened general movement as scored on the UPDRS (Meco et al., 2009). This novel antipsychotic acts by a partial agonism at the D₂ and 5-HT_{1A} receptors and antagonism of the 5-HT_{2A} receptor (Meco et al., 2009). Cannabinoid agonists have also been shown to reduce dyskinesia clinically in some L-DOPA treated patients, from their proposed action on receptors on the GPi (Sieradzan et al., 2001), although cannabis itself had no effect on dyskinesia in a double blind placebo controlled study (Carroll et al., 2004). Non-specific opioid receptor and specific δ -opioid antagonism with naloxone or naltrindole, respectively, resulted in a small yet significant reduction in LID in two small scale studies (Manson et al., 2001, Fox et al., 2004). Overall, the pharmacological approach to the adverse effects of L-DOPA treatment has had limited success at clinical trial stages, although there are a number of other agents that have shown a greater efficacy in experimental models of PD (Dekundy et al., 2007, Lundblad et al., 2002).

In animal models of PD L-DOPA is used to induce abnormal movements that closely mimic LID in patients, allowing specific systems and receptors to be targeted with pre-existing or

novel compounds, hence validating the model (Dekundy et al., 2007, Lundblad et al., 2002). Dopamine antagonists such as haloperidol can reduce dyskinesia by 99% in rodents (Johnston et al., 2005, Monville et al., 2005, Lundblad et al., 2005), but they completely suppress all voluntary motor function at effective doses. Noradrenergic and opioid modulators such as propranolol, clonidine, naloxone and yohimbine show some anti-dyskinetic effects in hemiparkinsonian rodents (Dekundy et al., 2007, Lundblad et al., 2002). Responses to opioid receptor modulation in particular are not uniform between studies, as both agonism of κ -opioid receptors and antagonism of μ - and δ -opioid receptors may result in a reduction in experimental LID (Henry et al., 2001, Ikeda et al., 2009). 5-HT_{1A} and 5-HT_{1B} receptor agonists and 5-HT_{2C} receptor antagonists have also shown some efficacy to minimise dyskinesia in rodents and primates (Dekundy et al., 2007, Munoz et al., 2008b, Carta et al., 2008d, Carta et al., 2008a). Cannabinoid agonists targeting cannabinoid receptor-1 (CB₁ receptors) such as WIN55,212-2 can also reduce dyskinesia experimentally (Morgese et al., 2009). Cholinergic modulators however have had no effect (Dekundy et al., 2007). Glutamate modulating drugs including amantadine have had the most promising effect on experimental dyskinesia; however, many of the compounds also influence the functionalities of other systems (Dekundy et al., 2007, Lundblad et al., 2002). Specifically, mGluR5 antagonists have been shown to reduce AIMs in rodent models, whereas mGluR1 antagonists exhibit more limited effect (Dekundy et al., 2006). The ability of two mGluR5 receptor antagonists, MPEP and MTEP, to reduced LID has also been shown in non-human primates (Morin et al., 2010). AMPA receptor antagonist drugs can also reduce dyskinesia by up to 75% (Kobylecki et al., 2010). LID can be prevented by NR1 and NR2b specific NMDA antagonists when given simultaneously to L-DOPA through treatment in non human primates (Ouattara et al., 2009). However, both pre-clinical research and clinical trials have shown that co-treatments are not ideal as they generally have little efficiency in targeting AIMs over general motor function and therefore other strategies are now sought to control LID.

The application of high frequency DBS directly into the GPi has shown marked improvements of hyperkinetic symptoms in patients (Kumar et al., 2000). However, complications using this technique include the difficult fine adjustment of frequencies necessary to gain maximal possible reduction in hyperkinesia without worsening bradykinesia, and a ‘wearing off’ effect seen in some patients a year or more post-surgery. Recently, GPi-DBS has been used to treat the most severe forms of dyskinesia; however, this is often compromised in favour of reduction in medication and STN stimulation to improve motor function (reviewed in Groiss et al., 2009).

1.5. Graft Induced Dyskinesia (GID)

1.5.1. Development and Possible Causes

The development of AIMs, 6-12 months after the transplantation of VM derived tissue, was first noted by Freed et al. and retrospective analysis has found this debilitating side effect to occur in the absence of L-DOPA (Freed et al., 2001, Freed et al., 2003, Ma et al., 2002). These abnormal movements have subsequently been termed ‘run away’ or graft-induced dyskinesia (GID). The development of dyskinesia was initially seen in a small number of patients (Freed et al., 2001), manifesting through what was subsequently described as a combination of hyperkinesia and dystonia symptoms, highlighted in (Olanow et al., 2009b, Olanow et al., 2009a, Olanow et al., 2003). These have been phenotypically described as ‘repetitive stereotypic alternating contractions of flexor and extensor muscles’ (Olanow et al., 2003), found in the face and limbs or generalised across the whole body (Freed et al., 2001). In some grafted patients, hyperkinetic movements required DBS therapy of the GPi or STN to decrease their severity (Freed et al., 2001). Table 1.3 describes the occurrence, onset and severity of GID in the three large scale clinical trials. AIMs were analysed in follow up studies or by retrospective analysis: -

Study	Reported	Patients affected	Time of development	AIM description	Treatment
Denver	Freed et al. 2001	15 %	1 year post transplantation	Severe debilitating dyskinesia	Amantadine and DBS (all)
Tampa	Olanow et al., 2003	56.5%	6-12 months post transplantation	Mild stereotypic movements of the lower extremities	DBS (small %)
Lund	Hagall et al., 2002	Not determined	40 months post transplantation	Mild to moderate choreiform movements	none

Table 1.3. Observations of GID in the three documented clinical trials of primary dopaminergic tissue transplantation.

GID is not causally linked with L-DOPA administration as AIM persist following the withdrawal of L-DOPA therapy post-operatively (Hagell et al., 2002, Winkler et al., 2005) and (reviewed in Lindvall and Bjorklund, 2004). Patients that have diurnal dyskinesia in response to L-DOPA preoperatively however may have a worsened ‘off’ phase dyskinesia and

improved ‘on’ phase dyskinesia postoperatively (Freed et al., 2001, Hagell et al., 2002, Olanow et al., 2009a). It is now considered that GID, develops a year or more following transplantation, and is not correlated with anti-parkinsonian effects (Hagell et al., 2002, Nova et al., 2004). In contrast other studies noted GID development in the first 12 months (Freed et al., 2001, Olanow et al., 2003). Timing of GID development may be important, as it seemingly occurs when a beneficial effect was noted, indicating that graft functionality or the withdrawal of immuno-suppression may be a risk factor for GID development (reviewed in Lane and Smith, 2010).

GID has led to the questioning of the future of transplantation as a viable treatment strategy for the field of PD. This has prompted much experimental research on the mechanistic cause of this phenomenon (detailed in section 1.9.) so that it may be reduced/ avoided in future clinical trials. In large GID is rare and although most patients exhibiting these AIMs find the side effects inconvenient they would not voluntarily forego the greater benefit of the graft for the elimination of the side effect.

1.5.2. Strategies for GID

Few pharmacological strategies have been used to negate dyskinetic side effects associated with cell transplantation in humans, not least because the phenomenon has only become apparent in the last decade and the number of patients affected is small. This better pharmacological management of this problem however may overcome political hurdles, to enable further clinical trials. Amantadine had limited success in reducing GID (reviewed in Lane et al., 2010), buspirone has shown some symptomatic relief in two grafted PD patients, associated with its 5HT_{1A} agonist properties (Politis et al., 2010, Politis et al., 2011a). D₁ and D₂ specific antagonists have been shown to reduce GID in the grafted rodent model of PD (Lane et al., 2009a). GID can also be reduced experimentally using 5-HT_{1A} and 5-HT_{1B} receptor agonists singly and to a greater extent in combination, although the exact mechanism of which is unclear (Lane et al., 2009a, Carta et al., 2010b). It is not known whether other anti-dyskinetic agents used for the treatment for LID (see section 1.4.2), will have any beneficial effect on the hyperkinesia caused by dopamine cell replacement strategies.

Although the precise electrophysiological consequences that cause abnormal movements following a dopamine rich transplant have yet to be elucidated both GPi and STN-DBS treatment strategies have been shown to cause improvements in some cases (Freed et al., 2004,

Herzog et al., 2008, Ma et al., 2002). However, transient benefits or no improvements have been recorded in some individuals using these measures, and thus experimental research is needed before the efficiency of DBS in transplanted patients is equal to that seen for the treatment of LID.

1.6. Animal models of PD

1.6.1. Pharmacological

The alkaloid reserpine was used to create the first animal model of PD (Carlsson et al., 1957, Carlsson et al., 1991). Reserpine causes the blockade of the vesicular monoamine transporter, preventing the reuptake of the neurotransmitter into vesicles of released or newly synthesised monoamines. It was the observation of the akinetic effects of reserpine on experimental rabbits and rats by Carlsson (1957) that first suggested that dopamine was a neurotransmitter in its own right (rather than just a precursor for noradrenaline). Further, in view of similarities to akinetic symptoms, it was first proposed that PD may involve a reduction in dopamine transmission within the basal ganglia (Carlsson et al., 1957). These symptoms prevail for 2-3 days before the replenishing of stores is enabled, allowing behavioural and neuro-chemical recovery. Carlsson et al. (1957) also observed that rigidity and akinesia in reserpine-treated rabbits could be alleviated by L-DOPA.

Methamphetamine is a lesser used pharmacological model of PD, which can deplete dopamine permanently, to cause a mild parkinsonian syndrome in the animals when off the drug. Administration of 2.5mg/kg, twice daily over 4 days reduces dopamine and 5-HT in the striatum, potentiated by pargyline (Jarvis and Wagner, 1985), and causes a loss of nigral dopaminergic neurons (Sonsalla et al., 1996), leading to the a permanent PD motor phenotype. Although this model is less commonly used due to side effects of thermal-dysregulation, and adverse psychological behaviours, ubiquitin and α -synuclein positive inclusions have been reported (Fornai et al., 2004). To mimic more closely the links of idiopathic PD to the farming and agricultural sector, rotenone and paraquat used as herbicides and pesticides, are seen to cause dopaminergic cell death in animal models, an effect believed to be mediated by an increase in free oxygen species (Anderson et al., 2007, Bove et al., 2005, Corasaniti et al., 1998, Greenamyre et al., 2003, Richardson et al., 2005). Although Lewy body-like inclusions have been reported in the brains of animals treated experimentally using these chemicals, non-

specific cell death, procedural difficulties in administration, inconsistency of lesions, and high death rates reduce the practical utility of these toxin models, which are consequently not commonly used in experimental PD research (reviewed in Greenamyre et al., 2003, Corasaniti et al., 1998).

Although models mentioned above have been used in the assessment of PD and analysis of the pathways of the basal ganglia, MPTP and 6-OHDA models are often preferred as they are well characterised, can mimic late stage PD, cause long-term maladaptive changes and dopamine depletion is stable (Jenner et al., 1984, Langston and Ballard, 1983, Ungerstedt, 1968) and (reviewed in Cenci et al., 2009, Jenner, 2009).

1.6.2. MPTP

The ability of MPTP to cause a fast severe parkinsonian phenotype in humans (Langston and Ballard, 1983), by promoting cell death within the SN, has led to its use in animal models to recapitulate the pathology and motor features of idiopathic human PD (Anichtchik et al., 2004, Boyce et al., 1984, Braungart et al., 2004, Jenner, 2003, Jenner et al., 1984). MPTP is a lipophilic by-product of the synthesis of mepethidine, it can cross the BBB with relative ease where it is then metabolised into MPP⁺ by MAO-B in non-neural cells. MPP⁺ is the active toxic metabolite which is taken up into neurons through the dopamine transporter (DAT). Cell death is induced by inhibition of complex I of the mitochondrial respiratory chain increasing the presence of free oxygen species (Nicklas et al., 1985). MPTP administration to mice and non-human primates selectively damages dopaminergic neurons of the midbrain, although there is evidence that other monoamine systems may also be affected (Luchtman et al., 2009, Perez-Otano et al., 1991). MPTP produces a rapid pattern of PD like cell death in mammals, and a stable lesion develops after a few weeks corresponding to the time at which behavioural deficits similar to clinical PD are observed (Jenner et al., 1984). In non human primates, the variation in the motor phenotype can be assessed with rating scales that are similar to that used to characterise PD in the clinic. Although typical inclusion body formation is not seen following MPTP toxicity (Fornai et al., 2005), aged primates and mice show an up-regulation in the expression of soluble α -synuclein (Halliday et al., 2009). MPTP has also been used to disrupt usual patterns of movement in *caenorhabditis elegans* (*C. elegans*) and zebrafish (Braungart et al., 2004, Anichtchik et al., 2004). Since primates are expensive to house and maintain, rodent based studies are often preferred. MPTP has species specific effects being

less potent in mice than in monkeys; and rats are even less susceptible to its neurotoxic effect (Boyce et al., 1984).

1.6.3. 6-OHDA

The catecholaminergic neurotoxin 6-hydroxydopamine (6-OHDA) is able to destroy dopaminergic terminals and cell bodies by inhibiting mitochondrial complexes I and IV as well as producing hydroxyl free radical species by auto-oxidation (Ben-Shachar et al., 1995, Glinka and Youdim, 1995, Ungerstedt, 1968). Motor behavioural deficits manifest in conjunction with cell loss in the SNc, beginning in the second week post-injection, and gradually progressing until a stable plateau is reached at day 28 (Blandini et al., 2007b). The unilateral 6-OHDA lesioned rat model of PD was developed by Ungerstedt in 1968 and has had a diverse use in the assessment of motor, cognitive and therapeutic aspects of Parkinson's disease (Perese et al., 1989, Kirik et al., 1998). To establish this model the neurotoxin can be injected stereotaxically into either the striatum, median forebrain bundle (MFB) or SN regions of the nigrostriatal pathway. The selectivity of 6-OHDA on the dopaminergic system is currently unclear and there is evidence that the neurotoxin can disrupt serotonergic and adrenergic systems, although this may be dependent on cannula type, species, 6-OHDA concentration and infusion rate of the neurotoxin (Fulceri et al., 2006, Bishop et al., 2009).

The hemi-parkinsonian rodent model, produced by the injection of 6-OHDA into one hemisphere, has been used widely to assess the role of the nigrostriatal pathway in motor function, to determine the degree of functional recovery following the transplantation of primary dopamine releasing cells (Torres et al., 2008, Mendez et al., 1996, Ishida et al., 1990, Mandel et al., 1990, Olsson et al., 1995, Dowd and Dunnett, 2004, Klein et al., 2009) and increasingly being utilised to explore the mechanisms underlying LID (Jankovic and Aguilar, 2008, Jankovic, 2008, Bordet and Destee, 1992, Kirik et al., 1998, Cenci et al., 1998), or GID (Carlsson et al., 2006b, Lane et al., 2009a, Lane et al., 2009b, Lane et al., 2006b, Steece-Collier et al., 2003). Although 6-OHDA is predominantly used in the rodent, other more basic models such as zebra fish, *C. elegans* and salamanders can also be used to assess the sensitivity to the drug and the testing of neuroprotective compounds (Anichtchik et al., 2004, Marvanova and Nichols, 2007, Nass et al., 2002, Parish et al., 2007). Interestingly, the salamander has a more progressive parkinsonian phenotype, similar in nature to that seen in the patient, yet deficits are not stable or long lasting. Overall the 6-OHDA lesion model is

non-selective among catecholamines, dopaminergic, noradrenergic and adrenergic pathways being equally susceptible to its toxic action. Nevertheless, two different strategies can be adopted, separately or together, to yield more selective dopaminergic cell death. First, stereotaxic techniques can permit selective placement of the toxin into a discrete area of the brain where only one principle pathway is present, such as targeting the coeruleocortical noradrenergic pathway by injection into the dorsal noradrenergic bundle caudal and dorsal to the substantia nigra (McGaughy et al., 1997). The ascending forebrain dopamine fibres from the ventral mesencephalon course together with noradrenergic fibres of the median forebrain bundle, so this strategy is not feasible at this level. However, the striatum itself receives a relatively sparse noradrenergic innervation, so that 6-OHDA injections placed directly into striatal terminal areas can yield relatively selective dopamine depletion (Debeir et al., 2005). A second strategy involves pretreatment with pharmacological inhibitors of catecholamine transport that block reuptake into some pathways but not others. Thus, administration of desipramine hydrochloride during stereotaxic surgery can be used to block uptake into noradrenaline (NA) neurons, thereby increasing selectivity of toxicity to dopamine pathways (Fink and Smith, 1980, Fulceri et al., 2006, Jeste and Smith, 1980). However this does not control for 5-HT uptake and physical damage caused by the cannula during the lesioning process but 5-HT neurons are less sensitive than catecholaminergic ones to 6-OHDA, and such cross-toxicity can be minimised by use of lower concentrations and slower delivery of the toxin (Fulceri et al., 2006). So relative selective can be achieved by judicious combination of toxin dose, site of delivery and pharmacological pretreatment, the parameters for which are best established empirically. However, the 6-OHDA model still differs in another way from dopamine loss in idiopathic disease, in that toxicity is essentially acute, and it does not allow for the progression of the disease with aging and typical regional spreading, as described by (Braak and Braak, 1990).

Behavioural tests are able to determine, with relative accuracy, the extent of dopaminergic neuron denervation in the unilateral 6-OHDA lesioned rat, though it is considered that the unlesioned side can overcompensate for unilateral motor deficits to some degree (Barneoud et al., 2000, Costall et al., 1976b, Costall et al., 1976c, Dowd et al., 2005b, Dunnett et al., 1981, Dunnett et al., 1988a, Kirik et al., 1998, Metz et al., 2005, Olds et al., 2006, Olsson et al., 1995, Perese et al., 1989, Schwarting and Huston, 1996, Woodlee et al., 2005), the bilateral model is less common, as loss of appetite and thirst is common (Pioli et al., 2008, Paille et al.,

2007, Sakai and Gash, 1994) and (reviewed in Zigmond and Stricker, 1989), which give rise to significant issues of maintaining good health and welfare of the experimental animals.

The standardisation of lesioning techniques and in depth behavioural analysis of the unilateral rat 6-OHDA model has led to its preference in the experimental PD field, and the size of the lesion is often assessed robustly with the use of amphetamine and apomorphine induced rotation (continued circling of mice through 360°). In unilateral models amphetamine causes dopamine release and subsequent stimulation of the dopamine receptors on the intact side, driving rotation in the ipsilateral (same side to the lesion) direction (Ungerstedt, 1971b) and apomorphine acts on the lesion-induced supersensitive receptors to induce rotation toward the contralateral (opposite to the lesion) direction (Ungerstedt, 1971a). Dopamine losses of 90% have been found to cause 5/7 turns per minute following an amphetamine (0.63-2.5mg/kg) or apomorphine (0.015-0.1mg/kg) challenge (Costall et al., 1976a, Costall et al., 1976b, Schmidt and Westermann, 1980). It was later found that dopamine losses in rats with partial lesions could be correlated to amphetamine, apomorphine and L-DOPA rotation (Hefti et al., 1980).

Simple motor behaviour in the unilateral model can also be assessed by a variety of hand tests that can indicate the extent of the lesion pre-mortem, useful where drug naive animals are needed. Commonly, motor deficits on the contralateral side are often compared to the ipsilateral side to the lesion, serving as an internal control. The cylinder test, first described by (Schallert et al., 2000) assesses the laterality of forelimb use in a novel environment, where MFB rat models typically express a 70% or higher usage of the ipsilateral limb. A similar bias is also seen in the corridor test, in which unilateral lesioned rats show lateralised differences, preferentially retrieving pellets located on the ipsilateral of the head, nose and snout, neglecting pellets positioned on the contralateral side (Dowd et al., 2005a, Dowd et al., 2005b). Sensorimotor dysfunction is also often tested using whisker stimulation leading to placing and grasping reactions (Woodlee et al., 2005). Deficits in the contralateral limb, with an overcompensation response in the ipsilateral paw, can be seen when using the skilled reaching test (staircase), when dopamine depletion is at 80% or more (Montoya et al., 1990, Montoya et al., 1991, Pagnussat Ade et al., 2009). The grip strength meter highlights clasp and forelimb movement deficits in rats with MFB lesions (Dunnett et al., 1998) and forelimb akinesia is also noted when conducting other stepping tests (Blume et al., 2009, Olsson et al., 1995) and gait analysis (Klein et al., 2009). The majority of these tests are essential to

determine a baseline on which to apply new therapies, yet have only been efficiently characterised in rats.

The effectiveness of some of the above mentioned tests has previously been reported in the 6-OHDA mouse (Iancu et al., 2005, Grealish et al., 2010b), however many have not been fully characterised for use this species. In mice a 31.5 fold increase in apomorphine rotation is seen following a dopamine depleting lesion and both amphetamine and apomorphine rotation is found to correlate with cell loss (Mandel and Randall, 1985). The skilled paw reaching ‘staircase’ test has also limited success when translated for use in the unilateral 6-OHDA mouse (Baird et al., 2001). The 70-75% usage of the ipsilateral limb in the cylinder and corridor test correlating to near complete destruction of dopaminergic neurons has also been shown in mice (Grealish et al., 2010b, Iancu et al., 2005), although strain and lesion type comparisons have not yet been established. General motor co-ordination and balance deficits in lesioned mice were also observed by means of the rotarod test (Iancu et al., 2005).

The optimisation of the hemi-parkinsonian mouse model is much needed as it will enable ‘proof of principle’ type experiments emphasising findings across species, and greatly facilitate testing of novel stem cell and genetic therapies. There are also a number of non-behavioural issues that need to be addressed for the optimisation of the 6-OHDA mouse. The success of the lesion may be dependent on the concentration and volume of 6-OHDA and the accuracy of the stereotaxic co-ordinates. This has varied extensively between previous mouse studies, the majority of which use striatal lesions owing to the ease of targeting the largest area in the nigro-striatal tract, see Table 1.4. Another important issue to resolve is improving survival post-surgery, since mortality rates over 80% have been reported previously (Lundblad et al., 2004b). The best target area along the nigrostriatal pathway must be balanced with the mortality caused by the lesion and the degree of interference with other systems such as forebrain 5-HT pathways which, like dopamine, have rich projections to the striatum.

<i>Conc</i> ¹	<i>Volume</i>	<i>Stereotaxic Co-ordinates (mm)</i> ²	<i>Strain</i>	<i>Sex</i>	<i>Reference</i>
16 µg/µl	4 µl	n/r	n/r	M	(Von Voigtlander and Moore, 1973)
4 µg/µl	4µl	AP= +5 (to occipital structure), ML= -2.2, DV= -3.5	Swiss	M	(Torello et al., 1983)
4 µg/µl	4µl	AP= +0.5, ML= -2.4, DV= -3.1	C57Bl/6	M/F	(Randall, 1984)
3.32 µg/l	4µl	AP= +4.8 (Lambda), ML= -1.7, DV= -3.0 and -2.7 (dura)	MNRI	M	(Brundin et al., 1986)
4 µg/µl	4µl	AP= +3 (to occipital structure), ML= -2.2, DV= -3.5	Swiss	M	(Thermos et al., 1987)
4 µg/µl	4µl	AP= +0.5, ML= -2.4, DV= -3.1	C57Bl/6	M	(Mandel and Randall, 1990)
2 µg/µl	2µl	AP= +0.4, ML= -1.8, DV= -3.5	C57Bl/6	M	(Bensadoun et al., 2000)
3 µg/µl	2x2 µl	(i) AP= +1.0, ML= -2.1, DV = -2.9 (ii) AP= +0.3, ML= -2.3, DV = -2.9	C57Bl/6	M	(Lundblad et al., 2004b)
3 µg/µl	2x 2µl	(i) AP= +1.0, ML= -2.1, DV = -2.9 (ii) AP= +0.3, ML= -2.3, DV = -2.9	C57Bl/6	M	(Lundblad et al., 2004b)
3 µg/µl	2x 2µl	(i) AP= +1.0, ML= -2.1, DV = -2.9 (ii) AP= +0.3, ML= -2.3, DV = -2.9	C57Bl/6	M	(Lundblad et al., 2005)
6 µg	n/r	AP = +0.8, ML= -1.0, DV= -2.5	A/J	M/F	(Liang et al., 2005)
3 µg/µl	3.9 µg or 5.4 µg	AP= -1.2, ML= ±1.1, DV= -5.0, with incisor bar set at ±0.0	CBA	F	(Iancu et al., 2005)
2.5 µg/µl	2x 2µl	AP= +0.5, ML= +2.4, DV -4.0 and -3.0 (dura)	C57Bl/6J / OlaHsd	M	(Pavon et al., 2006a)
3 µg/µl	2x 2µl	(i) AP= +1.0, ML= - 2.1, DV= -3.2 (ii) AP= +0.3, ML= - 2.3, DV= -3.2	C57Bl/7	M	(Santini et al., 2007)
2 µg/µl	2µl	AP= + 0.4, ML= - 1.8, DV= - 3.5	C57Bl/6	M	(Alvarez-Fischer et al., 2007)
4 µg/µl	2µl	AP= + 0.8, ML= -1.9, DV= - 2.6	C57Bl/6	M	(Richter et al., 2008)
2 µg/µl	1µl	AP= + 0.4, ML= - 1.8, DV= - 3.5	C57Bl/6 / SWISS / sv129	M	(Alvarez-Fischer et al., 2008)

Table 1.4. Parameters of mouse 6-OHDA lesions in published studies of the unilateral striatal lesion model. Concentration is based on free base 6-OHDA.HBr (1) and co-ordinates are calculated relative to Bregma, unless otherwise stated (2). Abbreviations: AP, anterior-posterior; ML, medial-lateral; DV, dorsal-ventral; M, male; F, female; n/r, Not reported. Published in Contemporary Models of Movement Disorders (Smith and Heuer, 2011).

1.6.4. Transgenic

PD is predominantly idiopathic. However, the use of genetic models highlights the mechanisms by which rare autosomal recessive and dominant mutations can cause the familial forms of the disease. The first gene mutation associated with PD was identified in a Greek family cohort (the 'Contorsi' kindred), within *SNCA*, the gene encoding for α -synuclein (Polymeropoulos et al., 1997). Since then, the aggregated protein has been found in various mutated forms in familial PD (Tong and Shen, 2009) and identified as a constituent protein in Lewy bodies (Spillantini et al., 1997). It is generally thought therefore that the protein plays a role in disease pathology, and hence a number of transgenic mice have been created with mutations in this gene to model PD. The first transgenic mouse made to mimic the synucleinopathy family of diseases was produced from the incision of human wild type α -synuclein under the PDGF β pan neural promoter (Masliah et al., 2000). Inclusion formation in these mice was seen in the cortex, hippocampus, olfactory bulb and occasionally in the SN. The stereotaxic injection of wild type or mutant α -synuclein into neurons, via a viral vector, leads to a progress loss of dopaminergic neurons in rodents and non-human primates (Eslamboli et al., 2007, Kirik et al., 2003). However, the development of these inclusions does not resemble the human form as the presence of α -synuclein fibrils is not seen, nor do they form the large spherical globular cytoplasmic structures, characteristic of Lewy bodies themselves.

LRRK2 is another gene in which mutations are associated with familial PD, and moderate overexpression of the human unmutated gene in mice causes an increase of striatal dopamine levels, inducing hyperactivity and enhanced performance in behavioural tests but, again, no overt Lewy body formation (Li et al., 2010). By knocking in human mutant LRRK2 into the same mice, the changes in motor function were ameliorated (Tong and Shen, 2009), yet deficits in dopamine handling detected including reduced striatal dopamine content, reduced vesicle release and a decrease in dopamine uptake. Other mice have been established to overexpress known heritable PD mutations in UCHL1 and PINK1 (Dawson et al., 2010, Setsuie et al., 2007, Zhou et al., 2007), to further models with changes in dopamine handling and inclusion bodies.

In all genetically modified mouse lines, cell death is typically less extensive than observed with 6-OHDA or MPTP neurotoxins and provide interesting models of early PD. However

they are not sufficient to bring about a robust motor deficit for the testing of novel treatments. The mechanistic similarity between genetic and idiopathic forms of the human disease is also currently unknown.

1.7. Dyskinesia Models

LID is a common motor side effect of current PD pharmacotherapy and causes debilitating AIMs. Effective animal models of LID therefore are essential to test new co-treatments that may reduce AIMs or to trial future interventions in a previously L-DOPA treated brain, mimicking that of the patient.

1.7.1. LID and GID in Primates

The first established animal model of LID was in the MPTP treated primate (Jolkkonen et al., 1995, Paxinos, 2001, Pearce et al., 1995). On first administration in akinetic monkeys, L-DOPA produced a marked anti-akinetic effect and greatly improved postural instability and gait (Jolkkonen et al., 1995). In these initial experiments oral L-DOPA was then given to common marmosets for three weeks and the recipients developed dystonic and choric AIMs seven days after the initiation of daily treatments, mimicking the rapid development of LIDs in advanced patients first given L-DOPA treatment, for example in the rare cases of MPTP toxicity in the case of the frozen addicts (Langston and Palfreman, 1995), or the introduction of L-DOPA soon after its discovery to postencephalitic patients (Sacks, 1973). Dyskinesias were found to be mimicked by dopamine receptor agonists after long-term treatment (Pearce et al., 1995) and related to doses of L-DOPA and peripheral COMT inhibitor entacapone given in combination (Paxinos, 2001). Furthermore, L-DOPA was found to restore levels of substance P depleted following MPTP, linking anti-parkinsonian effects of L-DOPA to physiological changes (Jolkkonen et al., 1995).

Models of LID are now predominantly rodent based as non-human primates are costly and stringently controlled by the Home Office in the UK. Moreover, GID has not been found in non-human primates and, notably, spontaneous AIMs have so far only been observed in humans. Thus GID is normally induced in grafted rodent, previously and chronically treated with L-DOPA, using amphetamine, at a dose where no AIMs or stereotypy is seen in either non-grafted 6-OHDA rats, nor in grafted rats not pretreated with L-DOPA.

1.7.1. LID in Rodents

A more recent model sprung from the recognition and acceptance that, following L-DOPA treatment, hemi-parkinsonian rats also exhibit AIMs which can be quantified (Cenci and Lundblad, 2007, Winkler et al., 2002b) and can be correlated physiological hallmarks within the striatum (Cenci et al., 1998, Andersson et al., 1999, Andersson et al., 2001, Andersson et al., 2003). In the rodent, dyskinesia can be induced by approximately 6mg/kg of L-DOPA, when less than 20% of dopamine remains in the lesioned striatum. Surprisingly, in all studies, a small proportion (typically 10-25%) of animals with equivalent dopamine depletion will remain non-dyskinetic (Lundblad et al., 2004b, Cenci et al., 1998). Where less dopamine denervation is observed, abnormal movements can only be initiated by a higher dose (Lundblad et al., 2004b, Winkler et al., 2002b). However the proportion of non-dyskinetic animals remains at a similar rate, and so is not primarily a dose related phenomenon. Specific AIM-physiological hallmark correlations and a definitive dose response curve of chronic L-DOPA treatment in mice, of different 6-OHDA lesion types, have not yet been defined to the same degree as the rat.

LID rating scales for 6-OHDA-lesioned rat and mice have been based on scoring individual components of the AIMs (including: body axis, forelimbs, hindlimbs and orolingual types) for their duration and severity (Cenci et al., 1998, Lundblad et al., 2004a, Winkler et al., 2002a). The scores from each component are then summed to give an overall severity rating. To examine AIMs, animals are placed singly in transparent rotometer bowls or cages following an injection with L-DOPA. Typically, behaviours are scored over one minute, every 20 or 30 mins for approximately 3 hours; as detailed further in Chapter 2. Animals within the same cohort will generally have varying levels of AIMs and those with scores that fall below a pre-determined threshold are considered 'non-dyskinetic' (Cenci and Lundblad, 2007). Assessment and induction of AIMs can be subject to interpretation by individuals and to the environmental conditions. It has also recently been found that the induction and severity of the abnormal movements can be modified by conditioned exposure to environmental cues and context, such that AIMs can even be triggered by paired association by saline alone (Lane et al., 2011). Consequently, the use of blind ratings in a standardised environment is important for consistent results.

The various behavioural components of dyskinesia are thought to arise through the stimulation of different anatomical parts of the denervated striatum. Whilst the administration of

amphetamine into the ventrolateral area specifically induces orofacial stereotypies (Kelley et al., 1988) forelimb, hindlimb and axial positional movements are more closely related to highly innervated dorsolateral areas (Brown and Sharp, 1995).

Although the 6-OHDA lesioned rodent has been invaluable to discovering mechanisms of L-DOPA action and to test new pharmacological co-treatment strategies, it does not completely model the full range of side effects observed following chronic treatment in man. There is disparity in the manifestation, pretreatment with agonists, presence of non-dyskinetics and time course of dyskinesia between humans and animal models. For example, it is usual for dyskinetic symptoms to manifest 5-10 years following L-DOPA therapy as the result of aberrant plasticity (Encarnacion and Hauser, 2008), while in the 6-OHDA lesioned rat AIMs are triggered several days after the initiation of L-DOPA, as lesions are near to complete. In the case for advanced degeneration in humans and subsequent L-DOPA treatment LID may too develop quickly (Langston and Palfreman, 1995, Sacks, 1973). Further, there may be species differences in the manifestation and severity of LID and, although similar, AIMs with different characteristics have been induced in the 6-OHDA lesioned mouse model previously (Lundblad et al., 2004b, Lundblad et al., 2005). A large scale comparison between all three lesion groups with correlations to histological measures has yet to be undertaken.

1.7.2. GID in Rodents

Embryonic VM grafts transplanted into the denervated striatum of rodents following unilateral 6-OHDA lesions standard models used to assess cell replacement in PD, and have been extensively optimised (Abrous et al., 1993, Arbuthnott et al., 1985, Bjorklund et al., 1981, Dunnett et al., 1983b, Dunnett et al., 1983a, Dunnett et al., 1988a, Dunnett et al., 1988b). Significant numbers of surviving primary dopaminergic cells in the lesioned striatum will cause a reduction of ipsilateral rotation to amphetamine, or an over compensation toward the contralateral direction (Bjorklund et al., 1980, Dunnett et al., 1988a). Psychostimulant-induced rotation has also been noted in mice (Thompson et al., 2009, Veng et al., 2002, Zhou et al., 1993, Shimizu et al., 1990, Brundin et al., 1989, Shimizu et al., 1988). Turning to amphetamine is usually a biphasic response with an initial high level of circling behaviour from the rapid release of dopamine from the graft, before a slower bell-shaped response (Fig 1.4), until a complete cessation of turning 6 hours post injection (Torres and Dunnett, 2007). A

proportion of the cohort will also develop AIMs in response to amphetamine, this group is now used to model GID (Carlsson et al., 2006b, Lane et al., 2006b).

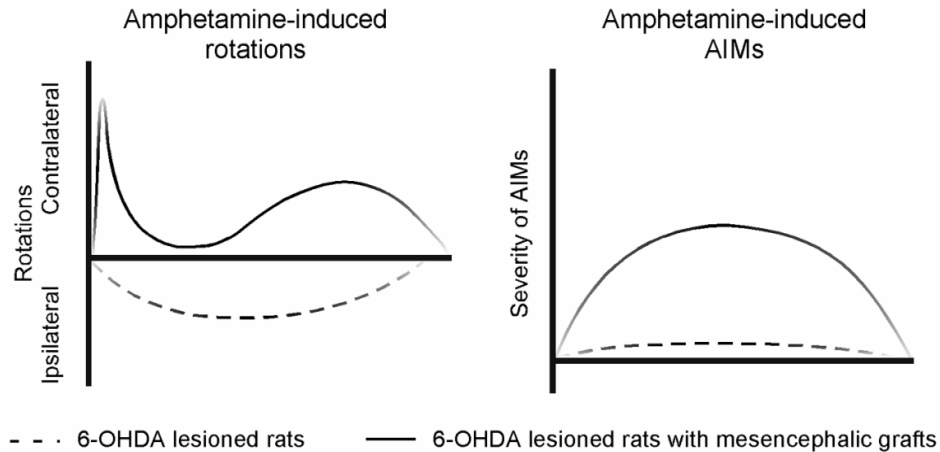


Fig. 1.4. Predicted time courses of amphetamine-induced rotation and AIMs in lesion only rats and those with additional dopaminergic transplants (Lane and Smith, 2010).

Spontaneous dyskinesia in transplanted 6-OHDA lesioned rats have been reported in two studies, although AIMs are transient in expression, sporadic and mild in severity (Vinueza et al., 2008, Lane et al., 2006b), therefore lacking the ability to be used as a GID model. Further, no spontaneous AIMs were seen without pharmacological stimulation when animals were subject to mild stress (Carlsson et al., 2006a). In the absence of a model in which GID is spontaneous, the reproducibility of amphetamine driven AIMs in the transplanted rat has enabled mechanistic insights into GID development, discussed in section 1.9.

The methodology of model production and the scoring of subsequent AIMs have now been standardised. Prior to transplantation, 6-OHDA lesioned rodents are primed with L-DOPA for 4 weeks to elicit LID as described by Winkler et al., (2002), thus causing long term changes in the denervated striatum; an important step in model development (Cenci and Konradi, 2010, Cenci et al., 2009, Picconi et al., 2003, Winkler et al., 2002b, Lane et al., 2006b). There is a greater tendency for amphetamine mediated AIMs in animals primed (by long-term L-DOPA treatment) for LID, although a proportion of the primed experimental cohort will still not develop dyskinesia; these animals are termed ‘non-dyskinetic’ (Lane et al., 2009a). AIMs in

grafted rodents vary in appearance yet on the whole look phenotypically similar to LID and are scored on the same rating scale as LID first devised by (Cenci and Lundblad, 2007, Winkler et al., 2002b). Typically LID is reduced by a graft (Garcia et al., 2011, Lee et al., 2000) and when L-DOPA is applied post-transplantation development of AIMs is restricted (Steece-Collier et al., 2009). It has also been reported that novel stereotypic behaviours can develop in L-DOPA treated animals following transplantation (Steece-Collier et al., 2003).

1.8. Mechanisms of LID

1.8.1. Circuitry and receptor Changes

A number of factors have been considered to effect the emergence and severity of LID in humans and animal models of PD; these predominantly include altered dopamine and glutamatergic inputs, dysregulation of dopamine release by the 5-HT system, vascular changes, neurogenesis and phenotypic shift of existing cells in the basal ganglia (Bishop et al., 2009, Darmopil et al., 2008, Dawson et al., 1991, Faucheux et al., 1999, Gil et al., 2010, Paille et al., 2004, Tande et al., 2006, Westin et al., 2006). Changes in direct and indirect pathway signalling are thought to be in part due to changes in G-protein coupled receptor (GPCR) levels that have been looked at in PD patients and hence extensively studied in the 6-OHDA lesioned rodent model.

Initially changes were identified at the receptor level, for example D₁ receptor levels were found to be elevated in the brains of PD patients regardless of L-DOPA treatment, whereas D₂ receptor increases were only seen in patients receiving no treatment (Seeman et al., 1987). These findings prompted much experimental work. 6-OHDA alone (in the absence of L-DOPA) caused a 37% and 35% increase in D₁ binding within the striatum and SN respectively, in comparison to the intact side and a 54% increase of D₂ binding in the striatum (Dawson et al., 1991). Changes of this nature were found within dorsomedial, dorsolateral, ventromedial and ventrolateral quadrants of the striatum (Gagnon et al., 1991). Similar lesion induced D₂ receptor changes have also been reported (Blunt et al., 1992, Savasta et al., 1992). In contrast, no increases in the expression of D₁ receptors were apparent in the lesioned brain compared to control animals (Savasta et al., 1992). Further analysis has shown that the density of D₁ receptors is reduced in the dorsolateral and ventrolateral medial striatum (Blunt et al., 1992). There have also been mixed reports on the change in receptor levels in response to L-DOPA treatment. It has been shown that no further changes in receptor levels were found with

L-DOPA treatment (Blunt et al., 1992). However, increases in D₁ and D₂ have been reported in another experiment for both chronic and acute treatment regimes (Rioux et al., 1993). Although receptor levels are disputed in the L-DOPA treated 6-OHDA lesioned brain, it is clear that receptors become supersensitive to the pulsatile delivery of dopamine agonists, and complex signalling cascade dysfunction arises (Section 1.8.2). Thus, an imbalance of the D₁ and D₂ mediated signalling of the direct and indirect pathway respectively is thought to be a major driver of dyskinesia.

Rodent studies have demonstrated that partial nigrostriatal dopamine depletion reduces the ability of corticostriatal neurons to undergo LTP, through changes in NMDA receptor subunit composition and acute L-DOPA treatment is able to rescue this dysregulation (Paille et al., 2010). Chronic administration nevertheless is sufficient to cause LID and this occurrence is associated with impaired synaptic depotentiation, a phenomenon which reduces the plasticity promoting mechanism LTP (Picconi et al., 2003, Picconi et al., 2008). Fast glutamate transmission in the striatum from cortical inputs is mediated by metabotropic glutamate receptors and antagonism of the mGlu5 receptor subtype reduces LID (Yamamoto and Soghomonian, 2009, Mela et al., 2007). There is also an apparent change in the ratio NR2A and NR2B NMDA subunit expression (by increase of the NR2B) on the post synaptic neurons of the striatum with L-DOPA treatment (Ouattara et al., 2009). Where this pattern of expression was disrupted, by altering membrane associated guanylate kinase protein levels, AIMs could be induced in non-dyskinetic rodents (Gardoni et al., 2006). In addition, AMPA receptors are thought to change in response to L-DOPA treatment (Calon et al., 2002, Ouattara et al., 2010), yet other studies have found no such change (Silverdale et al., 2002). The antagonism of AMPA receptors can also reduce the severity of AIMs in an L-DOPA treated models of PD (Konitsiotis et al., 2000).

It has been proposed that negative correlation exists between 5-HT and DA levels within the denervated striatum. Animals with LID have significantly higher 5-HT innervations in the ipsilateral striatum than non-dyskinetic groups (Gil et al., 2010). The sensitised contralateral rotational response to L-DOPA can be desensitised by intrastriatal infusion, only occurring where there was destruction of 5-HT projections within the striatum, indicating the importance of 5-HT in the rotational response to L-DOPA (Kaariainen et al., 2009). A substantial reduction of LID can also be caused by 5-HT_{1A} and 5-HT_{1B} agonist drugs (Munoz et al. 2008) and microinfusions of 8-OH-DPAT directly into the intact dorsal raphe can attenuate the

expression of LID (Bishop et al., 2009, Jaunaraajs et al., 2009, Tomiyama et al., 2005, Dupre et al., 2008, Munoz et al., 2008a, Eskow et al., 2009). In addition, dopamine depletion may also cause serotonergic sprouting (Zhou et al., 1991b). Although other neurotransmitter systems are unlikely to have a causal role in LID, they may have a secondary effect in controlling dyskinesia expression. Pharmacological evidence has shown that if L-DOPA is given in combination with μ and δ receptors/ α_2 -adrenergic receptor/ CB_1 receptor antagonist treatments then a reduction of abnormal movement occurs (Morgese et al., 2009, Dekundy et al., 2007, Lundblad et al., 2002), as discussed in section 1.3.2. This indirect modulation is likely as many of these receptors co-localise with dopamine, 5-HT and glutamatergic receptors on the same neuron and they therefore share common intracellular signalling pathways, partially negating the pathological molecular changes causing dyskinesia. It has also been found that receptors may not just be co-localised but form physical hetro-oligomer, influencing signalling further (Juhasz et al., 2008).

Post-mortem examination of PD patients that have previously received L-DOPA revealed notable micro-vascular remodelling, proposed to be caused by the synthesis of new endothelial cells, corresponding to the observed increase expression of endothelial growth factors (Faucheux et al., 1999, Yasuda et al., 2007). Newly formed neurons could be co-labelled with the proliferation marker BrdU, and markers of mature neurons, glia and endothelia could be found in striatum, GP, entopeduncular nucleus and SNr of L-DOPA treated rats (Westin et al., 2006). Proliferation to a lesser degree can also be found in the SNr of saline treated rats. The majority of newly formed cells reside within microvasculature and this is associated with an increase in vessel length. Further, dyskinetic rats have an increased albumin leakage, a sign of hyper-permeability, an integral component of angiogenesis, found within all areas of the basal ganglia (Westin et al., 2006). This suggests that long-term L-DOPA treatment causes vascular remodelling which is detrimental to beneficial effects of L-DOPA and newly proliferating endothelial cells are positively correlated with dyskinesia.

There is now growing interest in the emergence of TH positive cells first identified in the striatum of MPTP-treated primates (Jollivet et al., 2004). BrdU studies have shown that these are not formed by neurogenesis but rather represent cells already present in the striatum that have changed phenotype (Darmopil et al., 2008). Unilateral 6-OHDA lesioned mice also show this phenotypic shift of GABAergic striatal neurons towards a dopaminergic phenotype

(Francardo et al., 2011, Darmopil et al., 2008, Mazloom and Smith, 2006, Tande et al., 2006), but it remains unclear how this occurrence may relate to dopamine depletion in different areas of the nigrostriatal tract or the effect of L-DOPA treatment. These cells have a number of characteristics, namely, they are large, generally aspiny, stain positive for glutamic acid decarboxylase (GAD) and GABA without co-expression of calbindin, neuropeptide Y or parvalbimin, and they are thought to be GABAergic interneurons (Tande et al., 2006). TH positive cells can be colocalised with enkephalin and dynorphin and therefore there may be a subgroup of MSNs that have begun to express TH (Darmopil et al., 2008).

1.8.2. Regulators of G-protein Signalling (RGS) Dysfunction

G-protein coupled receptors (GPCRs) are localised to the plasma membrane of all neuronal cells and control synaptic and chemical detection, altering transduction with the basal ganglia (Schoneberg et al., 2007). GPCRs including dopamine receptors can be visualised by X-ray crystallography and have been found to have 6-7 trans-membrane domains that are structurally and functionally conserved between species (Palczewski et al., 2000). The α subunit of the G-protein initiates signal transduction from stimulation of the GPCR via its dissociation from β and γ subunits (Gether et al., 2002). Conformational changes of the α subunit from an active to an inactive form is rate limited by the hydrolysis of GTP to GDP (Milligan et al., 1990). There are two large families of GTP binding proteins; large G-proteins namely the Gi, Go and Gq subtypes and small G-proteins such as rap, ras, rho and rab. G-proteins have a variety of functions in the mammalian brain modulating all GPCRs and Ca^{2+} ion channels and consequently activating protein kinase C (PKC) or adenylyl cyclase- protein kinase A (PKA) pathways (Dolphin, 1990, Palczewski et al., 2000), ultimately leading to the activation of ERK and transcriptional dysregulation (Section 1.8.3).

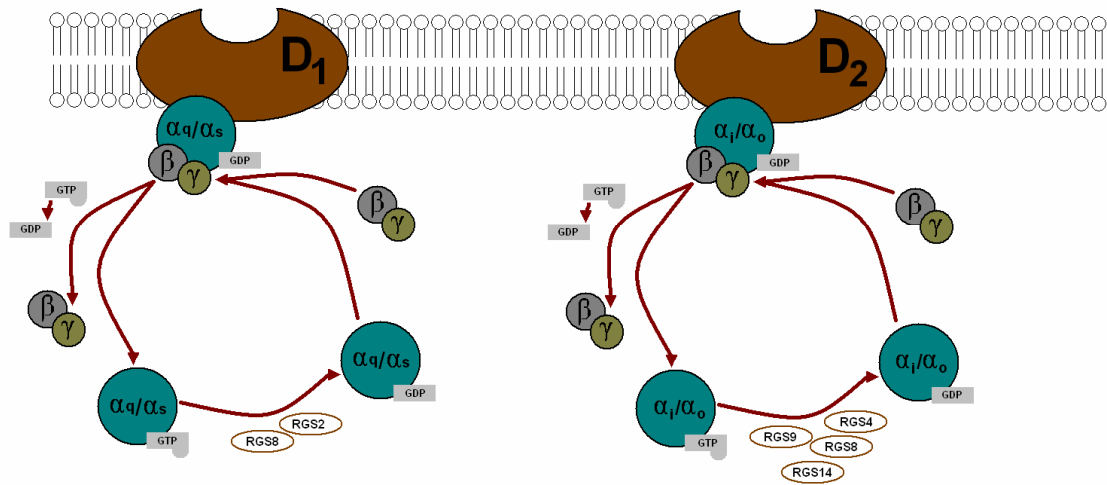


Fig. 1.5. The G-protein coupled receptor transduction following the stimulation of dopamine receptors of the D₁ and D₂ type. Dopamine receptors are differently modulated by regulators of G-proteins.

RGS proteins are powerful negative modulators of GPCRs that accelerate the inactivation of the alpha subunits. There are subtypes of RGS that are specific to GPCR, cell type and or location in the brain, shown in Fig 1.5, these regulators are transcribed from separate genes and are not produced by alternate splicing. RGS levels are differentially activated following dopamine denervation by 6-OHDA in the striatum, part of the post-synaptic compensatory mechanism for the reduction in dopamine levels. *RGS2*, *RGS5* and *RGS8* transcripts increase and *RGS9-2* and *RGS4* decrease following a lesion, in comparison to the intact control side (Geurts et al., 2003). In contrast, mRNA levels of *RGS3*, *RGS6*, *RGS7*, *RGS11* and *RGS12* were unchanged. Following prolonged reserpine treatment mRNA levels of *RGS2*, *RGS4*, *RGS5*, *RGS8*, *RGS9* and *RGS10* were found to be significantly decreased. Conversely, Taymans et al. (2002) did not detect such a change in *RGS2*.

There have been many studies which implicate the involvement of RGS dysregulation with movement abnormalities. *RGS4* is highly abundant and expressed ubiquitously throughout the cortex, striatum and hippocampus. A significant change in movement induced by opioids was produced in *RGS4* knockout mice (Grillet et al., 2005). *RGS4* polymorphisms are also implicated in the development of Schizophrenia and *RGS9-2* in dyskinesia associated with

anti-psychotic treatment (Guo et al., 2006, Seeman et al., 2007, Liou et al., 2009) and LID (Gold et al., 2007). *RGS9-2* is specific to the striatum and when this gene is knocked out *in vivo* motor coordination defects and changes in working/episodic memory manifest (Kovoor et al., 2005, Blundell et al., 2008). Viral-mediated overexpression of *RGS9* may cause D₁ and D₂ signalling to function in equilibrium; thereby reducing LID (Gold et al., 2007).

Selective dopamine antagonists and agonists such as L-DOPA cause an unusual pattern of RGS transcription which is currently disputed between groups. *RGS2* up regulation is seen 20 minutes after an L-DOPA injection of 50mg/kg in 6-OHDA lesioned rats, with no change observed in *RGS2*, *RGS4*, *RGS8* or *RGS9-2* transcripts (Geurts et al., 2002). In agreement, microarray work has highlighted that acute L-DOPA (single injection: 50mg/kg) is able to increase *RGS2* two hours post injection (El Atifi-Borel et al., 2009). Interestingly, no change in RGS was seen in when rats were treated daily for a number of weeks. Unfortunately the development of AIMs in response to L-DOPA was not characterised in this study and therefore correlations between LID and RGS could not be made. Conversely, another group has shown that a single injection of L-DOPA is able to increase *RGS2*, *RGS4* *RGS9-2* transcripts in the striatum of 6-OHDA lesioned rats (Ko et al., 2008, unpublished poster, PD U.K. York, Nov 3-4). It still remains to be found whether RGS transcript expression can be correlated to the severity of AIMs or whether the apparent upregulation differs depending on acute and chronic L-DOPA treatment, in either the 'off' or 'on' states with more standard doses of L-DOPA.

Therefore clarity into these basic transcription patterns is much needed in animal models to better understand LID. Clues into RGS mediated expression have been found, however, using selective antagonism of dopamine receptors, in intact rats (Taymans et al., 2004), see Table 1.5. Dopamine receptor agonists and antagonists dramatically changed the expression of *RGS2* and *RGS4* yet failed to alter the expression of *RGS8*, *RGS9* and *RGS10* (Taymans et al., 2003). mRNA expression was measured by autoradiographic *in situ*-hybridisation, and perhaps other methods such as qPCR might increase the sensitivity to be able to detect subtle differences. From investigations carried out by Taymans et al. (2004) it can be suggested that L-DOPA will also alter the expression of *RGS2* and *RGS4* to a greater extent than other RGS transcripts.

Dopamine receptor modulating drug	Action	RGS transcript	Expression	Response time (hours)
SKF82958	D1 agonist	2	↑↑ transient	0.5
SKF82958	D1 agonist	4	<i>nd</i> ¹	<i>nd</i> ¹
Haloperidol	D2 antagonist	2	↑↑ transient	0.5
Haloperidol	D2 antagonist	4	↓↓ transient	8
Quinpirole	D2 agonist	2	↓↓ transient	1-2
Quinpirole	D2 agonist	4	↑↑ transient	2-4
SCH23390	D1 antagonist	2	↓↓ transient	1-2
SCH23390	D1 antagonist	4	↑↑ transient	2-4

¹Not determined (*nd*)

Table 1.5. Specific dopamine receptor modulation by agonists and antagonists differently modulate the expression of RGS2 and RGS4. Table was created by observations discussed and quantified from (Taymans et al., 2004).

1.8.3. Intracellular Signalling

L-DOPA is associated with large scale neuroplastic changes, including changes in receptor levels, signalling throughout the basal ganglia and the proliferation of new cells. However, it is also essential to study the intracellular signalling changes to fully understand the origins of dyskinesia associated with L-DOPA.

The stimulation of the D₁ receptor induces a transcriptional upregulation of PDyn, while the stimulation of the D₂ receptor can block PPE transcription. In accordance, decreased expression of PDyn and an increase in PPE levels is a hallmark of PD (Sivam et al., 1986b, Sivam et al., 1986a, Young et al., 1986, Cenci et al., 1993), although L-DOPA cannot reverse the changes evoked in these biological markers. Instead L-DOPA induces a number of transcriptional changes via the mitogen-activated protein kinase (MAPK) signalling cascade (Pavon et al., 2006a, Santini et al., 2007, Wang et al., 1997). Stimulation of dopamine receptors causes the phosphorylation and subsequent activation of extracellular-signal-regulated kinases 1/2 (ERK), 20 minutes after L-DOPA injection, causing transcription by translocation of the protein into the nucleus (Wang et al., 1997, Impey et al., 1999, Pavon et al., 2006a). It should be noted however that the supersensitisation of dopamine receptors is a requirement of ERK dysregulation and is tightly controlled by a number of interacting proteins

downstream of the receptor itself. ERK activation causes short term transcriptional changes and long term changes in plasticity.

ERK activation causes the intra-nuclear phosphorylation of cAMP response element-binding (CREB) that acts on CRE and AP-1 promoter elements on a vast array of genes acting both immediately and over many weeks and months. High-throughput microarray screens suggest that these genes are involved in intracellular signalling, phosphorylation, secretion, translation, transcription, exocytosis and synaptic transmission (El Atifi-Borel et al., 2009). Chronic L-DOPA treatment is associated with a transcriptional and translational increase in PDyn within the striatum mediated by an upregulation of the FosB/ Δ FosB transcription factor (Cao et al., 2010, Lane et al., 2009b, Pavon et al., 2006b, Westin et al., 2001, Rodriguez et al., 2001, Doucet et al., 1996, Konradi et al., 2004). This expression of FosB/ Δ FosB is highly selective to areas without dopaminergic fibre innervation and is often most pronounced in the lateral striatum of 6-OHDA lesion models (Andersson et al., 1999, Andersson et al., 2003). FosB/ Δ FosB mediated transcription acts immediately and plays a causative role in dyskinesia, supported by the demonstration that viral mediated over expression of this gene induce AIMs in animal models (Cao et al., 2010, Andersson et al., 1999). Other immediate early genes (IEGs) are differently regulated by L-DOPA. JunD does not increase in response to chronic treatment (Valastro et al., 2007), *Zif*⁻²⁶⁸ expression increases only in striatonigral neurons and c-fos increases in the STN (Cao et al., 2010, Andersson et al., 1999, Valastro et al., 2007, Carta et al., 2008b).

In general ERK signalling is involved in several forms of synaptic plasticity (Thomas and Huganir, 2004). Many studies have so far focused on the role of ERK for memory consolidation in the hippocampus, although it is thought that ERK has a similar function within the basal ganglia. Plasticity in the form of LTP can be caused by the high frequency stimulation of post synaptic neurons by activation of glutamate receptors (Thomas and Huganir, 2004). Plasticity by ERK causes an increased activation and expression of AMPA receptors, leading to both structural and signalling changes (Patterson et al., 2010, Toyoda et al., 2009). It is also understood that ERK signalling can control long term depression (LTD), which is a neuro-plastic change caused by pre-synaptic low frequency stimulation acting on post synaptic NMDA and mGlu receptors (Thomas and Huganir, 2004). Evidence for the emergence of striatonigral plasticity has been found by the transcriptional induction of activity-regulated cytoskeleton-associated protein (ARC), an associated cytoskeleton protein

used for structural changes (Sgambato-Faure et al., 2005). Subsequently, gene screens have confirmed such changes and up-regulated genes involved in growth, synaptogenesis, neurogenesis and cell proliferation result from long term L-DOPA treatment (El Atifi-Borel et al., 2009, Konradi et al., 2004).

1.9. Mechanisms of GID

1.9.1. Causes of GID

GID does not have a single well-defined cause, and it is currently thought that this phenomenon may arise from an interaction of several factors. The first hypothesis put forward following the original report of GID by Freed et al (2001a) was that GID was caused by excessive dopamine from the transplant. Subsequently however, ¹⁸F-DOPA PET analysis on GID patients found that striatal dopamine was not excessive, but rather that dopamine was unevenly distributed with ‘hotspots’ in parts of the striatum, interspersed by widespread areas of denervation (Ma et al., 2002). Conversely, other clinical trial groups failed to find evidence of dopamine hotspots within the striatum of grafted patients (Hagell et al., 2002, Olanow et al., 2009a, Piccini et al., 2005). It has also been noticed that dyskinesia in some cases resembles ‘end-of-dose’ LID which occurs during sub-optimal levels of dopamine stimulation, indicating partial reinnervation of the striatum may be responsible for GID (Olanow et al., 2003). The experimental models of GID (described in section 1.7.2.) show there has been no correlation found between the number of transplanted cells or the size of the graft and the expression of amphetamine-induced AIMs (Lane et al., 2009b, Lane et al., 2006b). The location of the graft within the denervated striatum may also play a role in the development of amphetamine-induced AIMs; more caudally placed grafts show the greatest risk, yet have the most functional efficacy (Carlsson et al., 2006b). LID triggered in grafted rodent models is much reduced where a more even pattern of innervation is seen (Steece-Collier et al., 2003). Nevertheless, rare cases of spontaneous experimental GID have sporadically been reported, but only with highly focal grafts (Maries et al., 2006).

There have been a number of indicators to suggest that graft rejection may trigger AIMs (Soderstrom et al., 2008). The provision of immunosuppression was quite different in each of the 3 clinical trials reporting GID. In the Lund transplantation study, an immunosuppressive regime was applied for at least 2 years post surgery (Hagell et al., 1999), the withdrawal of

which coincided with the development of GID or worsening in some patients (Hagell et al., 2002). In the Tampa-Mt Sinai clinical trial there was also an association between peak development of GID at 6-12 months post-transplantation and the end of the 6 month immunosuppression period (Olanow et al., 2003, Olanow et al., 2009a). It is not clear whether this is coincidental, since in the grafted hemi-parkinsonian rat model the inflammation response caused by the introduction of interleukin-2 does not change the severity of AIMs (Lane et al., 2008). In agreement the incidence of GID was reported in the Denver-Colombia trial, where no immune suppression was used (Freed et al., 2001). Immunological aspects of transplantation therefore warrant further investigation.

The aberrant release of L-DOPA-derived dopamine from 5-HT terminals in the striatum is thought to be a major contributing factor to LID (Bishop et al., 2009, Dupre et al., 2008, Eskow et al., 2009, Gil et al., 2010). However, the contribution of this system to GID is poorly understood. The dissection of the VM from the developing embryo often contains a proportion of developing 5-HT neurons that are consequently transplanted, with the amount dependent on dissection technique. In the absence of dopaminergic neurons, transplants of 5-HT cells increase unregulated dopamine release, exacerbating LID experimentally (Carlsson et al., 2008). Furthermore, the proportion of dopamine to 5-HT neurons may be critical to achieve an optimal functional benefit of the graft and to reduce LID, but may not have a causal role in GID (Carlsson et al., 2008, Garcia et al., 2011). Generally, amphetamine-induced AIMs in rodent models may not be greatly influenced by the quantity of 5-HT neurons in the transplant or host 5-HT innervations (Carlsson et al., 2009, Carlsson et al., 2007, Garcia et al., 2011, Lane et al., 2009a). The contribution of 5-HT neurons may contribute to some cases to GID. In two select patients *in vivo* imaging techniques have shown excessive 5-HT innervation in the denervated striatum and when treated with 5-HT receptor agonists off medication dyskinesias were much reduced (Politis et al., 2010, Politis et al., 2011b).

Other factors including the stage of disease progression, neuronal loss and the severity of LID prior to transplantation may contribute to GID. In patients with preoperative dopamine loss restricted to the putamen there was a trend towards improved outcome, including lower 'off medication' abnormal movements (Piccini et al., 2005). This is backed by evidence that rodent models show a clear relationship between levels of LID pre-transplant and the development of

amphetamine-induced AIMs at the post-graft stage (Lane et al., 2006a). Specifically, L-DOPA priming causes an increase in GID severity in grafted rodents (Lane et al., 2009b).

As no single factor has been highlighted as the most likely cause of GID, it appears most likely that AIMs arise from several factors working synergistically. It is hoped that GID will be reduced in future clinical trials by the optimisation of the surgical procedure, precise dissection techniques and the appropriate appointment of PD patients.

1.9.2. Circuitry and receptor changes

Although there are multiple factors that may contribute to GID development, there is still a limited understanding of the precise system and intercellular mechanisms that underlie the expression of these abnormal movements. Also, there has not yet been any post mortem receptor analysis of the brains from GID sufferers. Indeed, the only experimental model available, by which the mechanisms of this side effect can be studied, is the amphetamine-induced, L-DOPA primed and grafted rodent. To date, studies have broadly shown that transplantation normalises both lesion and L-DOPA-induced D₁ and D₂ receptor expression within the reinnervated areas of the striatum (Blunt et al., 1992, Dawson et al., 1991, Gagnon et al., 1991, Lu et al., 1991, Rioux et al., 1993, Rioux et al., 1991, Savasta et al., 1992), although changes vary significantly between studies and there has not yet been a correlation of receptors and AIMs.

Electrophysiological changes leading to GID development have not yet been elucidated, yet evidence has been provided by transplanted patients that have subsequently undergone DBS. Two individuals from the Lund clinical trial received DBS treatment directed at either the GPi or STN, yet only GPi-DBS was successful at reducing off medication dyskinesia (Herzog et al., 2008), suggesting direct pathway involvement in GID. However, evidence from other trials suggests that the pathway is more complex. A small group of patients from the Denver-Colombia study received DBS directed at the GPi with apparent success (Freed, 2004, Ma et al., 2002), although only transient benefits were seen when the same area was targeted in the Tampa-Mt Sinai study (Cho et al., 2005). DBS to the STN was also found to be beneficial in a further 3 cases of GID from the latter study (Cho et al., 2005). From these case studies conclusions cannot be drawn as to the precise changes in basal ganglia function that contributes to GID. Again, both better models and a rational theoretical framework are required before appropriate treatment measures can be instigated with any confidence.

1.9.3. Transcriptional Changes

The post-receptor signalling changes in grafted rodents or humans that lead to GID remain poorly understood. A number of key studies show that IEG and regular striatal gene expression levels are altered by the dopamine released from newly transplanted cells, but these have not yet been related to AIMs. *c-fos* expression within an intact animal is increased by cocaine and amphetamine, and this phenomenon is blocked by a dopamine depleting lesion, but restored following grafting (Rodriguez et al., 1999). Furthermore, grafting alone can decrease basal FosB/ Δ FosB and PPE protein levels to pre-lesion levels (Maries et al., 2006, Vinuela et al., 2008, Carlsson et al., 2009). Transcript levels of *PPE*, *D₂* and the *GABA* synthesising enzyme glutamic acid decarboxylase 67 (*GAD 67*) were also normalised by a VM derived graft, although the lesion-induced down regulation of mRNAs coding for neuropeptide precursor preprotachykinin was unchanged (Winkler et al., 2003). In grafted rats the L-DOPA mediated increase in FosB/ Δ FosB is inhibited in the lateral striatal area, but the transplant does not negate the L-DOPA mediated increase in *c-fos* (Lane et al., 2009b). Overall however there was no association with abnormal movements and IEG expression in grafted rat model of GID and since FosB/ Δ FosB is known to play a causative role in LID, an alternate mechanism for GID development is therefore likely.

1.10. Aims of this Thesis

L-DOPA treatment and neural transplantation are viable methods for treating the motor symptoms of PD, although both the current pharmacological and potential transplantation approaches carry the risk of dyskinesia induction. These debilitating side effects are a significant problem in the current pharmacological treatment of PD, and this has jeopardised the futures of both primary embryonic and stem cell transplantation as therapeutic strategies. An understanding of the mechanisms of LID and GID are essential to either prevent or ameliorate these AIMS. The first process in gaining meaningful information is the optimisation and study in animal models of both conditions, starting with a well characterised model of PD.

This thesis has three main goals:

Firstly as the 6-OHDA lesioned mouse model of PD is poorly understood, inconsistently used, and weakly characterised in terms of motor deficits, LID expression and response to transplantation, I aimed to optimise all these aspects. Secondly, as the rat model of GID has previously been well established, this was utilised to explore the pharmacological responsiveness and potential underlying mechanisms of GID. Thirdly, further mechanistic insights into GID and LID were investigated by the measurements of RGS transcripts and proteins, with the aim of finding a new biological marker or ‘biomarker’ of dyskinesia.

Thus, the overall aims of the thesis were:

- 1) To characterise the 6-OHDA lesion mouse model of PD in terms of behavioural deficits and response to L-DOPA (Chapters 3 and 4).
- 2) To map the expression of RGS in response to L-DOPA challenge and the development of dyskinesia in mice (Chapter 5).
- 3) To establish the mechanisms of GID using pharmacological co-treatments in rats, with the aim of reducing it (Chapter 6).
- 4) To examine RGS and dopamine receptor expression in response to transplantation and GID in the rat (Chapter 7).
- 5) To characterise a mouse model of GID (Chapter 8).
- 6) To discuss the future of L-DOPA and transplantation treatment strategies (Chapter 9).

2. Methods

2.1 Animal Husbandry and Legislation

Adult male C57/Bl6 and CD1 mice and were housed 1-6 per cage and female *Sprague-Dawley* (SD) rats were house 1-4 per cage. Environmental conditions in holding rooms were monitored daily, in compliance with Home Office rules and regulations. Home cage dimensions are: L45cm, W28cm, D13cm (mouse) L54cm, W37cm, D21cm (rat). Standard living conditions were maintained at a 12 hour light /12 hour dark cycle, with hygienic animal bedding (Lignocel), nutritionally balanced maintenance diet of 14% protein (Harlan), water and environmental enrichment by cardboard tubing, present in the cage. All experiments were undertaken under a project 30/2498 and personal licence 30/8321 issued on behalf of the Secretary of State as part of the 1986 Animal Scientific Procedures Act (ASPA),.

2.2 Surgery Techniques

2.2.1 General Surgery considerations

Anaesthesia was induced with isoflurane carried by O₂ at a concentration of 5% (rat) and 4% (mouse) and placed in stereotaxic frame (KOPF). Anaesthetic maintenance was achieved with isoflurane at 2-3% (rat) and 3-0.5% (mouse) in constant NO₂ and O₂ at a ratio of 2:1. Co-ordinates were measured from bregma so that a hole could be drilled through the cranium using a stereotaxic drill (Foredom), at the desired location. A 30-gauge cannula was then positioned above the opening on an additional stereotaxic arm. 6-OHDA hydrobromide (Sigma) was calculated as the free base weight and dissolved in a solution of 0.2 mg/ml ascorbic acid in 0.9% sterile saline (Animal Care Limited). The neurotoxin was mechanically infused into the site at rate of 1µl/min using a 10µl Hamilton syringe driven by a compact infusion pump (975, Harvard), set at 1µl/min. The cannula was left in place for three minutes after which it was slowly removed and animals sutured with Vicryl (Ethicon). An aseptic technique was used throughout and animals were monitored continuously for appropriate respiration. Animals were left to recovery in a 30°C incubator until they were able to right themselves. Analgesic medication was given s.c at the time of surgery (Metacam) and post operative care carried out for 5 days. Mice received additional post-operative care for 2 weeks,

this included: mashed food, glucose saline (4 % glucose, 0.18 % saline, Animal Care Limited) s.c injections and health/ weight checks.

2.2.2 6-OHDA Lesions in Rats

A single 3 μ l injection of 6 μ g/ μ l (freebase concentration) of 6-OHDA hydrobromide (Sigma) was used to lesion all rats using the procedure detailed in Section 2.2.1. In rats stereotaxic co-ordinates were used to target the MFB relative to bregma and the dura surface (mm): AP= -3.9, ML= -0.9, DV= -6.9, nose-bar = -4.5; these were optimised for an increased lesion success rate by (Torres et al., 2011).

2.2.3 6-OHDA lesions in mice

The same equipment was used in mice and rats, with the exchange of ergonomically designed ear bars and mouth-piece for the mouse. Unilateral lesions were carried out by single or double injections of 6 μ g/ μ l (freebase concentration) of 6-OHDA hydrobromide (Sigma) into the right MFB (1 μ l) striatum (2x1.5 μ l) or SN (1.5 μ l) using the same delivery system as with the rat. The stereotaxic co-ordinates for mice were determined using the mouse brain atlas of (Paxinos, 2001) and expressed in mm relative to bregma. The efficiency of coordinates varies depending on strain, age, weight and sex as these factors denote brain size. MFB co-ordinates used for the C57/ Bl6 strain were optimised using the standard surgery procedure using cannulae loaded with trypan blue. 1 μ l of the dye was injected into the MFB, using a number of co-ordinates, to stain the end point of the cannula entry (Successful entry points are indicated in Fig. 2.1). Although all the co-ordinates chosen were able to hit the MFB, co-ordinate 3 was able to hit a more caudal location where the region was its largest point and was subsequently chosen for experiments in this thesis. The SN and striatal co-ordinates were already optimised by the Lund University group (Lundblad et al., 2004b) and used respectively for this strain (mm) **Str**: (i) AP = +1.0, L = -2.1, DV = -2.9; (ii) AP = +0.3, L = -2.3, DV = -2.9, **MFB**: Bregma AP = -1.2, L = -1.2, DV = -4.75 (co-ordinate 3) and **SNc**: AP= -3.0, ML= -1.2, DV=-4.5, with the nose bar set at 0 mm relative to the interaural line.

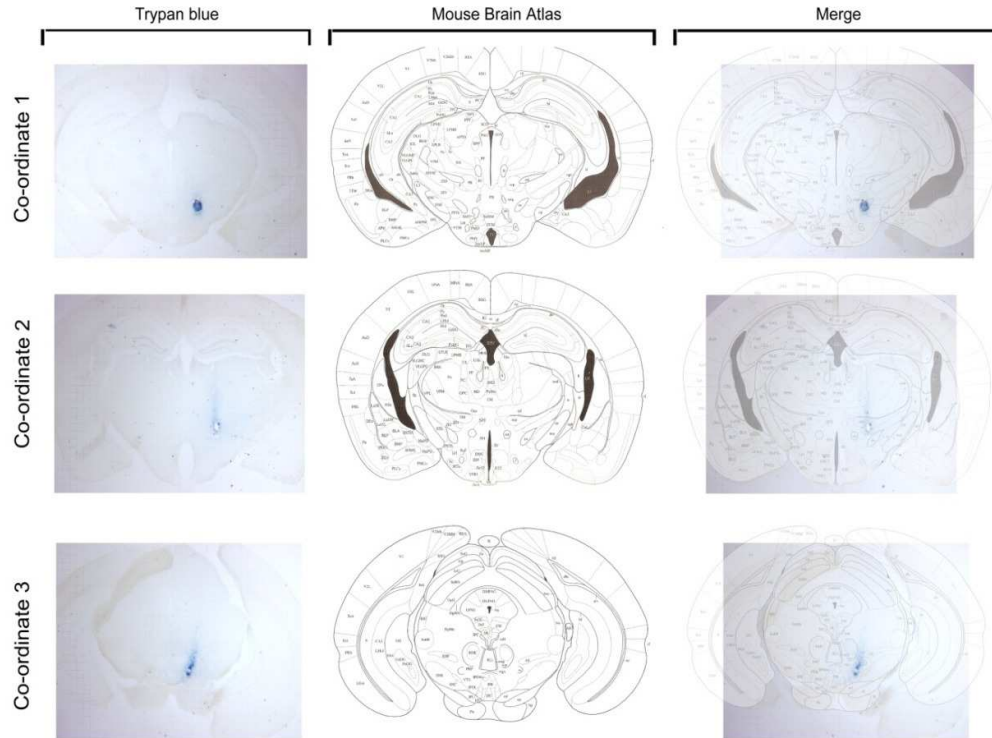


Figure 2.1. Optimisation of MFB lesion co-ordinates by the injection of 1 μ l of trypan blue. Co-ordinate 1: -AP: -0.7, ML: -1.2, DV: -4.75, co-ordinate 2: AP: -0.7, ML: -1, DV: -4.75 and co-ordinate 3: AP = -1.2, L = -1.2, DV = -4.75.

2.2.4 Grafting of primary dopamine tissue in Rats

Pregnant female SD rats were purchased from Charles River, where they were time mated to be carrying E13 aged embryos at the day of arrival, where E0 is considered the day after pairing overnight. Adult rats were killed at E14 by terminal anaesthesia using an intraperitoneal (i.p) injection of Euthatal (Park vet Group, U.K sodium pentobarbital, 50mg/ml, 1ml/kg) and cervical dislocation so that the intact uterus containing the embryos could be harvested. Embryos were then carefully removed from the uterine horns into Hanks Balanced Saline Solution (HBSS, Invitrogen, U.K). Ventral VM was dissected and prepared by methods described in Neural Transplantation (Dunnett, 1992), seen in Fig. 2.2.

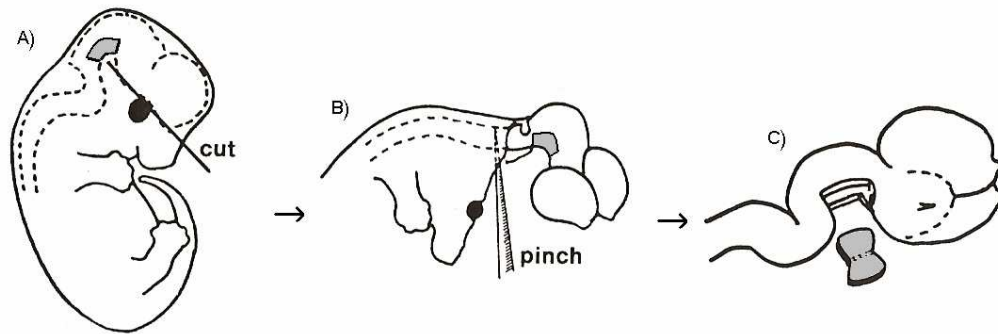


Fig. 2.2 Adapted from Dunnett and Björklund (1992). The spinal cord is severed and an initial cut is made to dissociate developing brain with the rest of the body. B) The skin is removed and the brain dissociated with the rest of the body. C) The VM is removed by three cuts; using iridectomy scissors. The first is a vertical cut toward the developing tectum, the second toward the dorsal thalamus and the third horizontally as an estimation of the VM area from the two vertical cuts. The meninges are then removed from dissociated VM and tissue pieces are pooled.

After three washes in HBSS, the VM tissue pieces were trypsinised (400 μ l (10 μ g/ml; Lorne Laboratories, U.K) and incubated for ten minutes at 37°C. Tissue pieces were allowed to settle and as much Trypsin as possible removed (200 μ l), without disturbing the tissue. Any remaining trypsin was inhibited (Sigma, U.K) for 20 minutes at 37°C. 200 μ l of the supernatant was then removed and 200 μ l of DNase was added, before further 5 minute incubation at 37°C. The supernatant was removed and fresh DNase was used to create a cell suspension that contained single cells and cellular aggregates, at a volume of 1VM/ 2 μ l. 2 μ l of sample was taken and mixed with 8 μ l of trypan blue solution (0.4% Sigma, U.K), for the viability and an estimation of total cells in suspension, by means of a haemocytometer.

2.2.5 Grafting of primary dopamine tissue in mice

Time mated pregnant female, C57/ B16 and CD1 mice were ordered in from Harlan to be E13 on the day of surgery. Lesioned mice were anaesthetised and restrained according standard surgery protocols (Section 2.2.2.). The dissection and cell suspension was carried out in accordance with the rat protocol (Dunnett, 1992), with the time in trypsin reduced to 5 minutes and the suspension adjusted to a concentration of 150,000 cells/ μ l. 1 μ l of the crude single cell suspension was injected into the lesioned striatum of mice with a Hamilton syringe at AP

+0.8mm: ML -1.7mm: DV-3.0mm relative to bregma, with the tooth bar set to 0mm relative to the interaural line. A further deposit of 1µl was placed at DV -2.8mm. Post-operative care and analgesia was provided for 5 days. Cell suspensions were kept at room temperature and mixed with a pipette before grafting into each animal.

2.3 Behavioural Techniques

2.3.1 General Behavioural Considerations

Behavioural tasks that could not be scored in real time were recorded with a 24x optical zoom digital video recorder (NVGSIS, Panasonic) and digital video-cassettes (TDK DV digital standard – 60minutes). Video recording was required where stated in this chapter and footage was replayed in slow-play mode, to ensure adequate frame-by frame *post hoc* analysis (Gaspar et al.). The testing environment was kept constant with respect to temperature, humidity, background noise level and smell. When possible, bias was avoided and all behavioural testing was conducted in a manner in which the investigator was blind to the treatment group. Specifically, animals in different treatment groups were mixed in cages and the investigator has no knowledge of which animals belong to which groups before the tests were complete. In the case of the pharmacological testing of drugs, an investigator blind Latin square paradigm was adopted remove the bias that previous high or low dosing may cause.

Precision sugar pellets of 20mg (Sandown Scientific) were used as a reward to motivate animals to perform the given task. Mice were required to be food restricted to 85% of their free feeding weight prior to the corridor and staircase tests. A sample of the sugar pellets was provided in the home cage to prevent neophobia during the test. Animals were also housed in small groups for the duration of feeding to prevent bullying that may result in unequal food consumption.

2.3.2 Drug Induced Rotation in the Rat

0.05mg/kg Apomorphine hydrochloride (Sigma) and 0.25-2.5mg/kg Methamphetamine (Sigma), given via the sub-cutaneous (s.c) and i.p routes respectively, were used to measure net rotational asymmetry in grafted rats. Doses were made based on free base weight and made in 0.9% saline (Animal care Limited, York). Rats were placed in computerised clear plastic rotometers (med Associates); dimensions: D: 35cm R:17.5cm. Software (Rotorat, Med

Associates) was adjusted to record rotations for 6 hours; parameters: full counts 360°, partial counts 90°, retrace 45° and time 5 min time bins. A minimum 3 day interval was introduced between amphetamine challenges for all experiments.

2.3.3 Spontaneous and Drug Induced Rotation in the Mouse

Spontaneous (non-pharmacologically induced) rotation in a novel environment in mice was previously reported by observations in an open field environment (Cenci and Lundblad, 2007), where dopamine released by exploring new surroundings causes turning toward the ipsilateral direction. Each mouse was placed in standard lab beakers (H:14cm, D:11.5cm) and allowed to explore the novel environment for 10 minutes. The video recorder was set up above the beakers to record the number of full rotations in each direction. These recordings were then analyzed *post hoc* and full rotations counted using fast-forward video playback reporting net rotations over the period (# clockwise - # anticlockwise).

Hemi-parkinsonian mice were also injected with 0.05mg/kg apomorphine (s.c.) or 2.5mg/kg methamphetamine (i.p.) dissolved into 0.9% saline (Animal care Limited, York) and placed back into the beaker to initiate a robust turning response in either the contralateral or ipsilateral direction respectively (See Figure 2.3). Both drugs were injected at a volume of 2ml/kg. Apomorphine is dissolved with the addition of 0.2% ascorbate and kept on ice and before use. The video recorder was set up above the beakers to record peak rotation; over 20 minutes, immediately following apomorphine injection or 20 minutes after methamphetamine injection. Drug induced rotation was only carried out after spontaneous rotation and a duration of 2 weeks separated amphetamine and apomorphine injections.

2.3.4 Automated Locomotor Activity

Animal activity was assessed using automated Med Associate hardware and MED-PC (IV) software over a 2 hour period. Fifteen animals were housed in individual plastic cages with three infrared beams crossing the base of each box; dimensions: L42cm; W26cm; D19cm. Animals were allowed to acclimatise to the cages 10 minutes before the start of the experiment. Beam breaks recorded from each crossing were totalled for each of the animals, to be used as the outcome measure.

2.3.5 Cylinder

As described previously in the 6-OHDA lesioned rat (Schallert et al., 2000), forelimb asymmetry was assessed by noting the paw used for each of the first 20 weight bearing rears made on the side of a glass cylinder measuring (H:14cm, D:11.5cm) in diameter (See Figure 2.3). In mice 2 mirrors were placed directly behind the cylinder so that a 360° view was seen by the observer. The session was videotaped and scored by detailed freeze frame analysis at a later date by an observer blind to the lesion status of the animals. Animals that failed to reach 20 touches were removed from the cylinder after ten minutes. Simultaneous ipsilateral and contralateral forelimb touches were excluded from the count. Since a novel spherical environment was needed for both spontaneous rotation and cylinder tests, these were carried out simultaneously.

2.3.6 Elevated Beam Test

In the rat, beam walking has been used to successfully show unilateral deficits following a 6-OHDA lesion (See Figure 2.3). The elevated beam test for mice was adapted from the rat based test (Allbutt and Henderson, 2007) and analyses the motor co-ordination and dexterity of right and left hindlimbs and forelimbs, where foot slips are recorded on ipsilateral and contralateral sides with respect to the lesion. Mice were made to transverse along an inclined ledge of decreasing width (80cm), before they were allowed to enter an enclosed (escape box) platform at the top. A foot slip was defined as paw misplacement where all digits entirely miss or slip off the narrow ledge of the beam, causing a noticeable imbalance in the body posture of the mouse.

On the first training day the elevated beam was placed on a bench top, such that the investigator could walk around the apparatus and see both sides. Mice were then placed facing outward, on the end of the elevated beam so they have to balance and turn inward. Mice were also placed in the enclosed space at the top of the beam and allowed to explore it for 5 minutes. On training day 2 each mouse was required to balance on the inner ledge to traverse the beam to the half way point three times, and on day 3 mice walked the whole beam to reach the platform once. On the test day, a video recorder was set up on one side of the beam so foot slips on this side could be scored *post hoc*. The investigator was positioned on the opposite side of the elevated beam, to count foot slips on that side (3 runs per mouse) in real time and

to record the time to transverse the beam.. For analysis, the two quickest times and corresponding foot slips averaged (outcome measure: foot slips count = # ipsilateral - # contralateral).

2.3.7. Corridor Test

The corridor test assesses lateralised sensory-motor integration, proprioception and neglect. A scaled down version of the rat apparatus was built, dimensions 2x: 60 cm x 4 cm x 15 cm. 10 pairs of adjacent 1cm pots containing 6 (20mg) sugar pellets (Sandown Scientific) were equally spaced at 5-cm intervals along the length of the corridor. Mice were habituated to the apparatus, on two days before testing; by the placement of sugar pellets randomly along the corridor floor and mice were free to explore for 20 min. Mice were food-restricted throughout (Section 2.3.1). The number of successful retrievals out of a total of 20 were recorded (= # ipsilateral - # contralateral), as defined by (Dowd et al., 2005a, Grealish et al., 2010b). The mouse was removed prior to twenty retrievals if 5 minutes had elapsed.

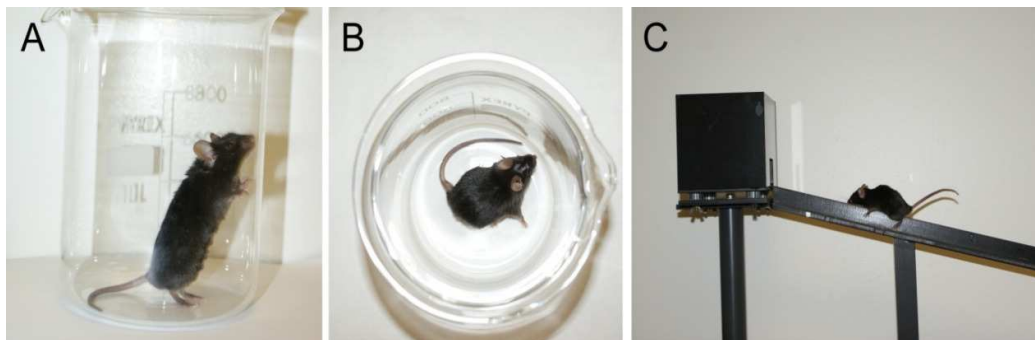


Figure 2.3. Photography of behavioural hand tests adapted from (Smith and Heuer, 2011) of the Cylinder (A), Apomorphine Rotation (B) and balance beam (C).

2.3.8. Staircase test

The staircase test (Campden Instruments, Loughborough, UK) for mice is an objective test of skilled forelimb use, described previously (Baird et al., 2001) and illustrated in (Smith and Heuer, 2011). In brief, the apparatus consists of start box with an adjoined testing section, fitted with a central plinth, onto which the mouse can climb so that there may be a narrow gap on either side. In these spaces are situated two staircases with eight steps of equal height, to

which two precision sugar pellets (20mg, Sandown Scientific) were placed in shallow wells. The apparatus is configured such that the mouse can only retrieve pellets from each staircase with the corresponding forepaw on that side. Therefore the total number of pellets removed provides a measure of reaching success and skilled forelimb use, for both ipsilateral and contralateral sides to the lesion.

The success of this test depends on food restriction to 85% of their free feeding body weight (mentioned above) and pre-training prior to the lesion. On the first day of training, mice were placed in the staircase apparatus for 20 min to explore and sugar pellets scattered on the plinth of the platform, and in the wells at each step of the staircases. All mice were then tested for 30 min daily until they reached a stable level of performance. The last three days of training were then averaged for use as a baseline (pre-lesion) performance measure. Post lesion data is similarly averaged over a 3-day block. For statistical analysis, reaching deficits are expressed in terms of the number pellets retrieved contralateral to lesion as a percentage of the number retrieved on the ipsilateral side.

2.3.9. Rotarod

The rotarod apparatus (Ugo Basile, Varese, Italy) was used to provide an overall assessment of motor coordination and balance (Alvarez-Fischer et al., 2008, Monville et al., 2006a, Ogura et al., 2005, Schallert et al., 2000). Mice received two training days of 3 trials at 12 rpm and 22 rpm, respectively. Trials lasted 300 s in total and were separated by at least one hour. On training days, mice that fell off the rotating beam were placed back on until the time had elapsed. On the test day, an accelerating protocol was used for each of the three trials (speed: 4 to 44 rpm over 300 s). The latency to fall was recorded as the outcome measure by the average of the two best trials (highest latencies).

2.3.10. Stepping test

The stepping test previously used for MPTP treated mice (Blume et al., 2009), was conducted using a modified protocol. The test was initiated by the placement of the mouse on a flat table where it was left to explore for 3 s. Subsequently the hind legs were elevated from the surface by the investigator with a grip at the base of its tail and gently pulling it backwards over a distance of 50 cm for 5 s. The test was recorded using a video camera and scored using frame-by-frame playback to count the number of adjusting steps the mouse made in total. All mice

were tested three times and the average number of adjusting steps for each side was expressed as bias score (# ipsilateral - # contralateral).

2.3.11. Gait analysis

Gait was analysed using the footprint method, used previously in rodents, where the fore paws and hind-paws were differently coloured using red and blue non-toxic water-based paint (de Medinaceli et al., 1982, Richter et al., 2008). Testing was conducted in the corridor apparatus, to encourage the mice to move in a straight and continuous line, with white absorbent paper secured to the floor that was cut to fit the entire length. The distance covered by three consecutive strides was recorded for each mouse.

2.3.12. Inverted Grid test

The inverted grid test is a measure of the grip strength of the forelimbs and hindlimbs of the mouse. To start the trial animals were placed onto the centre of a metal grid (home cage lid) with a rim of 4cm on which they were prohibited from climbing, allowing access to a rectangle of approximately 20 x 21 cm, as detailed in previous studies (Brooks and Dunnett, 2009, Brooks et al., 2004a, Dunnett et al., 1998). The grid was then slowly inverted and in a position 30 cm above the work bench. To dampen any falls, towels were placed directly below. The time the mouse spent grasping the grid without falling off was recorded, with a maximum cut off point of 300 s. Each mouse was tested three times with one hour gap between testing sessions. The average of the two best times for each mouse were used as the outcome measure.

2.4 Dyskinesia Assessment

L-DOPA methyl ester HCl and the peripheral DOPA decarboxylase inhibitor, benserazide HCl (Sigma) were dissolved in 0.9% saline immediately before use. The drugs were administered at the volume of 10ml/kg (rats) 2ml/kg (mice) in a single daily i.p. injection. AIMs were scored simultaneously to rotation in rats and simultaneously to locomotor activity in mice. All animals were scored once every 20 minutes for 3 hours. AIMs in grafted rats were scored with 2.5mg/kg of amphetamine for the same duration.

The AIMs scoring criteria is based on the specific rating scales (Cenci and Lundblad, 2007, Winkler et al., 2002b) as follows: Duration score (time out of one minute); 0= absent, 1=

present less than half the time, 2= present for over half the time, 3= present for the whole time but interruptible by an external stimulus (i.e. tapping sound), 4= present throughout but uninterruptible by external stimuli. Amplitude score (severity in one minute); orolingual; 1= repetitive chewing movements, 2= with tongue protrusions, axial; 1= consistent deviation of the head and neck to $\sim 30^\circ$, 2= deviation of the neck and head to between 30° and 60° , 3= deviation of head, neck and upper trunk of 60° to 90° , 4= consistent deviation to 90° with loss of balance; limb 1= small oscillatory movements of paw and distal forelimb, 2= low amplitude circular movements of the forelimb, 3= extension of the forelimb including displacement of the shoulder, 4= maximal amplitude movements of shoulder and limb. Duration and amplitude scores are the sum of all forelimb, hindlimb, orolingual and axial AIMs at all time points in the respective category. These are then in turn multiplied together to give a total integrated AIM score. Mice were classified as dyskinetic if they consistently displayed all categories of AIMs, between severity scores 2-4, when challenged with 2.5mg/kg of methamphetamine (Sigma). Animals were defined as non-dyskinetic exhibited either no or occasional AIMs of minimal severity, and scored no more than 2 at any given time, for any category for the duration of the testing session.

2.5 Molecular and Histological Techniques

2.5.1 General Technical Considerations

Techniques detailed below have been optimised within our group and variations for species are indicated. For the chemical and equipment suppliers see **Appendix (II)** and for the chemical composition of the solutions see **Appendix (III)**.

2.5.2 Perfusion

Animals are terminally anaesthetised with sodium pentobarbital (200mg/ml) (Euthetal, Merial) until total loss of reflex. The heart was exposed through cuts from below the sternum up to dorsal parts of the rib cage. Phosphate buffered saline (PBS) was trans-cardinally perfused into the left ventricle for 2mins and the right aorta was severed immediately after the start. Perfusion was then switched to 1.5% paraformaldehyde (PFA, Cal Biochem) in 0.1M PBS and allowed to perfuse for 3-6 minutes. Flow rates for pre-wash and fixative were 20ml/min (mouse) and 60ml/min (rat). Extra precautions for rats were undertaken for a fast efficient

perfusion; these include clamping the descending aorta and initiating perfusion in the ascending aorta. The whole brain was dissected and then post fixed in 4% PFA (Cal Biochem) in 0.1M PBS for 3 hours. The brains were then transferred to 25% sucrose (Fisher Scientific) in PBS until they were no longer afloat and the tissue was then stored at +4°C until further processing.

2.5.3 Snap freezing

Animals were killed by cervical dislocation and the whole brain dissected from the skull. The brain was placed in iso-pentane (methyl –2-butane 2 methylbutane isopentane, Fisher Scientific) on dry ice for 30 seconds and tissue was then stored at -80°C.

2.5.4 Immunohistochemistry

Perfused tissue (see tissue preparation) was cut at 40µm on a sliding sledge freezing microtome and collected into 96 well plates (Sero–Wel) flooded in TRIS buffered saline (TBS) with sodium azide (0.02%) at pH 7.4 to be stored at 4°C until required. A 1 in 6 series of sections was selected from the plates, put into a single pot and washed with TBS. Endogenous peroxidase activity was quenched by 10% H₂O₂ (VWR) in methanol (Fisher Scientific) before further washes in TBS. Non specific binding sites were blocked by 3% horse serum in TBS for 1 h. Tissue sections were then incubated in primary antibody for 16 h at room temperature with 3% serum at concentrations of 1:1000, TH (raised in rabbit, Chemicon), 1:15,000, 5-HT (raised in rabbit, Immunostar Inc) and 1:500 FosB (raised in rabbit, Santa Cruz) before a wash in PBS. Sections were incubated in biotinylated secondary antibody (anti-rabbit antibody raised in horse for TH, 1:200 for all stains). Sections were washed again in TBS and left in a Biotin-Streptavidin mixture, from a DAKO ABC kit (5µl A and 5µl B), for biotinylation. Prior to staining tissue was washed in TRIS non-saline (TNS) solution for equilibration. We visualised the tissue-bound antibody using a standard peroxidase-based method using the chromogen, 3-3'-diaminobenzadine (DAB kit, Vector Laboratories) in a 0.5mg/ml reaction (1:5 concentration) in TNS initiated by a 0.25% addition of hydrogen peroxide (H₂O₂). The reaction was stopped by submersion in TBS and sections were mounting on slides (Thermo scientific) coated in gelatine. Slides were air dried before dehydration in alcohol steps from 75-100% (Fisher Scientific) and xylene (VWR). Coverslips were then added with distyrene plasticizer and xylene (DPX). Routinely, some of the sections were processed excluding the primary antibody serving as a control for the stain.

Peroxidase based immunohistochemistry (ICH) was also carried out on fresh snap-frozen tissue. Sections were cut to a 30µm thickness on the cryostat and mounted directly onto super frost slides to be stored -80⁰C. The immunohistochemistry protocol remained the same but required an initial fixation step in 4% PFA before being left to air-dry overnight. A 20 min permeabilisation step in acetone and full evaporation of the solvent was also required before starting ICH.

Fluorescence ICH was undertaken in the same way as the peroxidase-based staining procedure, with the absence of the quench and DAB colour reaction steps. A 1 in 6 series of tissue sections were incubated in primary antibodies for 16 h at room temperature with 3% serum at concentrations of 1:1000, TH (raised in mouse, Chemicon) and 1:2000, GABA (raised in rabbit, Abcam), before a wash in TBS. Hoechst nuclear stain 1:10,000 was then added to the free floating sections and left for 10 minutes, before another wash in TBS. Sections were incubated in fluorescent secondary antibodies added together: anti-rabbit antibody (Green, Molecular probes); and anti-mouse antibody (red, Molecular probes), both at 1:200.

2.5.5 In-situ hybridisation - Probe synthesis

Oligonucleotides were designed using genetic sequences obtained from Ensemble online genomic database (ensemble.org) specific for that gene and species (See Appendix I). Forward and reverse primers were optimised for the following parameters: Primer length 20b +/- 2; primer Tm 55°C +/- 5; primer GC% 50 +/- 5; product length 300-800b. The specificity of the design was verified using an online Basic Local Alignment Search Tool (BLAST) against online nucleotide collections from the National Centre for Biotechnology Information (NCBI) (ncbi.nlm.nih.gov). Primers were manufactured by MWG Operon.

cDNA was made from fresh, adult murine tissue (See, 2.3.1- cDNA manufacture). This was then used in a polymerase chain reaction (PCR) reaction with the manufactured primers to create copies of the genetic sequence. The oligonucleotides were then chemically incorporated into a PCR II TOPO cloning vector (Fig. 2.4.) using a salt solution provided with the kit (Invitrogen).

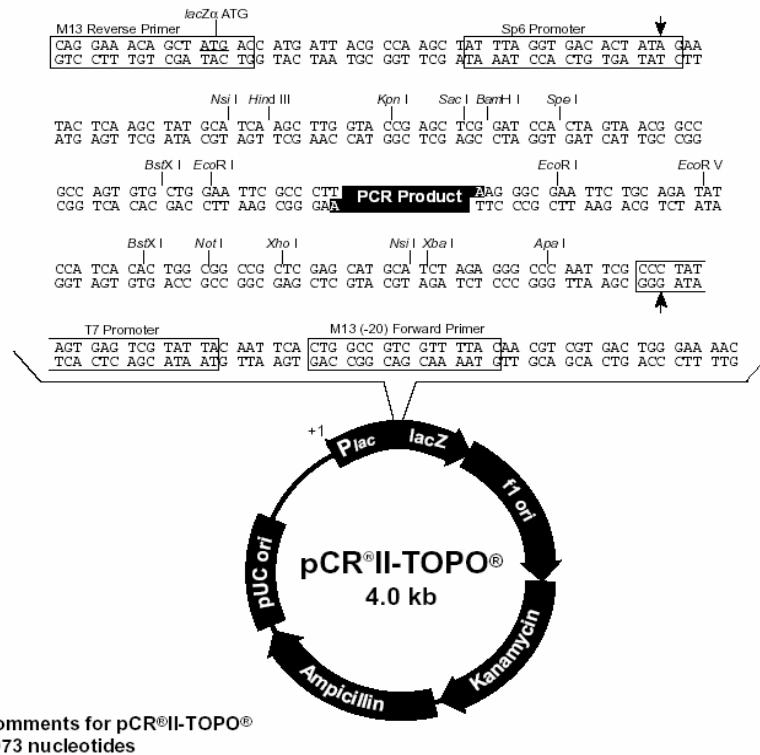


Figure 2.4. A base and enzyme map of the PCR II TOPO cloning vector. PCR insert sites and T7 and Sp6 promoter sites are indicated.

The PCR II TOPO cloning vector (Invitrogen) and PCR product was then transformed by heat shock at 42°C into Escherichia-coli (E-coli), one shot TOPO10 chemically competent cells, (Invitrogen) and plated on agar (Difco) - plates. Ampicillin (150mg/ml) was added to the agar before solidifying at a 1:1000 concentration. Several colonies were selected on the basis of antibiotic resistance and were grown through stages of S.O.B and LB media, with Ampicillin at the same concentration and were left at 37°C overnight. DNA was extracted from bacteria using the QIAprep high speed plasma min kit (QIGEN). Vectors were cut enzymatically using Apa I and Hind III (New England Biolabs) and run on a 1% agarose gel to screen for vectors that contain inserts, according to size in comparison to the PCR II TOPO cloning vector (Invitrogen) without an insert. Validation of vectors with correct PCR inserts, based on the nucleotide chain, was by sequencing from the T7 promoter region (DNA Sequencing Core, Molecular Biology Unit at Cardiff University, UK).

DNA vectors that contain inserts were cut enzymatically with either Kpn I or Xho I enzymes (New England Bio-Labs) in corresponding buffers over 2 hours at 37⁰C. Vectors were then checked for linearisation by separation with a circular plasmid on a 0.5% agarose gel. RNA was transcribed from the cut template from either Sp6 or T7 promoter regions using Sp6 or T7 polymerases (Boehringer) in the following reaction mixture: DIGNTPs (Boehringer), RNase inhibitor (Boehringer), 10x transcription buffer (Boehringer) and RNA free water (Ambion), for 2hours at 37⁰C. Following this DNA was digested with DNase I (Boehringer). The precipitation of RNA was then achieved by the addition of sodium carbonate at 60⁰C and then ammonium acetate on ice. Precipitates were collected by centrifugation at 6000rpm in a micro-centrifuge (5415R Eppendorf). RNA is finally washed in 100% ethanol and resuspended in a TE and formamide solution (1:1).

The efficiency of the DIG RNA oligonucleotide probe to detect complementary RNA was checked using 5 different probe concentrations, made by serial dilution of the concentrated stock into RNase free water (Ambion). These were then hybridised onto a nylon membrane blotted with RNA using a U.V. transillumination light box (UVP). The intensity of the stain was thus decided prior to starting *In-situ* hybridisation.

2.5.6 In situ hybridisation - Optimising

Whole brains were embedded in Cryo embedding compound (Bright) and 30µm thick serial sections were taken from these using a cryostat (Bright, microtome 5030) and directly mounted onto superfrost slides (Thermo Scientific). Temperature was maintained at the following: cutting chamber -35⁰C, mounting stage 30⁰C. The tissue was then permeabilised by digestion with protein kinase (PK, Roche) and fixed with 4% PFA (Cal Biochem). Time taken for these steps was adjusted to gain maximum clarity for visualisation at the end stage. Sp6 and T7 polymerised strands of RNA then acted as sense and anti-sense controls; these can differ with each manufactured probe, as the orientation of the insert in the DNA construct is unknown until optimisation.

2.5.7 In-situ hybridisation - Procedure

The fixed tissue sections were washed in PBS before carboxylation in 0.1% diethylpyrocarbonate (DEPC). Slides are washed again in PBS and 2x Sodium chloride-

sodium citrate (SSC) buffer. Sides were placed in staining tray flooded with formamide and 5xSSC solution (1:1) and 0.5mls of pre-hybridisation buffer were added to each slide for 3hours at 56°C. The probe was placed in hybridisation buffer and heated to 95°C for linearisation, before being added to the sections. The sections were covered with Nesco film and the tray left at 56°C overnight.

Excess probe was washed off the sections through a series of washes: 5xSSC, 2xSSC, 0.2xSSC, formamide with 0.2xSSC (1:1), and Tris Buffered Saline – Tween (TBS-T). The tissue is then blocked using 1% whole milk in TBS-T for 1hour before the addition of 0.5mls of anti-DIG antibody (Roche) in 1% whole milk (1:5000) to each slide. Excess antibody was then washed off through a series of washes in TBS-T before equilibration in 1x alkaline phosphatase (AP) with MgCl₂ (1M) before development in 100mg/ml of 4-Nitro blue tetrazolium chloride solution (NBT, Roche), and 50mg/ml 5-Bromo-4-chloro-3-indolyl-phosphate 4-toluidine salt solution (BCIP, Roche) in 1xAP. The reaction was left until an appropriate colour change occurred, in a staining tray flooded with 1xAP. The reaction was stopped in 1x Tris-Ethylenediaminetetraacetic acid (EDTA) solution (TE).

2.5.8 qPCR

The recording of the exponential amplification of specified DNA sequences in real time was achieved using a double stranded DNA fluorescent DYAMO SYBR green kit (Finnzymes). A standard PCR protocol was adopted and 10µl of the dye (containing a set concentration of dNTPs and MgCl₂) was added per well, with 1µl of cDNA and 0.5µl of each primer, in a translucent 96 well plate. Primers were made specifically for qPCR with a T_m of 60°C (See Appendix 1). The hot start Taq polymerase within the SYBR green was initiated by 95°C for 15 minutes in the machine. Amplification conditions used were 40 cycles of 95°C followed by 60°C for 30 seconds and 72°C for 30 seconds. Melt curves were generated from readings every 0.5°C between 53°C and 95°C. qPCR data was analysed by Opticon monitor 3 software and samples were always normalised to GAPDH levels in the same sample by the $\Delta\Delta C(t)$ method. Differential expression of mRNA is presented in terms of fold change (FC) to the initial variable always set at 1.

The $\Delta\Delta C_t$ method is used for relative quantification to a calibrator (the sample used to compare all other samples to). The sample RGS gene and GAPDH reference gene are normalised against variation in sample quality and quantity by the following: -

- $\Delta C(t)_{\text{sample}} = C(t)_{\text{target}} - C(t)_{\text{reference}}$
- $\Delta C(t)_{\text{calibrator}} = C(t)_{\text{target}} - C(t)_{\text{reference}}$

$\Delta\Delta C(t)$ is then calculated from the results from above : -

- $\Delta\Delta C(t) = \Delta C(t)_{\text{sample}} - \Delta C(t)_{\text{calibrator}}$

Expression of the target gene is normalised to the reference gene, remaining relative to the calibrator: $2^{-\Delta\Delta C(t)}$.

qPCR primers were tested by their capacity to display known changes of RGS expression in striatal tissue by apomorphine (1mg/kg) and methamphetamine (2.5mg/kg) in mice (See Fig. 2.5). Striata were dissected 30 minutes following the challenge and compared to striatal tissue taken from a mouse 30 minutes after a saline injection. In accordance with previous work apomorphine does not elicit a change in RGS2, RGS4, RGS8 or RGS9-2 at this time, as changes occur with complete wearing off of the drug up to 24 hours later (Hooks et al., 2008, Psifogeorgou et al., 2007, Garzon et al., 2005). In addition, increases in RGS2 (3 fold), RGS8 (0.5 fold) and RGS4 (0.5 fold) expression and decreases in RGS9-2 (1.5 fold) expression in the striatum and nucleus accumbens of rodents, as seen when using these optimised primers, have been reported in response to a single challenge of amphetamine previously (Burchett et al., 1999, Burchett et al., 1998, Schwendt et al., 2006). These changes in RGS gene expression following amphetamine and lack of change following injections of apomorphine in intact animals are in agreement with previous work and provide strong evidence that the primers are working efficiently.

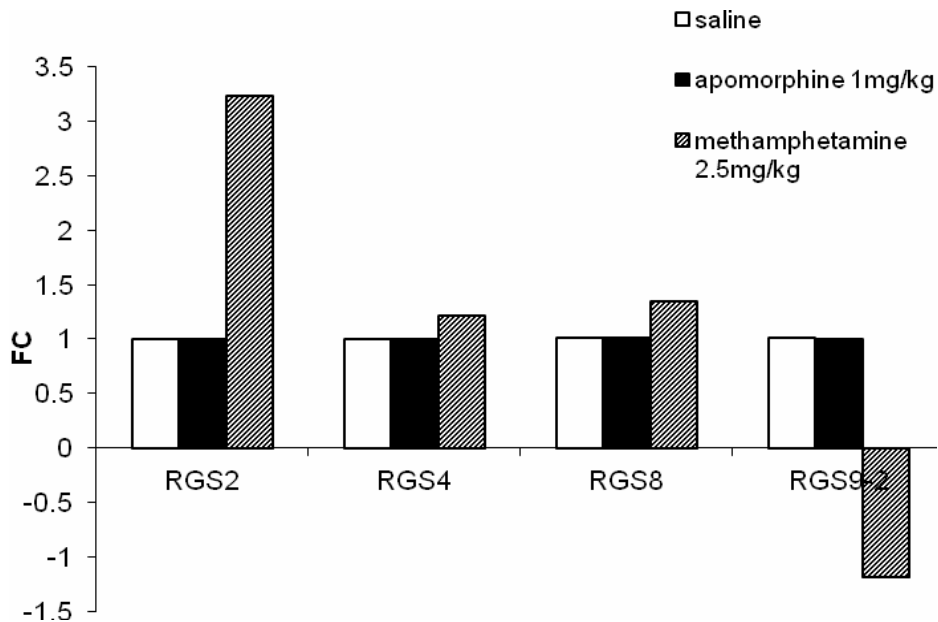


Figure 2.5. The testing of qPCR primers in tissue samples from intact mice, 30 minutes after a challenge of 1mg/kg of apomorphine or 2.5mg/kg of amphetamine.

2.5.9 Western Blotting- Protein Extraction

Proteins from the cytosolic fraction were isolated from dissected whole striata stored at -80°C . 300 μl of lysis buffer (stored at 4°C) was used to homogenise the tissue. The lysate was then transferred immediately to the centrifuge to be spun for 10 mins at 6500 rpm at $+4^{\circ}\text{C}$. Up to 150 μl of supernatant was then transferred a new Eppendorf (on ice) and an equal volume of 2x Laemmli (LB) buffer with 2-mercaptoethanol was added and mixed. The denaturation of proteins was achieved by boiling for 5mins at 95°C before replacing on ice. Denatured proteins were stored at -20°C until future use.

2.5.10 Western Blotting- Procedure

Prior to running proteins on SDS-PAGE, protein levels were normalised to ensure comparable levels of total protein were assessed. Total protein concentration was measured using a commercial protein assay kit (BioRad), based on the Bradford procedure (Bradford 1976). Homogenized protein samples were passed through a two layer polyacrylamide gel, consisting of a 6% upper “stacking gel” layer, followed by a higher concentration “resolving gel”, typically 10-20% acrylamide. The percentage of polyacrylamide contained in the resolving gel was altered according to the weight of proteins being assessed. Normalised levels of protein

were loaded into the stacking gel wells. Prestained protein weight marker ladder (Fermentas PageRuler Plus) was added to an additional well. Voltage and length of run time varied depending on the molecular weight of the protein being assessed.

Following electrophoresis, proteins were transferred from the polyacrylamide resolving gel to a PVDF membrane. Membranes were blocked in a solution of 3% non-fat milk (Marvel) in TBS-T for one hour. Blocking solution was removed and the membrane incubated in primary antibodies (RGS2: raised in rabbit from Abcam; RGS4: raised in goat from Santa Cruz; RGS9-2: raised in goat from Santa Cruz; TH: raised in rabbit from Chemicon) in 3% non-fat milk (Marvel) in TBS-T for overnight at +4°C. Primary antibody solution was removed and the membrane washed thoroughly in TBS-T. Samples were then incubated with anti-rabbit, anti-mouse or anti-goat secondary HRP conjugated antibodies (Amersham) for 1-2 hours. Protein bands were then imaged using the ECL or ECL+ chemi-luminescent detection systems in accordance with the manufacturers instructions (Amersham). Band intensities were analysed using AlphaImager 2200 analysis software. Following analysis, membranes were washed with TBS-T to remove ECL/ECL+. Membranes were reblocked and probed with antibody against β -actin (Abcam). Relative concentrations of test protein in samples were calculated by normalising band intensities against intensities of β -actin.

2.5.11 Tritiated Ligand binding Assays

Sections for radioligand binding were cut on the cryostat directly onto superfrost slides, from fresh frozen whole brains. Sections were allowed to air dry at room temperature, overnight before use. [³H]SCH23390 (Perkin Elmer) was used to assess D₁ receptor binding, based on the protocol of (Dewar and Reader, 1989). Sections were incubated in radioligand buffer 1 (See Appendix III) twice for 8 minutes at room temperature. 4.25 μ L of 0.5nM [³H]SCH23390 was mixed with radioligand buffer 1 for specific D₁ receptor binding and was mixed with radioligand buffer 1 and 10 μ M cis-flupenthixol (5mg/l) for non specific binding. Sections were left for 90 minutes at room temperature, washed in TRIS and deionised water for 2 minutes each and dried overnight.

[³H] Raclopride (Perkin Elmer) was used to assess D₂ receptor binding, based on the protocol of (Dewar and Reader, 1989). Sections were twice pre-incubated in radioligand buffer 2 (See Appendix III) for 8 minutes at room temperature. Specific binding was then initiated in the

same buffer with 100nM (100ul per 100ml) of ketanserin stock solution (5mg/ml stock in H₂O) and 2nM of [³H] Raclopride (17.4μl/100ml). [³H] Raclopride in radioligand buffer 2 was mixed with 10μM Sulpiride (3mg/l) for non-specific binding on adjacent sides with corresponding serial sections. All sections were left for 120 minutes at room temperature and washed in TRIS and deionised water for 2 minutes each and left to dry overnight.

For development and calibration slides were arranged in cassettes with the addition of two autoradiographic [³H] micro-scales (GE Healthcare) containing known high and low radioactivity levels. The high concentration strip emits radioactivity at 113.22- 4070Bq/mg and the low concentration strip at 3.774- 580.9 Bq/mg; each strip is split into 8 known radioactivity sections within these ranges. Amersham photographic Hyperfilm MP (GE Healthcare) was laid on the slides in darkness and cassettes were left for 3 months at 4°C. Radioactivity was then detected using a compact X4 imaging system (Xograph) with development and fixing solutions (Champion Photochemistry).

2.7 Quantification and Microscopy

2.7.1 General quantification and statistics

The statistical analysis used for each experiment is detailed in corresponding experimental chapters. SPSS (version 16) was used to deduce statistical significance for all Pearson's correlations, partial correlations, 1-3 way analysis of variance (ANOVA) and T-tests, and where appropriate post-hoc tests (as described in each chapter) were also implemented to specify significance to 95%*($P<0.05$), 99%**($P<0.01$) and 99.9%***($P<0.001$). Information on any relevant interactions, the total and error sum of square values, and stat value are also provided for each test.

Scores on behavioural tests and TH positive cell counts are expressed as a percentage of the intact side. Cell bodies were counted under a Leica light microscope in the VTA and SNc at the level of the medial terminal nucleus of the accessory nucleus of the optic tract interception as described by (Dowd and Dunnett, 2004). TH immuno-reactive cells within the striatum were counted in all sections from a 1 in 6 series through the mouse brain and corrected formulaically to deduce cell numbers in whole striatum. The quantification of RGS positive cells at different regions within the striatum and immunological staining of proteins within

cells was quantified by counting under a DMBRE Leica light microscope within a $600\mu\text{m}^2$ field, at 10x magnification. Half brains were visualised using a free standing Wild Makrozom M420 microscope (Switzerland). Images were taken by an Optronics camera and processed using Magnafire (2.1) software. Before quantification the investigator was blind as to which series of stained sections belong to which group. In addition groups were randomised in the blinding process. Upon completion of cell counting/ density analysis the investigator was informed of the blinding for analysis, thereby removing experimenter bias during quantification.

2.7.2 Determining Statistical Power

Group sizes for the experiments were determined by previous literature that has yielding significant results, for that particular kind of experiment: behavioural (Iancu et al., 2005), dyskinesia (Lundblad et al., 2005) and grafting/ histology (Lane et al., 2006). In addition we can calculate group sizes that will have enough power to show a statistically significant affect with a 1 tailed (i.e LID always expected to increase with big lesions and GID with large grafts) *a priori* power analysis test. The following have been calculated by the GPower statistical software (Erdfelder et al., 2006).

- Motor behavioural assessments: a total of 102 (critical t 100=1.66) would have an 80% power to yield a statistically significant result, for a medium effect size (0.5) at the alpha level of 0.05.
- Dyskinesia, molecular and biochemical analysis: a total sample size of 42 mice (critical t 40=1.68) would have an 80% power to yield a statistically significant result, for a predicted large effect size (0.8) at the alpha level of 0.05.

2.7.3 Quantification and Density Analysis with ImageJ

We assessed the density of TH- and 5-HT-immunopositive neurons in the dorsal and ventral striatum from images of every 6th section (taken with Leica DFC420 camera and Leica application V3.6 software) on ImageJ software (Version 1.42, National Institutes of Health, USA). A formula was used to convert default grey scale measurements into arbitrary optical density (O.D) values. Density was normalised to background levels of the corpus callosum and photographic sheet variances normalised to each other using a correction factor for the

difference in density based of the autoradiographic [3H] micro-scales (GE Healthcare). Control slides that have undergone the same procedure with the addition of competitive antagonists of corresponding receptors were measured and subtracted from test slide values. Equally for western blot analysis relative intensities of each band was quantified using density analysis software provided by ImageJ, and normalised corresponding GAPDH bands.

The low levels of background found within the striatum after a FosB stain allowed for automatic quantification of cell numbers using the ImageJ software. Photos for all regions and animals were taken the same day under DMBRE Leica light microscope without adjusting light levels at 10x magnification. The formula on ImageJ was adjusted to detect the maximum number of cells for their shape and size.

2.7.4 Analysis of Dopaminergic Grafts

Dopamine cell bodies densely stained with TH/5-HT by ICH or RGS DIG labelled oligonucleotide probes were counted in every sixth 40µm coronal brain section at a 200x magnification. The number from each section was then combined to give the total amount of dopamine neurons / RGS stained cells for each brain. The diameter of TH positive cells / RGS positive nuclei was deduced from by measuring at least 50 random positively stained cells under an Olympus BX50 microscope and Olympus C.A.S.T grid system. The total number of cells present in the graft was calculated using the Abercrombie correction formula (Abercrombie, 1946): -

$$T = F \times A \times M / (D/M)$$

T = total number of cells

F = frequency of sections

A = total counts for one animal

M = section thickness

D = average cell/nucleus area.

3. A Comprehensive Behavioural Assessment of the 6-OHDA lesioned mouse model of Parkinson's disease

Summary

The 6-OHDA lesioned rat is still the most commonly used model of PD, however due to the increasing availability of transgenic mice, mouse based tests and mouse derived cells, there has been much interest in a mouse version of the model. The comprehensive histological and behavioural assessments available for the rat are not as defined as those described for the mouse. This study examines the consequences of injecting 6-OHDA at three sites along the nigrostriatal tract (SN, MFB and striatum). This process caused distinct patterns of neuron depletion in the SNc, VTA and the denervation of dopaminergic fibre terminals in the striatum. Intense animal husbandry procedures ensured that the mortality rates remained high post lesion, a significant problem for some other studies. A large battery of motor hand tests evaluated behavioural deficits in all three models in comparison with intact control animals. Each of the lesion groups displayed marked behavioural deficits which correlated with histological measures to different degrees. The cylinder, corridor test, inverted cage lid, balance beam, rotarod, psycho-stimulant rotation (amphetamine and apomorphine) and spontaneous rotation correlated the most closely with cell loss within the SNc, and partial correlation analysis has shown the majority are dependent on SNc cell loss rather than that of the VTA.

Chapter 3 - Declaration

The experiments in this chapter were carried out in collaboration with PhD student Andreas Heuer (AH). Specifically he carried out the Staircase test, the inverted cage lid test, gait analysis, the rotarod, the stepping test and part of the histology. These tests were included in this thesis chapter with all others in order to allow completeness of the presentation and to be able to compare them in the discussion, but are indicated in the results section with the abbreviation AH.

3.1. Introduction

The in-depth behavioural analysis of the 6-OHDA lesioned model in the rat has led to a preference for its use in the experimental PD field. However, with the increased use of transgenics to explore different pathologies, the utility of a mouse model is clearly apparent. A limited number of studies have been carried out in the 6-OHDA lesioned mouse but at the time of starting this thesis there was little consistency between the surgical procedures, and behavioural assessments in conjunction with a worryingly low survival rate. The two predominant studies that have aimed to validate up to 4 behavioural hand tests to determine lesion extent and thus select animals for further study, used pre-selections by evaluating amphetamine-induced rotation (Iancu et al., 2005, Grealish et al., 2010b). Furthermore, it is unclear whether select psychostimulant induced rotation or drug free behavioural measures will show the most promising results when compared to each other (Mandel and Randall, 1985, Iancu et al., 2005). New motor and sensory-motor behavioural indicators of nigrostriatal damage and greater optimisation of the model to enhance survival, are necessary to make it a more robust and useable model of PD.

Rotational asymmetry remains the gold standard for the evaluation of the 6-OHDA lesion in the rat. Dopamine losses of 95% or more in the rat relate to a peak rotation rate of 7-15 turns per minute following an amphetamine (0.63-2.5mg/kg)/ apomorphine (0.015-0.1mg/kg) challenge (Costall et al., 1976a, Costall et al., 1976b, Schmidt and Westermann, 1980) and there are widely accepted relationships between dose and the extent of denervation (Hefti et al., 1980). This makes for highly predictive testing. Although up to a 31.5 fold change in directional bias has also been found in the mouse following an apomorphine challenge (Mandel and Randall, 1985), the reports of the rotational behaviour of the mouse model are highly variable, both in terms of outcome and technique (Francardo et al., 2011b, Grealish et al., 2010b, Iancu et al., 2005). The cylinder test, first described by (Schallert et al., 2000) assesses the laterality of forelimb use in a novel environment, and typically, rats with unilateral dopamine depletion will preferentially use the ipsilateral limb 70-90% of the time. Thus far reports are mixed as to the validity of this test in the mouse (Francardo et al., 2011b, Grealish et al., 2010b, Iancu et al., 2005). The corridor is used to discriminate lateralised differences of sensory-motor neglect. Rats show an ipsilateral bias of 75% following near complete neuronal degeneration of the striatum and SNc (Dowd et al., 2005b, Dowd et al.,

2005a), retrieving sugar pellets predominantly when placed on their ipsilateral side, ignoring those on the contralateral. When recently adapted for mice, similar levels of predictability for dopamine depletion were observed (Grealish et al., 2010b).

In the 6-OHDA rat model, deficits in the contralateral paw and a 10% overcompensation of the ipsilateral paw also manifest in the staircase test, when dopamine depletion is at 80% or more (Montoya et al., 1991, Montoya et al., 1990, Pagnussat Ade et al., 2009). The success of the staircase task, first devised for the *Sprague-Dawley* strain, has led to its adaptation for other strains of rat (Pagnussat Ade et al., 2009), mice (Baird et al., 2001) and models of other neurodegenerative diseases e.g. Huntington's disease and Stroke (Fricker et al., 1996, Peeling et al., 2001, Klein et al., 2007, Galtrey and Fawcett, 2007, Dowd et al., 2005b). Other behavioural assessments such as grip strength and adjusted stepping have consistently defined unilateral denervation through functional forelimb differences (Dowd et al., 2005b, Dunnett et al., 1998, Olsson et al., 1995, Paille et al., 2007), but these are not well adapted for use in the mouse.

Overall motor coordination and locomotion deficits can be assessed in hemi-parkinsonian rodents in open field, rotarod and beam walking paradigms (Koob et al., 1981, Fink and Smith, 1980, Fornaguera and Schwarting, 2002, Allbutt and Henderson, 2007, Iancu et al., 2005, Monville et al., 2006a, Ogura et al., 2005). In particular the latency to fall off the accelerating rotarod can correlate with 60% or greater loss of dopaminergic cells in mice (Iancu et al., 2005), however in the rat this test remains more discriminative to the extent of the lesion (Monville et al., 2006b).

This chapter focuses on clarifying the use of these various behavioural assessments in the mouse model of Parkinson's disease. Motor deficits were evaluated in three different lesion models to determine which may offer accurate predictors of 25- 90% unilateral dopamine depletion and to optimise some of the less frequently used behavioural tasks described previously in 6-OHDA rats and mice, and some which have not been used previously.

3.2. Experimental Design

A cohort of 105 male C57/Bl6 mice (Charles River, UK) was divided into 4 experimental groups. One group (n=15) served as untreated experimental controls whereas the other three groups (n = 30 in each) were designated for stereotaxic surgery. The staircase test required extensive pre-training (see Chapter 2) before surgery, which was carried out over 14 days, under a food restriction regime, where mice were maintained to 85% of their free feeding body weight. Mice were subject to unilateral lesions to the dopaminergic system, aimed at the SN, the MFB, or the striatum with co-ordinates optimised from trypan blue injections, confirming accuracy at the target site (see Chapter 2). An intensive daily animal husbandry regime was undertaken to ensure the full recovery of the mice. Six weeks post-lesion, mice were food-restricted to 90% of their free feeding weight and tested on the staircase and corridor test. Mice were allowed *ad libitum* access to food for all other behavioural hand tests that were carried out in the following order: staircase, corridor, balance beam, spontaneous rotarion, cylinder, rotarod, inverted cagelid, locomotor activity and separate amphetamine- and apomorphine-induced rotation sessions. At the end of testing, mice were used for a separate dyskinesia experiment (see Chapter 3) then were perfused transcardially with 1.5% paraformaldehyde, before brains were removed, post-fixed and stored in sucrose before processing. Brains were cut into coronal sections of 40 micrometers and a 1 in 6 series from each mouse was used to stain for TH, where density and cell counts in the SNc and VTA were quantified, detailed histological methods and modes of quantification as detailed in Chapter 2. The behavioural data were analysed using 1-way ANOVA, and Dunnett's *post-hoc* tests, using intact control groups as baseline. When appropriate a bias score was calculated as 100 x (ipsilateral paw or side/ contralateral paw or side). Behavioural results were used for bivariate correlation analysis with the histological measures of cell loss, using Pearson correlation coefficients (one-tailed). Finally, in select analysis co-correlation between SNc /VTA depletion was factored out using partial correlation analysis for each of the behavioural assessments.

3.3. Results

3.3.1. Mortality Rates and Weight

The insensitive husbandry regime achieved a low mortality rate for all groups, where death was evident within the first 10 days post-lesion and none were lost after this time (see Fig

3.1A). Survival rates depended upon lesion type where: Striatal >95%; MFB >80%; SNc >90%. All mice were given a highly palatable diet in an attempt to maintain body weight and therefore control mice put on weight over the two weeks of intensive animal husbandry, this was not seen in mice lesioned to the striatum and SNc where weight remained stable (Fig 3.1B). The MFB group had a reduced weight compared to all other groups for 10 days post surgery and compared to the baseline level (Fig 3.1B).

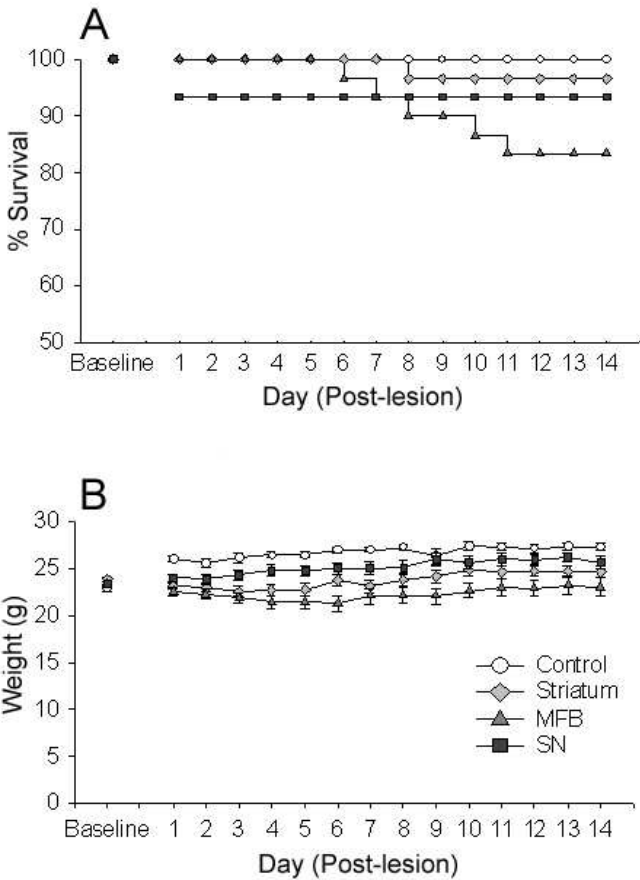


Fig. 3.1. Survival (A) and body weight (B) measures for 14 consecutive days post lesion plotted per group, where the baseline day was recorded at the day of surgery. Values are expressed as means \pm SEM.

3.3.2. Histological analysis of the lesions

6-OHDA reduced the numbers of TH positive neurons in the SNc ($F_{3,90} = 13.33$, $p < 0.001$) in all three lesion groups (Fig. 3.2A-B) and in the corresponding TH-fibre density in the dorsal striatum ($F_{3,89} = 17.57$, $p < 0.001$), significant reductions were observed for each type compared to intact controls (Striatum and MFB groups $p < 0.001$; SN $p < 0.01$). There was also significant cell loss in the VTA ($F_{3,90} = 9.05$, $p < 0.001$) and TH fibre density depletion in the ventral striatum ($F_{3,90} = 12.67$, $p < 0.001$), however only MFB and Striatum groups differed significantly from control ($p < 0.01$ and $p < 0.001$ respectively).

20-50% of the animals in all groups had near to complete lesions (>90% depletion), while a smaller number of animals in both the MFB and SN lesion groups had very small lesions (<25% depletion). The lesion success was highest in the Striatum lesion group where the majority of mice exhibited at least partial lesions (between from 25% up to >90% depletion). The variability of the lesions is considered further with subsequent correlation analysis against behavioural deficits. Mice with near to complete lesions were chosen from each group for use in another study, detailed in Chapter 4, where it is evident that group deficits are more pronounced (see section 4.3.1).

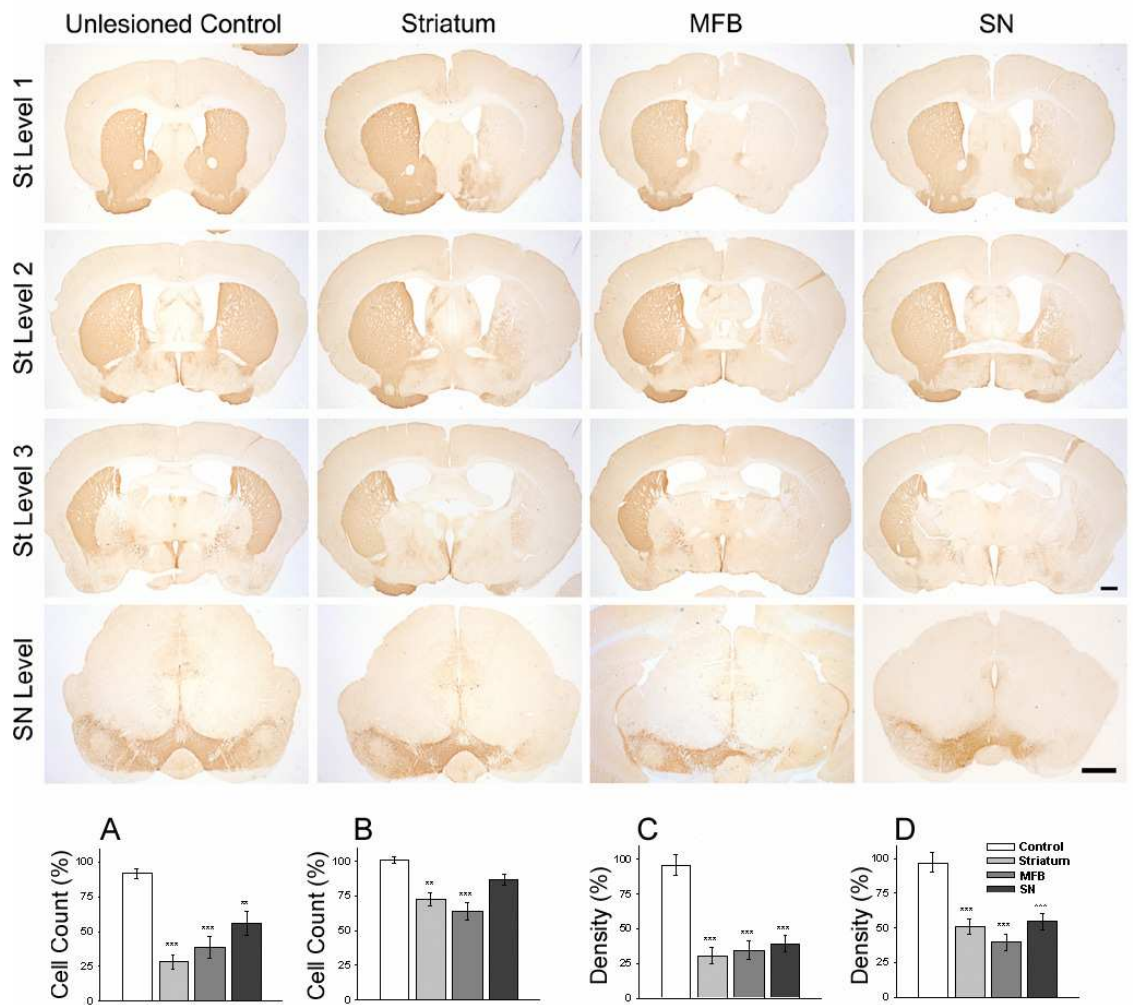


Fig. 3.2. Bright-field photomicrographs of representative sections for successful lesions of the Striatum (St) medial forebrain bundle (MFB) and substantia nigra (SN) groups compared to the intact controls. Sections were cut in the coronal plane and stained for TH. Sections were taken at the approximate levels: (St Level 1) +1.0mm, (St Level 2) -0.2mm, (St Level 3) -1.3mm, and (SN Level) -5.2mm from Bregma. Scale bar represents 1mm for all levels. Cell counts were expressed as percent of contralateral for SNc (A) and VTA (B). Striatal density measures of TH positive fibres are expressed as percent of contralateral for the dorsal striatum (C) and ventral striatum (D). Graphs are annotated at the $p < 0.05^*$, $p < 0.01^{**}$ and $p < 0.001^{***}$ level of significance. Values are expressed as means \pm SEM.

3.3.3. Group effects on motor deficits

There were a number of tests that showed no differences between lesion groups and non-operated controls (Fig 3.3.), including staircase (Group, $F_{3,91} = 0.58$, $p = ns$) and adjusting stepping tests ($F_{3,85} = 1.63$, $p = ns$), undertaken by AH, and horizontal locomotor activity ($F_{3,91} = 1.51$, $p = ns$). A trend was noted for group effects of lesion-induced deficits on the balance beam test (Fig. 3.3C; $F_{3,90} = 2.65$, $p = 0.054$), and when the MFB group is directly compared to unlesioned controls a significant performance deficit was found ($p < 0.05$). Performance on the corridor test was impaired in mice with MFB or striatal lesions (Fig. 3.3B; $F_{3,91} = 4.62$, $p < 0.01$, post hoc $p < 0.01$ for both groups). The striatal group showed specific deficits in the cylinder test (Fig. 3.3D; $F_{3,91} = 4.25$, $p < 0.01$, post hoc $p < 0.05$). The inverted cage lid test, performed by AH, was used as a measure of grip strength was able to detect lesion deficits compared to the intact control group (Fig. 3.3H; Group, $F_{3,91} = 3.59$, $p < 0.05$), however *post hoc* analysis showed this only to be true for the Striatum lesion group ($p < 0.05$). The latency to fall from the rotating rod was significantly different between the other lesion groups and the from the control group (Fig. 3.3E; Group, $F_{3,91} = 3.76$, $p < 0.05$), where all lesion groups reached significance to varying degrees (SN and Striatum, $p < 0.05$ MFB, $p < 0.01$).

Rotational deficits proved to be one of the most robust measures to determine group lesion effects. Significant differences were noted between lesioned mice with methamphetamine induced rotation (Fig. 3.3K; $F_{3,90} = 4.33$, $p < 0.01$), apomorphine induced rotation (Fig. 3.3L; Group, $F_{3,85} = 6.09$, $p < 0.05$) and by spontaneous rotation (Fig. 3.3J, $F_{3,91} = 10.59$, $p < 0.001$). Methamphetamine was able to induce ipsilateral rotation in all groups (Striatum, $p < 0.01$; MFB, $p < 0.001$; SN, $p < 0.05$), where as apomorphine-induced rotational differences were only seen in Striatum ($p < 0.05$) and MFB ($p < 0.01$) groups. Significant spontaneous total net ipsilateral rotation was seen exclusively in mice with an MFB lesions, where $p < 0.01$.

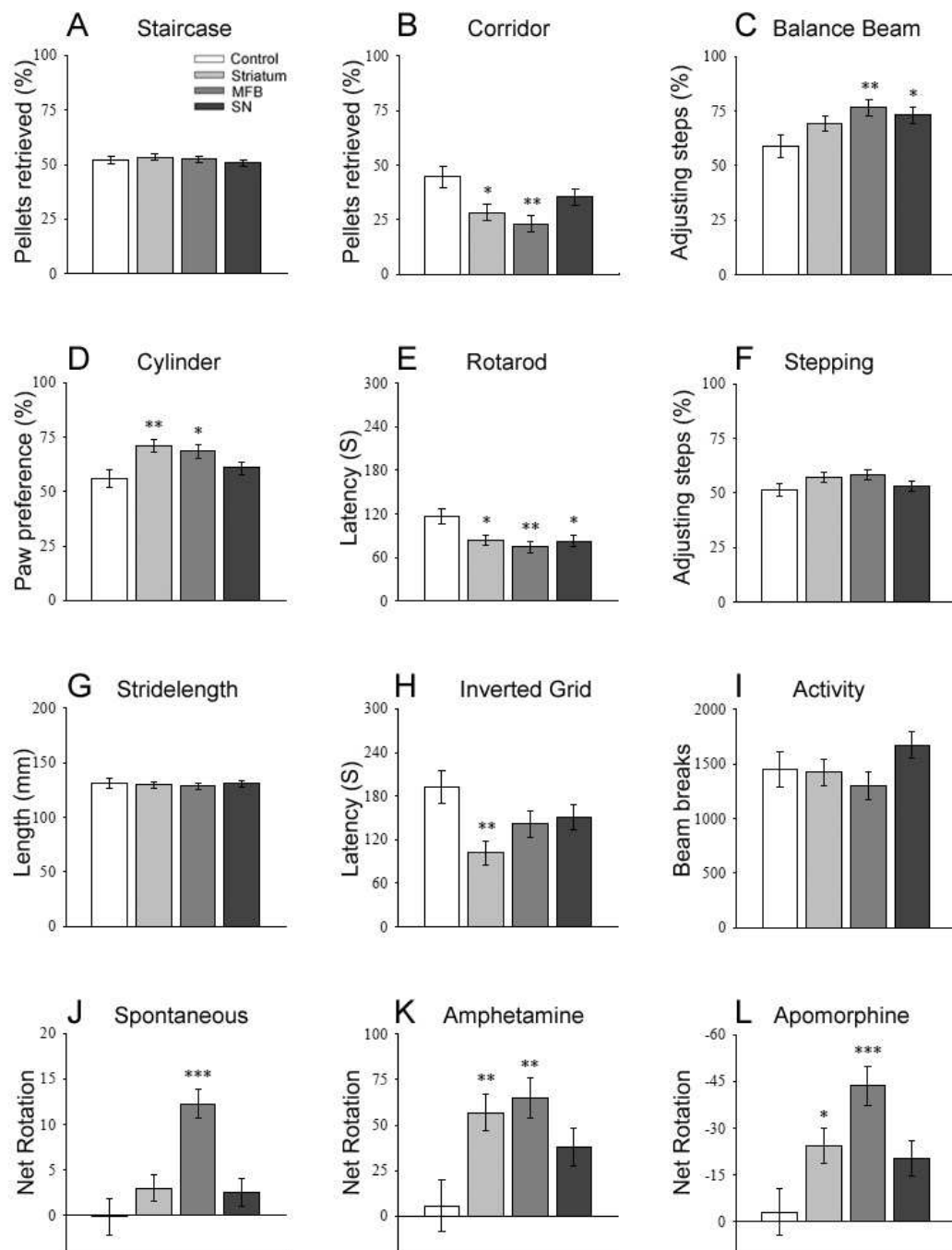


Fig. 3.3. Effects by group on select behavioural hand tests compared to unlesioned controls. Graphical representations of the following are shown: pellets retrieved on the staircase (A), pellets retrieved on the corridor (B), foot slips on the balance beams (C), paw preference on the cylinder (D), Latency to fall on the rotarod (E), stepping test (F), stride length (G), grip strength by the grip test (H), locomotor activity (I), percentage of spontaneous turns (J), percentage of turns from 2.5mg/kg of methamphetamine (K) and percentage of turns from 0.05mg/kg of apomorphine (L). Significant differences determined by a 1-way ANOVA are indicated by $p < 0.05$ *, $p < 0.01$ ** and $p < 0.001$ ***. Values are expressed as means \pm SEM.

3.3.4. Correlation of Motor Deficits and Lesion Extent in the SNc

Without pre-selection of animals by rotation, group effects may have been masked by the presence of mice with partial and failed lesions, therefore a comprehensive correlation analysis was performed to determine the relationship between cell loss in the VTA and SNc and all of the behavioural hand tests performed (Table 3.1 and Table 3.2 respectively).

The proportion of dopaminergic cell bodies remaining in the SNc in the lesioned side could be correlated to total spontaneous rotation ($r = -0.485$, $p < 0.01$), total amphetamine rotation ($r = -0.694$, $p < 0.01$), total apomorphine rotation ($r = 0.548$, $p < 0.01$), the cylinder test ($r = -0.581$, $p < 0.01$) and the corridor test ($r = -0.557$, $p < 0.01$) (Table 3.1). The percentage of cells remaining in the SNc was weakly correlated to the stepping test ($r = -0.254$, $p < 0.01$) and gait analysis ($r = 0.184$, $p < 0.05$), undertaken by AH. The staircase, inverted cage lid, and basal locomotor activity did not correlate with the percentage of TH positive cells in the SNc on the ipsilateral side. Although a high proportion of the hand tests undertaken could be correlated to the percentage of TH positive cells remaining on the ipsilateral side, few reached significance when each group was considered separately. Nevertheless the cylinder and amphetamine tests could be robustly correlated to the percentage of TH positive cells remaining in the SNc, in all lesion groups (Table 3.1). In contrast, the total number of spontaneous rotations and performance on the corridor test was only correlated to the cells counts in the SN and MFB lesion groups.

Partial correlation analysis uses the percentage of cells remaining in the VTA as a covariate, so that it may be excluded as a confounding factor in the evaluation of correlation with SNc cell loss. With this statistical analysis the overall deficits correlated significantly with SNc cell loss on the balance beam (Fig. 3.4A; $r = -0.186$, $p < 0.05$), the corridor test (Fig 3.4B; $r = 0.440$, $p < 0.001$), the rotarod (Fig. 3.4C; $r = 0.175$, $p = 0.05$), the cylinder test ($r = -0.385$, $p < 0.001$), total spontaneous rotation ($r = 0.356$, $p < 0.001$), total amphetamine induced rotation ($r = 0.630$, $p < 0.001$), and total apomorphine induced rotation ($r = -0.200$, $p < 0.05$). Assessment by partial correlation has also shown that significant trends, found with standard bivariate Pearson's correlations, also remain for individual groups, therefore reinforcing the sensitivity of these tests to specific losses of neurons in the SNc.

Hand test/ Group	Overall	Striatum	MFB	SN
Rotarod	0.304 **	0.036	0.215	0.309
Cage lid	0.171	0.027	-0.132	0.052
Amphetamine Rot (total)	-0.698 **	-0.623 **	-0.810 **	-0.619 **
Apomorphine Rot (total)	0.548 **	0.359 *	0.665 **	0.476 **
Spontaneous Rot (total)	-0.485 **	-0.153	-0.671 **	-0.630 **
% Balance Beam	-0.399 **	-0.104	-0.283	-0.778
% Cylinder	-0.581 **	-0.336 *	-0.751 **	-0.442 *
% Corridor	0.557 **	0.317	0.529 **	0.734 **
% Staircase	-0.076	-0.202	-0.009	-0.015
% Stepping Bias	-0.254 **	0.223	-0.205	-0.269
Gait (stride length left)	0.184 *	0.087	-0.009	0.248
Activity Perseverative	0.136	-0.009	0.258	0.110

Table 3.1. Pearson's correlation coefficients between percentage of cells remaining in the SNc of mice lesioned to the striatum, MFB and SNc and deficits on a battery of motor hand tests. Significance is indicated by $p < 0.05$ * and $p < 0.01$ **. Values are expressed as means \pm SEM.

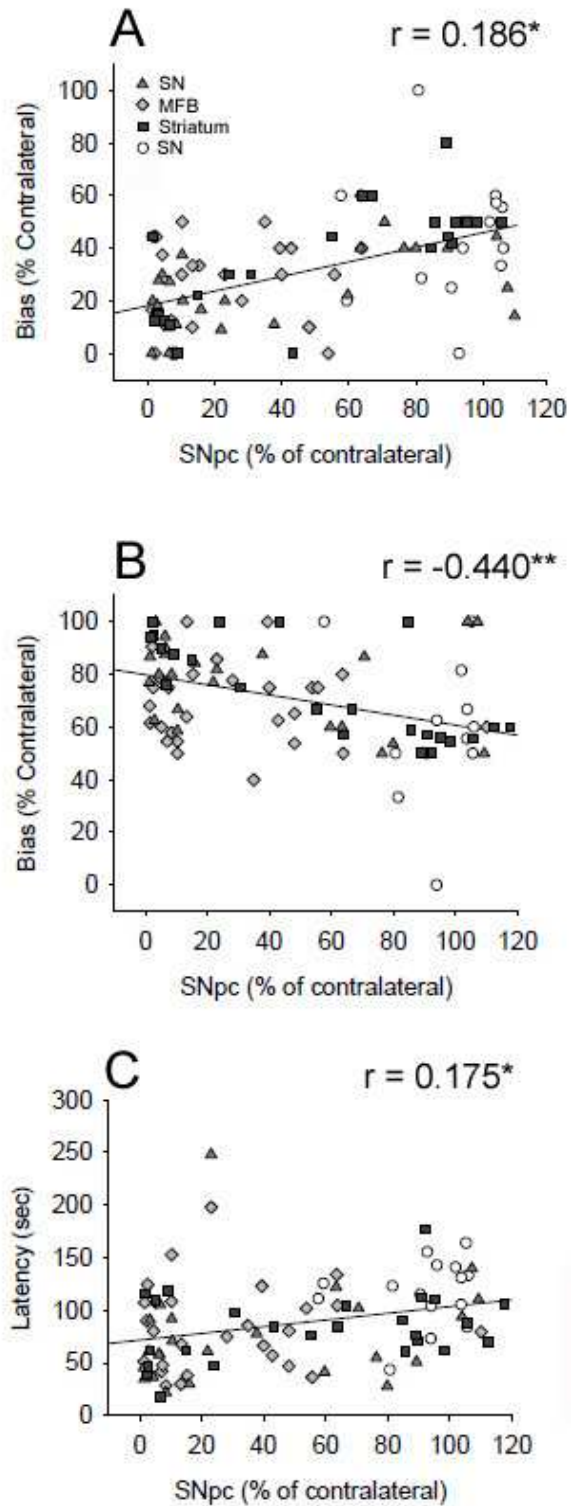


Fig. 3.4. Pearson's correlations between percentage of cells remaining in the SNc of mice lesioned to the striatum, MFB and SNc and deficits on the balance beam (A), corridor (B) and rotarod (C). Significance is indicated by *, $p < 0.05$ or **, $p < 0.01$.

3.3.5. Correlation of Motor Deficits and Lesion Extent in the VTA

The correlations between the percentage of dopaminergic cell bodies preserved in the VTA and performance on each of the behavioural tests are indicated in Table 3.2. The proportion of remaining cells in the VTA for all groups correlated robustly with performance on the cylinder test ($r = -0.516, p < 0.01$). Moderate to weak correlations were also evident between the VTA cell counts and deficits incurred on the balance beam test ($r = -0.425, p < 0.01$), the stepping test ($r = 0.400, p < 0.01$), total amphetamine-induced rotations ($r = -0.698, p < 0.01$), the corridor test ($r = 0.383, p < 0.01$), total spontaneous rotations ($r = -0.485, p < 0.01$), total apomorphine-induced rotations ($r = 0.450, p < 0.01$) and performance on the rotarod ($r = 0.275, p < 0.01$). All other tests did not reach significance. When assessing each group individually, the percentage of remaining VTA cells correlated significantly with behaviour on the corridor and balance beam tests for the MFB and SN lesion group. Conversely the cylinder test correlated significantly with VTA dopamine depletion in the Striatal and MFB lesion groups. Total amphetamine mediated turns and the stepping tests were exclusively correlated to the Striatal lesion group and spontaneous rotation only with the MFB group.

When controlling for the remaining percentage of SNc cell counts with partial correlation analysis, overall correlations between cells remaining in the VTA with the performance on the cylinder test ($r = -0.238, p < 0.05$) and balance beam ($r = -0.244, p < 0.05$) remained significant, whereas all other tests that had previously been deemed significant by Pearson's correlation analysis (Table 3.2), failed to reach significance in the present analysis.

Hand test/ Group	Overall	Striatum	MFB	SN
Rotarod	0.275 **	0.018	0.296	0.171
Cage lid	0.080	-0.325 *	-0.254	0.368 *
Amphetamine Rot (total)	-0.698 **	-0.623 **	-0.810 **	-0.619 **
Apomorphine Rot (total)	0.548 **	0.359 *	0.665 **	0.476 **
Spontaneous Rot (total)	-0.485 **	-0.153	-0.671 **	-0.630 **
% Balance Beam	-0.425 **	-0.322	-0.408 *	-0.653 **
% Cylinder	-0.516 **	-0.340 *	-0.797 **	-0.180
% Corridor	0.383 **	-0.035	0.568 **	0.532 **
% Staircase	0.016	-0.234	0.213	0.317
% Stepping Bias	0.400 **	0.374 *	0.333	0.209
Gait (stride length left)	0.081	-0.063	0.297	0.151
Activity Perseverative	0.156	-0.019	0.185	0.252

Table 3.2. Pearson's correlation coefficients between percentage of cells remaining in the VTA of mice lesioned to the striatum, MFB and SN with deficits on a battery of motor hand tests. Significance is indicated by $p < 0.05^*$ and $p < 0.01^{**}$. Values are expressed as means \pm SEM.

3.4. Discussion

This study uses 9 different hand tests and drug-induced rotation without initial screening, ensuring that groups with a wide range of denervation are able to display group differences between lesion placements and dopamine cell loss levels. Since behavioural and histopathological differences were found between mice lesioned at different levels of the nigrostriatal pathway, this study provides a randomised and blind assessment and comparison of the three hemi-parkinsonian models currently used in the literature. The data gathered from this investigation has allowed for the fullest behavioural characterisation of 6-OHDA lesioned mice to date. In previous studies, no more than four hand tests have been used to quantify deficits in mice with near to complete lesions, and only following prior screening with psychostimulant induced rotation. This has the effect of skewing the data, excluding mice with partial or poor lesions (Grealish et al., 2010b, Iancu et al., 2005). The differences between previous studies to those shown here, the outcome of lesion surgery, behaviour and histological correlates are discussed below.

3.4.1. 6-OHDA Lesion Efficiency

All 6-OHDA lesions produced a marked degeneration of the dopaminergic neurons in the midbrain and denervation of TH immuno-positive fibres in the striatum. There were clear differences in lesion efficiency between the three target sites of 6-OHDA injection, with the Striatal lesion group having the most successfully lesioned mice, the most marked cell loss on the ipsilateral side and had the smallest within-group variability. This is in contrast to the MFB and SN groups; there were a larger proportion of mice with very small and partial lesions, although mice that have died are likely to have near complete lesions, biasing the lesion success rate ('very small', 'partial', and 'near to complete' are defined in section 3.3.2.). As expected, successful lesions aimed at the MFB were near to complete, extending their degeneration in the midbrain, to parts of the VTA and hence ventral striatum, as shown previously using this lesion type (Kirik et al., 1998, Grealish et al., 2008a, Francardo et al., 2011a). Lesions targeted at the SN produced more focal dopaminergic cell depletion, largely sparing the VTA and ventral striatum. MFB lesions produced the largest depletion of cell bodies in the SNc and VTA, denoting the degradation of fibres in the whole striatum. The degree of degeneration in the ventral striatum and VTA was more variable and less severe in the other two lesion groups, with dopamine depletion primarily restricted to the SNc and the dorsal striatum in the majority of cases. Discussed below are how these unique patterns of

denervation, and the different proportion of mice with ‘very small’ and ‘near to complete’ lesions in each group, impact on survival and behavioural outcome measures.

3.4.2. Mortality Rate Improvement

This study also highlights that 6-OHDA lesion efficiency has direct consequences on the survival of mice. The surgical and husbandry protocols used previously have led to reported death rates of up to 80% of mice, which appears to have resulted in a shift from the use of MFB lesions to those of the striatum and SN. This is probably based on the presumption that non-specific or bilateral damage is caused during this lesion, which is quite close to the brain midline. In particular high mortality rates have been reported with lesions aimed at the MFB (Grealish et al., 2010b, Cenci and Lundblad, 2007, Lundblad et al., 2004b). However, following a stringent post-surgical care regime, mortality and weight loss in this study were minimal, and the survival rate in the MFB lesioned group was greater than 80%, in agreement with another recent study (Francardo et al., 2011b). All animals required post-surgical care for two weeks, but this was most needed for the MFB lesion group, which is likely to be due to both dopaminergic and non-dopaminergic depletion to mesocorticolimbic projections outside the nigrostriatal pathway itself. The levels of dopaminergic depletion likely remain the largest contributing factor to survival, since MFB lesions typically spare less neurons. There was no evidence from any of the lesion types that the bilateral loss of dopaminergic neurons occurred, suggesting that this is not the cause of high mortality in other studies. Lesion site along the nigrostriatal pathway dictates the approximate latency to death post-surgery, for example death on the first few days following the lesion is possible if 6-OHDA is injected directly to the SN. Mice are likely to die in the second week after MFB and Striatal lesions as the neurotoxin is delayed from reaching the SN by retrograde transport (Alvarez-Fischer et al., 2008, Marinova-Mutafchieva et al., 2009, Walsh et al., 2011, Blandini et al., 2007a). Low mortality rates due to limited drinking and eating may also be linked to limbic functions of the ventral striatum, therefore the greater sparing of the VTA in SN and Striatal lesioned groups may have contributed to enhanced survival.

3.4.3. Deficits on Behavioural Tests

Group deficits caused by the lesion on behavioural tests remain one of the most important and reliable means to initially screen for adequate dopamine depletion, without pre-selection of mice with the biggest lesions. In this study the success of hand tests to determine group

deficits in comparison to their unlesioned counterparts depend on the initial site of 6-OHDA injection. The cylinder and inverted cage lid tests were only useful in distinguishing Striatal lesions, whereas the corridor test was able to detect a group deficit in mice with MFB and Striatal lesions. The novel corridor test has been shown to be sensitive to unilateral 6-OHDA lesions aimed at the mouse SN (Grealish et al., 2010b), however here no SN group effects were observed on this task. These differences most likely result from selection of the experimental cohort and their respective overall degree of cell loss. In the previous study, 40 mice were selected from 122, to represent all subjects of a defined mild, intermediate and severe lesion type (Grealish et al., 2010b), where even mice with a mild lesion had a 71% reduction of dopaminergic SNc cells. The present study did not remove any mice from the lesion cohorts and hence incorporated a wider range of dopamine depletions, most likely resulting in the lack of effect of the corridor test in distinguishing SN lesions. The cylinder test results presented here are comparable to those seen in the unilateral lesion rat models of PD (Lundblad et al., 2004b, Grealish et al., 2010b, Iancu et al., 2005). The lack of deficits in gait, was reiterated in another mouse study (Grealish et al., 2010b), and these are in contrast to the outcome of this test in unilateral 6-OHDA rat model (Grealish et al., 2008a, Kirik et al., 1998, Olsson et al., 1995). Equally, gait analysis has been shown to be sensitive to abnormalities in gait of transgenic and lesioned rodents (Brooks et al., 2004b, Carter et al., 1999, Schallert et al., 1978), but was not sensitive enough to detect differences in this study. In this study the balance beam test detected deficits in MFB and SN groups compared to intact control mice, thus indicating that gait for controlled movements may have been impaired, however these may partly depend on the lack of co-ordination. In addition, basal locomotor activity did not show significant differences between any of the groups, in agreement with the Lundblad et al. (2004) study. Locomotor activity was one of the last tests to be carried out and it is possible that the lack of movement change was due to spontaneous recovery, as there was reportedly a small effect shortly after the lesion in another study (Lundblad et al., 2004b). As an automated system was used, behavioural observations used in an open field test were not possible and changes in grooming, rearing and time spent on the inside quadrant may have been missed.

Drug-induced rotation remains the most widely used measure of unilateral dopamine depletion. However, its use in the mouse has given mixed success to date. In the literature, a wide range of doses of amphetamine and apomorphine have been used (amphetamine: 0.25-8mg/kg and apomorphine: 0.01- 4mg/kg) (Grealish et al., 2010b, Randall, 1984, Iancu et al., 2005, Mandel and Randall, 1985, Von Voigtlander and Moore, 1973, Brundin et al., 1986,

Torello et al., 1983) with similarly variable outcomes. Amphetamine-induced rotation was the most sensitive behavioural measure and was able to identify robust differences in all lesion groups. Apomorphine-mediated rotation was a good measure of MFB and Striatal lesions but failed to determine dopamine denervation in the SN group. High doses of apomorphine used in some studies would have produced strong stereotypic behaviours, slowing movement overall and confounding results (Iancu et al., 2005). In this study 0.05 mg/kg apomorphine was informative of dopamine cell loss, in all three lesion groups and no stereotypic behaviour was observed, although the effect size was small for lesions aimed directly at the SN. In mice it is common to give multiple apomorphine injections over a number consecutive days, to increase the rotational response prior to the test day (Grealish et al., 2010b). In this present study, mice only received a single injection, administered on the day of testing, yet a robust turning response was seen. It can therefore be suggested that priming the animals with apomorphine is not only unnecessary, but causes long term post-synaptic changes that may confound the results from other behavioural tests, and which is likely to render the mice unsuitable for use in other experiments, such as those centred around chronic L-DOPA treatment (see Chapter 4). Spontaneous rotation in a novel environment was only noted in the MFB group. It can be speculated that dopamine is released by anxiety from the novel environment causing ipsilateral locomotion. A high degree of dopamine denervation is needed to drive this effect, and dopamine release by remaining terminals in SN and Striatal groups is enough to overcome the effect of the anxiety-mediated dopamine release on the contralateral side.

3.4.3. Correlations between Midbrain Cell Loss and Behavioural Deficits.

Overall effects by group do not allow for the analysis of how accurate these tests are at selecting for various levels of dopamine depletion. Therefore, a correlation analysis was used. The most highly correlative tests with behavioural outcome measures, gave a large enough and consistent deviation between ‘very small’, ‘partial’ and ‘near to complete’ lesions. Behavioural assessment by correlation revealed that drug mediated rotation, spontaneous rotation, corridor test, cylinder test, and balance beam were sensitive to dopaminergic depletion of the SNc, even when using a partial correlation to exclude potentially confounding VTA cell loss. Conversely, there were also a number of tests which were correlated to remaining cells of the VTA, however when controlling for remaining SNc cell percentage by

partial correlation, the stepping test and the gait analysis were no longer significant, suggesting that this effect was at least partially driven by the influence of the SNc.

Interestingly, when you exclude the variance caused by VTA cell loss, the corridor test became correlated with remaining SNc cell percentage of this group, whereas performance on the cylinder test was no longer significant. These provide an important insight on the mechanisms of these hand tests and suggest that there may be a mesolimbic element influenced by the ventral striatum in the cylinder test, which might also be detrimental to the capacity to retrieve pellets in a linear corridor test. The MFB group deficits were the most correlative to cell loss in the SNc, even when controlling for VTA co-correlation. This may have resulted from the high degree of intra-group lesion variability and is suggestive that high losses of cells in the SNc may be alone enough to cause deficits on these tests regardless of VTA damage. Using partial correlation analysis there were no longer influences of the VTA on any rotational measure. It suggested that VTA damage of 30% found in our mice were not sufficient to alter rotation further than that driven by SNc cell loss, in agreement with the rat model (Moore et al., 2001). Interestingly, VTA cell losses of 60% or greater may reduce amphetamine hyper-responsiveness and amphetamine-induced rotation (Koob et al., 1981, Moore et al., 2001), not seen in this study. The models presented here may therefore reflect the patterns of cell loss in late stage PD patients where A10 neurons are largely spared. These results demonstrate that the sensitivity of the behavioural tasks to motor deficits varies in magnitude and deficits are differentially correlated with cell loss in the SNc and VTA. It can be suggested from this data that the use of multiple tests in the assessment of hemi-parkinsonian mice is important. The best approach may be the use of a drug-induced rotation, followed by a small number of behavioural tests, without rotation pre-selection. However, tests used will be dependent on lesion type. Further, these studies report the first use of spontaneous rotational assessment and the balance beam test for the assessment of mouse lesions, thereby validating their use in MFB and MFB/SN lesion groups respectively.

3.4.4. Conclusions

The typical survival rate of between 95-100% seen in hemi-parkinsonian MFB lesioned rats (Torres et al., 2011) is still near impossible to achieve in the mouse, however intensive post-operative care enabled mortality rates to be kept to a minimum ensuring meaningful results and compliance with home office rules for this type of procedure. Overall, intra-striatal neurotoxin

injections caused clear motor impairments, likely due to the relative hit rate consistency and reduced variability of lesions between mice. Targeting the neurotoxin to the SN or MFB was more variable, although in successfully lesioned mice the overall level of ipsilateral dopaminergic cell loss in the SNc and VTA was greater. This study has allowed for a comprehensive evaluation of motor impairments and dopaminergic loss in three 6-OHDA models. Deficits in mice can be assessed robustly in hemi-parkinsonian mice to rival threshold levels of deficit established in the rat. This was found to be achieved regardless of 6-OHDA injection site; although this study demonstrates the need to choose suitable tests specifically for each lesion type. Tests indicated in Table 3.3 show those that could be used for groups of mice of each type (without excluding mice by any other motor deficit measure), based off both group deficit measures and ability to correlate to dopamine loss (Table 3.3).

Hand test/ Group	Striatum	MFB	SN
Rotarod			
Cage lid			
Amphetamine Rot	XXXXXXXXXX	XXXXXXXXXX	XXXXXXXXXX
Apomorphine Rot	XXXXXXXXXX	XXXXXXXXXX	XXXXXXXXXX
Spontaneous Rot	XXXXXXXXXX	XXXXXXXXXX	XXXXXXXXXX
Balance Beam			
Cylinder			
Corridor	XXXXXXXXXX	XXXXXXXXXX	XXXXXXXXXX
Staircase			
Stepping			
Gait			
Activity			

Table 3.3. Summary table of the most sensitive tests that may be used for each lesion type, as defined both by group deficit and the correlative capacity of each test to the degree of dopamine depletion. Group deficits on behavioural hand tests are indicated in grey, where mice with very small (<25%), partial (26 – 89%) and near to complete lesions (>90%) are all included. Checked squares indicate the 4 most highly correlative hand tests to cell loss in the SNc when controlling for losses in the VTA.

Furthermore, I conclude that drug-mediated rotation, spontaneous rotation, corridor test, cylinder test, and balance beam tests are the most reliable and sensitive for indicating the degree of dopamine depletion. This detailed optimisation of the 6-OHDA mouse proved invaluable in the latter parts of this thesis, where the model enabled new insights into changes the molecular biomarkers of L-DOPA function (Chapter 5), and in the transplantation of mouse-derived primary foetal dopamine cells that were a pre-requisite for the creation of a mouse model of GID (Chapter 8). Prior to these studies however the in-depth characterisation of AIMS induced by escalating doses of L-DOPA in the three 6-OHDA lesion models are described (Chapter 4).

4. Assessment of L-DOPA induced dyskinesia in the 6-OHDA-lesioned mouse

Summary

The location of the 6-OHDA lesion along the nigrostriatal pathway determines the extent and pattern of neuropathology, behavioural phenotypes and responses to the dopamine precursor L-DOPA. The objectives of this chapter were to examine the relationship between lesion extent and development of LID and to determine if these tasks could be predictive of dyskinesia development. Mice were lesioned with 6-OHDA lesions of the striatum, MFB and SN and tested on a variety of motor tasks established for use in rats and mice (discussed fully in Chapter 1). The most impaired animals in each lesion group were given L-DOPA in progressively increasing doses and assessed for LID at each stage. Many of the motor tests correlated with the extent of nigrostriatal dopamine depletion but only rotarod, apomorphine-induced rotations and locomotor activities were potentially predictive of the development of dyskinesia at 6mg/kg and 25mg/kg of L-DOPA. The losses of dopaminergic fibre innervation and sparing of serotonergic density in the ventral and dorsal striatum also differed depending on lesion location along the nigro-striatal tract and these neuropathological patterns were also correlated with LID. In addition, the expression of FosB/ Δ FosB was differently upregulated in the striatum and NAcc regions in dyskinetic mice according to lesion type.

4.1 Introduction

PD patients are commonly treated by the administration of the dopamine receptor agonists and with disease progression, the dopamine precursor L-DOPA. However, administration of L-DOPA over a prolonged period of time leads to the development of choreic and/or dystonic AIMs termed dyskinesia. These behaviours were first modelled in the MPTP-treated primate (Jenner et al., 1984) and more recently the 6-OHDA lesioned rat, which has been well validated and established as an accurate, more affordable means of assessing the dyskinesiogenic potential of L-DOPA (Cenci et al., 1998). In rats, the extent and location of the lesion causes variation in the severity and onset of dyskinesia in a dose responsive manner and chronic L-DOPA therapy is associated with an increase in prodynorphin within the striatum mediated by an upregulation of the FosB/ Δ FosB transcription factor and other immediately early genes (Cao et al., 2010, Lane et al., 2009b, Pavon et al., 2006b, Westin et al., 2001, Rodriguez et al., 2001, Doucet et al., 1996). Subsequently, AIMs in both rats and mice have been validated and hence can be scored on specifically designed rating scales (Cenci and Lundblad, 2007, Winkler et al., 2002b), however in mice LID has not been fully validated and the best injection site of 6-OHDA along the nigrostriatal pathway for the development and hallmarks of AIMs has not yet been established. The most popular theory of LID development is that spared 5-HT neurones in the lesioned hemisphere cause the sporadic and unregulated release of dopamine, causing AIMs through uncontrolled post-synaptic simulation. Hyperinnervation of 5-HT has been found in rodent and primate models PD (Maeda et al., 1994, Gil et al., 2010, Rozas et al., 1998b, Maeda et al., 2003b, Zhou et al., 1991a), although the extent at which 5-HT fibre innervations contribute to the AIMs is unknown and debated, with little research carried out in the mouse model.

Motor and AIMs trends following L-DOPA have not been studied in detail and it remains to be seen if patterns established are equal to that of the rat. Prolonged daily L-DOPA treatment of 25mg/kg in rats with a full unilateral nigrostriatal lesion, and causes a ‘wearing off’ of the duration and increase in magnitude of the rotational response from the second to the third week of treatment, not seen in the terminally lesioned group (Papa et al., 1994, Marin et al., 2004). An increase locomotor sensitisation over time has not yet been reported in mice however a dose dependent increase in rotation was seen in Striatal and MFB groups (Lundblad et al., 2004a). Here we aim to compare dose dependent rotational differences and overall locomotion in lesioned mice in response to L-DOPA.

Another important factor to consider is whether histological markers, that have previously been linked with LID (levels of: TH, 5-HT and FosB/ Δ FosB), may be differently correlated with AIMs depending on lesion type. Results in this chapter will analyse whether these three models allow for varying destruction of 5-HT and TH fibres, and complete or partial destruction of the nigrostriatal pathway. Further, these histological were correlated with FosB/ Δ FosB protein expression in post-synaptic cells following L-DOPA, as this has previously been correlated to the denervation of TH immuno-reactive fibres in mice and rat 6-OHDA lesion models (Andersson et al., 1999, Andersson et al., 2003, Francardo et al., 2011b, Lundblad et al., 2004b).

The emergence of TH positive cells in the striatum of lesioned animals has triggered much interest of late, found in humans, MPTP treated non-human primates and unilateral 6-OHDA lesioned mice (Darmopil et al., 2008, Mazloom and Smith, 2006, Tande et al., 2006, Francardo et al., 2011b). TH neurones in the striatum were not found to be the result of neurogenesis and previous co-localisation studies have pointed towards a phenotypic shift from previously exclusive GABAergic cells to dopaminergic like cells (Darmopil et al., 2008, Tande et al., 2006). TH cells were found to be expressed 1 week post lesion and appear to be maintained by long-term L-DOPA treatment (Darmopil et al., 2008). However, it is still unclear how the presence of these cells correlates to dopaminergic cell loss within the SNpc and AIM development in response to L-DOPA in each lesion type.

In Chapter 3 it was shown that dopaminergic histological changes post lesion may be correlated with behavioural deficits seen on a wide range of hand tests. It remains unclear however if motor hand test scores can be used to predict animals which will become the most dyskinetic following L-DOPA priming and also whether the criteria, used to determine lesion extent, differs from that used to discriminate AIM development. Therefore this chapter compares both AIMs initiated at escalating doses of L-DOPA between each lesion group, and correlations of dyskinesia scores at 6mg/kg and 25mg/kg of L-DOPA with deficits on behavioural hand tests and histological measures.

4.2 Experimental design

The outline of this chapter is indicated in Figure 4.1. 120 adult male mice were used in this study. 6-OHDA was injected unilaterally in the SN (n=35), MFB (n=35), and striatum (n=35), with a group of intact control animals (n=10). Surgical procedures are detailed in Chapter 2. Surviving mice were then subject to an array of motor hand tests, see Chapter 3. In this study, 10 mice from each lesion group were chosen for dyskinesia assessment, all displayed significant contralateral akinesia and motor coordination deficits on the cylinder, apomorphine rotation, amphetamine rotation and corridor compared to unlesioned controls. Hence ‘failed’ and ‘partially lesioned mice’ (defined in Chapter 2) were likely excluded for the purpose of these experiments. All mice were treated daily with L-DOPA and AIMs assessed every 3-4 days. L-DOPA methyl ester HCl and the peripheral DOPA decarboxylase inhibitor: benserazide HCl (Sigma Aldrich) were dissolved in 0.9% saline immediately before use. The drugs were injected at the volume of 10ml/kg in a single daily intraperitoneal (i.p.) injection. Chronic treatment with L-DOPA was administered for daily for 64 days and consisted of four phases with incremental doses: -

- Phase 1 (days 1-13): all groups, at 2 mg/kg of L-DOPA with 2 mg/kg of benserazide.
- Phase 2 (days 14-40): all groups, 6mg/kg of L-DOPA with 6mg/kg of benzerazide.
- Phase 3 (day 41-55): all groups, 12 mg/kg of L-DOPA and 12 mg/kg of benzerazide.
- Phase 4 (days 56-59): all groups, 25mg/kg of L-DOPA and 12mg/kg of benzerazide*.

*the SN group continued to received L-dopa for a further 5 days as behaviours had not reached a plateau.

Animals were killed using terminal anaesthesia with perfuse fixation 24 hours after the last injection and brains harvested for histology.

For statistical analysis behavioural measures in corridor, grip strength, rotarod, balance beam, apomorphine rotation, amphetamine rotation, spontaneous rotation, staircase, activity and cylinder tests and TH positive cell counts are expressed as a percentage of the intact side. Cell bodies were counted under the Lecia light microscope in the VTA and SNpc at the level of the medial terminal nucleus of the accessory nucleus of the optic tract interception as described by (Dowd and Dunnett, 2004). The dencity of TH- and 5-HT-immunopositive neurons were assessed in the ventral and dorsal striatum, from images of every 4th section (taken with Leica

DFC420 camera and Lecia application V3.6 software) using the Zeiss imager 22 Fluorescence microscope with Axiovision 4 software and on ImageJ software (Version 1.42, National Institutes of Health, USA) and TH and 5-HT density levels were normalised to density levels of the corpus collosum. SPSS (version 16) was used to deduce statistical significance for all correlations and ANOVAs with Dunnett *post hoc* tests. TH cells within the striatum were counted in all sections from a 1 in 6 series through the mouse brain and corrected formulaically to deduce cell numbers in whole striatum.

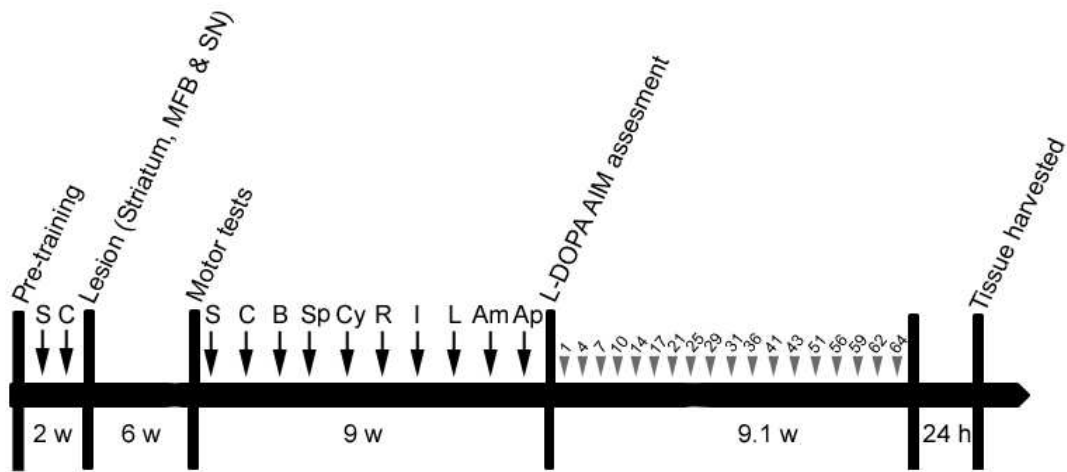


Fig. 4.1. Graphical representation of the experimental design. Motor tests were carried out consecutively: Staircase (S), Corridor (C), balance beam (B), spontaneous rotation (S), cylinder (Cy), rotarod (R), inverted cage lid (I), locomotor activity (L) amphetamine rotation (Am) and apomorphine rotation sessions (Ap). Grey arrow heads indicate the days in which dyskinesia was scored. Times are indicated in hours (h), days and weeks (w).

4.3 Results

4.3.1. Behavioural deficits in mice with 6-OHDA lesions of the Striatum, MFB or SN

Deficits on motor tests carried out prior to L-DOPA treatment were not significantly different between lesion only and L-DOPA treated lesion groups. Compared to non-operated controls, there was an overall lesion effect of dopaminergic depletion on behaviour (Table 4.1). Lesioned animals showed deficits in the rotarod ($F_{3,69} = 28.76, p < 0.001$), the balance beam ($F_{3,69} = 5.34, p < 0.01$), inverted cagelid ($F_{3,69} = 2.91, p < 0.05$), time on balance beam ($F_{3,69} = 2.92, p < 0.05$), cylinder ($F_{3,69} = 4.51, p < 0.01$), staircase ($F_{3,69} = 3.31, p < 0.05$), corridor ($F_{3,69} = 3.04, p < 0.01$), and basal locomotor activity ($F_{3,69} = 3.83, p < 0.01$). Rotational behaviours also demonstrated a clear lesion effect in total apomorphine ($F_{3,69} = 9.18, p < 0.001$), total amphetamine ($F_{3,69} = 4.80, p < 0.01$) and total spontaneous ($F_{3,69} = 16.33, p < 0.001$) test paradigms. Specific deficits according to lesion type were noted by pair wise comparisons as indicated on Table 4.1, where deficits were less pronounced for individual lesion groups.

Lesion Type / Hand test	Intact Control	Striatum	MFB	SN
Rotarod	131.65 ± 6.08	66.75 ± 5.95***	45.82 ± 2.89***	77.15 ± 6.97***
Cagelid	215.26 ± 30.85	117.47 ± 11.09*	155.84 ± 17.91	153.09 ± 24.60
Amphetamine rot (total)	26.72 ± 6.84	81.61 ± 6.60***	87.55 ± 11.88***	72.34 ± 11.47***
Apomorphine Rot (total)	2.70 ± 0.39	29.41 ± 4.44***	59.65 ± 9.43***	33.10 ± 6.16***
Spontaneous Rot (total)	8.20 ± 0.78	12.90 ± 1.45	22.35 ± 2.31***	8.70 ± 0.76
% Balance Beam	68.62 ± 8.13	73.52 ± 3.07	73.9 ± 3.22*	80.21 ± 3.59
% Cylinder	57.82 ± 2.12	77.18 ± 3.43*	73.41 ± 3.21*	66.37 ± 3.91
% Corridor	36.69 ± 6.04	18.69 ± 3.42*	16.81 ± 3.07*	27.17 ± 4.41
% Staircase	49.85 ± 2.33	49.61 ± 0.69	52.98 ± 0.76*	46.14 ± 2.41
Beam time	13.59 ± 2.57	16.79 ± 1.42	20.90 ± 1.16	17.27 ± 1.68
Activity Preseverative	663.40 ± 27.43	631.70 ± 46.99	469.50 ± 25.70	710.50 ± 80.93
Activity non-preseverative	1320.70 ± 76.13	1382.60 ± 147.61	1137.70 ± 71.45	1429.40 ± 191.03

Table 4.1. Deficits in mice lesioned at the level of the striatum, MFB or SN compared to intact controls on a battery of motor hand tests (mice with failed and partial lesions excluded). Significant differences are indicated by $p < 0.05^*$, $p < 0.01^{**}$ and $p < 0.001^{***}$. Values are expressed as means ± SEM.

4.3.2 Histological comparison of mice with 6-OHDA lesions of the Striatum, MFB or SN

Mice were pre-selected from the cohort used in Chapter 1 to have substantial TH cell losses based on motor hand tests. Fig. 4.2A-H show representative photomicrographs of TH and 5-HT neuronal loss present in all lesion groups. Dopamine depletion in the SNc was consistently high in all lesioned mice (Fig. 4.2M; $F_{3,69} = 14.80$, $p < 0.001$;) compared to intact controls, which was also reflected in a substantial reduction in dorsal TH density levels. Overall there was also a substantial loss in the percentage of cells remaining in VTA (Fig. 4.2N; $F_{3,69} = 11.63$, $p < 0.001$) and this was reflected in corresponding TH fibre loss in the ventral striatum. Mice lesioned at the SN or striatum had a greater sparing of fibres in the ventral striatum than those with an MFB lesion, yet a high depletion was seen in all groups (Fig. 4.2P; $F_{3,69} = 13.05$, $p < 0.001$).

The sparing of 5-HT fibres were highly variable within groups (Fig. 4.2I-L), yet little sparing was evident in both the dorsal (Fig. 4.2Q; $F_{3,69} = 3.14$, $p < 0.05$) and ventral striatum (Fig. 4.2R; $F_{3,69} = 3.15$, $p < 0.05$). Specifically, a lack of sparing in dorsal and ventral striatum 5-HT density was only seen in the MFB lesioned group ($p < 0.05$), with no difference between lesion only and L-DOPA treated lesioned mice.

Fig 4.3 illustrates that the most significant increase in FosB/ Δ FosB levels was found within the dorsal striatum in all lesion groups (A-H) where there was a significant effect of L-DOPA treatment (Fig. 4.3I; $F_{2,67} = 23.43$, $p < 0.001$) compared to lesion only mice and levels seen in the intact control group. For the dorsal region there was also an effect of lesion type ($F_{3,69} = 21.04$, $p < 0.001$), where the highest FosB/ Δ FosB expression found in the L-DOPA-treated MFB lesioned group compared to SN or striatal lesioned groups receiving the same treatment ($p < 0.001$). When assessed in the NAcc core the number of FosB/ Δ FosB positive cells was only significantly increased in the Striatal lesioned group following L-DOPA treatment (Fig. 4.3J; $p < 0.05$). L-DOPA treatment also increased the number of FosB/ Δ FosB positive cells ($F_{2,67} = 18.69$, $p < 0.001$; Fig. 4.3k) within the NAcc shell region, with no overall difference between lesion type.

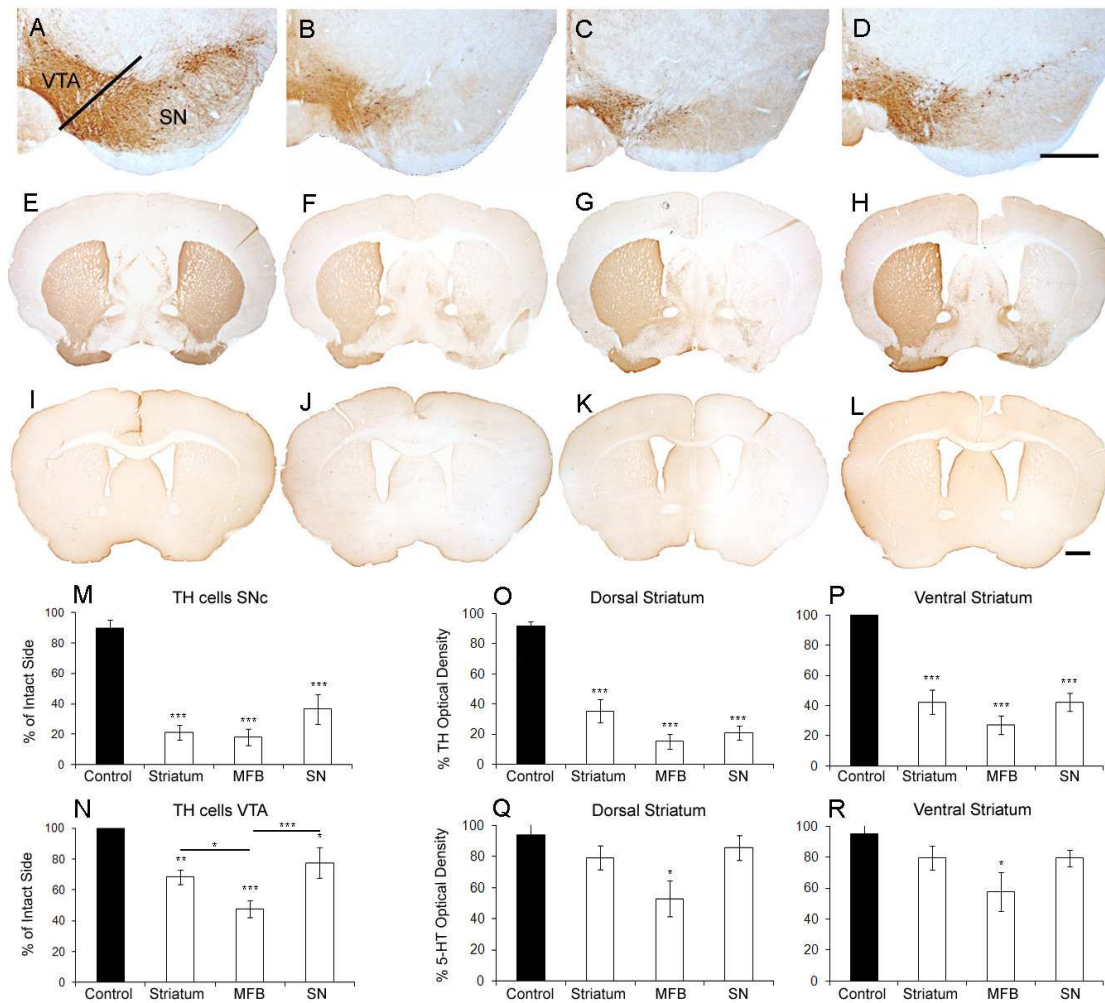


Fig. 4.2. Photomicrographs of the SNc in mice, immunostained with TH, in an unlesioned control mouse (A) and mice with a 6-OHDA lesion of the Striatum (B), MFB (C) and SN (D) (Scale bar 400 μ m). Photomicrographs are also shown for whole forebrain sections immuno stained for TH (E-H) and 5-HT (I-L) on (scale bar 2mm). % TH cell loss from the SNc and VTA is shown for the 6-OHDA lesioned, L-DOPA-treated groups compared to the unlesioned side (M,N). Optical density was used to measure relative TH and 5-HT expression in the dorsal striatum and ventral striatum for each lesion type (O-R). Significant deviations from intact control animals and between lesion groups are indicated by $p < 0.05^*$, $p < 0.01^{**}$ and $p < 0.001^{***}$. Values are expressed as means \pm SEM.

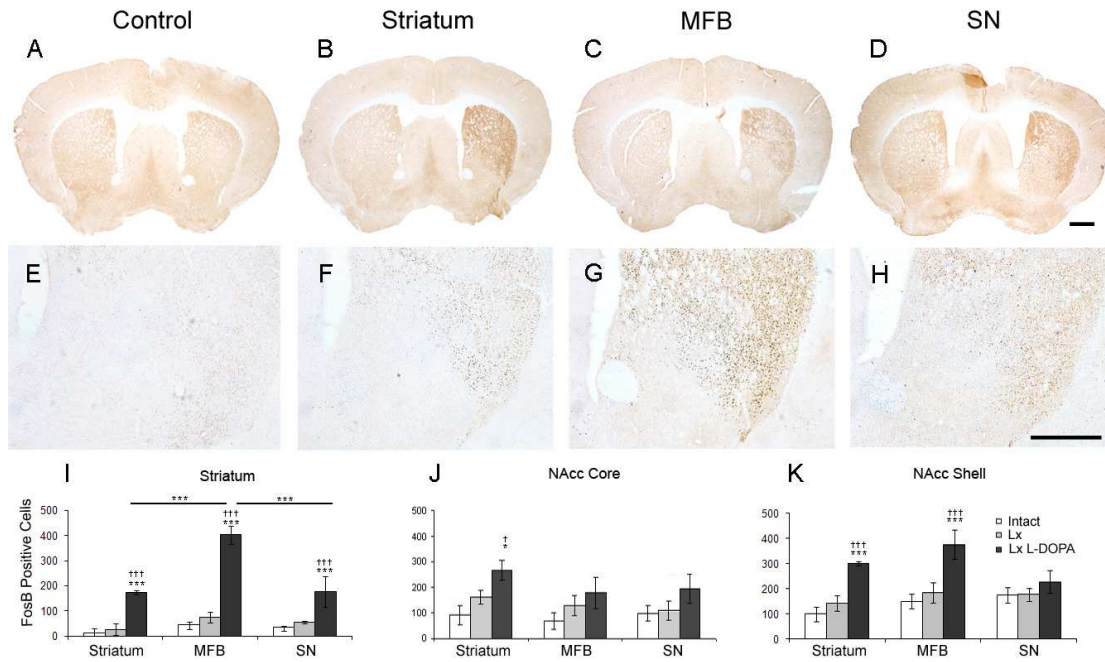


Fig. 4.3. Photomicrographs of sections immuno-stained for FosB/ Δ FosB on mice with a 6-OHDA lesion of the striatum, MFB and SN compared to unlesioned controls (scale bar 2mm; A-D) and at 5x magnification FosB/ Δ FosB (E-H), where the scale bar shown is 500 μ m. The number of FosB/ Δ FosB positive cells within the whole striatum, NAcc core and NAcc shell were counted (I-K). Significant differences from intact control animals and between L-DOPA treated groups are indicated by $p < 0.05^*$, $p < 0.01^{**}$ and $p < 0.001^{***}$. Values are expressed as means \pm SEM.

4.3.3 L-DOPA-induced AIMs, activity and rotation.

The analysis of LID in each lesion group was only undertaken in animals with the largest behavioural deficits, indicating a near to complete lesion, as rodents with partial lesions are not responsive to low dose L-DOPA (Winkler et al., 2002b, Francardo et al., 2011b). In general, AIMs in all lesioned mice treated with chronic L-DOPA, increased at each dose over the course of L-DOPA administration ($F_{4,108} = 15.42, p < 0.001$). Moreover, there was a difference between the magnitude of the AIMs that were expressed the lesion groups and the L-DOPA dose at which AIMs were first exhibited (Group, $F_{2,27} = 14.15, p < 0.001$; Group x Phase, $F_{8,108} = 7.71, p < 0.001$). Fig. 4.4A-B highlights that the lowest dose of L-DOPA (2mg/kg) induced minor AIMs only in the mice with MFB lesions. The MFB lesion group continued to express AIMs at progressively higher levels as the L-DOPA dose was increased in phase 2 (6mg/kg), phase 3 (12mg/kg) and phase 4 (25 mg/kg), compared to SN and Striatal lesion types. In addition, the SN and Striatal groups did not display significant AIMs until phase 3 (12mg/kg), but the severity of AIMs then increased further at phase 4 (25mg/kg). AIMs in the MFB group were consistently greater than those in the SN and Striatal groups throughout all phases (Fig. 4.4B).

Horizontal L-DOPA induced locomotor activity increased between 2mg/kg and 6mg/kg and remained significantly elevated for higher doses (Fig. 4.4 C,D; $F_{4,108} = 5.19, p < 0.001$). There was no significant overall effect of lesion type, although there was a significant Group x Phase interaction (Fig. 4.4C,D; $F_{8,108} = 3.71, p < 0.001$). Further, the percentage of animals of the total cohort that displayed L-DOPA driven turning behaviour, recorded as an observation in the activity cage, gradually increased over the 4 phases (Fig. 4.4E). A dose-dependent increase in total net rotations ($F_{1,28} = 4.21, p < 0.05$) was also noted, between the plateau phases 2 (6mg/kg) and 4 (25mg/kg). Subsequent *post hoc* analysis found this trend was only significant in the Striatal group (Fig. 4.4F; $p < 0.05$).

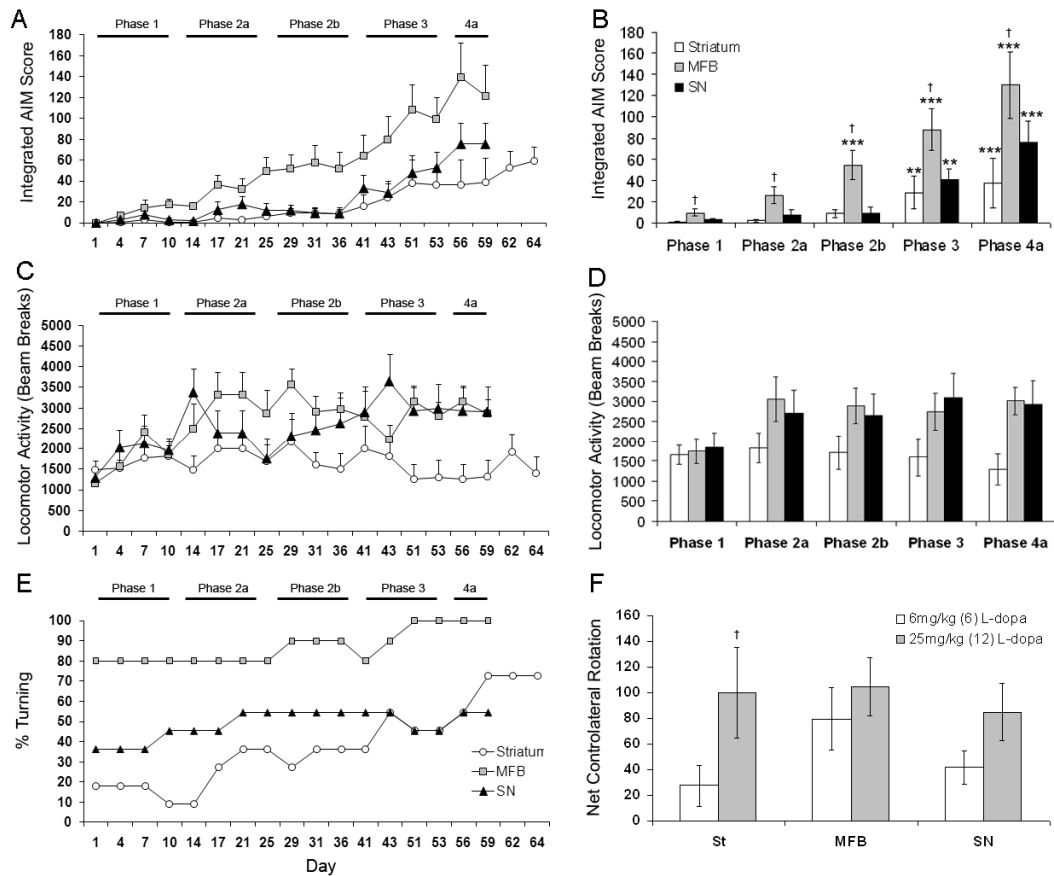


Fig. 4.4. AIMs induced by L-DOPA administration, in mice with striatal, nigral or MFB 6-OHDA lesions scored on the Cenci and Lundblad rating scale each day (A) and averaged for each phase (B), where phase 1 = 2(2)mg/kg (days 1-13), phase 2 = 6(6)mg/kg (days 14-40), phase 3 = 12(12)mg/kg (days 41-55) and phase 4 = 25(12)mg/kg (days 56-59); brackets indicate dose of benzerazide used. Simultaneous horizontal locomotor recorded scored each day (C) and mean activity are shown (D). Also displayed are the percentage of mice in each group that turned in response L-DOPA treatment by day (E) and net contralateral rotations for each lesion type scored at 6mg/kg and 25mg/kg (F). *post hoc* comparisons from are indicated as $p < 0.01^{**}$ and $p < 0.001^{***}$ and compared to the MFB group at each phase as $p < 0.05^{\dagger}$. Significance found between rotational bias between 6mg/kg and 12mg/kg are annotated as $p < 0.05^{\dagger}$. Values are expressed as means \pm SEM.

4.3.4 Correlation of dyskinesia with behavioural hand test scores.

The severity of AIMs at the end of phases 2 and 4 were correlated with motor defects on a select hand tests. Table 4.2 indicates all partial Pearson's correlation between AIMs and behavioural hand test scores, with SNc depletion as a control factor. Contralateral rotation in response to L-DOPA correlated with AIMs in all lesioned mice at 6mg/kg ($r=0.422$, $p<0.01$) and 25mg/kg ($r=0.445$, $p<0.01$). Table 4.2 also shows that a greater number of motor deficit tests correlate to AIMs induced by 25mg/kg of L-DOPA than 6mg/kg, as AIMs were at maximum levels. At 6mg/kg AIMs in all mice were only correlated with total apomorphine driven turns ($r= 0.305$, $p<0.05$), latency to fall on the rotarod ($r= -0.508$, $p<0.01$) and total spontaneous turns ($r=0.541$, $p<0.01$). In contrast AIMs driven by 25mg/kg were correlated to both non- perseverative locomotor activity ($r= -0.460$, $p<0.05$) and perseverative locomotor activity ($r= -0.420$, $p<0.05$) and but were no longer correlated to tests at the lower dose.

When considering each lesion type (Table 4.2) the most consistent correlations with AIMs at 6mg/kg between groups were found on deficits recorded on the rotarod (Striatum: $r= -0.558$, $p<0.05$, MFB: $r= -0.763$, $p<0.05$; SN: $r= -0.784$, $p<0.01$). There were also clear general trends in all groups for correlation to apomorphine and amphetamine rotation. Further analysis showed that scores on the rotarod remained correlated with AIMs elicited by 2mg/kg ($r= -0.498$, $p<0.01$) but not 12mg/kg or 25mg/kg. In contrast correlations driven by 25mg/kg were found with perseverative locomotor activity and non-perseverative locomotor activity, but were only noted in MFB and SN lesion groups ($p<0.01$). Furthermore strong correlations between total apomorphine rotations ($p<0.001$) and rotarod ($p<0.05$) with AIMs at 25mg/kg were only seen in MFB lesioned mice.

<i>Hand test/AIMs</i>	<i>Overall</i>	<i>Str</i>	<i>MFB</i>	<i>SN</i>	<i>Overall</i>	<i>Str</i>	<i>MFB</i>	<i>SN</i>
	6mg/kg				25mg/kg			
L-DOPA Rot (6mg/kg)	0.422**	0.882***	-0.200	-0.492	N/A	N/A	N/A	N/A
L-DOPA Rot (25mg/kg)	N/A	N/A	N/A	N/A	0.445**	0.692*	0.045	0.041
Rotarod	-0.508**	-0.558*	-0.763*	-0.784**	-0.285	-0.440	-0.620*	-0.517
Cagelid	0.001	-0.317	-0.201	-0.519	-0.135	0.122	-0.507	-0.445
Amphetamine rot (total)	0.140	0.454	0.308	0.339	-0.320	0.194	-0.337	-0.110
Apomorphine Rot (total)	0.305*	0.389	0.415	0.684*	0.304	-0.268	0.896***	0.552
Spontaneous Rot (total)	0.541**	0.039	0.284	0.110	0.350	0.524	0.505	0.208
Balance Beam	0.066	0.003	0.197	0.309	0.105	-0.183	0.431	0.026
Cylinder	0.034	0.309	-0.431	-0.707*	0.139	0.567	-0.497	-0.439
Corridor	-0.182	-0.229	-0.400	-0.367	-0.198	-0.268	-0.324	-0.147
Staircase	0.156	0.170	-0.267	-0.092	0.154	-0.214	-0.395	-0.357
Beam time	0.194	0.437	0.114	0.092	0.105	0.026	-0.183	0.431
Activity Preseverative	-0.298	0.301	-0.310	-0.586	-0.420*	-0.260	-0.772**	-0.682*
Activity non-preseverative	-0.214	-0.319	-0.241	-0.546	-0.460**	-0.182	-0.699*	-0.695*

Table 4.2. Pearson's correlation coefficients between average AIMs at peak responses to 6mg/kg and 25mg/kg with L-DOPA induced behaviours and tests of motor function, with confounding correlations between AIMs and % of cells remaining in the SNc controlled for. Correlation co-effects are indicated for the total L-dopa treated cohort and for each lesion type, where $p < 0.05^*$, $p < 0.01^{**}$ and $p < 0.001^{***}$. † indicates where correlation coefficient could not be deduced as all animals rotating 100% to the contralateral side of the lesion in the MFB group.

4.3.5 Correlating AIMs with histological measures

AIM scores could be correlated with TH, 5-HT and FosB/ Δ FosB differently depending on dose and lesion type. It can be seen from Table 4.3 that there was a correlation between cell loss within the SNc with AIMs score at 25mg/kg ($r = -0.533$, $p < 0.01$) and the VTA with AIMs score at 6mg/kg (Table 4.3; $r = -0.596$, $p < 0.01$). When looking more closely at individual lesion groups AIMs were correlated significantly in the MFB group with respect to cell counts within the SNc ($r = -0.577$, $p < 0.05$) and the SN group with respect to the VTA ($r = -0.577$, $p < 0.05$). Table 4.3 also shows that TH density in the dorsal striatum was correlated with AIMs at 6mg/kg ($r = -0.341$, $p < 0.05$) and at 25mg/kg ($r = -0.596$, $p < 0.01$). Similar trends in density were seen in respect to the ventral striatum at 25mg/kg ($r = 0.554$, $p < 0.01$) with an overall trend at the lower dose.

There was also a weak overall positive correlation with ventral 5-HT density and AIMs (Table 4.4) at 6mg/kg ($r = 0.325$, $p < 0.05$) and dorsal density at 25mg/kg ($r = 0.343$, $p < 0.05$). In addition, L-DOPA induced AIMs were moderately correlated to 5-HT density only in the MFB group at 6mg/kg, within the ventral striatum ($r = 0.616$, $p < 0.05$) and dorsal striatum ($r = 0.618$, $p < 0.05$). However this trend was lost at high dose L-DOPA and was not found in mice with SN or Striatal lesions.

FosB/ Δ FosB cell counts within the striatum, NAcc core and NAcc shell were correlated to the development of AIMs in all three different unilateral lesioned mouse models (Table 4.5). At phase 2 (6mg/kg) AIMs and FosB/ Δ FosB cell counts are only positively correlated in the NAcc shell region ($r = 0.583$, $p < 0.05$). At 25mg/kg FosB/ Δ FosB is highly correlative to dyskinesia in the striatum ($r = 0.754$, $p < 0.01$) and NAcc core ($r = 0.525$, $p < 0.01$) in all mice. This striatal FosB/ Δ FosB upregulation in response to L-DOPA persists in striatum ($r = 0.852$, $p < 0.01$), MFB ($r = 0.583$, $p < 0.05$) and SN ($r = 0.713$, $p < 0.05$) groups, despite overt differences between the severity of AIMs in the three groups at phase 4 (25mg/kg). FosB/ Δ FosB levels do not correlate significantly with AIMs present from 2 or 12mg/kg of L-DOPA although a trend can be noted in the latter dose. In addition, a positive correlation was noted between L-DOPA induced rotation at 25mg/kg and FosB/ Δ FosB positive cells in the NAcc shell in MFB lesioned mice ($r = 0.664$, $p < 0.05$).

<i>AIMs/TH</i>	<i>TH Cells (SN)</i>	<i>TH Cells (VTA)</i>	<i>TH Density (Dorsal)</i>	<i>TH Density (Ventral)</i>
Overall (6mg/kg)	-0.310	-0.521**	-0.341*	-0.229
Str (6mg/kg)	0.128	0.102	0.043	-0.172
MFB (6mg/kg)	-0.544	-0.550	-0.416	-0.529
SN (6mg/kg)	-0.379	-0.544	-0.415	-0.529
Overall (25mg/kg)	-0.533**	-0.267	-0.596**	-0.554**
Str (25mg/kg)	-0.527	-0.55	-0.591*	-0.602*
MFB (25mg/kg)	-0.577*	-0.452	-0.522	-0.653*
SN (25mg/kg)	-0.548	-0.577*	-0.522	-0.563*

Table 4.3. Pearson’s correlations between average integrated AIMs at 6mg/kg and 25mg/kg with cell counts within the SNpc and VTA and TH density values within the dorsal and ventral striatum of L-DOPA treated mice. Statistically significant correlation co-efficients overall and specifically for mice lesioned to the striatum, MFB and SN are indicated by $p<0.05^*$ and $p<0.01^{**}$.

<i>AIMs/TH</i>	<i>5-HT Density (Cortex)</i>	<i>5-HT Density (Ventral)</i>	<i>5-HT Density (Dorsal)</i>
Overall (6mg/kg)	0.263	0.325*	0.245
Str (6mg/kg)	0.226	0.051	0.193
MFB (6mg/kg)	0.433	0.616*	0.618*
SN (6mg/kg)	0.980	-0.054	0.168
Overall (25mg/kg)	0.054	0.127	0.343*
Str (25mg/kg)	0.450	-0.020	0.042
MFB (25mg/kg)	0.131	0.432	0.415
SN (25mg/kg)	-0.100	-0.020	0.188

Table 4.4. Pearson’s correlations between integrated AIMs at 6mg/kg and 25mg/kg with 5-HT density values in the dorsal and ventral striatum. Statistically significant correlation co-efficients overall and specifically for mice lesioned to the striatum, MFB and SN are indicated by $p<0.05^*$ and $p<0.01^{**}$.

<i>AIMs/</i>	<i>FosB Cells (Str)</i>	<i>FosB Cells (NAcc core)</i>	<i>FosB Cells (NAcc shell)</i>
Overall (6mg/kg)	0.217	0.199	0.316*
Str (6mg/kg)	0.216	0.390	-0.23
MFB (6mg/kg)	0.317	0.164	0.583*
SN (6mg/kg)	0.272	-0.052	0.138
Overall (25mg/kg)	0.754**	0.525**	0.298
Str (25mg/kg)	0.852**	0.469	0.195
MFB (25mg/kg)	0.357	0.733*	0.483
SN (25mg/kg)	0.713*	0.138	0.418

Table 4.5. FosB/ Δ FosB cell counts within NAcc core, NAcc shell and whole striatum correlated with total integrated AIM scores in L-DOPA treated mice. Statistically significant correlation co-efficients overall and specifically for mice lesioned to the striatum, MFB and SN are indicated by $p < 0.05^*$ and $p < 0.01^{**}$.

4.3.6 *Quantification of TH positive cells in the striatum of 6-OHDA lesioned mice*

TH positive cells were identified in the striatum of all lesioned mice (Fig. 4.5A-C). They appear medium sized, displayed apparently aspiny projections (Fig. 4.5G) and were darker in appearance in L-DOPA treated groups. TH positive cells were also increased significantly in number by L-DOPA treatment compared to lesion only controls (Fig. 4.5D-F). TH immunopositive cells in the striatum of lesioned mice also co-expressed GABA (Fig. 4.6), even after chronic L-DOPA treatment. The distribution these cells were ubiquitous across the lesioned striatum with little observed difference between counts in the dorsal and ventral striatum. There was a significant increase of TH cell occurrence by L-DOPA treatment in the whole striatum ($F_{1,59} = 12.19, p < 0.001$) and where dorsal ($F_{1,59} = 14.68, p < 0.001$), ventral ($F_{1,59} = 8.11, p < 0.01$) regions were considered separately. No differences however were found between lesion types. *Post hoc* analysis has further shown that significant changes were seen in the whole striatum in MFB ($p < 0.001$) and SN ($p < 0.001$) lesioned groups, but was not seen in mice receiving a Striatal lesion.

The number of TH expressing cells in the whole striatum correlates with the percentage of cell loss within the SNc in L-DOPA treated mice receiving either MFB or SN lesions but not non-L-DOPA treated groups (Fig. 4.5J,K; $r = -0.690$ and $r = -0.811$ respectively, where $p < 0.01$ for both). AIMS present at phase 4 (25mg/kg) were also correlated to the number of TH positive cells in the striatum in all lesioned animals ($r = 0.539, p < 0.01$). With the confounding correlations between cell loss in the SNc taken into account and factored into the partial correlation, AIM development was only correlated to TH cells in the L-DOPA treated MFB group ($r = 0.642, p < 0.01$).

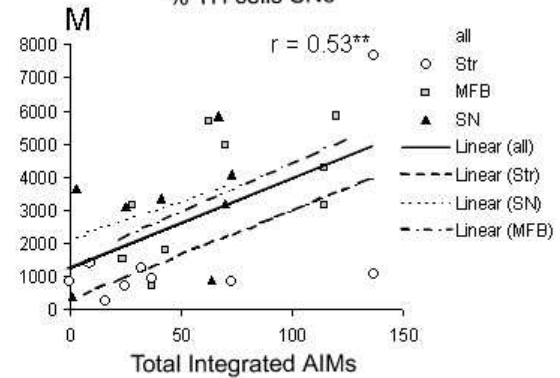
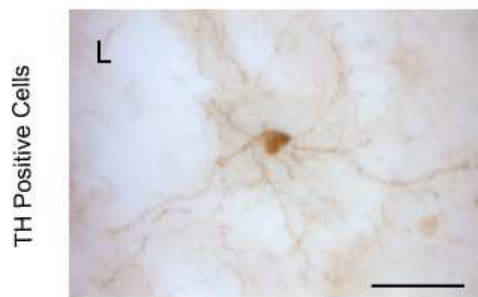
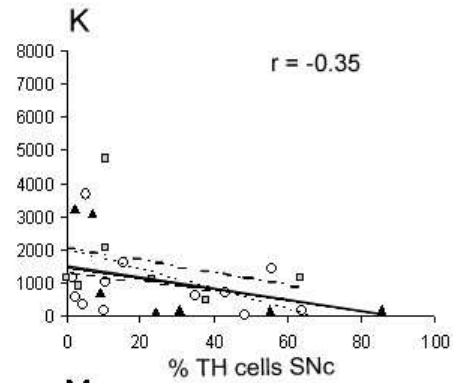
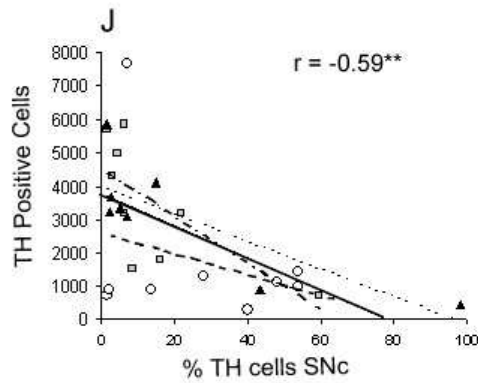
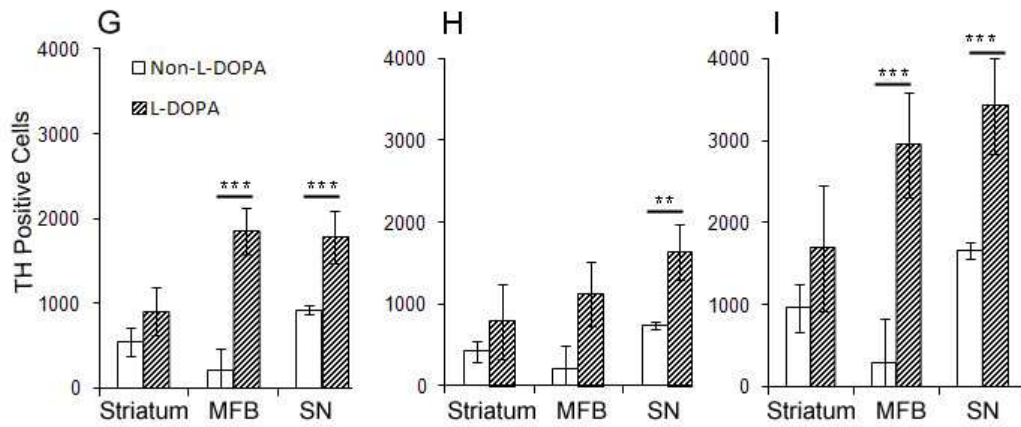
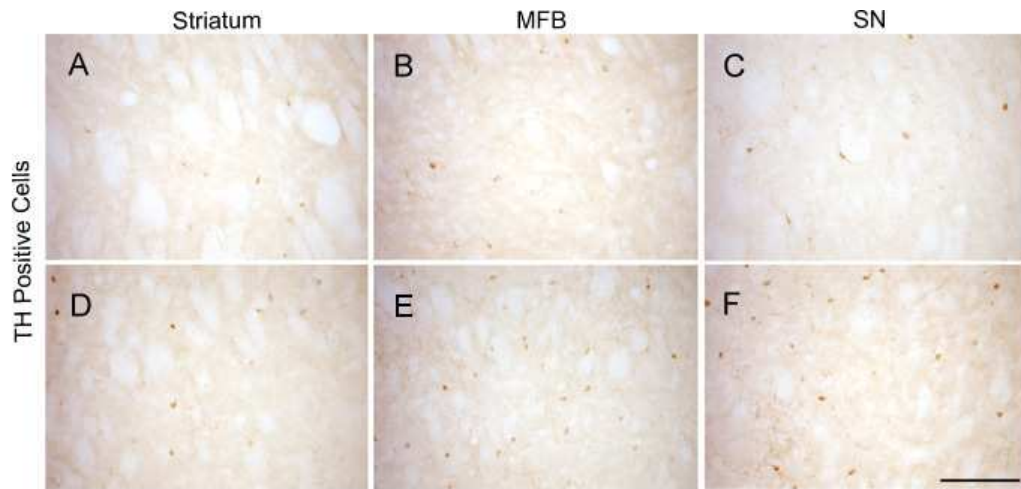


Fig. 4.5 Photomicrographs of TH immunopositive cells in the striatum of lesion only controls (A, Striatum; B, MFB; C, SN) and L-DOPA treated groups (D, Striatum; E, MFB; F, SN); scale bar is 200 μ m. A high magnification image is shown in (scale bar 50 μ m; L). TH immunopositive cells were quantified in L-DOPA and non-L-DOPA treated groups in the dorsal (G), ventral (H) and whole (I) striatal areas. TH immunopositive cells were correlated with % cell loss in the SNc of Non-L-DOPA treated (J) and L-DOPA treated lesioned mice (K) and total integrated AIMs (25mg/kg; M). Specific values and lesion trends are indicated for the Striatal lesion group by circle outlines and dashed lines, the MFB group by filled circles and dotted lines and SN group by filled triangles and dashed-dotted lines. Significant whole correlation coefficients and increases in TH cell numbers in L-DOPA treated mice are labelled as $p < 0.01^{**}$ and $p < 0.001^{***}$. Values are expressed as means \pm SEM.

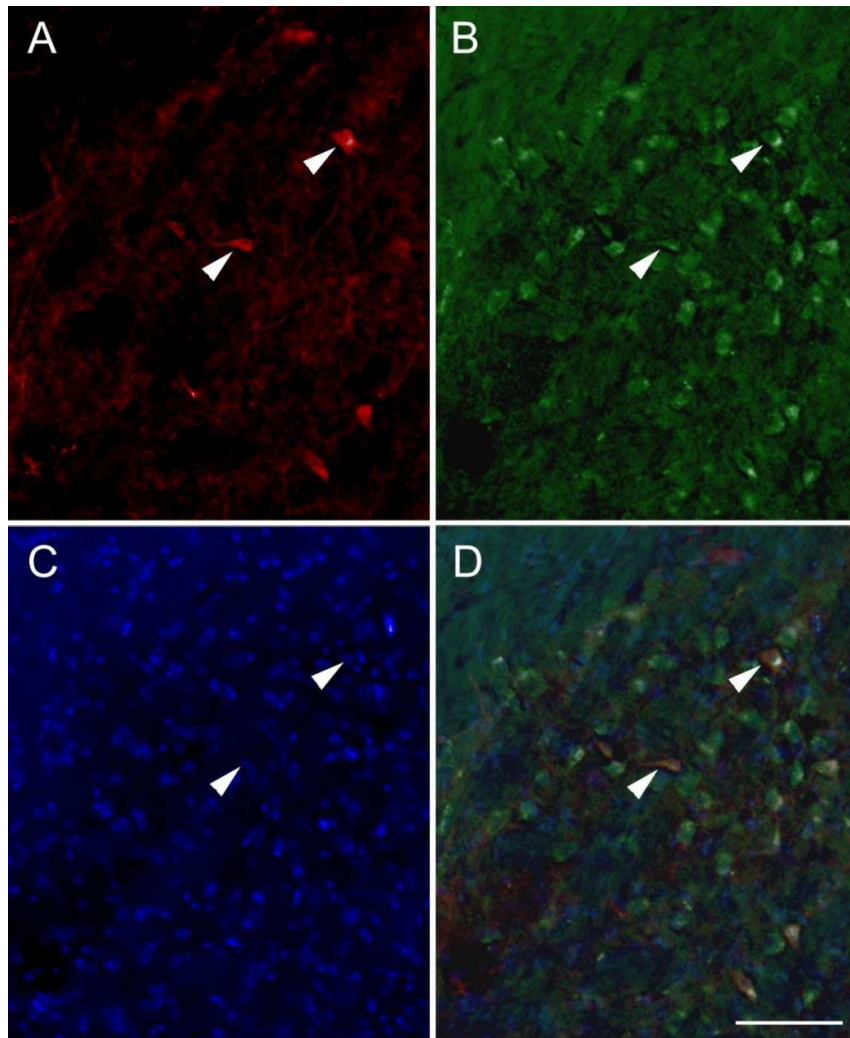


Fig. 4.6. Photomicrographs of sections immune-stained for TH (A), GABA (B), Hoechst (C) and merged (D). Arrow heads indicate cells expressing all markers. Scale bar = 100 μ m.

4.4 Discussion

The progression of AIMs, locomotion and rotation that manifest from phases 1-4 (6-25mg/kg) is reliant on the degree of depletion in the VTA and SNc. In addition, we find that TH fibre depletion, 5-HT fibre depletion and FosB/ Δ FosB positive cell upregulation in the striatum correlate with dyskinesia expression at both 6mg/kg and 25mg/kg of L-DOPA. All selected lesioned mice displayed deficits on motor hand tests before the initiation of L-DOPA treatment, and a proportion these deficits can correlate both to dyskinesia expression and to cell loss in the SNc. A small proportion of the behavioural tests remained predictive of subsequent AIM expression, even once allowance is made (by partial correlation analysis) for the extent of dopamine cell loss. These data suggest that mice can be preselected for future dyskinesia experiments to express severe AIMs following chronic L-DOPA treatment both on the basis of cell loss and directly by deficits on motor hand tests.

4.4.1. *Histological characterisation of the lesions*

The greatest losses of TH positive neurons in the SNc were seen in Striatal and MFB groups with a more moderate depletion in the SN lesion group. Differences in the levels of 5-HT depletion and non-nigral dopamine cell losses were also obvious between lesion types. VTA dopamine cell loss was the most depleted in the MFB lesion group, with a higher degree of sparing produced by Striatal and SN lesions. It can be assumed that the targeting of a lesion on a specific nucleus may produce focal denervation with extensive sparing at the nucleus periphery. This is in contrast to cases where the toxin is focally injected into a compact fibre bundle where the toxin can be transported and hence degeneration spreads along the length of the fibre pathway.

Post lesional 5-HT was not spared in the MFB lesion group and was likely due to the loss of 5-HT fibres, although this was highly variable between individual mice. This contrasts with the only other study to examine 5-HT changes in 6-OHDA lesioned mice, in which no differences in whole striatal 5-HT levels were observed following MFB lesion (Francardo et al., 2011b). This may be due to procedural differences, the total quantity of 6-OHDA infused in this study was less than the one presented here and was administered through a fine glass capillary as opposed to a metal cannula. These two factors may have produced less non-specific damage in their study, leading to a more selective dopaminergic lesion. Also whole 5-HT levels as measured by HPLC are not directly comparable to density as storage capacity may have

increased allowing more 5-HT to be stored with fewer fibres. It can be proposed however that the 5-HT depletion may not be a disadvantage so long as they are considered, and maybe of further use to study dyskinesia in animal models. There is a positive correlative relationship between total integrated AIM score and 5-HT density when using dopamine cell loss in the SNc as a covariate. Given that in PD there is a significant serotonergic depletion, this may be valuable in the study of PD and of particular relevance to the study of L-DOPA mediated behaviours. There is growing evidence that in the absence of dopaminergic terminals, dopamine is synthesised, stored and released in 5-HT terminals. Although they contain AADC so that L-DOPA may be converted, they are unable to regulate the release of dopamine (Arai et al., 1995), since they lack the normal feedback mechanisms of autoreceptors. These data show that the aberrant pulsatile monoamine release is a major factor in the development of LID, in agreement with other studies (Scatton et al., 1983, Carta et al., 2007). This relationship warrants further investigation, as 5-HT changes in PD models and their contribution to dyskinesia is debated and appears to be dependent upon age at time of lesion, lesion type and maybe species (Gil et al., 2010, Maeda et al., 2003a, Rozas et al., 1998a, Zhou et al., 1991b).

FosB/ Δ FosB expression was induced significantly in the striatum and NAcc regions in all lesioned mice. It is evident that high fosB/ Δ FosB expression in the NAcc in MFB lesion groups is mediated by the lack of TH fibre innervation of this area, a pattern well established in the striatal region (Andersson et al., 1999, Andersson et al., 2003, Francardo et al., 2011b, Valastro et al., 2007, Westin et al., 2001). The ventral striatal density loss seen in the MFB group can be attributed to high levels of neuronal loss in the VTA resulting from optimised stereotaxic co-ordinates. Although other studies have not looked specifically in the NAcc, striatal FosB/ Δ FosB expression has previously been found to be highest in MFB lesion mice compared to Striatal lesioned groups (Francardo et al., 2011b), also consistent with our findings. Dyskinetic mice with SN lesions also have an increase in FosB/ Δ FosB expression in the dorsal striatum which is comparable to the Striatal lesion group, with less expression in the ventral striatum owed to sparing of TH fibres in that location. In addition, cocaine-induced sensitisation can induce increases of FosB/ Δ FosB in the NAcc shell (Brenhouse and Stellar, 2006), analogous to levels shown here, indicating the likely role of L-DOPA in supersensitisation specifically in this region.

4.4.2. Lesion effects on L-DOPA dyskinesia

Here we show a comprehensive longitudinal analysis of the dyskinetic responses of mice with lesions of the striatum, MFB and SN, through a range of L-DOPA doses. In previous studies, AIMs in mice with unilateral MFB or Striatal lesions were triggered by doses in the range of 6mg/kg and 18-20mg/kg respectively (Lundblad et al., 2002, Lundblad et al., 2004b, Francardo et al., 2011b). Those with MFB lesions started to show dyskinesia at 6mg/kg, whilst Striatal or SN lesion mice developed AIMs at 12mg/kg, lower than previously found. These studies also found a lower severity of AIMs following Striatal and SN lesions in C57/Bl6 mice compared to the MFB group even at a 25mg/kg dose of L-DOPA. In this study 6-OHDA lesions caused equivalent dopamine cell loss in the SNc in the Striatal group using the same strain (Lundblad et al., 2002, Lundblad et al., 2004b), yet cell loss was significantly less compared to MFB group, which is likely to be the primary reason why dyskinesia were evoked at a lower dose. We report similar striatal lesion extents compared to a recent study (Francardo et al., 2011b) with a dose almost twice as high, indicating the difficulty of depleting the entire striatum with the chosen 2x1.5µl volume.

Mice that show few or no AIMs and are termed ‘non-dyskinetic’ (defined as having an integrated AIM score of less than 20). The dyskinetic status of lesioned mice is in part due to dose: at low doses, some animals only show few AIMs (non-dyskinetic) however long term treatment at higher doses increases the severity of AIMs gradually over time until a plateau is reached, here AIMs may surpass threshold levels and mice are considered ‘dyskinetic’. Following chronic treatment in rats with Striatal and MFB lesions approximately 20-35% of the cohort will continue to be classified as ‘non-dyskinetic’ with the moderate dose of 9-11mg/kg (Winkler et al., 2002b). In this study we found only 7% of MFB lesion mice were non-dyskinetic at 6mg/kg and this is consistent with studies of LID where low levels or the absence of non-dyskinetic mice were seen (Lundblad et al., 2004b, Lundblad et al., 2005). Conversely, 60% of Striatal lesion mice were non-dyskinetic at 6mg/kg (Francardo et al., 2011b), while few mice from our cohort had significant AIMs at that dose. The lack of mice that could be scored below the dyskinetic threshold at higher doses suggests that AIMs may also in part relate to species differences in basal movements and plasticity. Kinetic differences in exploratory movement, including the observation that mice have faster grooming behaviours could contribute to AIM scores by some investigators. The dose-dependent progressive development of AIMs also illustrates that the impact of apomorphine was likely minimal and priming was still permitted.

Dyskinetic priming and maintenance in mice lesioned directly at the level of the SN was observed for the first time in our cohort. AIM expression patterns are highly comparable to the striatum group likely due to similar levels of VTA cell loss. Animals in both groups remain largely non-dyskinetic until 12mg/kg and have AIMs of a similar magnitude. Strong L-DOPA driven contralateral rotations in the MFB group and correspondingly high horizontal locomotor activity are likely caused by the extensive VTA damage. This response is likely to manifest in the same manner as amphetamine and apomorphine mediated turning traits (Olds et al., 2006), arising from psychostimulant evoked supersensitisation in the NAcc.

Chronic exposure to L-DOPA pre- and post-synaptic changes, and causing a worsening of symptoms (Stocchi, 2006), this is often referred to as a ‘wearing off’ effect approximately two weeks after the start of treatment. Some studies have shown that long term L-DOPA treatment in hemi-parkinsonian rats causes a shortened rotational response and an increase in magnitude from the second to the third week of treatment (Papa et al., 1994, Marin et al., 2004). There is speculation that this may be related to high doses or the lesion site as this response is not seen in rats following a striatal lesion. In this study we found no evidence of ‘wearing off’ of the AIMs or rotational response, regardless of dose. At 6mg/kg it was also found that dyskinetic mice have a higher rotational rate compared to non-dyskinetic groups (Francardo et al., 2011b) and dose-dependent increases in rotation were also reported in Striatal and MFB mice (Lundblad et al., 2004b). In this cohort of mice AIMs can be positively correlated to L-DOPA-mediated rotation in the Striatum group, suggestive of the previously reported relationship, and in contrast no trend was found for the MFB group likely due to the lack of non-dyskinetic mice.

4.4.3. Behavioural prediction of susceptibility to dyskinesia

Dopamine depletion in the SNc correlates with the extent of AIMs present at 6 and 12mg/kg irrespective of lesion type. Equally a selection of motor hand tests can be correlated to AIM severity at 6mg/kg and 25mg/kg, even when controlling for confounding SNc depletion by partial correlations. Therefore tests correlating to AIMs may offer useful predictors of dyskinesia even before L-DOPA is given, however the predictability of the motor hand test is dependent both on L-DOPA dose and on lesion type. AIMs at 2mg/kg and 6mg/kg are

correlated to the rotarod scores prior to L-DOPA dosing but not at higher doses, indicating both a ceiling effect from maximal AIM development and the sensitivity of the test to distinguish potential dyskinetic mice. At higher doses the correlative nature of AIMs with basal horizontal activity measures and apomorphine induced rotations may reflect uncontrolled for lesion differences, since this is exclusively found in the MFB group. Nevertheless, these tests can be used to predict dyskinesia in specific future experiments using bundle lesions. These data suggest that risk factors for LID development may reflect the interplay of other neurotransmitter systems, differences in plasticity and other maladaptive physiological changes and go beyond dopamine cell loss in the SNc which is currently used as the 'gold standard' predictor of dyskinesia.

4.4.4. TH expression in striatal neurons

TH immunopositive cells can be found within the striatum of 6-OHDA lesioned rodents, MPTP treated primates and humans with PD (Huot and Parent, 2007, Darmopil et al., 2008, Mazloom and Smith, 2006, Tande et al., 2006, Francardo et al., 2011b, Jollivet et al., 2004, Mura et al., 2000). In rodent studies the highest number of TH positive cells is typically found 3-7 days after a 6-OHDA lesion, steadily decreasing from then on (Darmopil et al., 2008), with an apparent resurgence upon L-DOPA treatment (Francardo et al., 2011b). The new presence of TH cells does not arise from neurogenesis, or from the result of a full phenotypic shift, as these cells have been shown to still retain GABA as their primary neurotransmitter (Tande et al., 2006). This study also shows that cells retain a GABAergic phenotype even following chronic L-DOPA treatment. TH immunoreactive cells were detected ubiquitously in the denervated striatum of MFB lesion mice and that further L-DOPA treatment causes an increase in the number of these cells. No significant increase was detected in the Striatal lesion group and high variability between mice was obvious. Interestingly, the increase in TH cells in the SN group is more comparable to that seen in mice with MFB lesions even though other parameters shown in this report, including AIM expression, found more similarities between the SN and Striatal lesions. This highlights the need for lesion selection to be carefully considered, in the light of the anticipated outcomes of the study.

TH cells residing within the striatum of non-L-DOPA treated mice were not correlated with % cell loss within the SNc and this is likely because of the very low number of cells detectable in these lesion only groups, while cell loss was highly correlated with TH cells in L-DOPA

treated mice, comparable to previous findings (Francardo et al., 2011b). In a previous mouse study, L-DOPA was started 1 week after the Striatal lesion and given over a shorter duration (Darmopil et al., 2008). However, TH cell levels and changes were similar to those described here, despite a delay of several months between lesion surgery and the start of L-DOPA treatment in this present study. Our longitudinal study therefore shows two interesting findings; firstly that although TH cell numbers have been reported to decrease from 7 days post lesion, those cells still maintain the ability to express TH when prompted by L-DOPA, despite a long delay between the lesion and start of treatment. Secondly, high doses and prolonged L-DOPA treatment does not cause a further increase in TH cell number, to that reported previously.

4.4.5. Conclusions

AIM expression and locomotor responses caused by L-DOPA are differentially expressed in mice lesioned at different locations along the nigrostriatal pathway. This is likely to be the result of differences in VTA dopamine losses and 5-HT fibre innervation. Longitudinal L-DOPA driven responses in mice lesioned to the SN had distinct behavioural and histological characteristics compared to mice with MFB and Striatal lesions. In addition, FosB/ Δ FosB is differentially upregulated in the striatum according to lesion type. Furthermore, expression patterns of FosB/ Δ FosB in the NAcc reflect specific ventral dopamine losses, underpinning locomotor measures. The emergence of TH positive cells is also enhanced by L-DOPA in all three mouse models and is related to cell losses and AIM development. We also find that behavioural measures can be used to predict LID distinctly to dopamine cell loss correlates and combining both measures would provide a more appropriate selection procedure to study LID. Information generated from this chapter has been used to assess the expression of RGS following chronic and acute treatment regimes (Chapter 5) and was proved useful for the creation of a mouse model of GID (Chapter 8).

5. Regulators of G-Protein Signalling as a Hallmark of Dyskinesia?

Summary

RGS genes have previously been shown to be dysregulated by single injections of L-DOPA, dopamine agonists/ antagonists and select psychostimulants, and I hypothesise may play a role in the priming response to L-DOPA. Unilaterally dopamine depleted mice were primed with L-DOPA for 21 days. They displayed AIMs and contralateral rotation in comparison to similarly lesioned mice that were given a single injection, in whom AIMs were absent but rotation was still initiated. Post-mortem, basal levels of *RGS2*, *RGS4*, *RGS8* transcripts were identified in the striatum and cortex of wild-type mice whereas *RGS9-2* was exclusively found the striatum. RGS transcripts were found to be differently regulated by acute and chronic administration of 10mg/kg L-DOPA, with *RGS2* transcripts increased in the striatum (analysed by qPCR and density analysis from *in situ* hybridisation) and *RGS4*, *RGS8* and *RGS9-2* unchanged. *RGS2* expression however differed depending on long-term (multiple L-DOPA challenges over 21 days) or single L-DOPA challenges. These data were upheld by further quantification of the numbers of *RGS2* positive cells. *RGS2* gene expression was not correlated with AIMs and increased *RGS2* protein translation.

5.1. Introduction

GPCRs exert intra-cellular signalling consequences, by the activation of specific pathway components, caused by the dissociation of $G\alpha$ and $G\beta\gamma$ subunits, in which regulators of G-protein signalling (RGS proteins) are the rate-limiting step. RGS proteins promote GTP hydrolysis of the alpha subunit thereby controlling the rate at which G-proteins can exert post-receptor signalling mechanisms in a negative feedback mechanism. The ERK pathway, dysregulated in L-DOPA-induced dyskinesia, is regulated by GPCRs that stimulate PKA and activate CREB mediated transcription of other genes with CRE promoters. RGS proteins have the potential to down-regulate a significant number of pathways in the basal ganglia and may therefore be future targets for the modulation of LID in PD.

L-DOPA causes functional sensitisation of dopamine receptors and although the exact mechanism remains unclear, RGS proteins may play a key role in mediating this response. Certainly, RGS9-2, the RGS protein expressed selectively in medium spiny neurons of the striatum has been implicated in L-DOPA induced receptor sensitisation as viral-mediated over-expression of this gene reduced the severity of AIMs without worsening the beneficial effect of L-DOPA (Gold et al., 2007). IEGs and *RGS9-2* expression have been considered the ‘transcriptional hallmarks’ or post-mortem ‘biomarkers’ of post-receptor sensitisation to L-DOPA and dyskinesia (Cenci et al., 1993, Cenci et al., 1998, Andersson et al., 1999, Andersson et al., 2001, Berton et al., 2009, Cao et al., 2010, Pavon et al., 2006a) and, in the case of IEGs may actually play a causal role (Andersson et al., 1999).

In intact rodents *RGS2*, *4*, *8* and *9-2* are the most abundant RGS mRNA transcripts in the brain (Grafstein-Dunn et al., 2001, Burchett et al., 1999, Burchett et al., 1998, Gold et al., 1997), and have distinct regional expression patterns. *RGS2* mRNA has been localised to the neocortex, piriform cortex, striatum, hippocampus and locus coeruleus in the adult brain (Grafstein-Dunn et al., 2001, Taymans et al., 2002). The absence of *RGS2* in the GP is suggestive of its function in the striatonigral (direct) pathway. *RGS4* is also highly expressed in the cortex, thalamus and striatum and weakly expressed in the SN, yet *RGS8* is ubiquitously expressed throughout most of the rodent brain including the striatum and SN, with particular density within the Purkinje cells of the cortex (Gold et al., 1997). *RGS9-2* is most dense within the striatal area, with some expression in the medial hypothalamus (Gold et al., 1997). Specific striatal quadrant expression patterns have not been well characterised.

In intact animals, *RGS* gene expression is modulated by pharmacological agents and specific dopamine and glutamate receptor agonists and antagonists (Bishop et al., 2002, Burchett et al., 1999, Burchett et al., 1998, Psifogeorgou et al., 2007, Schwendt et al., 2006, Taymans et al., 2005a, Taymans et al., 2004, Taymans et al., 2003). Differential changes in RGS levels have been shown following selective dopamine denervation by 6-OHDA in the striatum, thought to play a part in the post-synaptic compensatory mechanism for the reduction in dopaminergic innervation (Geurts et al., 2003). *RGS2*, *RGS5* and *RGS8* mRNA transcripts increase and *RGS9-2* and *RGS4* decrease following nigro-striatal dopamine depletion, in comparison to the intact control side (Geurts et al., 2003). In contrast, mRNA levels of *RGS10* and other RGS transcripts that are weakly expressed in the striatum (*RGS3*, *RGS6*, *RGS7*, *RGS11* and *RGS12*) were unchanged. Prolonged reserpine treatment which depletes monoamine levels, without causing loss of the neuronal projections, causes mRNA levels of *RGS2*, *RGS4*, *RGS5*, *RGS8*, *RGS9-2* and *RGS10* to decrease (Geurts et al., 2003). Conversely, Taymans et al. did not detect such a change in *RGS2* with 6-OHDA injections (Taymans et al., 2005b). RGS9-2 proteins were found to be markedly decreased in the striatum of MPTP treated mice and unilateral 6-OHDA lesioned rats increasingly over 0-6 weeks and *RGS4* was upregulated in both cases (Yin et al., 2010). Conversely another study has found RGS9-2 protein levels to be unchanged by MPTP in primates (Gold et al., 2007), in contrast to findings in PD patients (Tekumalla et al., 2001). In humans RGS9-2 was inversely correlated with putamen levels of the dopamine transporter, dopamine and dopamine metabolites (Tekumalla et al., 2001). Changes in RGS that accompany dopamine denervation in models and humans remain unclear, and conflicting results do not provide a clear baseline upon which to measure the effect of L-DOPA.

There are few studies that have looked at the role of L-DOPA in modulating RGS expression in the dopamine-depleted striatum. In intact animals *RGS2* was transiently and rapidly upregulated by a single injection of L-DOPA (50mg/kg) after 30 minutes, and this effect negated by co-administration with a D₁ receptor antagonist, but not with a D₂ receptor antagonist (Geurts et al., 2002). Interestingly, L-DOPA alone did not change *RGS4* expression in the intact brain, yet co-treatment with a D₁ antagonist caused a significant enhancement in *RGS4*, measured 30 minutes after injection. A large gene expression array analysis showed that 50mg/kg of L-DOPA given twice daily for 10 days induced *RGS2* upregulation in the 6-OHDA lesioned brain of dyskinetic rats, but was unchanged by a single injection of the same dose 2 hours post injection (El Atifi-Borel et al., 2009). These L-DOPA mediated changes

may not be representative of standard doses of L-DOPA used experimentally. In accordance with this theory 6mg/kg of L-DOPA given over 21 days increased *RGS2*, *RGS4* and *RGS9-2* transcription in the 6-OHDA lesioned rodent brain, compared to saline treated controls (Conference proceedings ko, 2008). In both the studies using either 50mg/kg or 6mg/kg transcript expressions were not compared to AIMS.

This study firstly aims to confirm existing expression patterns of *RGS2*, *RGS4*, *RGS8* and *RGS9-2* in the intact mouse using *in situ* hybridisation, so they may subsequently be used as a baseline to look at changes following a 6-OHDA lesion and L-DOPA treatment. This study specifically compares RGS transcript levels under single and long-term L-DOPA (10mg/kg) treatments, at 1 hour (during the peak of expression of L-DOPA-induced behaviours) and 24 hours post-injection (where conversion to dopamine is complete and hence there is a complete absence of L-DOPA mediated behaviours), in both intact and lesioned striatum, using several semi-quantitative techniques. To draw mechanistic conclusions on any changes seen, this study also looks at the relative protein levels of RGS, using the same treatment groups.

5.2. Experimental Design

95 adult C57/Bl6 mice were used in this study (outlined in Fig. 5.1 and Table 5.1). 85 of these were lesioned unilaterally with 6-OHDA directed at the MFB (methods detailed in Chapter 2). 76 were had sufficient dopamine depletion indicated by spontaneous rotational assessment (confirmed to be useful in selecting mice with an 80% cell loss or more in the SNc in: Chapter 3). The first group of mice received a single injection of 10mg/kg of L-DOPA with 10mg/kg of benzerazide and killed either 1 h post injection (n=15), with a subset killed 24 hours post-injection (n=14). A second set of mice received 21 days of daily L-DOPA at the same dose and killed 1 hour post injection on the last day (n=13), where AIMs were scored in all mice at day 20. Another group of dyskinetic mice, also receiving 21 days of treatment, were sacrificed 24 hours after the last injection on day 22 (n=13). Mice from the long-term L-DOPA treatment group were split for biochemical and molecular analysis according to approximately equal total net rotation (20 minutes post L-DOPA injection) and total integrated AIM scores. Lesion control mice were treated with daily saline injections for 21 days and killed 24 hours after the last injection (n=9). Intact control groups were also included from this initial cohort, where mice were either subject to 21 days of L-DOPA (n=5) or saline (n=5).

At the end of testing the brains were dissected, snap frozen and sections cut on the cryostat. Sections were taken from a 1 in 6 series and stained for TH by immunohistochemistry and *RGS2* and *RGS4* by *in situ* hybridisation, where density levels were quantified by ImageJ and RGS positive cells counted in defined areas of the striatum, detailed in Chapter 2. Rotation and AIMs were analysed by either 1-way ANOVA or Students t-test. Differences between relative RGS densities and cell counts between groups were determined using 2-way ANOVA and Dunnett's *post hoc* comparisons. Pearson's correlations were then compared between AIMs and the previously mentioned semi-quantitative measures of RGS.

Technique/ Group	Saline non-Lx	Saline Lx	L-DOPA S (on)	L-DOPA S (off)	L-DOPA LT (on)	L-DOPA LT (off)
<i>In situ</i> hybridisation (n)	4	3	9	8	7	7
qPCR (n)	3	3	3	3	3	3
Western Blott (n)	3	3	3	3	3	3

Table 5.1 indicates the number of mice (n) used in each experiment group. Abbreviations: non-lesioned (non-Lx), lesioned (Lx), single injection (S), after 21 days of L-DOPA: long-term injection (LT), 1 hour post injection: on L-DOPA (on) 24 hours post injection: off L-DOPA (off).

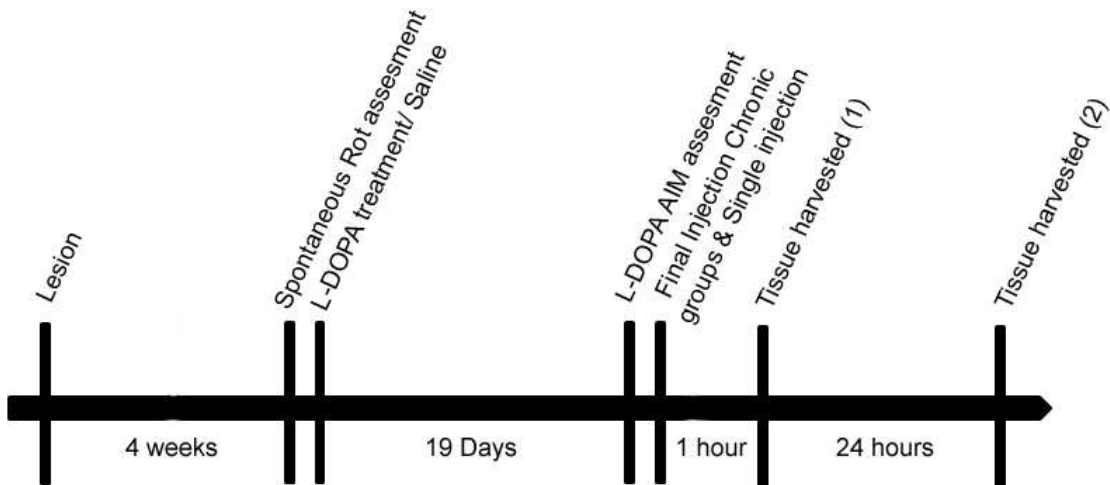


Fig. 5.1. Time line depicting behavioural assessments in mice and times of tissue collection that have contributed to experiments in this chapter.

5.3. Results

5.3.1. Localisation of *RGS2*, *RGS4*, *RGS8* and *RGS9-2* in the Rodent Brain.

The distribution of *RGS2*, *RGS4*, *RGS8* and *RGS9-2* positive cells stained by non-radioactive *in situ* hybridisation, throughout the murine brain at the level of the striatum, is indicated in Fig. 5.2 and detailed in Fig. 5.3. These *RGS* gene transcripts are expressed throughout the striatum. In addition, *RGS2*, *RGS4*, and *RGS8* positive cells can be seen throughout the cortex. *In-situ* hybridisation riboprobes were designed 'in house' and therefore much care was taken to ensure specific binding, hence control riboprobes with the reverse sequence are sufficient negative controls (Fig. 5.3B,F,J,N and Fig. 5.3D,H,L,P). The distribution of *RGS8* and *RGS9-2* is ubiquitous across the striatum whereas the density of *RGS2* and *RGS4* increases from the medial-lateral direction, shown in Fig. 5.3A and Fig. 5.3E respectively.

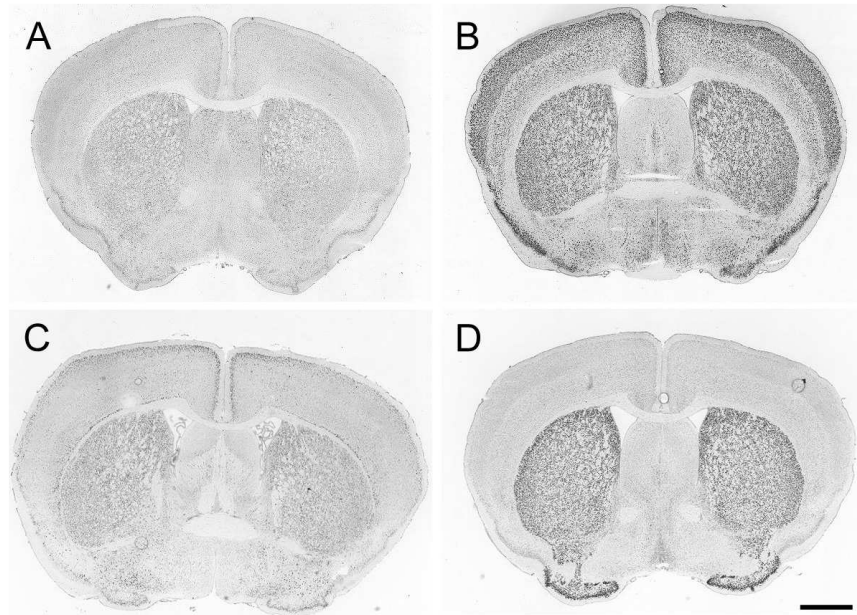


Fig. 5.2. Photomicrographs showing coronal sections through the brain of C57/Bl6 mice after *in situ* hybridisation with riboprobes designed for *RGS2* (A), *RGS4* (B), *RGS8* (C) and *RGS9-2* (D). Scale bar is equal to 2mm.

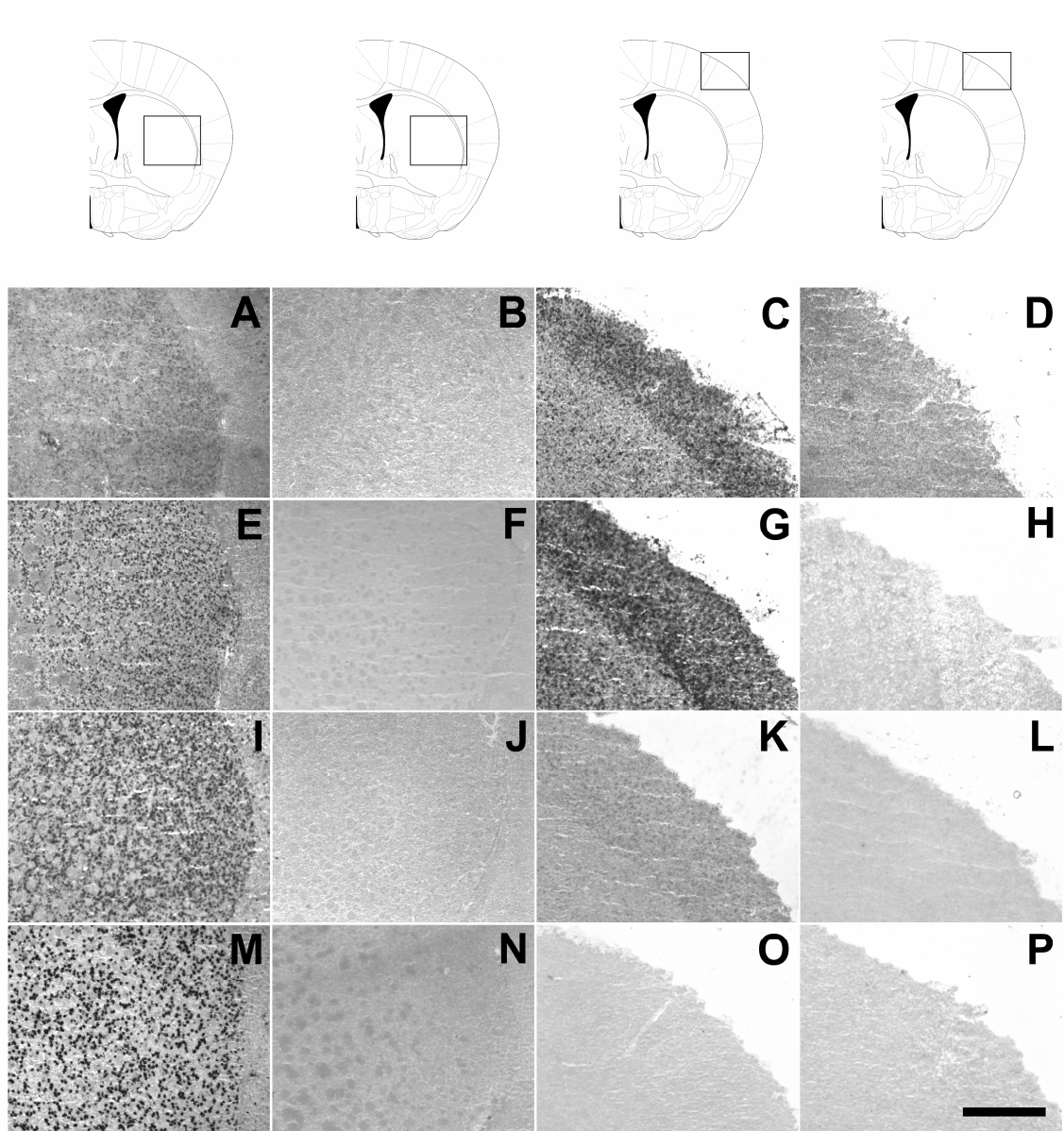


Fig. 5.3. Photomicrographs of the regional expression patterns of *RGS2* (A-D), *RGS4* (E-H), *RGS8* (I-L) and *RGS9-2* (M-P) positive cells throughout the brain, at the level of the striatum in intact mice. Striatal (A, E, I and M) and cortical (C, G, K and O) distributions are presented. Anti-sense control sections in adjacent sections are shown for striatal (B, F, J and N) and cortical (D, H, L and P) areas. Scale bar equals 1mm.

5.3.2. Dyskinesia and Rotational Assessment

Only mice receiving long term L-DOPA treatment (21 days) displayed AIMs above threshold levels (Fig. 5.4A,B), based on defined rating scales (Cenci and Lundblad, 2007, Winkler et al., 2002b). In mice receiving a single injection of L-DOPA no AIMs were observed. Mice in the long-term L-DOPA treatment group were split into three groups for subsequent biochemical and molecular experiments, based on equivalent total integrated AIM scores (Fig. 5.4B; $F_{2,23} = 0.33$, $p = ns$) and total net rotation (Fig. 5.4C; $F_{2,23} = 0.29$, $p = ns$). Mice receiving a single injection were split into corresponding groups based only on equivalent total net rotation (Fig. 5.4D; $F_{2,26} = 0.36$, $p = ns$). Total net contralateral rotation was highest in mice receiving long term L-DOPA injections compared to the single treatment ($T = 2.26$; $p < 0.05$).

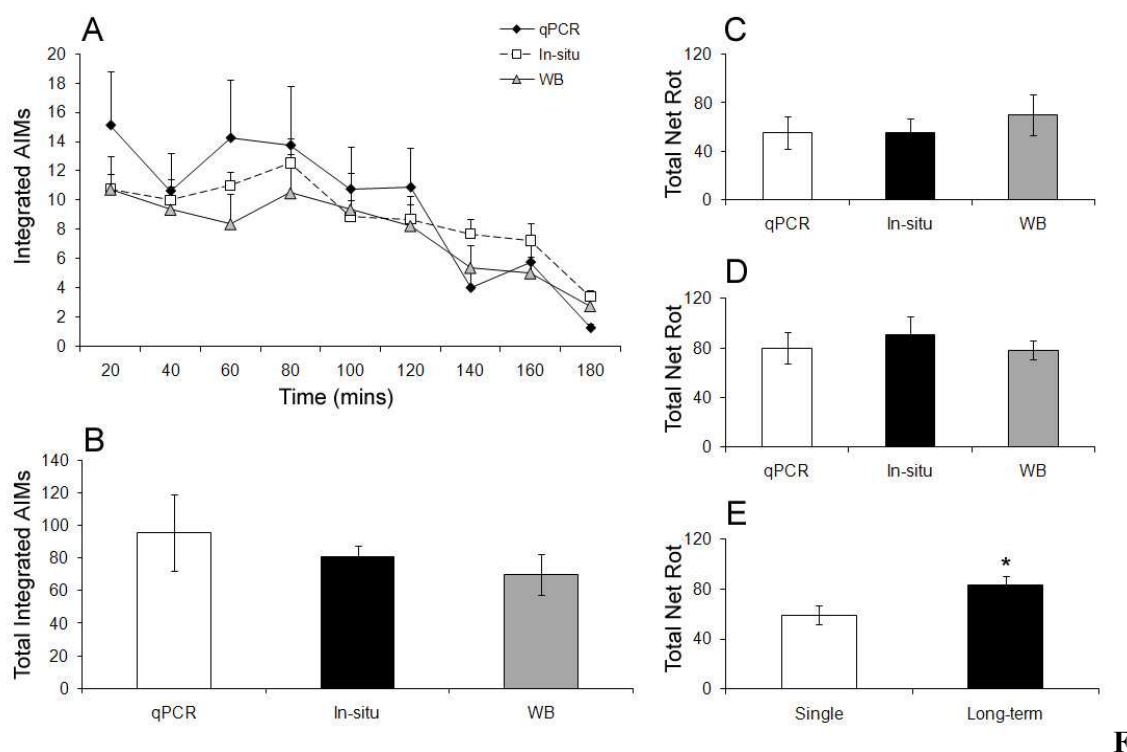


fig. 5.4. Integrated AIMs in 6-OHDA lesioned mice, timecourse of scores at 20 min intervals (A) and totals (B) for mice receiving 21 days of L-DOPA treatment. Total net rotations, scored over 20 minutes were recorded in all lesioned mice receiving either a single injection of L-DOPA (C) or long term treatment (D), for each biochemical analysis groups. Total net rotations for all mice in single treatment or long-term groups were also averaged (E). Significant differences between groups are annotated by $p < 0.05^*$. Values are expressed as means \pm SEM.

5.3.2. Striatal RGS mRNA Expression by qPCR

There were a small number of relative changes, in the expression of RGS transcripts normalised to *GAPDH* levels, between treatment groups (Fig. 5.5), compared to saline-treated intact mice, which were used as a baseline. Semi-quantitative PCR analysis demonstrated that *RGS2*, *RGS4*, *RGS8* and *RGS9-2* mRNA expression was largely unaffected by the lesion, in comparison to both the intact side of lesioned mice and unlesioned controls. In the control groups there was no difference between (a) L-DOPA/ saline treated intact mice, (b) for either acute or chronic treatment groups, (c) between on and off L-DOPA/ saline conditions in intact mice or (d) saline treated lesion mice, therefore control groups were pooled by intact or lesioned parameters (termed Saline non-lesioned/ Saline lesioned from here in). *RGS2* was found to increase 6-fold in the lesioned striatum 1 hour after a single L-DOPA injection or 4-fold after 21 days of L-DOPA treatment (Fig. 5.5A). The expression of *RGS2* on the intact side was approximately double that of basal levels in an intact controls post L-DOPA injection, in single and long-term treatment groups. There was also a smaller increase in the expression of *RGS2* 24 hours post L-DOPA injection, for both single dose and long-term groups. There were no relative changes observed in the expression patterns of *RGS4*, *RGS8* and *RGS9-2* (Fig. 5.5B-D).

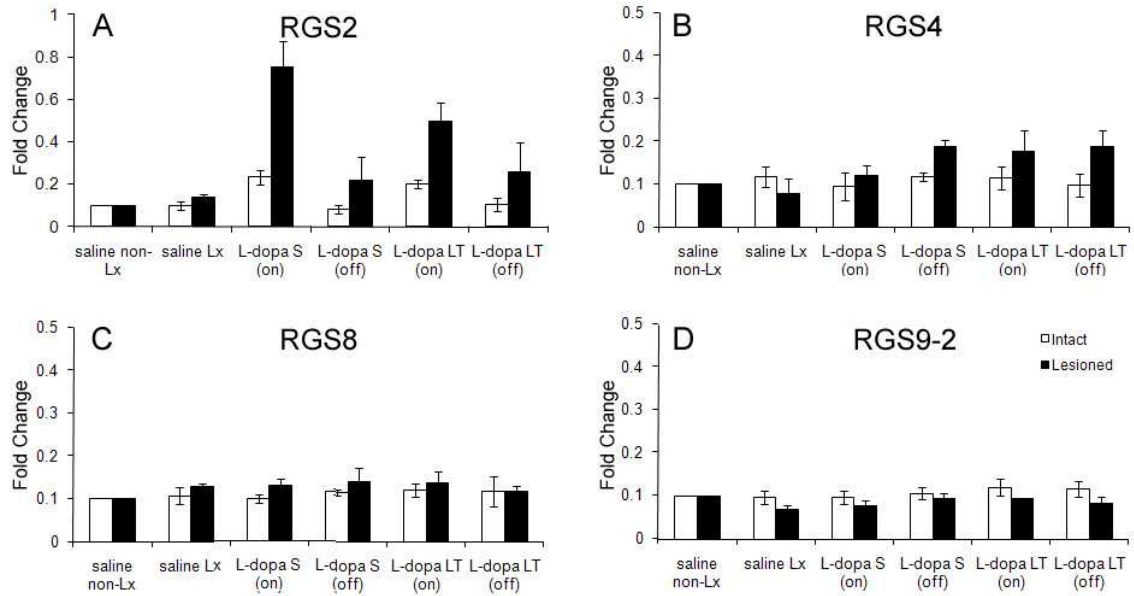


Fig. 5.5. Relative RGS gene expression changes determined by qPCR derived from the $\Delta\Delta C_t$ quantification method, normalised to the expression of *GAPDH* ‘housekeeping’ gene. The relative expression of *RGS2* (A), *RGS4* (B), *RGS8* (C) and *RGS9-2* (D) in intact and lesioned mice treated with saline (Saline non-Lx and Saline Lx respectively), following a single injection of L-DOPA in lesioned mice (L-DOPA S on), 24 hours following a single injection of L-DOPA in lesioned mice (L-DOPA S off), 1 following 21 days of chronic L-DOPA treatment (L-DOPA LT on) and 24 hours following 21 days of chronic L-DOPA treatment (L-DOPA LT off). Values are expressed as means \pm SEM.

5.3.3. Regional mRNA Expression of RGS by In situ Hybridisation

Optical density measurements of the whole striatum were used to measure lesion extent by TH presence and as a semi-quantitative measure RGS expression changes (Fig. 5.6.) TH immunohistochemistry was performed on adjacent sections to RGS *in situ* hybridisation and dopaminergic fibre loss was evident on the ipsilateral striatum compared to the intact side ($F_{1,68} = 53.40, p < 0.001$), and compared to intact control mice ($F_{5,68} = 4.92, p < 0.01$). There was an increase in the relative density of RGS2 with L-DOPA treatment, where there were significant differences between groups ($F_{5,68} = 3.82, p < 0.01$) and sides ($F_{1,68} = 19.14, p < 0.001$). RGS4 expression was increased between intact and lesion sides ($F_{1,68} = 4.55, p < 0.05$) but not between groups ($F_{5,68} = 0.89, p = ns$). Both single injections and long-term L-DOPA triggered upregulation of RGS2 on the lesioned striatum, 1 hour post injection (Fig. 5.6D), $p < 0.01$ for all. Increases of RGS2 were also seen 24 hours after L-DOPA injection in both single and long term groups. No change of density levels were noted for either RGS8 (Fig. 5.6F; group: $F_{5,68} = 0.36, p = ns$ side: $F_{1,68} = 2.46, p = ns$) or RGS9-2 (Fig. 5.6G; group: $F_{5,68} = 1.11, p = ns$ side: $F_{1,68} = 1.18, p = ns$).

The increased density of RGS2 in the lesioned hemisphere is exclusively seen after L-DOPA treatment (Fig. 5.7A-F) and is not seen in intact and lesion only mice, although there was a trend for increased density on the intact side of lesioned mice in the long-term treatment group. Few RGS2 positive cells could be detected prior to L-DOPA administration by *in situ* hybridisation, however following L-DOPA treatment a greater number of cells could be quantified (Fig. 5.7Ai-Fi).

L-DOPA-induced RGS2 upregulation was not uniform across the striatum (Fig. 5.8.). Specifically, RGS2 cell increases between lesion and intact sides were found in: the anterior medial striatum (Fig. 5.8A; $F_{1,68} = 29.99, p < 0.001$), dorsal medial striatum (Fig. 5.8B; $F_{1,68} = 11.15, p < 0.01$) and ventral lateral striatum (Fig. 5.8C; $F_{1,68} = 21.29, p < 0.001$). There was no change in the number of RGS2 positive cells on lesion and intact sides of the motor cortex (Fig. 5.8D; $F_{1,68} = 3.98, p = ns$), however there was a noticeable increase in RGS2 cells with L-DOPA treatment between groups ($F_{5,68} = 4.92, p < 0.01$). *Post hoc* comparisons show that this

was only observed in mice that were chronically treated with L-DOPA and killed during drug activity (Intact: $p < 0.01$; Lesion $p < 0.05$).

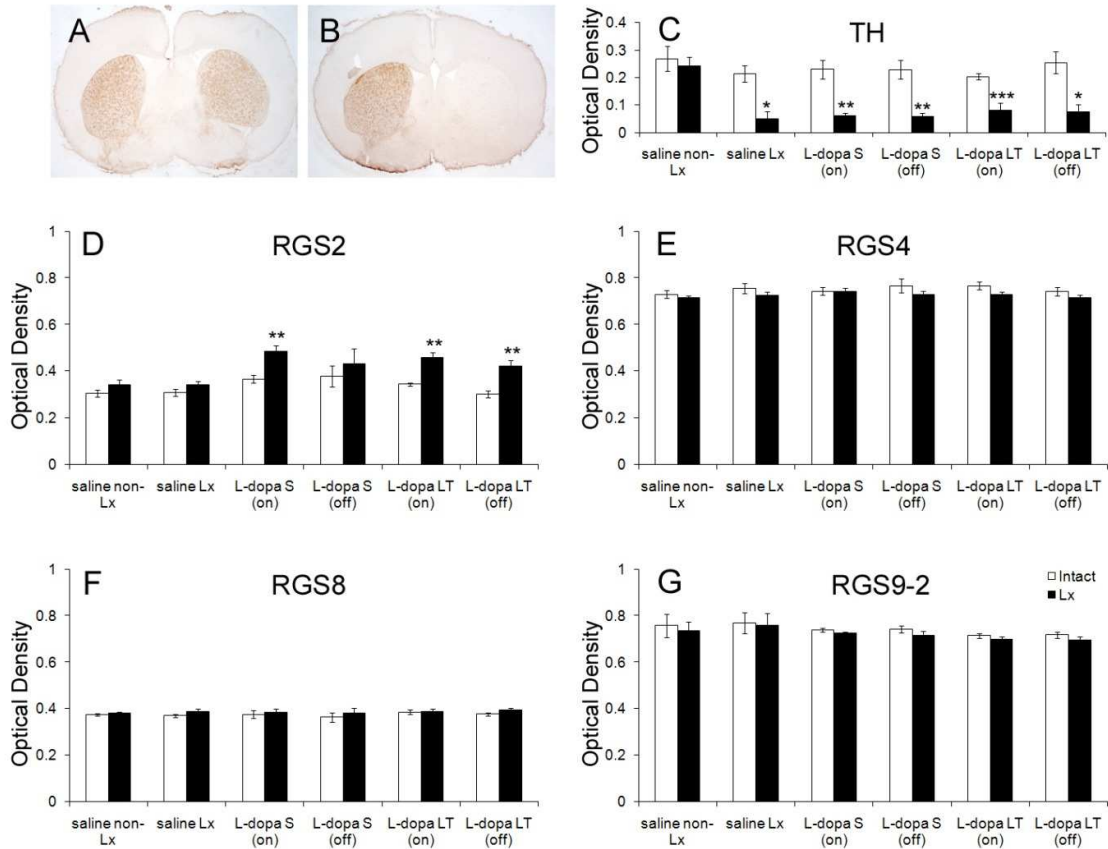


Fig. 5.6. Lesion extent derived from optical density measurements of TH immunohistochemistry (A-C) and relative *RGS* gene expression changes by L-DOPA, determined by optical density measurements of the striatum, following *in situ* hybridisation (D-G). Relative densities of *RGS2* (D), *RGS4* (E), *RGS8* (F) and *RGS9-2* (G) in intact and lesioned mice treated with saline (Saline non-Lx and Saline Lx respectively), 1 (L-DOPA S on) and 24h (L-DOPA S off) following a single injection of L-DOPA in lesioned mice 1(L-DOPA LT on) and 24h (L-DOPA LT off) following 21 days of chronic L-DOPA treatment and 24 hours. Significant differences between intact and lesion sides within a group are annotated by $p < 0.05$ *, $p < 0.01$ ** and $p < 0.001$ ***. Values are expressed as means \pm SEM.

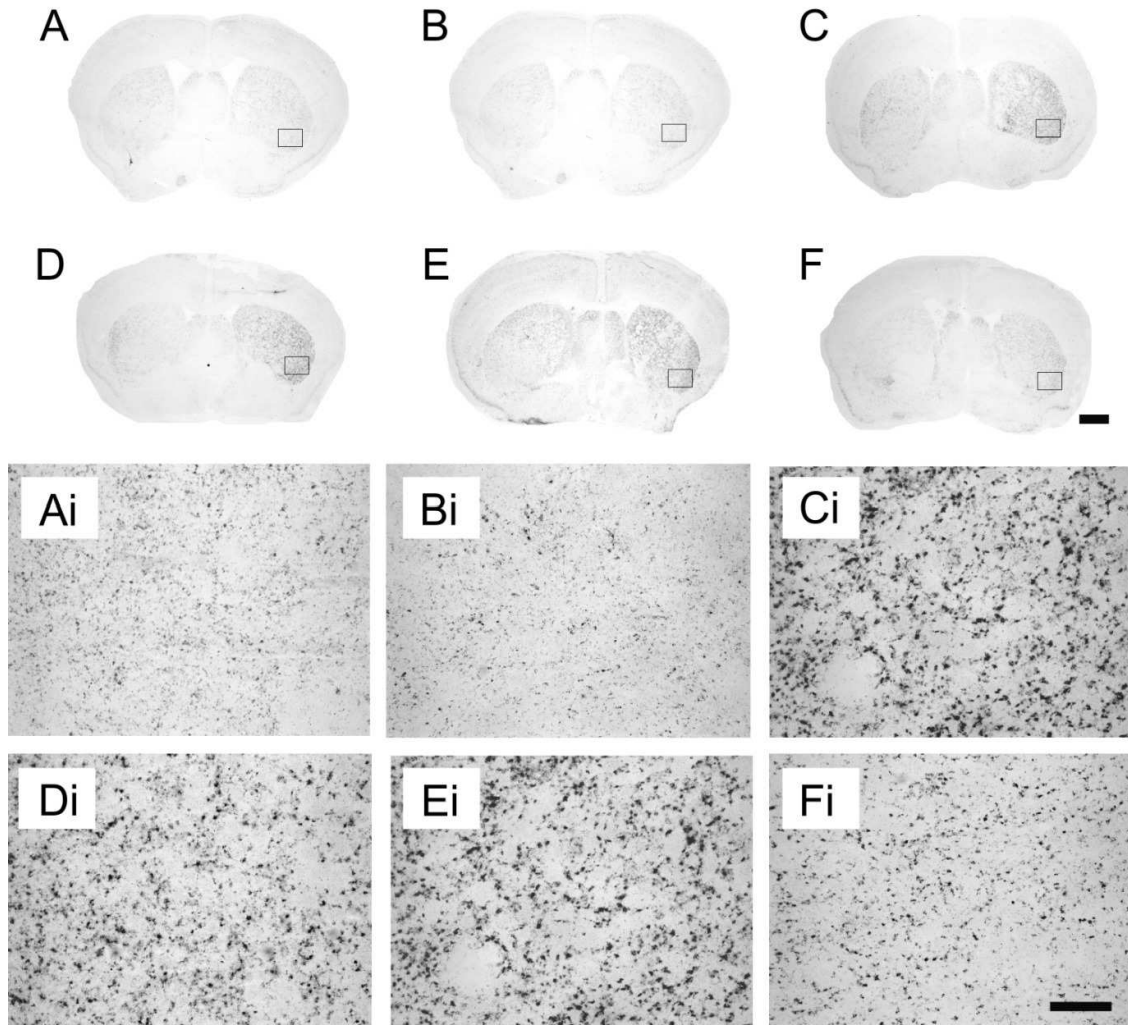


Fig. 5.7. Representative photomicrographs of *RGS2* positive coronal sections, from *in situ* hybridisation, through the dorsal striatum (A-F) and 10x magnification of *RGS2* positive cells (Ai –Fi), in the ventrolateral striatum of the lesioned side (right). Representative images from intact mice treated with saline (A, Ai), 6-OHDA lesioned mice treated with saline (B, Bi), 1 (C, Ci) and 24 h (D, Di), following acute administration of L-DOPA. 1h (E, Ei) and 24h (F, Fi) following 21 days of chronic L-DOPA treatment. Scale bar for images of whole section images equals 1mm and for photomicrographs of cells equals 400 μ m.

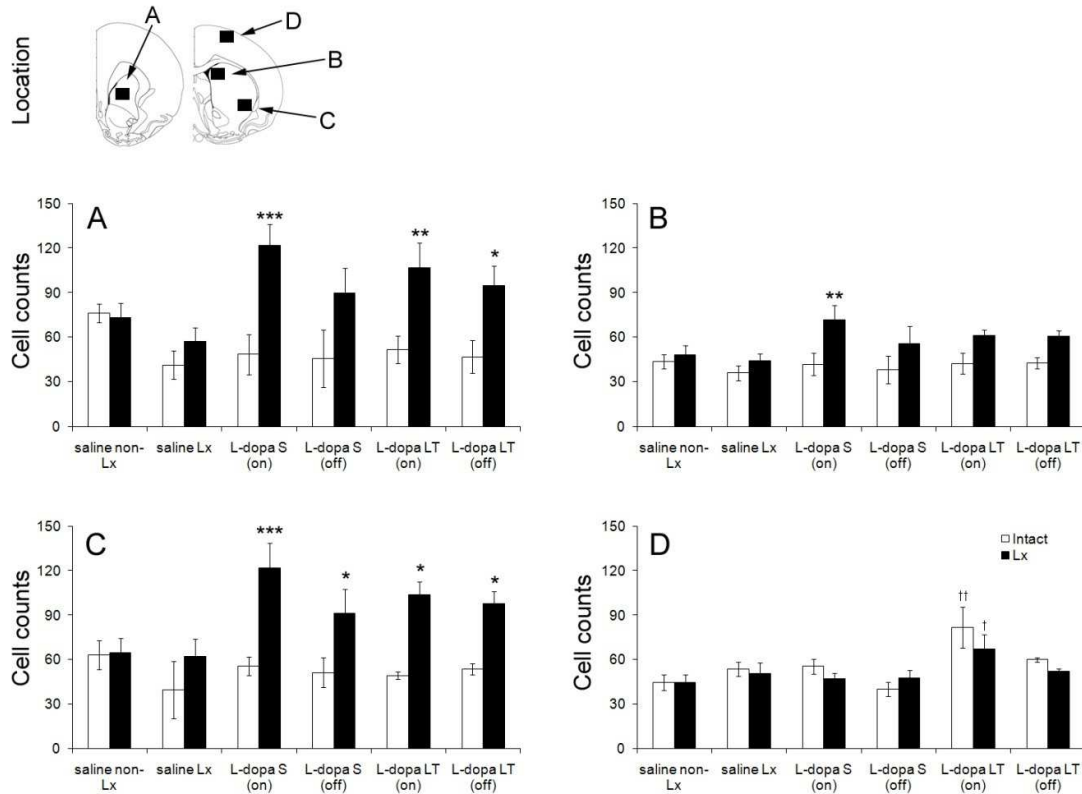


Fig. 5.8. *RGS2* positive cell counts in an 1mm² area of the anterior medial striatum (A), dorsal medial striatum (B), ventral lateral striatum (C) and motor cortex (D) for intact and lesioned mice treated with saline (Saline non-Lx and Saline Lx respectively), 1 (L-DOPA S on) or 24 (L-DOPA S off) following a acute administration of L-DOPA in 6-OHDA lesioned mice, 1 (L-DOPA LT on) and 24h (L-DOPA LT off) following 21 days of chronic L-DOPA treatment. Significant differences between intact and lesion sides are indicated by $p < 0.05^*$, $p < 0.01^{**}$ and $p < 0.001^{***}$ and between intact saline mice in as $p < 0.05^\dagger$ and $p < 0.01^{\dagger\dagger}$. Values are expressed as means \pm SEM.

5.3.4. Correlations of RGS Expression with LID and Rotation

There were few correlations between *RGS2* with dyskinesia and rotation (Table 5.1). A negative correlation was only found between AIMs and *RGS2* expression in the anterior medial striatum ($r = -0.881$, $p < 0.05$) in mice, 24 hours after the final injection of 21 days of L-DOPA treatment. There was also a negative correlation between total contralateral rotation and *RGS2* expression in mice receiving the same treatment ($r = -0.896$, $p < 0.01$), within the dorsomedial striatal region.

	<i>Density</i>	<i>RGS2 Cell counts</i>			
	<i>Whole striatum</i>	<i>Anterior medial striatum</i>	<i>Dorsal medial striatum</i>	<i>Ventral lateral striatum</i>	<i>Motor cortex</i>
<i>AIMs (LT on)</i>	0.655	0.781	0.771	0.708	0.764
<i>AIMs (LT off)</i>	0.107	-0.881*	-0.564	-0.006	-0.143
<i>Rot (LT on)</i>	-0.280	0.431	0.340	0.249	0.660
<i>Rot (LT off)</i>	0.004	0.089	-0.896**	-0.058	0.733
<i>Rot (ST on)</i>	0.170	-0.028	0.596	0.649	0.034
<i>Rot (ST off)</i>	-0.056	-0.177	0.892	-0.780	-0.744
<i>Rot (LT + ST on)</i>	-0.209	0.353	0.442	-0.458	0.571
<i>Rot (LT + ST off)</i>	-0.023	-0.147	0.199	0.176	0.129

Table 5.1. Pearson's correlation co-efficients between total integrated AIMs and total net contralateral rotation with the expression of *RGS2*, quantified through density measurements and cell counts from *in situ* hybridisation. Abbreviations: long-term (LT), short-term (ST), abnormal inhibitory movements (AIMs), rotation (Rot), on (on L-DOPA – 1 hour post injection) and off (off L-DOPA – 24 hours post L-DOPA). Significance is annotated as $p < 0.05^*$, $p < 0.01^{**}$.

5.3.5. Changes in RGS protein Expression

Levels of *RGS2*, *RGS4*, and *RGS9-2* did not differ between lesion and intact sides (Fig. 5.9), where samples were normalised appropriately (indicated by standardised levels of β -actin). Protein concentrations of *RGS2* were increased on both lesion and intact sides, after long-term treatment compared to a single injection (Fig. 5.9; $T = 3.31$, $p < 0.05$), seen at both 1 hour and 24 hours post injection (groups pooled). No significant differences between *RGS4*, *RGS8*,

RGS9-2 and β -actin were found. 6-OHDA caused a reduction in TH expression on lesioned sides compared to intact sides ($T= 8.46, p<0.01$) (data not shown).

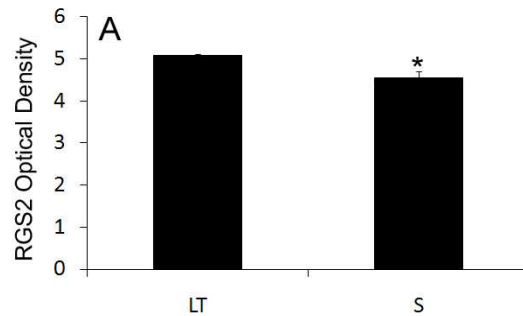
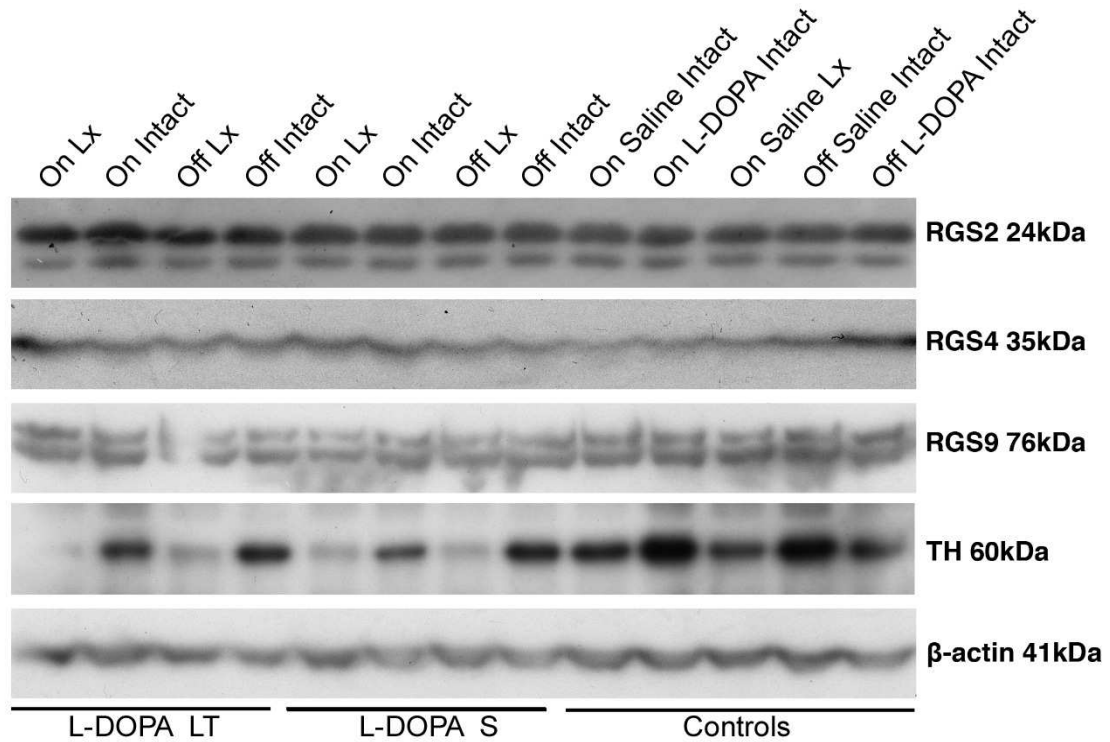


Fig 5.9. Photomicrographs depicting Western blot analysis of RGS2, RGS4, RGS9-2, TH and β -actin. Whole protein lysate concentrations were normalised for all groups and specific proteins identified by their respective molecular weights. Abbreviations: Long-term (LT), single injection (S), Lesion (Lx), on (on L-DOPA – 1 hour post injection) and off (off L-DOPA – 24 hours post L-DOPA). Optical density analysis of RGS2 all LT compared to all S groups (A). Significance is annotated as $p<0.05^*$. Values are expressed as means \pm SEM.

5.4. Discussion

5.4.1 *RGS expression is not differently modulated by the 6-OHDA lesion*

There was no effect of 6-OHDA on any of the RGS transcript expression, measured by qPCR or *in situ* hybridisation. This is in contrast with a previous study in which increases of *RGS2* and *RGS8* were found in 6-OHDA lesion rats, accompanied by decreases in *RGS4* and *RGS9-2* (Geurts et al., 2003). Differences between these two studies may have arisen as a result of the surgical techniques applied, as Geurts et al. (2003) inhibited non-specific depletion of noradrenergic fibres by the prior administration by desipramine and 6-OHDA toxicity was increased by the MAO inhibitor pargyline. Changes in this present study may therefore have been masked by the depletion of non-dopaminergic fibres (evident with MFB lesions, shown in Chapter 4) or a lower toxicity. This discrepancy may also be due to timing, as previously rodents were culled 3 weeks post-lesion (Geurts et al., 2003), in comparison to 7 weeks in this study, therefore RGS changes may occur under times of denervation, but are subsequently normalised. Accordingly, cell loss in the SN is still ongoing at 21 days after a terminal or MFB 6-OHDA injection (Blandini et al., 2007b, Grealish et al., 2008b). There was no effect of the lesion on *RGS2* expression in another studies (El Atifi-Borel et al., 2009, Taymans et al., 2005b), where rats were culled 4-7 weeks post lesion, consistent with our findings. These data show for the first time that the lack of change in *RGS2* in the lesion only condition is also shown in the hemi-parkinsonian mouse model, since all previous RGS studies have utilised the rat model.

Protein levels of *RGS2* are not changed following MPTP administration (mice) or 6-OHDA injection (rats) from 1-6 weeks post lesion (Yin et al., 2010), reflecting both the protein and gene expression changes of this study. In contrast *RGS9-2* was found to be decreased and *RGS4* increased 6 weeks after 6-OHDA injection (Yin et al., 2010), not shown in this present study after 7 weeks. As time courses were comparable and the antibodies were bought from the same company, these discrepancies may be due to surgical procedure or species used.

5.4.2. Lesion and Intact Differences in *RGS2* Expression by L-DOPA

L-DOPA mediated changes in *RGS2* mRNA levels were generally confined to the lesion side. This is unusual however since dopamine receptors do not need to be supersensitised in order to trigger the transcription of *RGS2* within the striatum (Taymans et al., 2004, Taymans et al., 2003). It can be postulated therefore that the intact system dopamine is better controlled and receptors are normosensitive, therefore leading to significantly less transcription. Upregulation on the lesioned side supports findings of two other studies where an increase in *RGS2* was reported two hours post injection (El Atifi-Borel et al., 2009, Geurts et al., 2002). Interestingly, this research suggests that dopamine synthesised from its precursor, behaves as a partial D₁ agonist (increasing *RGS2* only on the lesioned side), as opposed to full agonist action where equal transcript increases were noted on both sides (Taymans et al., 2004). Equally this may be due to the fact that dopamine levels are maintained by intact dopamine neurones. In this study however protein changes and qPCR expression changes were found on both sides after long-term treatment, although in the latter were much smaller on the intact. Therefore even where transcriptional differences between lesion and intact sides were seen, long-term L-DOPA causes a normalisation of increased *RGS2* protein expression on both sides.

5.4.3. *RGS2* Dysregulation

RGS increases were seen both following a single administration of L-DOPA or after 21 days exposure. This is in contrast to previous microarray analysis where *RGS2* expression, in lesioned rats was no longer upregulated after chronic L-DOPA treatment of twice daily injections of 50mg/kg (El Atifi-Borel et al., 2009). Discrepancies between studies may be due to treatment strategies. This high dose, given twice daily may have caused a reduced duration of L-DOPA response and a shift in the peak expression of *RGS2*. Therefore *RGS2* expression may have been missed. Certainly, the administration of 25mg/kg of L-DOPA, twice daily causes a shortening in the duration of L-DOPA mediated motor effects (Papa et al., 1994).

A high dose of L-DOPA (50mg/kg) was used in two studies to give both a 0.25 fold upregulation in *RGS2* measured by *in situ* hybridisation (Geurts et al., 2002) and a 2.4 fold increase by microarray analysis (El Atifi-Borel et al., 2009). The data presented here show that the approximate level of the mRNA increase (qPCR: 2.5 fold; Density: 0.20 fold; Cell count: 2

fold) is sustained despite using a much lower dose of L-DOPA (10mg/kg). Detectable transcript changes in *RGS2* by either single or long-term L-DOPA injections were not matched with protein changes (approximately 0.10 fold). Cells are therefore likely to sustain adequate modulation of D₁ receptors and other GPCRs by RGS2. However protein increases, seen only after long-term L-DOPA treatment, may indicate changes after priming and supersensitisation of dopamine receptors. The low level of L-DOPA used in this study is clinically relevant and therefore data presented in this chapter may reflect neuropathological, transcriptional and protein changes in PD patients receiving long-term treatment. An in-depth characterisation of RGS changes in PD patients of different stages and varied LID states is much needed.

RGS2 expression was only increased in the motor cortex after chronic L-DOPA treatment and may therefore reflect long-term changes in this region. Interestingly the increases in *RGS2* within the motor cortex were not confined to a single hemisphere. Bilateral changes in cortical stimulation have previously been associated with dopamine depletion (Viaro et al., 2011). Unilateral 6-OHDA lesions can change the area of stimulation by a given electrode on both ipsilateral and contralateral sides (Viaro et al., 2011), reflecting long-term neuroplastic changes. Caution must be taken when interpreting the results presented in the present study as the bilateral action of L-DOPA on cortical function is currently unknown, thus warranting further investigation.

5.4.4. *RGS2* Dysregulation ‘Off’ and ‘On’ L-DOPA

In this study RGS transcript levels were compared 1 h post L-DOPA injection when mice were rotating (indicating a near to complete lesion), in single and long-term treatment groups, compared to basal levels 24 hours after injection (when all L-DOPA was metabolised). In two other studies 30 minute and 2 hour time points were chosen as corresponding ‘on’ groups (El Atifi-Borel et al., 2009, Geurts et al., 2003). This is the first study to compare basal levels of RGS after L-DOPA treatment in the 6-OHDA lesioned mouse. These data suggest that *RGS2* remains elevated despite the lack of dopamine stimulation 24 hours post injection, however qPCR analysis shows that upregulation is much reduced at this later time point. Protein levels were also elevated at times on and off L-DOPA. In agreement to this observation *RGS2* remains elevated in the 6-OHDA lesion brain, above baseline levels, for 8 hours after the injection of a D₁ agonist (Taymans et al., 2004). As *RGS2* is increased at times on and off L-

DOPA, it is unlikely to be related to the expression of AIMS, indicated by few significant correlations with either AIMS or rotation.

5.4.5. Methodological Considerations

There are a number of confounding factors which must be considered when analysing RGS proteins. A source of viable antibodies is much needed to explore regional changes of dysregulation at the protein level, as it may not be matched to that of the mRNA transcript. For example, RGS2 protein and mRNA expressions were in the cortex and striatum of untreated rat brains, but not in the SNc where only mRNA transcripts were localised (Taymans et al., 2002). Since only non-commercially available RGS antibodies are efficient enough to use in immunohistochemistry, specific monoclonal antibody production may give a greater insight L-DOPA induced changes throughout the striatum. Nevertheless the combination of the three semi-quantitative methods for RGS analysis presented in this study provides a useful and valuable tool to monitor RGS expression.

Further, 2 hours of acute resistance stress in mice can cause an up regulation of 8 RGS genes expressed in the mouse brain, where *RGS2* was down regulated within the striatum and *RGS9-2* and *RGS4* in the prefrontal cortex (Kim et al., 2010). It was therefore important to expose control animals to saline injections, avoiding bias induced by stress, although levels of stress were much lower in this study. It is also unlikely that LID induces stress, as the anxiety level of rats remains unchanged with AIM expression (Kuan et al., 2008). Therefore this study controls for factors in which other studies have not done, providing an good experimental design with sufficient controls, that can be used in future studies to monitor other potential post-mortem biomarkers of LID.

5.4.6. Conclusions

RGS proteins play a key role in the downstream signalling cascade of GPCRs abundant in the striatum, where RGS2 and RGS8 have been linked with the functionality of the D₁ receptor and RGS4 and RGS9-2 of the D₂ receptor (Taymans et al., 2004, Taymans et al., 2003). Seven weeks post-lesion RGS were not changed in the striatum at the transcript or protein level, indicating usual RGS regulation of GPCRs in post-synaptic cells of the striatum. *RGS2*, *RGS4*, *RGS8* and *RGS9-2* are differently regulated by L-DOPA. Specifically, increased levels of *RGS2* were found after single injections and long-term L-DOPA treatment, although protein increases were only seen in the latter, indicating long-term maladaptive changes in GPCR signalling. In addition, *RGS2* expression changes were seen at times on L-DOPA (where AIMs and/ or rotation were present) and off L-DOPA (where AIMs and rotation were absent); hence few correlations between AIM/ rotation and transcript levels were found. *RGS2* expression is therefore inefficient to be used as a post-mortem biomarker or hallmark of LID. Chapter 7 will look at basal levels of *RGS2* and *RGS4* transcripts for their potential to be used as a pre- requisite biomarker of GID in rats, following the pharmacological manipulation of GID with known modulators of GPCR signalling (Chapter 6).

6. The Pharmacological Modulation of Experimental Graft-Induced Dyskinesia

Summary

Exploring the pharmacology of amphetamine-induced AIMs using compounds with known activity in reducing LID may shed some light on the relationship between these two forms of treatment-induced dyskinesia in PD. 6-OHDA lesioned rats were primed with L-DOPA for 21 days, before receiving transplants of E14 VM derived tissue into the denervated striatum. Following neuronal maturation of the graft, animals were challenged with 0.25mg/kg, 0.5mg/kg, 1.25mg/kg and 2.5mg/kg of methamphetamine, in a randomised Latin square paradigm, to elicit dyskinesia and rotational locomotion, which were recorded simultaneously. 16 rats from the group were selected, with a range of abnormal inhibitory movements (AIMs), and given 2.5mg/kg of methamphetamine co-administered with a pharmacological challenge at high and low doses: - SCH-22390 (D₁ antagonist), raclopride (D₂ antagonist), nafadotride (D₃ antagonist), naloxone (μ opioid antagonist), WIN55,212-2 (CB₁ agonist), yohimbine (α_1 and α_2 adrenergic receptor antagonist), CP94253 (5-HT_{1B} agonist), 8-OH-DPAT (5-HT_{1A} agonist), amantadine (NMDA antagonist), MK-801 (NMDA antagonist), MTEP (mGluR5 antagonist) and IEM1460 (AMPA antagonist). Non-dyskinetic animals were used as controls throughout. AIMs were decreased with SCH-22390, raclopride, and to a lesser extent nafadotride, accompanied by a decrease in net contralateral rotation. Co-administration of methamphetamine with amantadine, MTEP and IEM1460 did not alter the AIMs score. Interestingly, AIMs in response to MK-801 were increased and a reversal of rotation behaviour was observed. The dyskinesia caused by L-DOPA in lesioned models and methamphetamine in grafted models is differently modulated by pharmacological agents, indicating an alternate mechanism of AIM expression. Furthermore, the dopaminergic, 5-HT and glutamate systems are likely to have a fundamental role in the development of GID. This is reinforced by findings in chapter 7 in which the graft normalises the lesion and L-DOPA driven increase in dopamine receptors.

6.1 Introduction

Restoration of depleted striatal dopamine levels, by the implantation of embryonic tissue derived from the VM of human foetuses, has led to the amelioration of the motor symptoms of PD in some patients, (Freed et al., 2001, Olanow et al., 2003, Redmond, 2002, Redmond et al., 1993). A major roadblock in the development of this novel therapy is the occurrence of off-medication dyskinesia in 15-56% of patients depending on the clinical trial, commonly occurring as a combination of hyperkinesia and dystonia (Freed et al., 2003) and (reviewed in Lane and Smith, 2010, Winkler et al., 2005). These spontaneous GID are present in the absence of L-DOPA, although unfortunately spontaneous GID cannot be observed following grafting into rodent models of PD. However, post-transplantation AIMs can be evoked by the administration of methamphetamine (Lane et al., 2006b), which are significantly more prevalent in animals that have been primed with L-DOPA before grafting (Lane et al., 2009b). 2.5mg/kg of methamphetamine may initiate AIMs in some animals and 1.5mg/kg has been found to give maximum rotational bias in rats (Lane et al., 2009b, Torres et al., 2008, Torres and Dunnett, 2007). The dose relationship of amphetamine in relation to both AIMs and locomotion scores has not yet been fully explored in the same cohort.

As the result of the small number of transplanted patients with GID, few pharmacological compounds have been trialled with the aim of reducing GID. Currently, amantadine is the only clinically available compound that is known to reduce LID with some efficacy (Sawada et al., 2010, da Silva-Junior et al., 2005, Godwin-Austen et al., 1970), and this may represent an avenue that we can exploit to treat GID. Amphetamine-induced AIMs in rats can be reduced experimentally in grafted lesioned rodents using D₁ and D₂ receptor antagonists, indicating the necessity of dopamine receptor activity in mediating the response (Lane et al., 2009a, Monville et al., 2005). Furthermore, the 5-HT_{1A} receptor agonist (8-hydroxy-2-(di-n-propylamino) tetralin (8-OH-DPAT) also show efficacy to reduce AIMs with only a small worsening in locomotor score (Lane et al., 2009a), although the exact mechanism of which remain unclear. It is not known whether other anti-dyskinetic agents, used for the treatment for LID, will have any beneficial effect on the hyperkinesia caused by dopamine cell replacement strategies. Here we have selected a range of compounds targeting multiple systems known to affect the basal ganglia and motor function.

There have been a number of key studies to show the efficiency of both clinically available and novel anti-dyskinetic drugs in the 6-OHDA lesioned and L-DOPA treated rat. Dopamine antagonists such as haloperidol can reduce LID significantly, but also inhibit locomotor activity in lesioned rodents (Johnston et al., 2005, Monville et al., 2005, Lundblad et al., 2005). Yohimbine and naloxone show some anti-dyskinetic effects in hemi-parkinsonian rodents by their α_1 agonist and μ -opioid antagonist properties respectively (Dekundy et al., 2007, Lundblad et al., 2002). Overall locomotion was reduced by yohimbine but remained unchanged with naloxone, indicating that the former has a global suppressive effect on locomotion. The 5-HT_{1A} receptor agonist 8-OH-DPAT and 5-HT_{1B} receptor agonist CP94253, have also shown some efficacy to minimise dyskinesia in rodents and primates (Dekundy et al., 2007, Munoz et al., 2008b, Carta et al., 2008d, Carta et al., 2008a), while L-DOPA driven locomotion remain largely unimpaired. Cannabinoid agonists targeting CB₁ receptors such as WIN55,212-2 can also reduce dyskinesia experimentally without effecting the anti-akinetic effect of L-DOPA (Morgese et al., 2009). The weak NMDA receptor antagonist amantadine has the most promising effect on experimental dyskinesia (Dekundy et al., 2007, Lundblad et al., 2002), and has a significant effect in dyskinetic PD patients (Sawada et al., 2010, Wolf et al., 2010), although the compound has some anticholinergic properties and causes dopamine and NA release (Nastuk et al., 1976), yet does not greatly affect L-DOPA driven locomotion (Dekundy et al., 2007, Lundblad et al., 2002). In contrast, the non-competitive NMDA receptor antagonist MK-801 reduces dyskinesia, but only at doses that worsen parkinsonism, suppressing the beneficial effects of L-DOPA, reflected in reduced rotation in the animal model (Paquette et al., 2010). Furthermore, MK-801 has been found to reverse rotation after long-term L-DOPA treatment (Engber et al., 1994), possibly through synergistic actions with D₁ receptor agonism (Fenu et al., 1995). The AMPA-mGluR5 receptor subunit specific antagonist 3-((2-Methyl-4-thiazolyl)ethynyl)pyridine (MTEP) is able to reduce the severity of LID and lessen contralateral rotations in response to L-DOPA (Dekundy et al., 2006). The open-channel blocker of AMPA receptors 1-trimethylammonio-5-(1-adamantane-methylammoniopentane) dibromide hydrobromide (IEM1460) has shown specific action to reduce AIMs without effecting rotarod performance levels seen with L-DOPA treatment (Kobylecki et al., 2010).

In the initial part of this study the relationship of AIM score and rotation at escalating doses of methamphetamine was analysed. Subsequent experiments presented in this chapter have two overall aims, firstly to understand the mechanism of methamphetamine induced AIMs and

locomotion in the transplanted model of GID, and secondly to discover the anti-dyskinetic potential of compounds designed to target dopaminergic, adrenergic, opioid, cannabinoid, 5-HT and glutamergic receptors, known to reduce LID.

6.2 Experimental Design

Sixty female SD rats were lesioned with 6-OHDA using stereotaxic surgery procedures and subjected to experiments outlined in Fig. 6.1. All successfully lesioned rats (those rotating greater than 7 turns per minute with methamphetamine (2.5mg/kg) were treated with L-DOPA (6mg/kg with 6mg/kg of benzerazide in saline) daily for 3 weeks. Rats classified as dyskinetic in response to L-DOPA were grafted using dissociated VM from developing E14 SD embryos. Rats were classified as dyskinetic if they consistently displayed all categories of AIMs, between severity scores 3-4, whereas non-dyskinetic rats exhibited either no or occasional AIMs of minimal severity (Winkler et al., 2002b). Further details of AIM scoring and transplantation techniques are detailed in Chapter 2. Transplants were allowed to develop *in vivo* for 16 weeks before a second methamphetamine (2.5mg/kg) test to assess AIMs. 32 selected rats (N=21 dyskinetic and N=11 non-dyskinetic) were used to determine the dose responsive nature of AIMs and rotation, where 0.25, 0.5, 1.25 or 2.5mg/kg methamphetamine was administered by i.p injection at twice weekly intervals in a Latin square design. Histological analysis of the grafts is outline in Chapter 7.

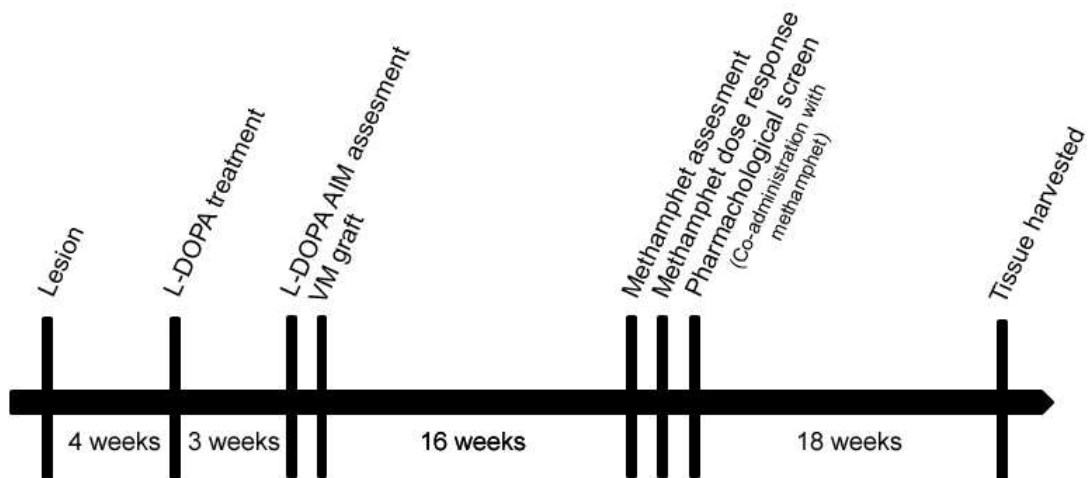


Fig. 6.1. Time line of experimental design to look at the pharmacological modulation of methamphetamine induced AIMs in grafted hemi-parkinsonian models of PD.

16 rats selected from the cohort used for the above dose response experiment were tested with drugs known to modulate LID. In this group rats either exhibit high (N=11 dyskinetic) or negligible (N=5 non-dyskinetic) AIM scores. Pharmacological agents and corresponding doses were chosen on their proficiency to ameliorate AIMs elicited in response to L-DOPA in the hemi-parkinsonian rat model as found in our laboratory (See supplementary Table 2) and as reported in the literature (Dekundy et al., 2007, Kobylecki et al., 2010, Lundblad et al., 2002, Lundblad et al., 2005, Morgese et al., 2007, Munoz et al., 2009, Munoz et al., 2008b, Rylander et al., 2009). SCH23390, raclopride, nafadotride, naloxone, WIN55, 212-2, yohimbine, CP94253 8-OH-DPAT, amantadine, MK-801, MTEP and IEM1460 were co-administered with 2.5mg/kg of methamphetamine (at doses specified in Table 6.1), twice weekly with 72 hours or more between sessions. Each drug was given at a high and low dose in a Latin square paradigm and the drug completely washed out before the next set of administrations. AIMs were scored over 3 hours post-amphetamine injection and rotations measured for 6 hours post injection. All drugs doses, primary receptor action, injection time in relation to methamphetamine (2.5mg/kg) administration, route and method of dissolving are indicated in Table 6.1.

Integrated AIM scores and net rotation were expressed as totals over the whole session and temporally in 20 minute and 10 minute time bins respectively. A 1-way ANOVA with repeated measures was used for statistical analysis to compare total integrated AIMs between dyskinetic rats in response to methamphetamine alone, low dose co-treatment and high dose co-treatment. 2-way ANOVAs with Dunnett's *post hoc* tests were used to determine the difference in total net rotational response between drug administrations, for both dyskinetic and non-dyskinetic groups. Since only one dose was used for the AIM assessment using yohimbine a paired t-test was used to determine statistical significance. Two sample t-tests were used for quantifying dyskinetic and non-dyskinetic differences between rotational scores using low dose CP94253.

Drug	Principle Action	Doses	Time relative to mAmphet (mins)	Route	Sol	Supplier	Ref
SCH23390	D1 antagonist	0.05 and 0.2 mg/kg	-20	i.p	Saline	Sigma	(Monville et al., 2005)
Raclopride	D2 antagonist	0.5 and 2 mg/kg	-20	i.p	Saline	Sigma	(Monville et al., 2005)
Nafadotride	D3 antagonist	0.6 and 1mg/kg	-20	s.c	Saline	Tocris	(Monville et al., 2005)
Naloxone	κ and δ opioid antagonist	4 and 8mg/kg	+5	s.c	Saline	Sigma	(Lundblad et al., 2002)
WIN55, 212-2	CB1 agonist	1 and 2.5 mg/kg	-15	i.p	Saline	Sigma	(Morgese et al., 2007)
Yohimbine	$\alpha 1$ and $\alpha 2$ antagonist	10mg/kg	-30	i.p	Water	Sigma	(Dekundy et al., 2007)
CP94253	5-HT1B agonist	1.5 and 3mg/kg	-20	s.c	Saline	Tocris	(Munoz et al., 2008b)
8-OH-DPAT	5-HT1A agonist	0.05 and 0.1 mg/kg	-20	s.c	Saline	Sigma	(Munoz et al., 2008b)
Amantadine	NMDA antagonist	20 and 40 mg/kg	-30	i.p	Saline	Sigma	(Lundblad et al., 2005)
MK-801	NMDA antagonist	0.03 and 0.3 mg/kg	-30	i.p	Saline	Sigma	(Paquette et al., 2010)
MTEP	mGluR5 antagonist	1.25 and 6.25 mg/kg	0	i.p	Water	Tocris	(Rylander et al., 2009)
IEM1460	AMPA antagonist	1 and 3 mg/kg	0	i.p	Water	Tocris	(Kobylecki et al., 2010).

Table 6.1. Table highlighting all pharmacological agents used in combination with methamphetamine (2.5mg/kg). Information shown (left to right): - principle receptor action site, dosage used in experiment, administration time relative to methamphetamine injection (i.p), administration route, solution requirements (sol), supplier and reference (ref) for their use LID modulation in 6-OHDA lesioned rats. N.B supplier locations are listed in Appendix II.

6.3 Results

6.3.1. Methamphetamine Dose Response

There was dose dependent effect of methamphetamine on AIMs ($F_{4,120}= 22.11, p<0.001$) and total contralateral rotation ($F_{4,120}= 19.33, p<0.001$), pair wise comparisons are shown in Fig. 6.2A and C. Rats classified as dyskinetic exhibited AIMs that were significantly different to the non-dyskinetic group ($F_{1,30}= 24.95, p<0.001$) however rotational scores did not differ between dyskinetic and non-dyskinetic groups ($F_{1,30}= 0.94, p=ns$), although at the highest dose there is a trend for an increased turning response in non-dyskinetic animals. The emergence of AIMs above threshold levels (scores above 40) on a specific rating scale (Cenci et al., 1998) could be seen with 0.5-1.25mg/kg of methamphetamine, however rats were only highly dyskinetic when doses of 1.5 or 2.5mg/kg were used. Interestingly the highest change in the expression of AIMs in the dyskinetic group was between 1.5mg/kg (85.19 ± 14.08) and 2.5mg/kg (181.71 ± 20.13). This is in contrast to the highest recorded rotational bias, which was seen at 1.5mg/kg. In addition, the classic ‘two peak’ response to the methamphetamine injection was only seen at doses 1.5 and 2.5mg/kg, Fig. 6.2D.

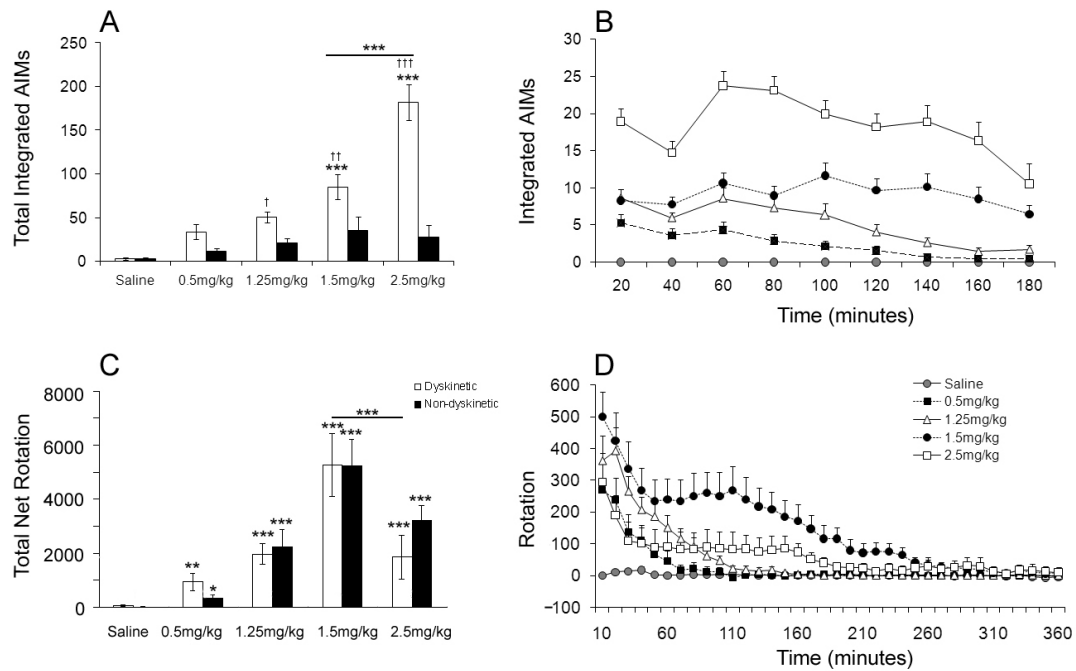


Fig. 6.2. The dose response of hemi-parkinsonian grafted rats previously primed with 6mg/kg of L-DOPA. Rats were subject to either saline, 0.5mg/kg, 1.25mg/kg, 1.5mg/kg or 2.5mg/kg in a randomised Latin square paradigm. Integrated AIMs scores were expressed as totals over 3 hours (A) and in 20 minute time bins (B), with dyskinetic (white) and non-dyskinetic (black). Net contralateral rotations were also analysed as total turns over 6 hours (C) and in 10 minute time bins over the duration (D). Significant changes in AIMs and rotation from 0.5mg/kg and saline baselines respectively, are annotated by $p < 0.05^*$, $p < 0.01^{**}$ and $p < 0.001^{***}$. Differences between the scores found for dyskinetic group at 1.5mg/kg and 2.5mg/kg are also indicated accordingly. Significant dose dependent changes between dyskinetic and non-dyskinetic groups are indicated by $p < 0.05^\dagger$, $p < 0.01^{\dagger\dagger}$ and $p < 0.001^{\dagger\dagger\dagger}$. Values are expressed as means \pm SEM.

6.3.2. Dopamine Receptor Antagonism

The co-administration of the D₁ antagonist SCH23390 at the highest dose significantly reduced total AIMs by 38% compared to those induced by methamphetamine (2.5mg/kg) alone (Fig. 6.3A: $F_{2,22}= 6.12, p<0.01$). Similarly, a 61% decrease in AIMs was noted using the highest dose of the D₂ antagonist raclopride (Fig. 6.4A: $F_{2,22}= 4.34, p<0.05$). Total AIMs remained lowest between 20 and 100 minutes in comparison to methamphetamine for both SCH23390 and raclopride challenges, shown in Fig. 6.3B and 6.4B respectively. SCH23390 caused a decrease in contralateral rotation (Fig. 6.3C: $F_{2,28}= 4.88, p<0.05$), with no difference seen in both dyskinetic and non-dyskinetic groups (Fig. 6.3C: $F_{1,14}= 0.25, p=ns$). Dose dependent decreases in rotation occurred at the highest dose of raclopride (Fig. 6.4C: $F_{2,28}= 4.88, p<0.05$), with no discrepancy between dyskinetic and non-dyskinetic types (Fig. 6.4C: $F_{1,14}= 0.57, p=ns$). Rotation was decreased at both in the initial and second peak following SCH23390 administration, yet with raclopride the effect was predominantly in the second peak.

Co-administration with the D₃ receptor antagonist nafadotride however did not cause a significant reduction in amphetamine-induced AIMs in dyskinetic animals (Fig. 6.5A: $F_{2,22}= 2.20, p=ns$), although a trend was noted. There was also no change in the total rotational responses ($F_{2,28}= 0.24, p=ns$) or between dyskinetic and non-dyskinetic groups ($F_{1,14}= 0.40, p=ns$), Fig. 6.5C.

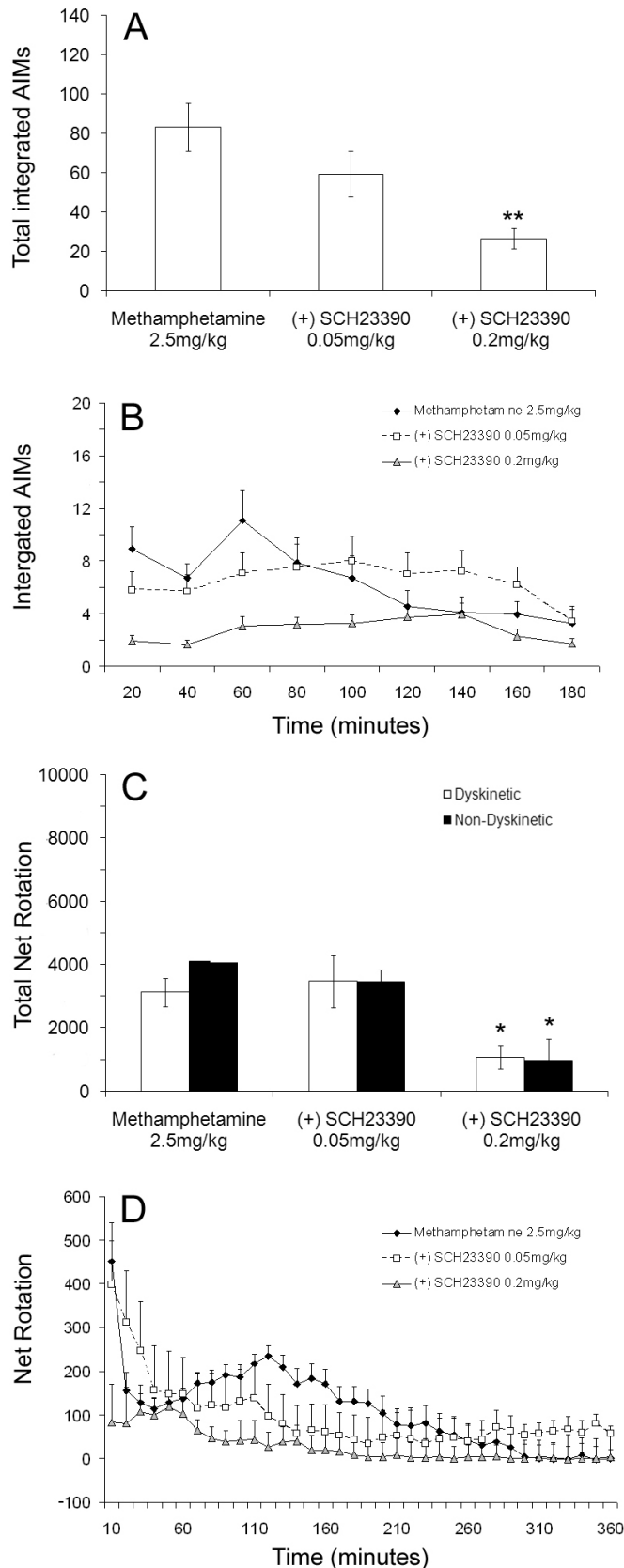


Fig. 6.3. Total integrated AIMs initiated by methamphetamine (2.5mg/kg) alone and with (+) SCH23390 at a low dose (0.05mg/kg) or a high dose (0.2mg/kg) (A). Integrated AIMs were scored every 20 min for 3 h in response to methamphetamine and in combination with SCH23390 doses (B). Total net contralateral rotations were recorded with the same doses over 6 h (C). Rotational asymmetry for all animals was recorded over 10 min intervals for the duration (D). Significant differences between the combination treatment and methamphetamine alone, are indicated by $p < 0.05^*$, $p < 0.01^{**}$. Values are expressed as means \pm SEM..

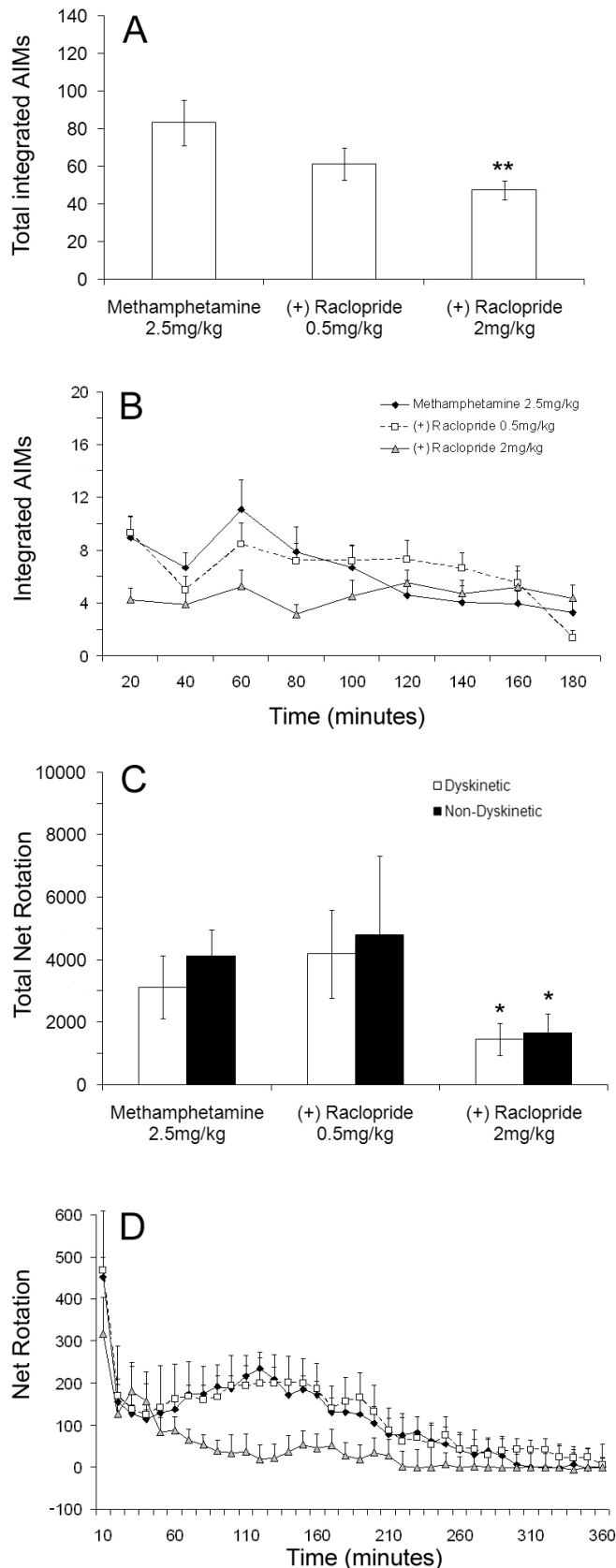


Fig. 6.4. Total integrated AIMs initiated by methamphetamine (2.5mg/kg) alone and with (+) Raclopride at a low dose (0.5mg/kg) or a high dose (2mg/kg) (A). Integrated AIMs were scored every 20 min for 3 h in response to methamphetamine and in combination with Raclopride doses (B). Total net contralateral rotation was record with the same doses over 6 hours (C). Rotational asymmetry for all animals was recorded over 10 minute intervals for the duration (D). Significant differences between the combination treatment and methamphetamine alone, are indicated by $p < 0.05^*$, $p < 0.01^{**}$. Values are expressed as means \pm SEM.

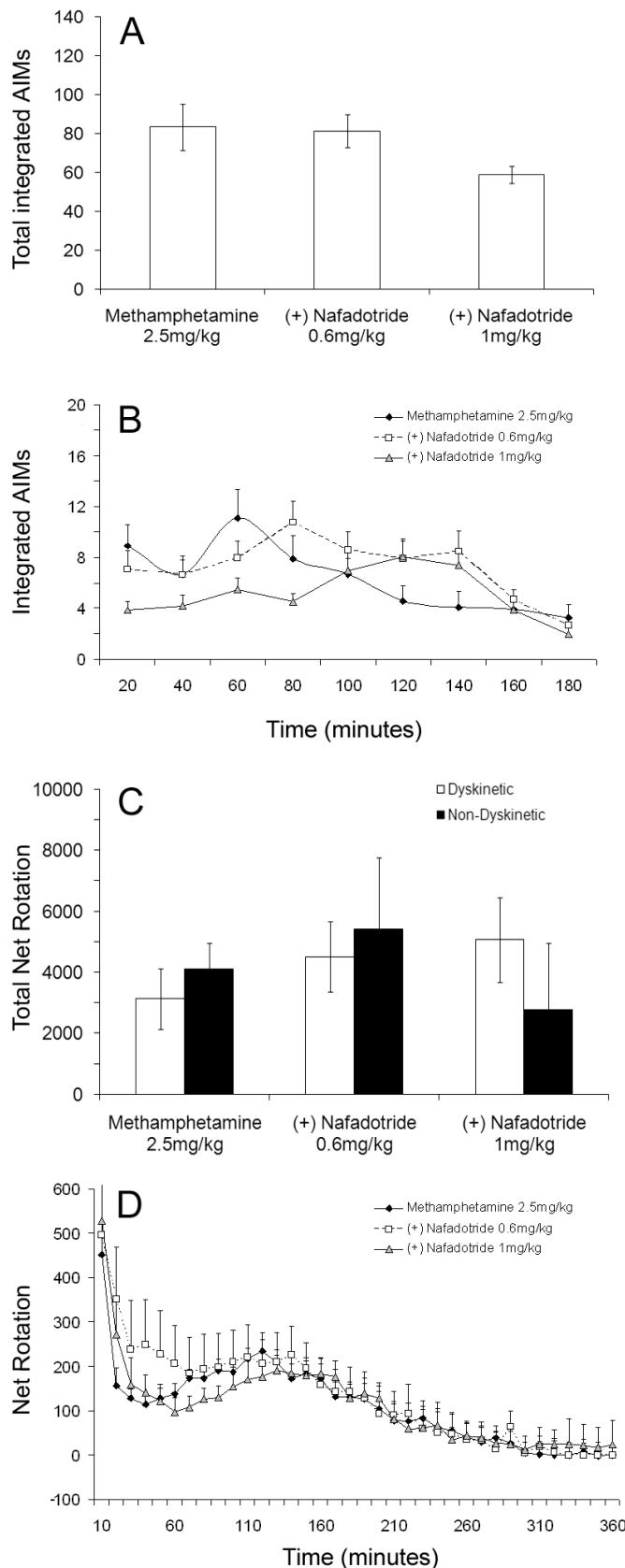


Fig. 6.5. Total integrated AIMs initiated by methamphetamine (2.5mg/kg) alone and with (+) Nafadotride at a low dose (0.6mg/kg) or a high dose (1mg/kg) (A). Integrated AIMs were scored every 20 min for 3 h in response to methamphetamine and in combination with Nafadotride doses (B). Total net contralateral rotation was recorded with the same doses over 6 h (C). Rotational asymmetry for all animals was recorded over 10 min intervals for the duration (D). Values are expressed as means ± SEM.

6.3.3. Opioid Receptor Antagonism

The μ -opioid receptor antagonist naloxone did not significantly alter total integrated AIMs in response to methamphetamine (Fig. 6.6A: $F_{2,22}= 0.36, p=ns$). Conversely, there was a small suppression of total rotational scores with the highest dose of naloxone ($F_{2,28}= 4.11, p<0.05$) with no difference between dyskinetic and non-dyskinetic groups ($F_{1,14}= 0.22, p=ns$), Fig. 6.6C. This bias was most apparent on the second peak of the rotational response, between 70-160 minutes (Fig. 6.6D).

6.3.4. Cannabinoid Receptor Agonism

Total integrated AIMs were unchanged (Fig. 6.7A: $F_{2,28}= 0.53, p=ns$) between treatments. Further, the CB₁ receptor antagonist WIN55, 212-2 did not alter total net rotations in response to methamphetamine ($F_{2,42}= 0.04, p=ns$), between either dyskinetic and non-dyskinetic groups ($F_{1,14}= 1.20, p=ns$), Fig. 6.7C. Small temporal changes in rotation were apparent using the high and low doses of WIN55, 212-2 (Fig. 6.7D). The second methamphetamine-induced peak in rotation, usually occurring between 100-130 minutes, was shifted to 160-190 minutes.

6.3.5. Adrenergic Receptor Antagonism

The α_1 and α_2 -adrenergic receptor antagonist yohimbine was only used at the low dose since an adverse reaction was noted. A minority of the grafted rats developed predicted pulmonary odema and were observed to be highly anxious. When using the low dose however no change in total AIM expression was evident (Fig. 6.8A: $T= -0.38, p=ns$). There was no apparent change between methamphetamine induced total rotation and that with the addition of yohimbine ($F_{1,14}= 0.03, p=ns$) or between dyskinetic and non-dyskinetic groups ($F_{1,14}= 0.31, p=ns$), Fig. 6.8C. Yohimbine altered the contralateral rotation pattern over time (Fig 6.8D), where the initial peak usually occurring before the first 10 minutes was postponed until 15 minutes, abolishing the second rotational peak.

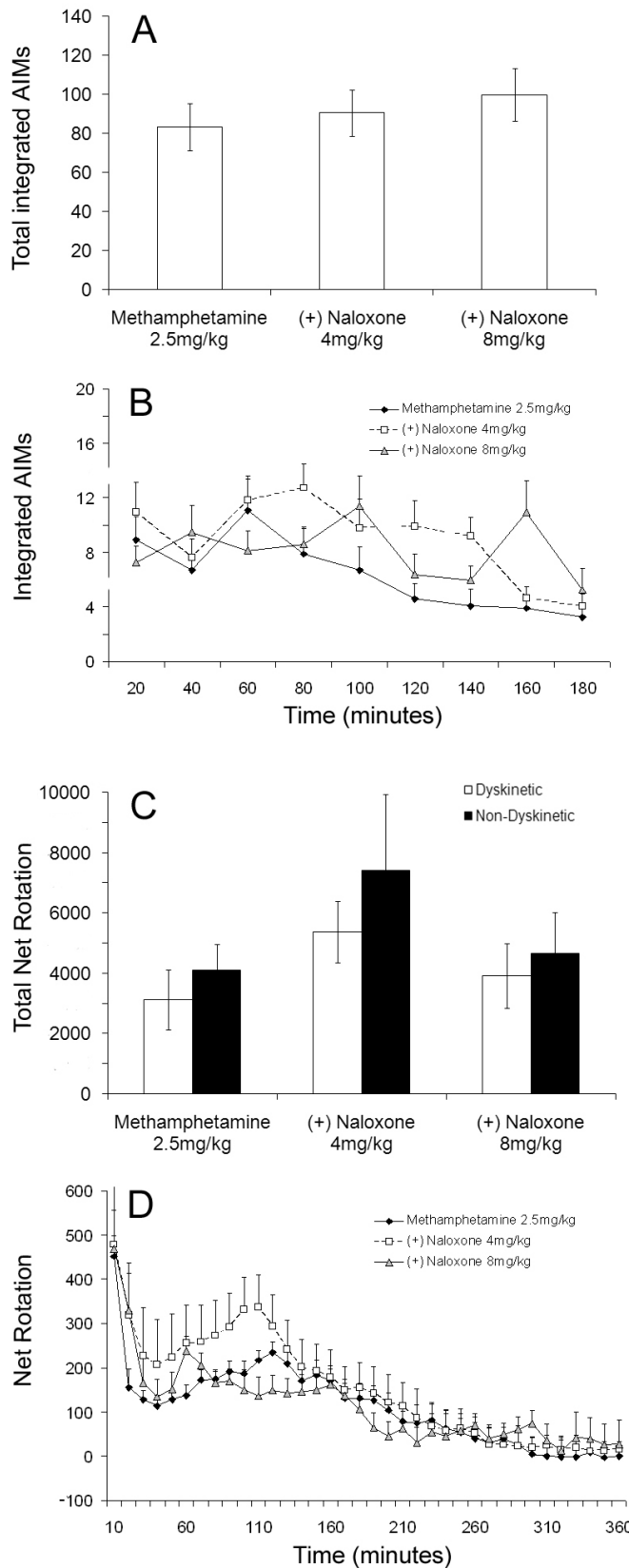


Fig. 6.6. Total integrated AIMs initiated by methamphetamine (2.5mg/kg) alone and with (+) Naloxone at a low dose (4mg/kg) or a high dose (8mg/kg) (A). Integrated AIMs were scored every 20 min for 3 h in response to methamphetamine and in combination with Naloxone doses (B). Total net contralateral rotation was recorded with the same doses over 6 h (C). Rotational asymmetry for all animals was recorded over 10 min intervals for the duration (D). Values are expressed as means \pm SEM.

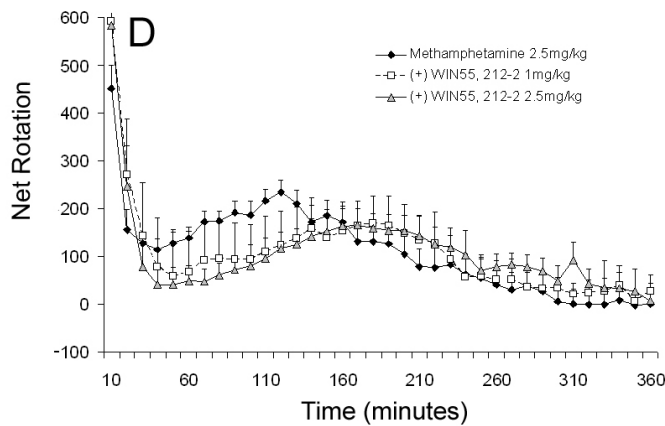
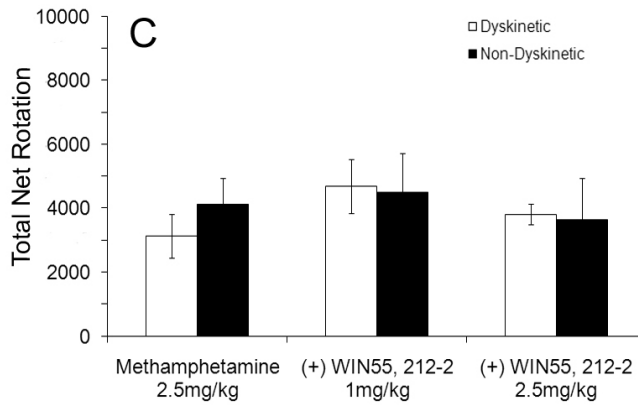
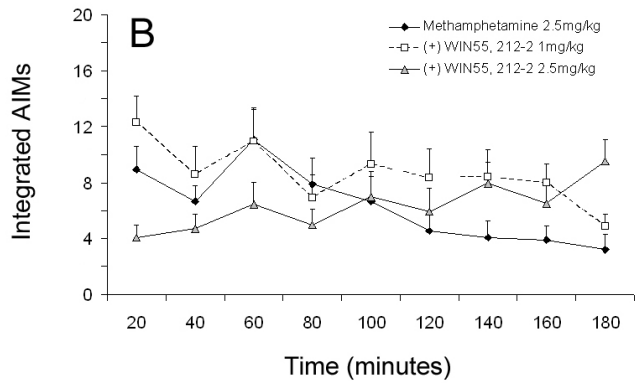
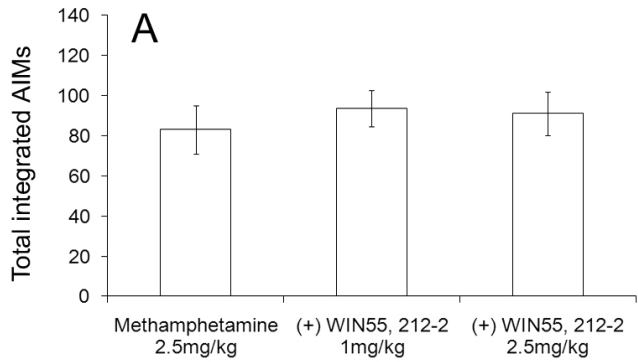


Fig. 6.6. Total integrated AIMs initiated by methamphetamine (2.5mg/kg) alone and with (+) WIN55, 212-2 at a low dose (1mg/kg) or a high dose (2.5mg/kg) (A). Integrated AIMs were scored every 20 min for 3 h in response to methamphetamine and in combination with WIN55, 212-2 doses (B). Total net contralateral rotation was recorded with the same doses over 6 h (C). Rotational asymmetry for all animals was recorded over 10 min intervals for the duration (D). Values are expressed as means ± SEM.

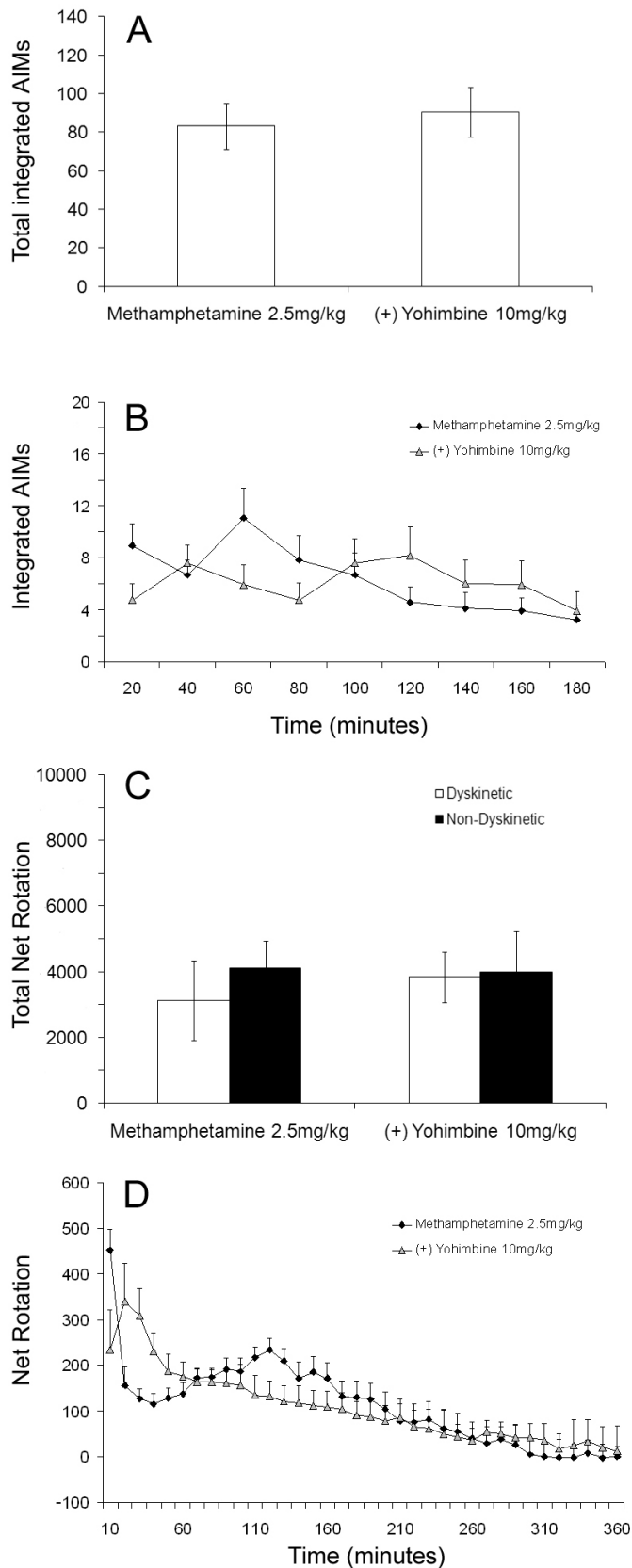


Fig. 6.8. Total integrated AIMs initiated by methamphetamine (2.5mg/kg) alone and with (+) Yohimbine at a dose of 10mg/kg (A). Integrated AIMs were scored every 20 min for 3 h in response to methamphetamine and in combination with Yohimbine doses (B). Total net contralateral rotation was recorded with the same doses over 6 h (C). Rotational asymmetry for all animals was recorded over 10 min intervals for the duration (D). Values are expressed as means ± SEM.

6.3.6. 5-HT Receptor Agonism

The action of the 5-HT_{1B} receptor agonist CP94253 (3mg/kg) caused a significant reduction in AIMs compared to methamphetamine alone (Fig. 6.9A: $F_{2,22} = 3.46$, $p < 0.05$). Primarily decreases were observed in the first 100 min of the scoring session (Fig. 6.9B), thereafter appearing similar in magnitude to those seen with methamphetamine alone. A dose dependent reduction in total AIMs was also seen with the specific 5-HT_{1A} receptor agonist 8-OH-DPAT (Fig. 6.10A: $F_{2,22} = 5.85$, $p < 0.01$). There was no difference between the total rotational response to CP94253 and methamphetamine (Fig. 6.9C) compared to methamphetamine alone ($F_{2,28} = 0.30$, $p = ns$), however there was a difference between dyskinetic and non-dyskinetic groups ($F_{1,14} = 4.91$, $p < 0.05$). *Post hoc* tests reveal that the latter difference was only evident at the low dose ($p < 0.05$). 8-OH-DPAT treatment did not alter total net rotation ($F_{2,28} = 0.70$, $p = ns$), with no differences between dyskinetic and non-dyskinetic groups ($F_{1,14} = 2.64$, $p = ns$) (Fig. 6.10C). Co-administration of CP94263 altered the time course of the rotational response with a gradual increase in rotations between 130 and 360 minutes without an identifiable second peak in the response, in contrast to the methamphetamine only time course. Dyskinetic and non-dyskinetic groups responded differently, where the early rotational responses in non-dyskinetic rats was suppressed for the early phase of the response (Fig. 6.11; $T = -2.60$, $p < 0.05$) before being normalised (Fig. 6.11; $T = -1.48$, $p = ns$). CP94263 treatment also caused a small biphasic response in AIM expression (Fig. 6.9B) where dyskinesia is much reduced between 20 and 140 minutes and increased above the methamphetamine baseline at 180 minutes, mirroring the rotational response.

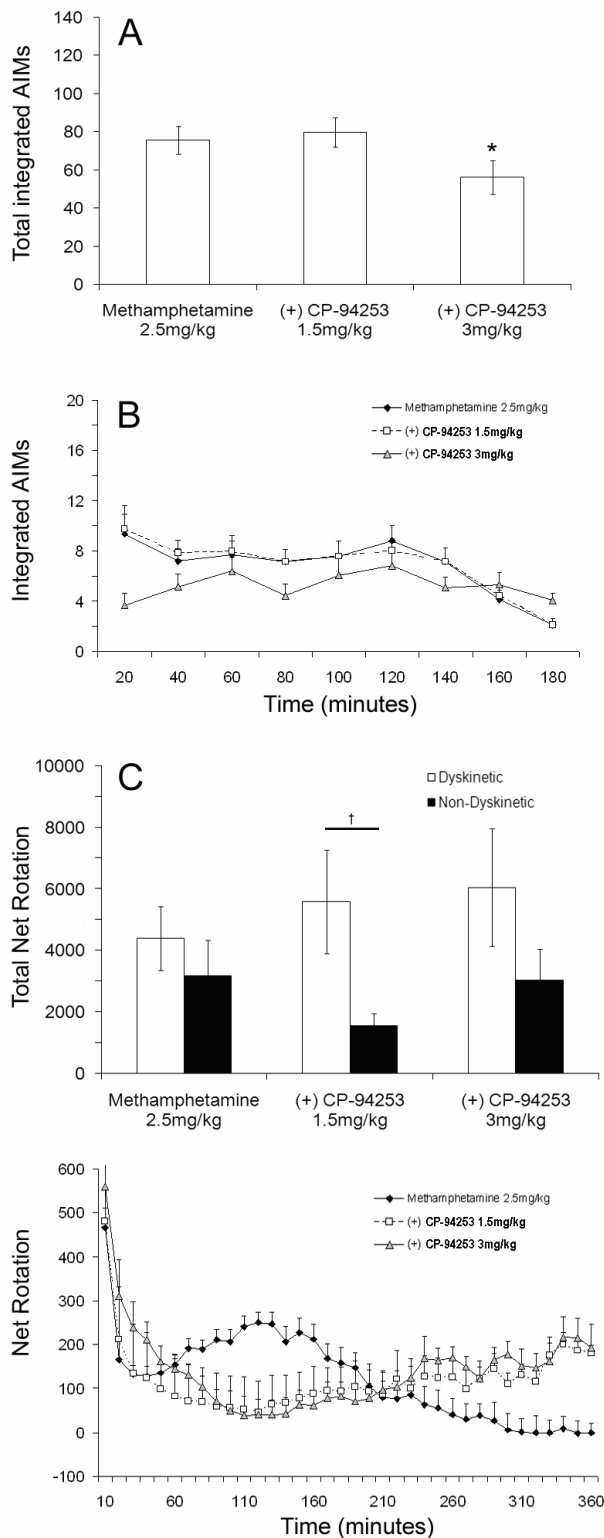


Fig. 6.9. Total integrated AIMs initiated by methamphetamine (2.5mg/kg) alone and with (+) CP-94253 at a low dose (1.5mg/kg) or a high dose (3mg/kg) (A). Integrated AIMs were scored every 20 minutes for 3 hours in response to methamphetamine and in combination with CP-94253 doses (B). Total net contralateral rotation was recorded with the same doses over 6 hours (C). Rotational asymmetry for all animals was recorded over 10 minute intervals for the duration (D). Significant differences between the combination treatment and methamphetamine alone is indicated by $p < 0.05^*$. Dyskinetic and non-dyskinetic differences were also present, where $p < 0.05^\dagger$. Values are expressed as means \pm SEM.

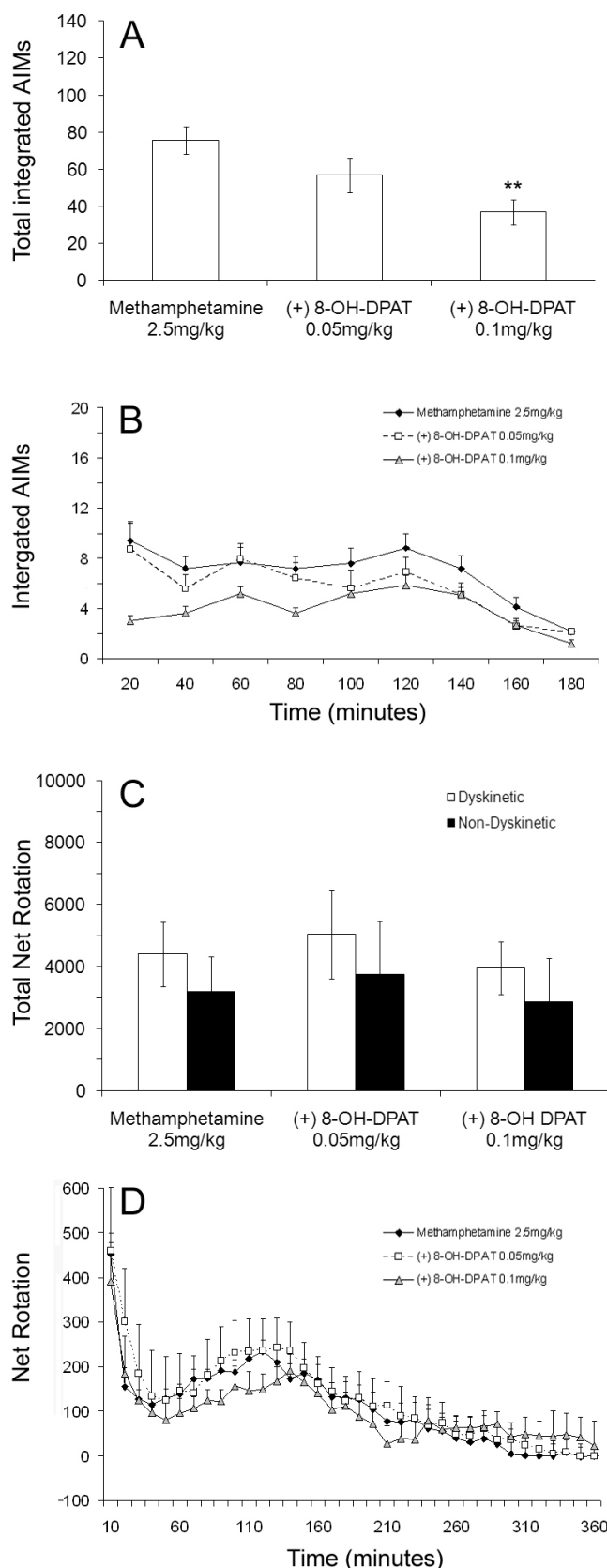


Fig. 6.10. Total integrated AIMs initiated by methamphetamine (2.5mg/kg) alone and with (+) 8-OH-DPAT at a low dose (1.5mg/kg) or a high dose (3mg/kg) (A). Integrated AIMs were scored every 20 minutes for 3 hours in response to methamphetamine and in combination with 8-OH-DPAT doses (B). Total net contralateral rotation was recorded with the same doses over 6 hours (C). Rotational asymmetry for all animals was recorded over 10 minute intervals for the duration (D). Significant differences between the combination treatment and methamphetamine alone is indicated by $p < 0.01^{**}$. Dyskinetic and non-dyskinetic differences were also present, where $p < 0.05^{\dagger}$. Values are expressed as means \pm SEM.

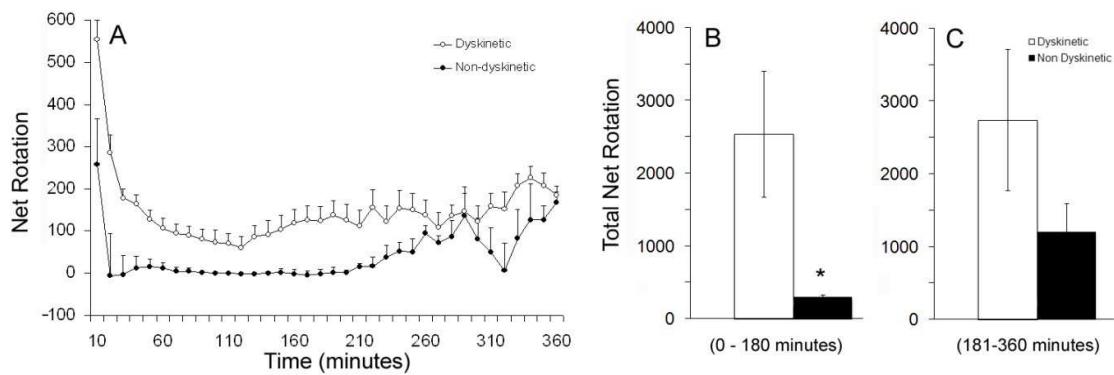


Fig. 6.11. Temporal dyskinetic and non-dyskinetic differences in rotation present when co-administrating methamphetamine with CP94253 low dose (1.5mg/kg) (A). Total net contralateral rotations are also shown from 0-180 min (B) and 181-360 min (C). Statistical significance between groups was deduced by a 2 sampled T-test and annotated as $p < 0.05^*$. Values are expressed as means \pm SEM.

6.3.7. Glutamate Receptor Antagonism

The NMDA receptor antagonist amantadine had no effect on the AIMs response to methamphetamine (Fig. 6.12: $F_{2,22}= 1.42$, $p=ns$). Conversely, the NMDA receptor antagonist MK-801 increased total AIMs (Fig. 6.13A: $F_{2,28}= 11.17$, $p<0.001$) at the highest dose, resulting from abnormally high dyskinetic responses at 100-140 minutes (Fig 6.13B). When the total integrated AIM score is split into sub-components (Fig. 6.14A-D), dyskinesia was significantly increased in the forelimbs ($F_{2,22}= 3.47$, $p<0.05$) and hindlimbs ($F_{2,22}= 3.71$, $p<0.05$) of the grafted cohort, with the biggest change recorded the axial form of the movement ($F_{2,22}= 11.14$, $p<0.001$). No changes in orolingual movements were noted ($F_{2,22}= 0.60$, $p=ns$). The increase in AIMs was mainly the result of increased duration of the response in each recording interval (Fig. 6.14E: $F_{2,22}= 16.14$, $p<0.001$), although amplitude scores were also increased (Fig. 6.14F: $F_{2,22}= 3.68$, $p<0.05$).

Total contralateral turns did not differ between groups when treated with amantadine ($F_{1,14}= 3.76$, $p=ns$) or between treatments ($F_{2,22}= 0.68$, $p=ns$), shown in Fig. 6.12C. An abnormal rotational response was observed with MK-801 co-administration (Fig. 6.13C), where a dose dependent reversion in rotation was clear ($F_{2,28}= 19.24$, $p<0.001$), with no differences between dyskinetic and non-dyskinetic subgroups ($F_{1,14}= 0.37$, $p=ns$). Total net rotational scores with high dose MK-801 were significantly different to methamphetamine alone ($p<0.001$) and although this was not reiterated at low dose there was a clear absence of the second rotational peak, with almost no net rotation in any direction between 70 and 360 minutes (Fig. 6.13D).

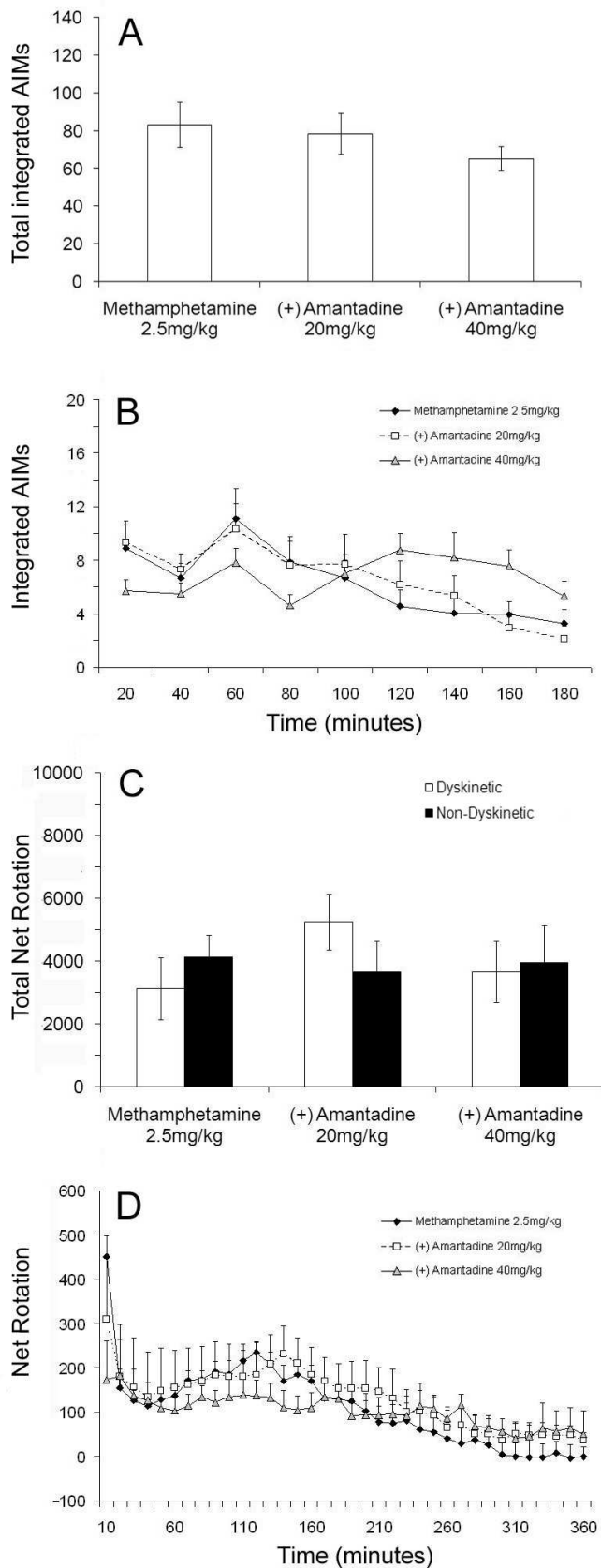


Fig. 6.12. Total integrated AIMs initiated by methamphetamine (2.5mg/kg) alone and with (+) amantadine at a low dose (20mg/kg) or a high dose (40mg/kg) (A). Integrated AIMs were scored every 20 minutes for 3 hours in response to methamphetamine and in combination with amantadine doses (B). Total net contralateral rotation was recorded with the same doses over 6 hours (C). Rotational asymmetry for all animals was recorded over 10 minute intervals for the duration (D). Values are expressed as means \pm SEM.

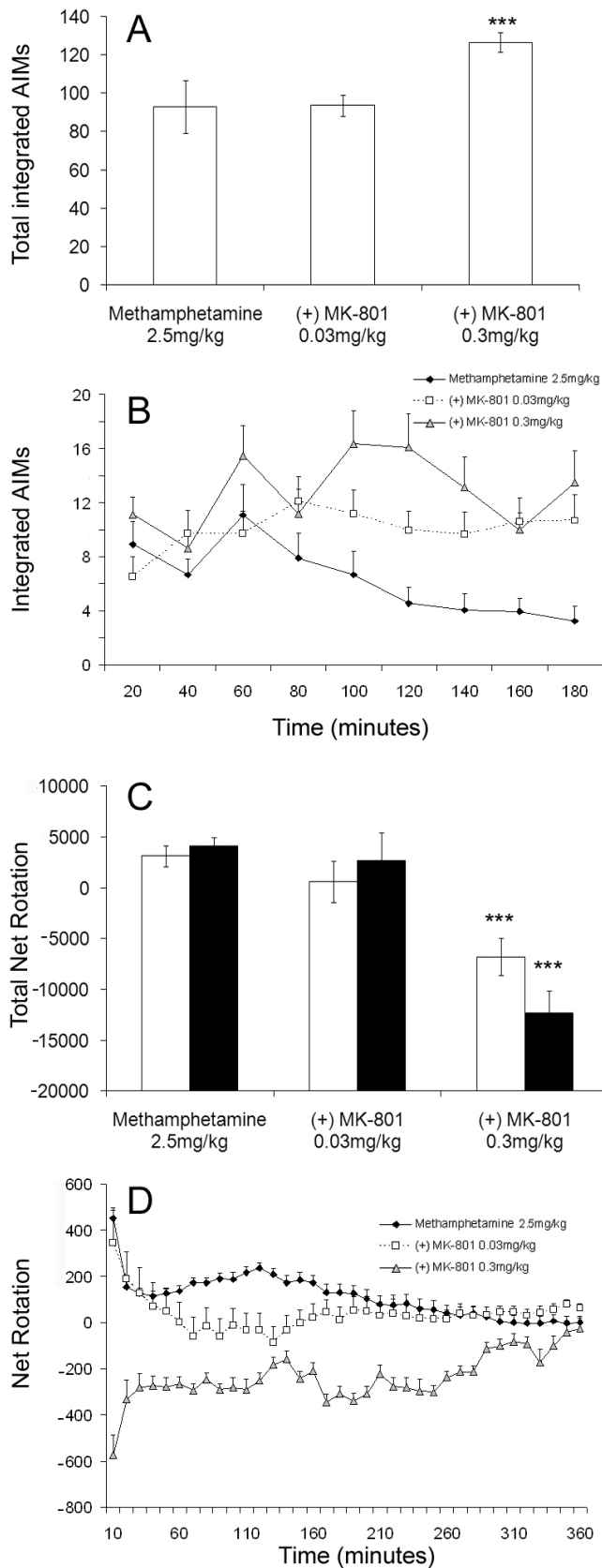


Fig. 6.13. Total integrated AIMs initiated by methamphetamine (2.5mg/kg) alone and with (+) MK-801 at a low dose (0.03mg/kg) or a high dose (0.3mg/kg) (A). Integrated AIMs were scored every 20 min for 3 h in response to methamphetamine and in combination with MK-801 doses (B). Total net contralateral rotation was recorded with the same doses over 6 h (C). Rotational asymmetry for all animals was recorded over 10 min intervals for the duration (D). Significant differences between the combination treatment and methamphetamine alone are indicated by $p < 0.001$ ***. Values are expressed as means \pm SEM.

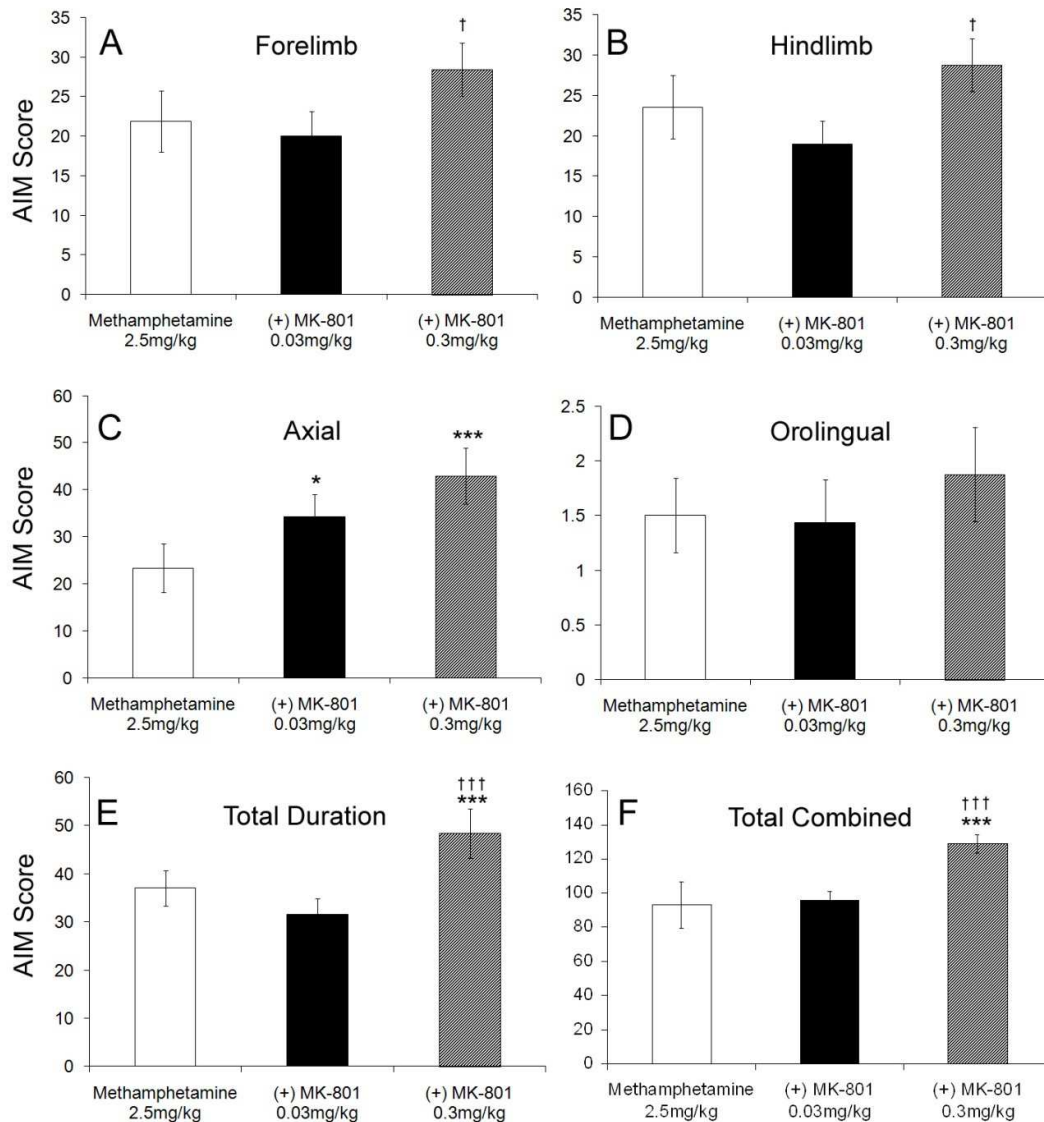


Fig. 6.14. The sub-categorisation of AIM score in response to methamphetamine alone (2.5mg/kg), with the addition of low dose MK-801 (0.03mg/kg) or high dose MK-801 (0.3mg/kg). AIM components assessed were forelimb (A), hind limb (B), axial (C), orolingual (D), total AIM severity (E) and total AIM amplitude (F). A Tukey post hoc test revealed significant differences attest between methamphetamine and with MK-801 treatment at the low dose, annotated by $p < 0.05^*$ and $p < 0.001^{***}$. Differences between high and low doses indicated by $p < 0.05^\dagger$ and $p < 0.001^{\dagger\dagger\dagger}$. Values are expressed as means \pm SEM.

The mGlu5 receptor subunit antagonist MTEP used in combination to methamphetamine had no effect on the expression of AIMs (Fig. 6.15A: $F_{2,22} = 0.66$ $p=ns$). There was a small decrease in total number of rotations with administration of the high dose ($F_{2,28} = 4.30$, $p < 0.05$) but no difference between dyskinetic and non-dyskinetic groups ($F_{1,14} = 0.44$, $p=ns$), Fig. 6.14C. The total rotational decrease can be attributed to a specific decrease in the second peak of rotational behaviour (Fig 6.15D).

The voltage-dependent open-channel blocker of AMPA receptors, IEM1460, did not affect AIMs at either dose (Fig. 6.16A: $F_{2,22} = 1.36$, $p=ns$), but reduced total rotations ($F_{2,28} = 4.04$, $p < 0.05$), with no difference between dyskinetic and non-dyskinetic groups ($F_{1,14} = 0.66$, $p=ns$), Fig 6.16C. At the low dose a small decrease in the second rotational peak was apparent (Fig 6.16D).

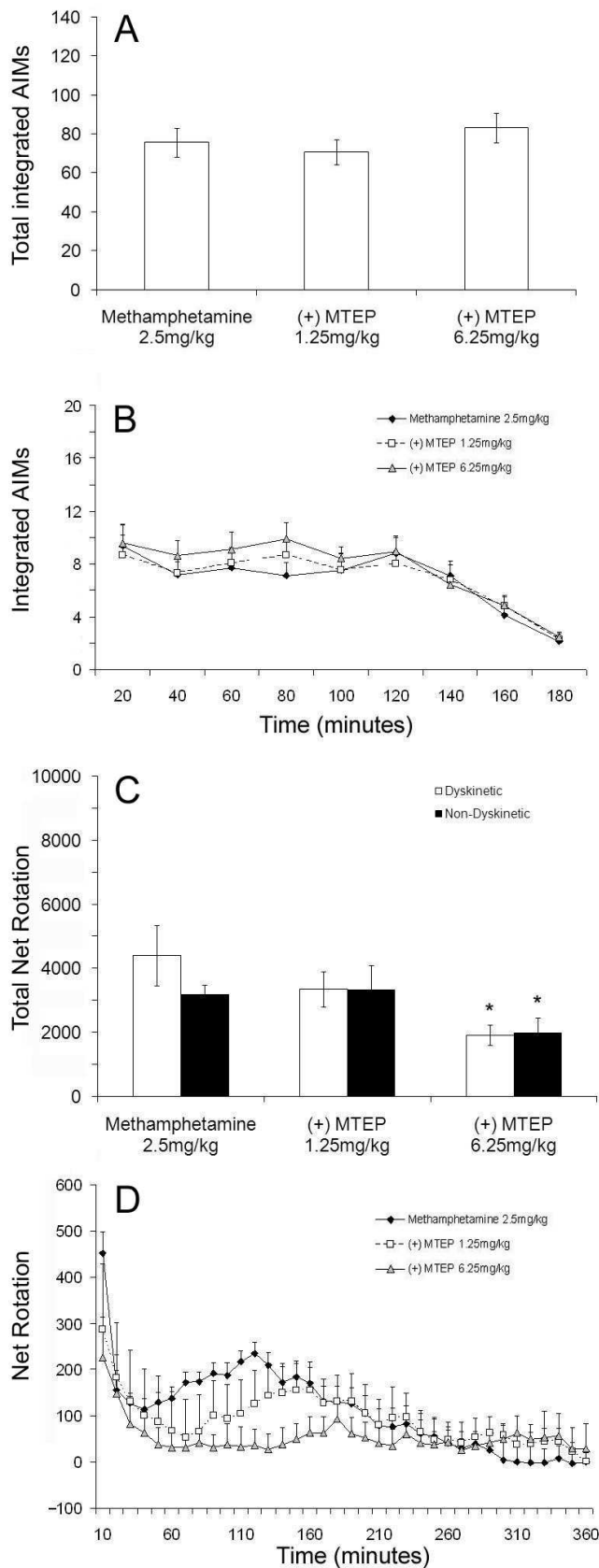


Fig. 6.15. Total integrated AIMs initiated by methamphetamine (2.5mg/kg) alone and with (+) MTEP at a low dose (1.25mg/kg) or a high dose (6.25mg/kg) (A). Integrated AIMs were scored every 20 minutes for 3 hours in response to methamphetamine and in combination with MTEP doses (B). Total net contralateral rotation was recorded with the same doses over 6 hours (C). Rotational asymmetry for all animals was recorded over 10 minute intervals for the duration (D). Significant differences between the combination treatment and methamphetamine alone are annotated by $p < 0.05^*$. Values are expressed as means \pm SEM.

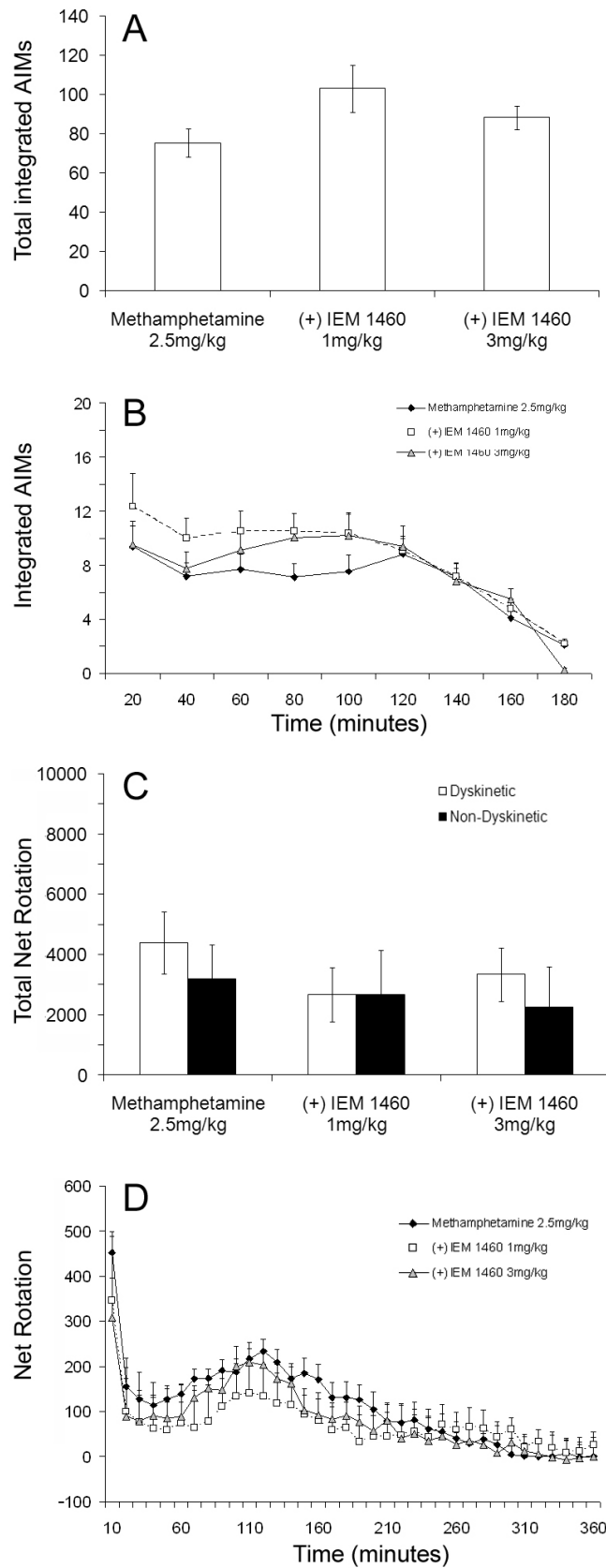


Fig. 6.16. Total integrated AIMs initiated by methamphetamine (2.5mg/kg) alone and with (+) IEM-1460 at a low dose (1mg/kg) or a high dose (3mg/kg) (A). Integrated AIMs were scored every 20 minutes for 3 hours in response to methamphetamine and in combination with IEM-1460 doses (B). Total net contralateral rotation was recorded with the same doses over 6 hours (C). Rotational asymmetry for all animals was recorded over 10 minute intervals for the duration (D). Values are expressed as means ± SEM.

6.3.8. Results Summary

Table 6.2 illustrates the drugs known to reduce LID and their impact on reducing amphetamine-induced dyskinesia in the grafted hemi-parkinsonian model. Dopamine and 5-HT modulating agents did reduce AIMs and altered total and temporal patterns of net contralateral rotation. With the exception of MK-801 the NMDA, AMPA and mGlu receptor antagonists did not decrease AIMs, yet locomotor activity measured by rotation was suppressed at the highest doses. Excluding MK-801, where total integrated AIM changes did occur, these were ubiquitous across all subtypes (see supplementary data: Table 1).

Drug	LID	L-DOPA Loco	Ref	mAmphet GID	mAmphet Loco	Ref
SCH23390	↓↓↓	↓↓↓	(Monville et al., 2005)	↓↓↓	↓↓↓	(Lane et al., 2009a)
Raclopride	↓↓↓	↓↓↓	(Monville et al., 2005)	↓↓↓	↓↓↓	(Lane et al., 2009a)
Nafadotride	↓↓	↓↓	(Monville et al., 2005)	↓	---	
Naloxone	↓↓	---	(Lundblad et al., 2002)	---	↓	
WIN55, 212-2	↓↓	---	(Morgese et al., 2007)	---	---	
Yohimbine	↓↓	↓↓	(Dekundy et al., 2007)	---	---	
CP94253	↓↓	---	(Munoz et al., 2008b)	↓↓	↓*	
8-OH-DPAT	↓↓	---	(Munoz et al., 2008b)	↓↓	↓	(Lane et al., 2009a)
Amantadine	↓↓	---	(Lundblad et al., 2005)	---	---	
MK-801	↓↓	↓↓	(Paquette et al., 2010)	↑↑	↓↓↓†	
MTEP	↓↓	---	(Rylander et al., 2009)	---	↓↓	
IEM1460	↓↓	---	(Kobylecki et al., 2010)	---	↓	

Table 6.2. A comparison of the pharmacological modulation of LID and methamphetamine (2.5mg/kg)-induced GID in unilateral 6-OHDA lesioned rats. Table annotated as: - mildly decreased (↓), mildly increased (↑), moderately increased (↑↑), moderately decreased (↓↓), greatly increased (↑↑↑), greatly decreased (↓↓↓), unchanged (---), reversion in rotation (†) and dyskinetic/ non-dyskinetic group differences (*).

6.4 Discussion

6.4.1. *Methamphetamine Dose Response*

The reduction/ reversion in amphetamine-mediated turning following transplantation have long been established (Bjorklund and Stenevi, 1979, Dunnett et al., 1981). Both stereotypic and rotation responses have previously been shown to be dependent upon dose (Lane et al., 2009b, Torres and Dunnett, 2007), but this is the first data to illustrate the same effect with post-transplantation AIMs. This study also highlights the disparity between AIMs and rotational responses, increasing the validity of their assessment as two different parameters of post-transplantation activity of the graft. Maximal rotational responses were triggered by 1.5mg/kg of methamphetamine, whereas the highest AIM scores were recorded at 2.5mg/kg. Lower doses (0.5mg/kg and 1.25mg/kg) were sufficient to cause both AIMs and rotational bias to equivalent levels that were significantly less than observations at 1.5mg/kg and 2.5mg/kg. The conflict between the increase in AIMs and decrease in rotation rate may reflect the direct competition between these behaviours, since locomotion is limited by the limb/ axial dyskinesia and dystonia. However these data suggest that something different underlies this difference, since rotation is only slightly higher in the non-dyskinetic group. Methamphetamine induces dopamine efflux from the transplant and reduces dopamine influx via direct interaction with DAT transporters (reviewed in Fleckenstein et al., 2007), with the efficacy of this mechanism seemingly greatest at 1.5mg/kg. This balance may be shifted at 2.5mg/kg, favouring reduced and dysregulated dopamine release. Interestingly, the same biphasic response and rotational severity is observed in grafted rats that have not been primed with L-DOPA (unpublished observations Lane EL, Steece-Collier et al., 2009, Torres and Dunnett, 2007) Thus indicating the super-sensitisation of dopamine receptors does not mediate turning in response to methamphetamine.

6.4.2. *Dopamine Receptor Antagonism*

The inhibition of methamphetamine-induced dyskinesia and contralateral turning behaviour by D₁ and D₂ antagonists, SCH-23390 and raclopride respectively, suggests that dopamine released from the graft acts on D₁ and D₂ receptors in the striatum to trigger these behavioural responses. These findings by (Lane et al., 2009b) were reproduced here and AIMs score reduction, accompanied by a decrease in locomotion, was of equal magnitude to their effect on

experimental LID (Johnston et al., 2005, Monville et al., 2005, Lundblad et al., 2005). These data also suggest robust turning response and methamphetamine driven GID is not greatly modulated by D3 receptors. In contrast both D₃ agonism and antagonism are able to reduce LID in MPTP treated primates, with the latter also negating the therapeutic benefit of L-DOPA (Bezard et al., 2003). Since antagonism with nafadotride caused no change in rotational asymmetry it is likely that the small reduction in dyskinesia may be explained by the partial D₂ antagonistic properties of the drug. In addition, other more specific D₃ binding compounds have no effect on mediating amphetamine-driven ipsilateral rotation after a 6-OHDA lesion, where receptors are found to be down-regulated (Robinet and Bardo, 2001). It is therefore unlikely that D₃ receptors are further altered post graft. D₂ receptors within the graft are likely to modulate dopamine release caused by methamphetamine, thus further modulating extracellular dopamine levels presynaptically. Levels of D₁ and D₂ receptors within the denervated striatum and transplanted tissue are compared between dyskinetic and non-dyskinetic groups in Chapter 7.

6.4.3. Opioid Receptor Antagonism

Naloxone had a small effect of reducing the rotational asymmetry from 75-150 minutes post injection, although had no effect on GID. The null effect on AIMs can be explained in part by the lack of μ -opioid receptors in dorsomedial regions, as receptors mainly reside within the NAcc core and rostral VTA (Soderman and Unterwald, 2008). These results are in contrast to its use in the modulation of experimental LID (Dekundy et al., 2007). Rotational changes are likely to be post-synaptic and mediated by dopamine receptor intracellular signalling, since D₁ and D₂ receptors can be colocalised with μ -opioid receptors and are coupled with adenylyl cyclase-5, implicated in motor function (de Gortari and Mengod, 2010). In addition, specific μ -opioid receptor-mediated G-protein activation is significantly enhanced in the basal ganglia and cortex of L-DOPA-treated dyskinetic primates (Chen et al., 2005) and therefore naloxone may cause an anti-dyskinetic effect by altering opioid specific GPCR intracellular signalling. It is currently unknown if specific opioid G-protein mediated signalling is dysregulated or normalised in grafted rodent models.

6.4.4. Cannabinoid Receptor Agonism

The CB₁ receptor antagonist WIN55, 212-2 reduced the rotational response between 25-100 minutes, without decreasing the expression of methamphetamine induced GID during this or any other time point during the observation time. The localisation of CB₁ receptors in ventral

striatal regions may mediate the locomotor response, preferentially to the abnormal movements. This contrasts with the reduction of LID in rats with the same compound (Morgese et al., 2007), although this result can be debated, since clinical trials using oral cannabis did not improve dyskinetic symptoms (Carroll et al., 2004). The collective action of cannabinoid agonists is seemingly unlikely to warrant evaluation as a treatment of GID. The lack of effect of CB₁ modulation are threefold, since they are unlikely to be found in the graft as they have only been localised to striatonigral neurones, are substantially reduced in the 6-OHDA lesioned brain (Walsh et al., 2010) and unchanged by L-DOPA treatment (Casteels et al., 2010). Nevertheless this is an important drug for continued clinical investigation, as there is much research in regard to LID and may have some modular and co-modulator roles in pharmacological management of GID.

6.4.5. Adrenergic Receptor Antagonism

Dyskinesia or turning behaviour was not affected by 10mg/kg of yohimbine and proportions of the cohort exhibited adverse side effects including pulmonary oedema. Tolerance issues and cardiovascular side effects associated with the targeting of the α_2 adrenergic receptor have been reported following testing in phase II clinical trials for the treatment of LID (Fox et al., 2008a). The additional antagonist actions on 5-HT_{1A}, 5-HT_{1B}, and D₂ have not been excluded as mechanisms through which the positive effects of yohimbine on LID may be mediated, although do not explain the lack of effect with GID. It is reasonable to assume that a higher dose would have negated GID but could not be trialled due to extreme side effects in combination with amphetamine administration. The adrenergic antagonistic properties drug to cause an inhibition of dopamine release from host terminals should be sufficient to decrease turning and dyskinetic behaviour, however the presence of α_1 and α_2 receptors on dopamine neurones on the graft are unknown.

6.4.6. 5-HT Receptor Agonism

The 5-HT_{1A} receptor agonist (8-OH-DPAT) and the 5-HT_{1B} receptor agonist (CP-94253) reduced the total integrated AIM score, largely due to a reduction over the first 80 minutes of testing; this reduction in AIMs with 8-OH-DPAT is consistent with previous findings (Lane et al., 2009a). 5-HT release is blocked by action at receptors on the dorsal and medial Raphe nucleus or on the 5-HT terminals themselves when given 8-OH-DPAT and CP-94253 respectively. The dual route of these responses has led to the previous finding that combined 5HT_{1A} and 5HT_{1B} treatment causes a further reduction in L-DOPA induced AIMs (Carta et al.,

2008a), this could also be applied to the grafted model in future studies. Activation of presynaptic 5HT_{1A} receptors on glutamate and 5-HT terminals by CP-94253 causes an increase in extracellular 5-HT levels reducing the synaptic release of glutamate and 5-HT and controlling dysregulated release. Under these principles AIM reduction is likely to be a combined modulation of grafted 5-HT neurones, host 5-HT terminals and corticostriatal connections.

CP-94253 did not alter total contralateral rotations but the time course reveals a biphasic action, the second peak in rotation being prevented by both doses, with turning remaining constant between 225-360 minutes. CP-94253 acts as a monoamine reuptake inhibitor causing the accumulation of 5-HT and dopamine in the brain which may relate to the delayed and prolonged increase in rotation in the latter half of the experiment. Interestingly, 5-HT_{1B} agonists injected directly into the VTA can enhance methamphetamine-induced hyperlocomotion (Papla et al., 2002). Therefore the action of this drug in the VTA may contribute to the enhancement of methamphetamine-induced rotation seen toward the end of the session and the sustained AIM expression above baseline seen at 180 minutes.

To probe the role of 5-HT in GID, 11CDASB PET scans carried out on 2 of the patients grafted in the London/Lund study (Hagell et al., 1999). These revealed high binding of the 5-HT transporter, and thereby assumed high levels of 5-HT neurons in the grafted putamens (Politis et al., 2010). Levels were significantly higher than both neurologically normal controls and patients with PD (Politis et al., 2010). Both patients had GID and were blindly challenged with buspirone which reduced the abnormal movements as assessed by a clinician also blind to the treatment status. Although supportive of a role of 5-HT in the GID these data should be interpreted with caution as only 2 grafted patients were studied, both of whom had GID, no grafted patients without GID were evaluated. Furthermore, buspirone has a notable D₂ receptor antagonist activity which could also be expected to have this effect, assuming excessive dopamine release is driving the GID. The α_1 , and α_2 -adrenergic receptor antagonist action of buspirone is unlikely to have a direct effect on spontaneous abnormal movements, as seen by this study, although it may have a synergistic effect to reduce GID in combination with 5-HT agonist and D₂ antagonist actions. It is evident that agonist action on 5-HT release by the host terminals and 5-HT cells in the graft can modulate GID to a certain extent, but it is unclear whether this is a causative neuro-pathological mechanism, since the relationship between grafted 5-HT cells and host fibres with dyskinesia has not fully been explored.

Certainly research with the model of amphetamine-induced AIMs has shown no such relationship to host or transplant derived 5-HT innervations (Lane et al., 2009a) and although the clinical relevance of the rodent model is disputed, grafts with a high proportion of 5-HT cells in the transplants were observed in patients without GID (Mendez et al., 2008).

6.4.7. *Glutamate Receptor Antagonism*

There was no change in AIMs when the NMDA receptor antagonist amantadine was given with methamphetamine, equally in the in patients with LID amantadine only has an effect in a proportion of patients and efficiency of the drug may wear off after several months (Sawada et al., 2010, Wolf et al., 2010). The drug may act like other NMDA receptor antagonists on LID, such that AIMs are only reduced when parkinsonism is increased (Paquette et al., 2010, Paquette et al., 2008). Since methamphetamine driven locomotion did not change with amantadine perhaps a higher dose than those used in LID would bring about these changes in GID. Although clinically available for the treatment of dystonia or LID, this compound is one of the least specific and potent NMDA receptor antagonists. Amantadine also acts as a dopamine releasing agent, and also has anticholinergic properties (www.accessdata.fda.gov) that may be partly responsible for the decrease in LID, yet had these properties fail to effect methamphetamine driven AIMs/ rotation. The lack of effect of amantadine could be due to a similar competing mechanism since methamphetamine too causes dopamine release in addition to replacing dopamine in vesicles and inhibiting dopamine metabolism (reviewed in Fleckenstein et al., 2007).

Abnormal movements were increased by the highest dose of MK-801, accompanied by a reversal in rotation to pre-graft levels. This bizarre turning behaviour may be explained by the action MK-801 to increase dopamine in the SN and VTA (Wedzony and Czyrak, 1996, Wedzony et al., 1996). In this instance dopamine will have a greater effect on the dopamine receptors on the intact side, resulting in an ipsilateral bias. Previously authors have similarly reported that high doses of MK-801 are also able to cause a reversal in rotation caused by L-DOPA or dopamine agonists in lesioned rats (Boldry et al., 1995) and enhance turning where dopamine is injected intrastrially in intact rats (St-Pierre and Bedard, 1995, St-Pierre and Bedard, 1994). In intact animals MK-801 causes a down-regulation of *RGS2* in the striatum, that parallels an enhancement of adenylyl cyclase (Taymans et al., 2005a). This is in contrast to amphetamine and dopamine mediated upregulation of *RGS2* gene expression. *RGS2*

expression reduction could therefore play a causal role in the reversal of rotation seen in our animals, as RGS proteins are inhibitory to the cAMP pathway associated with dopamine receptors and locomotion. MK-801 given in combination with apomorphine is able to negate the priming effect on D₂ receptors (Pollack and Strauss, 1999) and can increase the turning responses and c-fos expression to D₁ agonists (Fenu et al., 1995), highlighting the strong functional connection between receptor types. High doses of L-DOPA and MK-801 however caused a worsening of scores on simple behavioural tasks assessing asymmetry deficit restoration by L-DOPA (Paquette et al., 2010). MK-801 could therefore cause an increase in the AIM score due to a lack of balance and co-ordination, therefore resulting in an increased parkinsonian phenotype. A loss of balance may also arise because the change in rotation occurred yet the lateralised dyskinesia in hind and fore limbs was constant, thus segregating the locomotor and dyskinesia mechanisms in the striatum. High axial and hindlimb AIM scores may therefore be the result of loss of balance.

MTEP was selected because of its known anti-LID properties in the rodent model (Dekundy et al., 2006) and because mGluR5 (Testa et al., 1994), expressed heterogeneously throughout the cortex and striatum. The antagonism of mGluR5 however did not cause a decrease in amphetamine-induced GID, only a reduction in contralateral rotation. It seems likely that MTEP may actually be increasing dyskinesia as a substantial reduction in rotation (an indicator of global motor suppression) is often accompanied by a decrease in AIMs. Co-administration of MTEP in LID states not only causes a reduction in AIMs but also abolishes pathological hallmarks of dyskinesia i.e. reversal of L-DOPA-induced up-regulation of PPE (Kobylecki et al., 2010). PPE has not yet been studied in relation to amphetamine driven AIMs with MTEP, but this aspect warrants further investigation. The lack of effect of MTEP may also be due to the absence/ presence of the mGluR5 receptor on grafted cells, which currently remains unknown. Nevertheless, the studies presented here indicate a different mechanism of amphetamine induced AIMs compared to those triggered by L-DOPA (perhaps through the simultaneous function of the graft and super-sensitised striatum), as mGluR5 antagonists suppress L-DOPA induced AIMs, yet mGluR1 antagonists have no effect (Dekundy et al., 2006, Rylander et al., 2010, Mela et al., 2007).

IEM 1460 was used to antagonise AMPA receptors without GluR2 subunits (GluR2 is expressed largely within the cortex), however had little effect on behaviour in contrast to LID where these receptors are critically involved in the initiation and subsequent expression of AIMs (Kobylecki et al., 2010). In the same study IEM 1460 was also found to normalise PPE and PPD expression in the lateral striatum. IEM 1460 may also be directly affecting the graft and the expression of AMPA receptor subunits quantified. GluR2/3 and GluR4 are highly expressed on developing dopamine cells 4 weeks post grafting, correlating with behavioural recovery, whereas the maturation of GluR1 subunits is prolonged until 12 weeks (Ishida et al., 2002), yet this later time point is associated with dyskinesia. Therefore GluR1 antagonism may be more advantageous in GID. Overall this indicates that GID is likely the result of graft integration, in addition to that of the long-lasting changes triggered by L-DOPA priming, requiring different pharmacological treatments compared to LID.

6.4.8. Conclusions

The dosage of methamphetamine is critically important for the manifestation of severe AIMs and locomotion, at 2.5mg/kg dose dyskinetic movements are high, yet strong net contralateral rotation is compromised from that seen at 1.5mg/kg. Furthermore, many of the pharmacological agents that have shown efficacy to reduce AIMs in humans and animal models, as the result of long term L-DOPA therapy, do not appear to reduce amphetamine driven dyskinesia in the grafted rodent model. It can therefore be concluded that GID and LID are mechanistically distinct and dopamine, 5-HT and glutamate are likely to be the key neurotransmitter systems involved in the development of AIMs arising from the dopamine rich transplant. It is clear from the literature that little is known about how levels of each receptor change following transplantation and whether this procedure can reverse L-DOPA receptor states. Therefore it is also unknown whether dyskinetic and non-dyskinetic grafted rats in response to methamphetamine have different receptor expression patterns. It is hoped that transgenic mice (i.e. specific receptor and functional protein knock-outs) may be used in the future to determine the mechanism of GID; however this first requires the creation of a non-transgenic grafted mouse model of amphetamine-induced AIMs (Chapter 8). Furthermore, a greater analysis of the dopamine receptors and associated molecular correlates of amphetamine-induced AIMs may also provide clues into the mechanism underlying GID (Chapter 7).

7. Neural Correlates of Amphetamine Induced Dyskinesia in the Grafted Rat Model

Summary

Unilateral 6-OHDA lesioned rats were primed with L-DOPA for 21 days, 1 month post surgery, before they were transplanted with rat E14 VM tissue in the denervated striatum. Dopaminergic grafts were allowed to mature in the absence of L-DOPA treatment for 16 weeks. Contralateral turning behaviour was elicited in response to 2.5mg/kg of methamphetamine in all grafted animals and 60% developed additional AIMs, not seen in lesion only rats. These data show that graft size (as determined by 5-HT/ TH cell counts) correlates with AIMs, although cell counts of either type do not differ between rats grouped into dyskinetic and non-dyskinetic cohorts. D₁ and D₂ dopamine receptor binding analysed by density analysis were found to be upregulated in response to the lesion and normalised following transplantation, however receptor expression was not uniform throughout the striatum. Cells within the grafted tissue were found to contain mRNA transcripts for both *RGS2* and *RGS4*, however the former was the most highly expressed and accordingly was correlated with AIMs. It was further found that *RGS* expression in the grafted tissue does not follow that of the adult SNc and VTA, but rather reflects embryonic levels at the time of transplantation, or a change induced by graft development in a novel environment.

7.1. Introduction

Transplantation of developing dopaminergic tissue into the dopamine depleted striatum of PD patients has led to improvement of the motor phenotype of some patients (Lindvall et al., 1989, Madrazo et al., 1988, Freed et al., 1995, Freed et al., 2001, Redmond, 2002, Redmond et al., 1993). However this novel technique has been shown to cause dyskinesia that can be initiated and sustained off medication (Freed et al., 2001). Although the spontaneous nature of this side effect cannot be reproduced in transplanted animal models, AIMs can be initiated by the administration of amphetamine in grafted rats (Lane et al., 2009a, Lane et al., 2006b). A number of factors have been found to correlate with AIMs in transplanted rats, differing according to each individual transplant. Graft placement, L-DOPA pre-treatment and the proportions of 5-HT neurones within the graft have been found to modulate the expression of AIMs (Carta et al., 2008c, Carlsson et al., 2006b, Lane et al., 2009b), although the latter correlate has been disputed (Garcia et al., 2011, Lane et al., 2009a). To date there has been little evidence to suggest correlates between the number of transplanted dopamine cells/ size of the graft and the expression of amphetamine-induced AIMs (Lane et al., 2009b, Lane et al., 2006b, Lane et al., 2008).

In addition, dopamine rich transplants also change the expression of dopamine receptors. The density analysis of [³H] radioligand binding assays show that dopamine depletion causes an increase in D₁ and D₂ receptors in the striatum and following a dopamine rich transplant, there is an apparent renormalisation of dopamine receptor levels, although results have been mixed and may be dependent on time post-lesion (Dewar et al., 1990, Myleson et al., 1991, Blunt et al., 1992, Narang and Wamsley, 1995). Transplantation has also been found to increase [³H] DAT binding and cause a normalisation of [³H] D₁ and [³H] D₂ levels compared to the intact side in the striatum and SN (Dawson et al., 1991). Other studies have shown regional differences in binding, where a large reduction of [³H] D₁ and [³H] D₂ density levels in the immediate graft vicinity and a smaller reduction throughout the rostral and caudal striatum (Gagnon et al., 1991, Rioux et al., 1991). No further change in D₁ and D₂ receptor levels are observed in L-DOPA treated grafted rats (Rioux et al., 1993). Where no previous lesion induced change in [³H] D₁ density is seen however [³H] D₁ levels are reduced compared to lesion only controls following transplantation (Savasta et al., 1992).

This chapter aims to look at the levels of D₁ and D₂ dopamine receptors and corresponding post-receptor regulators of G-protein signalling (*RGS2* and *RGS4*) within the graft and denervated striatum, to find how the transplant alters basal levels with respect to lesion only animals. The quantities and correlations of 5-HT/ TH and RGS positive cells in the graft were also compared, with the aim of discussing reasons behind observed differences. The ultimate goal of this research was to test whether dopamine receptors and RGS transcript expression in cells could be used as a new ‘biomarker’ for rats that will become dyskinetic in response to amphetamine and/or AIM severity.

7.2. Experimental Design

47 rats were used for the experiments presented in this chapter. All rats were adult female SD rats (Harlan) that had previously received a unilateral 6-OHDA injection to the MFB (Outlined in Chapter 2). Four weeks post-lesion rats received 21 consecutive days of L-DOPA and benzerazide (10mg/kg each), given by s.c injection. Rats were then transplanted with a single cell suspension derived from E14 VM tissue, from time mated SD females (Harlan) and the graft left to mature for 16 weeks, in the absence of any treatment. Methamphetamine (2.5mg/kg) was then used to induce contralateral turning and AIMs (in transplanted rats), given no more than twice per week.

Transplanted rats were separated into two groups, matched on similar AIM scores, to be culled either by perfusion from immunohistochemistry (N=16) or a schedule 1 technique so that the brains could be snap frozen (N=31) for *in situ* hybridisation. All rats were sacrificed more than 48 h after the final methamphetamine injection, where the presence of AIMs was absent. Groups were generated from rats that were dyskinetic (perfused: N=11; snap frozen: N=14) and non-dyskinetic (perfused: N=5; snap frozen: N=11), with remaining animals serving as intact and lesioned controls. Six E14 rat embryo heads, snap frozen immediately following dissection, were also used for these experiments. Paraformaldehyde fixed tissue issue was processed for the analysis of TH and 5-HT positive cells and snap frozen tissue to monitor basal cell expression of *RGS2* and *RGS4*, following protocols highlighted in Chapter 2. Consecutive sections of snap frozen tissue at the level of the striatum were used to determine levels of D₁ and D₂ receptor levels by [³H] SCH23390 and [³H] Raclopride autoradiography, also described in detail in Chapter 2.

Student T-tests were used to compare total numbers of TH and 5-HT cells in the grafted tissue of dyskinetic and non-dyskinetic rats and Pearson's analysis were used to measure correlations between cell numbers with the expression of AIMs and graft volumes. Dopamine receptor levels were measured by density analysis on imageJ (methods outlined in Chapter 2) and a 1-way ANOVA was used to compare differences between groups. Two-way ANOVAs with Dunnett's *post hoc* tests were used to compare levels of *RGS2* and *RGS4* labelled cells in the graft vicinity, in defined areas throughout the striatum and in comparison to TH labelled cells.

7.3. Results

7.3.1. 5-HT and TH Cell Analysis in the Graft

It is clear from the photomicrographs in Fig. 7.1A-Bi that the E14 VM transplants were rich in dopaminergic (TH) and serotonergic (5-HT) cell types. Further stereology analysis confirmed that TH and 5-HT cell numbers were directly correlated to the volume of the graft (Fig. 7.1C: $r = 0.93$, $p < 0.001$; Fig. 7.1Ci: $r = 0.893$, $p < 0.001$). On average there was approximately double the amount of 5-HT cells compared to TH types. In addition, there was no difference between either cell type in dyskinetic and non-dyskinetic groups (Fig. 7.1D: $T = 0.74$, $p = \text{ns}$; Fig. 7.1Di $T = 0.76$, $p = \text{ns}$). Total integrated AIMs elicited following an injection of 2.5mg/kg methamphetamine were correlated to TH (Fig. 7.1E: $r = 0.31$, $p < 0.05$) and 5-HT (Fig. 7.1Ei: $r = 0.23$, $p < 0.05$) labelled cells. However when the percentage of 5-HT cells in the graft were considered with respect to total integrated AIM scores (Fig. 7.2), no significant correlation was found (Fig. 7.2: $r = -0.13$, $p = \text{ns}$).

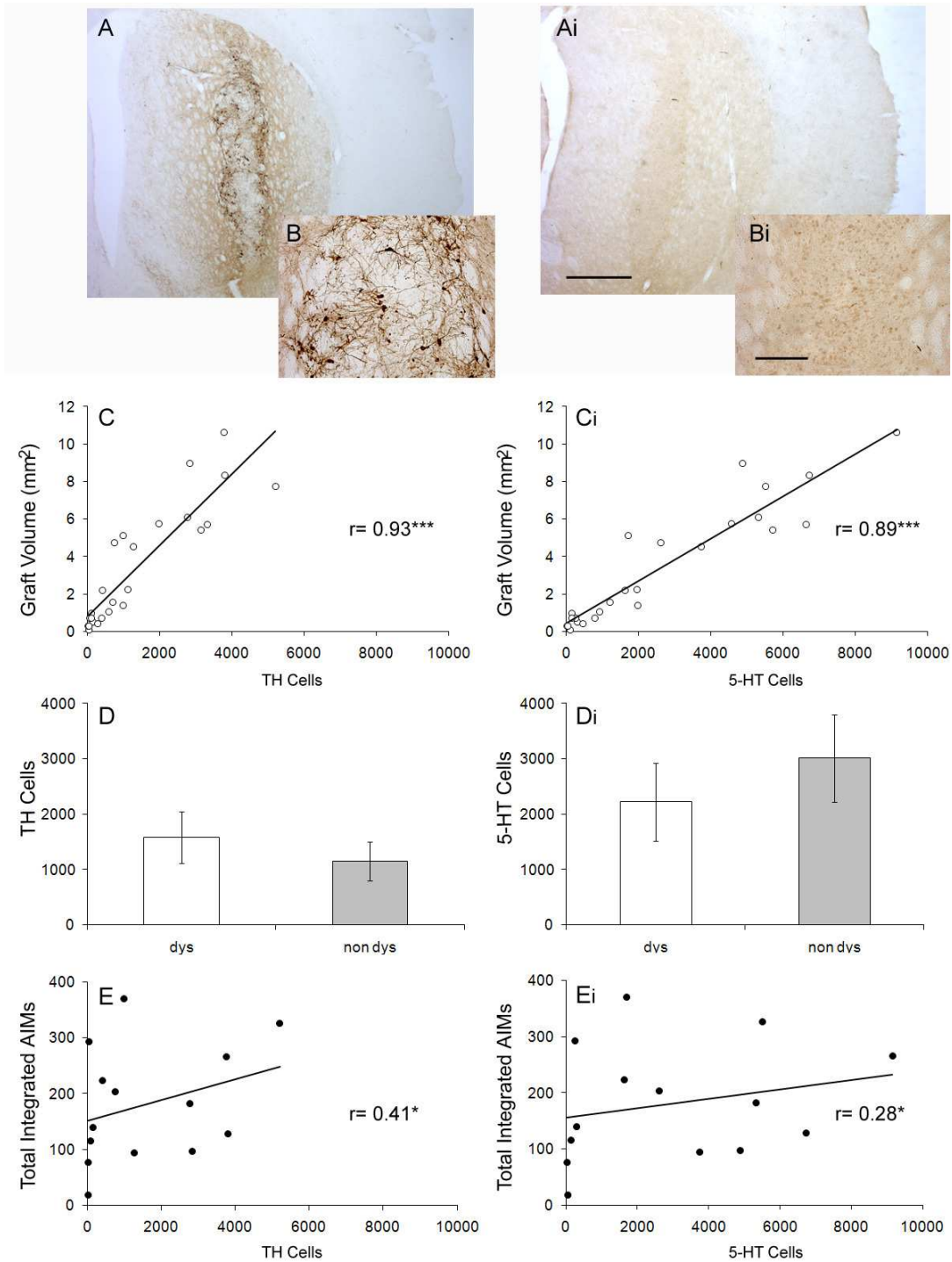


Fig. 7.1. Cell analysis of dopaminergic (A-E) and serotonergic types (Ai- Ei) in transplanted hemi-parkinsonian rats. Photomicrographs of transplanted TH (A-B) and 5-HT (Ai-Bi) cell types, where scale bar is 1mm (1.6x magnification) and 200 μ m (10x magnification). The

proportion of 5-HT and TH positive cells are directly correlated to graft volumes (C, Ci), where significance found by Pearson's analysis is annotated by $p < 0.001^{***}$. Numbers of TH and 5-HT cells were also compared between dyskinetic and non-dyskinetic groups in response to 2.5mg/kg of methamphetamine (D, Di) and total integrated AIMs displayed by dyskinetic animals were correlated to cell counts (E, Ei), where significance is denoted by $p < 0.05^*$. Values are expressed as Mean \pm SEM.

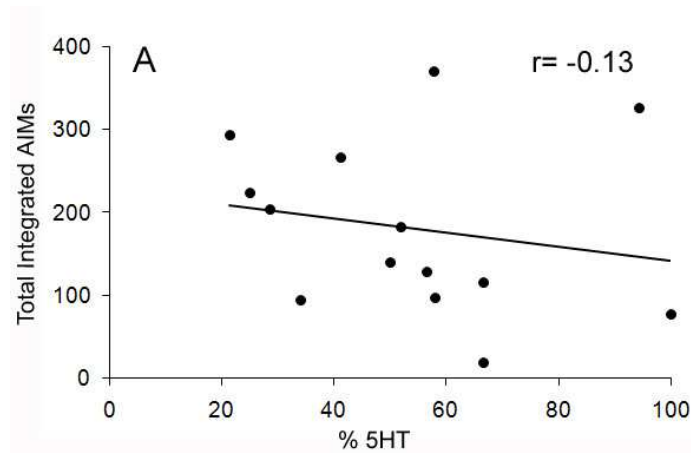


Fig. 7.2. Correlation between total integrated AIMs and the % of 5-HT labelled cells in the graft compared to that of TH (A). No significance was found using Pearson's correlation statistical test.

7.3.2. Dopamine Receptor Levels

D₁ and D₂ receptor levels were quantified in transplanted rats using [³H] SCH23390 and [³H] Raclopride autoradiography respectively. As shown in Fig. 7.3C-D,H-I a moderate increase in dopamine receptor binding was observed in 6-OHDA lesioned rats relative to intact controls. D₁ receptor binding increases however were unable to reach the 95% level of significance (Fig 7.3A; $F_{3,27} = 0.29$, $p = ns$), whereas D₂ receptor levels were significantly increased in the lesioned striatum (Fig. 7.3B; $F_{3,27} = 3.44$, $p < 0.05$). Following the transplant of VM derived tissue, receptor levels appear to be normalised, where the density of the striatum is considered as a whole. The photomicrographs of transplanted rats reveal that changes in receptor levels were not uniform within the denervated striatum (Fig. 7.3E-F, J-K), and transplanted nigral cells appear to have a lower density of both D₁ and D₂ receptors. The highest expression of both receptor types could be observed within the lateral region of the striatum. There was a significant difference between striatal areas for D₁ binding optical densities (Fig. 7.3M; $F_{1,46} = 24.12$, $p < 0.001$), with no change between dyskinetic and non-dyskinetic groups ($F_{1,46} = 0.22$, $p = ns$). The same pattern was noted for D₂ receptor binding, where density values were significantly decreased in the grafted area compared to the lateral striatum (Fig. 7.3N; $F_{1,46} = 57.84$, $p < 0.001$), with no change between dyskinetic and non-dyskinetic groups ($F_{1,46} = 0.02$, $p = ns$). No significant Group*Area interactions were observed for D₁ or D₂.

Furthermore, optical density binding values, in the striatum of dyskinetic rats, were not correlated to total integrated AIMs scored in response to 2.5mg/kg of amphetamine (D₁: $r = 0.09$, $p = ns$; D₂: $r = 0.07$, $p = ns$), data not shown.

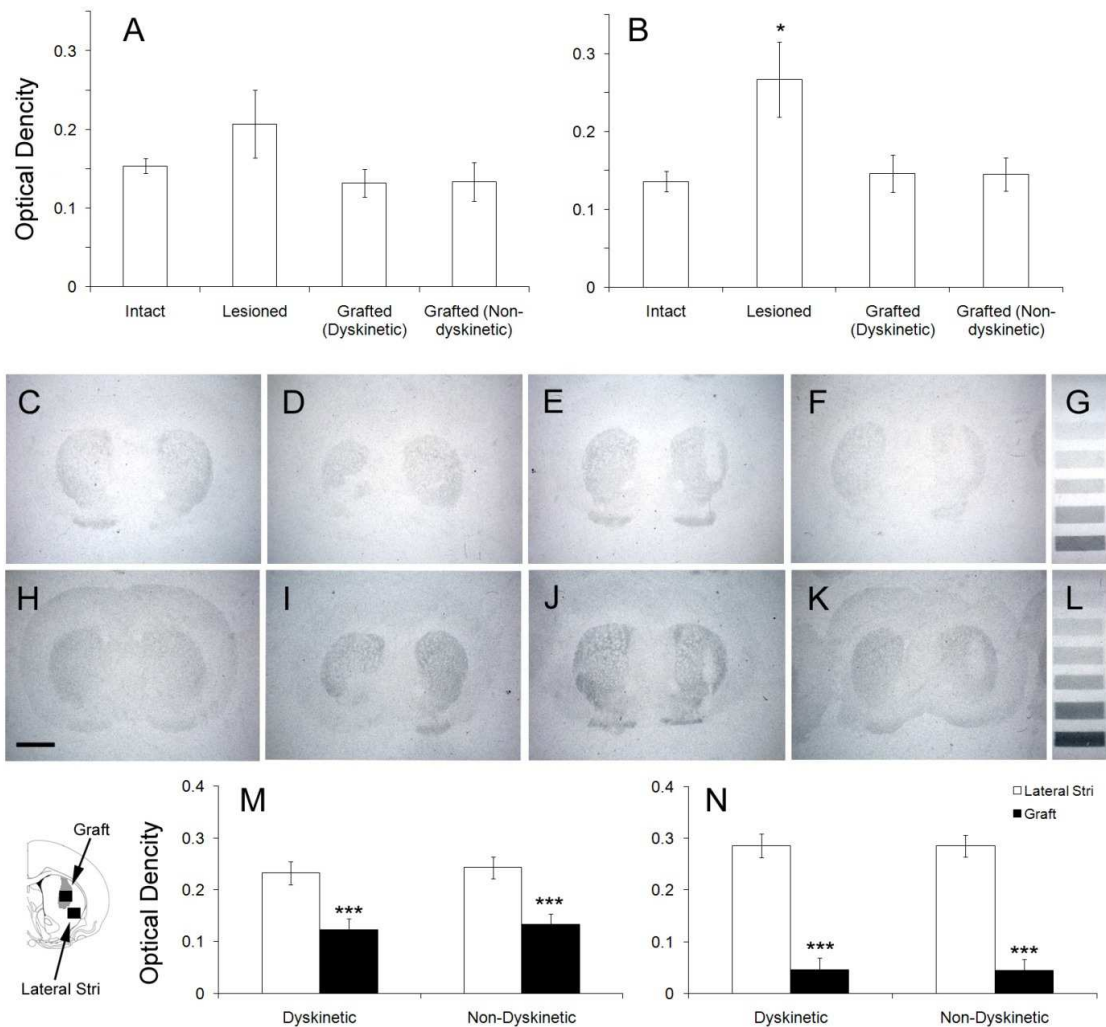


Fig. 7.3 Relative optical density analysis of D₁: [³H] SCH23390 (A) and D₂: [³H] Raclopride binding (B). Photomicrographs of developed photographic hyperfilms for corresponding [³H] SCH23390 (C-F) and [³H] Raclopride binding (H-K), where scale bar shown as 2mm. Intact (C,H), Lesioned (D, I) and Grafted dyskinetic (E,J) and Grafted non-dyskinetic groups (F,K) are shown, and [³H] Audiographic micro cassettes used for normalisation for corresponding dopamine receptor binding compounds are shown (G, L). Differences between the [³H] SCH23390 (M) and [³H] Raclopride (N) density levels within the transplant vicinity and the lateral striatum are indicated for dyskinetic and non-dyskinetic rats. Significant differences from intact control animals and between graft and host lateral striatal areas, are indicated by $p < 0.05^*$ and $p < 0.001^{***}$. Values are expressed as Mean \pm SEM.

7.3.3. *RGS* Transcript Levels

The photomicrographs in Fig. 7.4 show that the basal levels of *RGS2* and *RGS4* expression differ in the dopamine rich transplant. *RGS2* is of high abundance within the vicinity of the graft where as *RGS4* is of a much lower expression (Fig. 7.4A-F). The amount of *RGS2* and *RGS4* positive cells residing in the graft was also quantified by stereology in relation to numbers of TH positive cells. *RGS4* expression was significantly lower compared to that of *RGS2* and TH (Fig. 7.4G; $F_{2,46} = 21.71$, $p < 0.001$), yet there was no discernable difference between dyskinetic and non-dyskinetic groups ($F_{1,23} = 2.38$, $p = ns$), with no Group*Cell marker interaction. In accordance, Fig. 7.4H shows that the numbers of TH positive cells residing within the graft could be correlated to those expressing *RGS2* ($r = 6.64$, $p < 0.01$) but not *RGS4* ($r = 0.06$, $p = ns$). *RGS2* positive cells present in the graft of dyskinetic rats in the absence of amphetamine, were not correlated to previously scored amphetamine AIMs, even when confounding TH cell number-AIM correlations were removed by partial analysis ($r = 0.09$, $p = ns$), data not shown. Further, there were no correlations between the number of 5-HT cells in the grafted tissue and the quantities of either *RGS2* ($r = 0.12$, $p = ns$) or *RGS4* ($r = 0.19$, $p = ns$), data not shown.

RGS2 and *RGS4* were also differently expressed and altered by the transplant in the denervated striatum of transplanted rats, in the absence of methamphetamine, shown in Fig. 7.5. Fig. 7.5A indicates that within a defined area of the anterior medial striatum neither the lesion nor transplant were able to alter levels of *RGS* positive cells from those of unlesioned controls ($F_{3,54} = 2.07$, $p = ns$) and numbers of cells quantified with each *RGS* probe were equal ($F_{1,54} = 3.30$, $p = ns$). In the dorsomedial striatum (Fig. 7.5B) the lesion and transplant were unable to alter levels of *RGS* positive cells seen in unlesioned controls ($F_{3,54} = 0.38$, $p = ns$), however a small overall decrease in the levels of *RGS4* was apparent ($F_{1,54} = 4.51$, $p < 0.05$). In the medial striatum (an area directly over the transplant in grafted dyskinetic and non-dyskinetic groups) *RGS2* expression remained high following a lesion and transplant, whereas *RGS4* expression was much reduced in transplanted dyskinetic and non-dyskinetic groups (Fig. 7.5C; Group: $F_{3,54} = 16.83$, $p < 0.001$; Probe: $F_{1,54} = 25.96$, $p < 0.001$; Group*Probe $F_{3,54} = 14.00$, $p < 0.001$), confirming stereology findings. It is apparent from Fig. 7.5D however that *RGS4* cell counts were lower than those of *RGS2* in the ventrolateral striatum, for lesion and grafted groups ($F_{1,54} = 4.51$, $p < 0.05$) and in addition *RGS2* positive cells were found to be increased

post-lesion and further increased following a dopamine rich transplant, compared to intact controls ($F_{3,54} = 2.98$, $p < 0.05$).

It was further shown that both *RGS2* and *RGS4* are present in the adult VTA and SN (Fig. 7.6A-B), yet *RGS4* is absent from the VM of developing E14 embryos, despite the presence of *RGS2* and TH at this stage (Fig 7.6D-F).

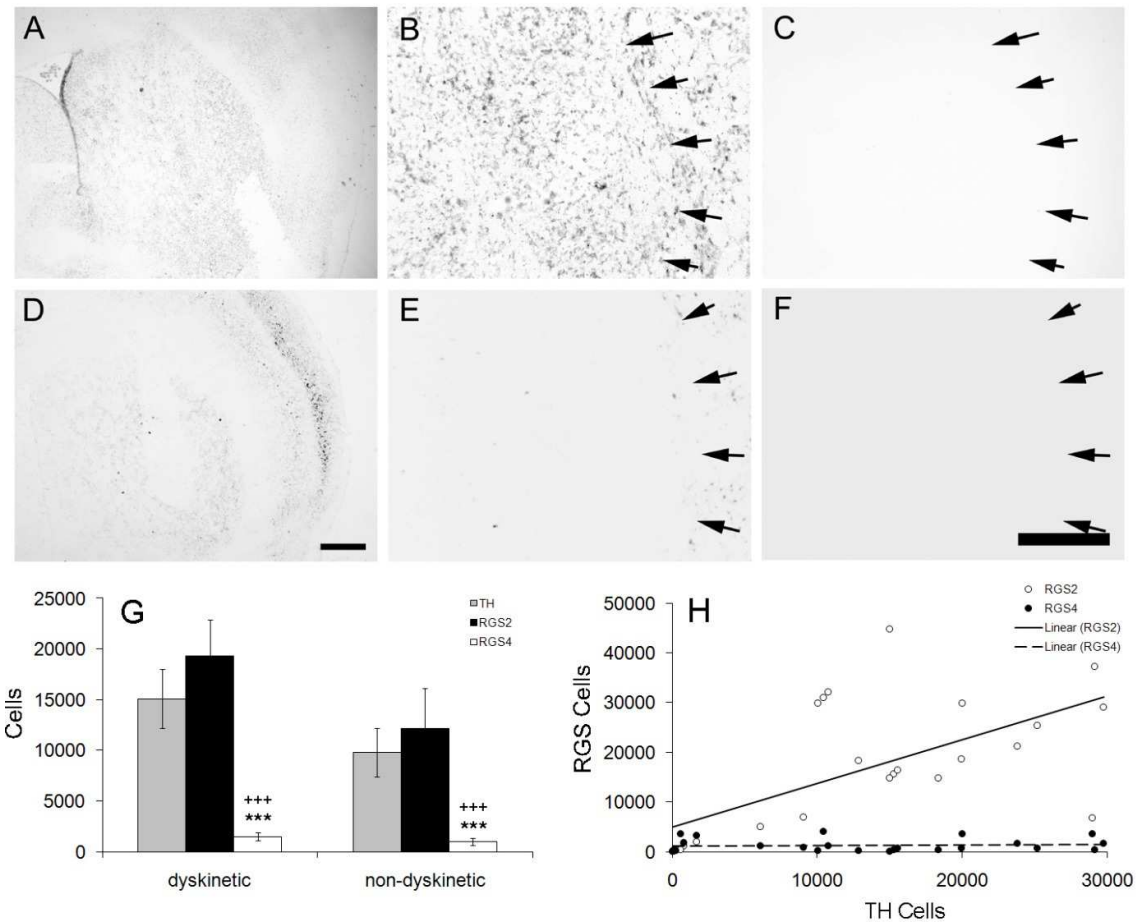


Fig. 7.4. Photomicrographs depicting *RGS2* (A-B) and *RGS4* (D-E) expression by *in situ* hybridisation in the rat E14 VM grafted tissue, with antisense oligonucleotides to respective probes used as negative-controls (C,F). Arrows indicate the graft host border. Scale bar = 1mm (A,D) and scale bar = 200µm (B-C,E-F). Cell counts of *RGS2*, *RGS4* (*in situ* hybridisation) and TH (immunohistochemistry) within the whole graft were quantified using stereology for both dyskinetic and non-dyskinetic groups (G) and RGS positive cells were then correlated with the amount of TH positive cells (H). Significant differences in the expression of TH cell numbers and those of *RGS2* and *RGS4* are annotated by $p < 0.001^{***}$ and $p < 0.001^{+++}$ respectively. Values are expressed as Mean \pm SEM.

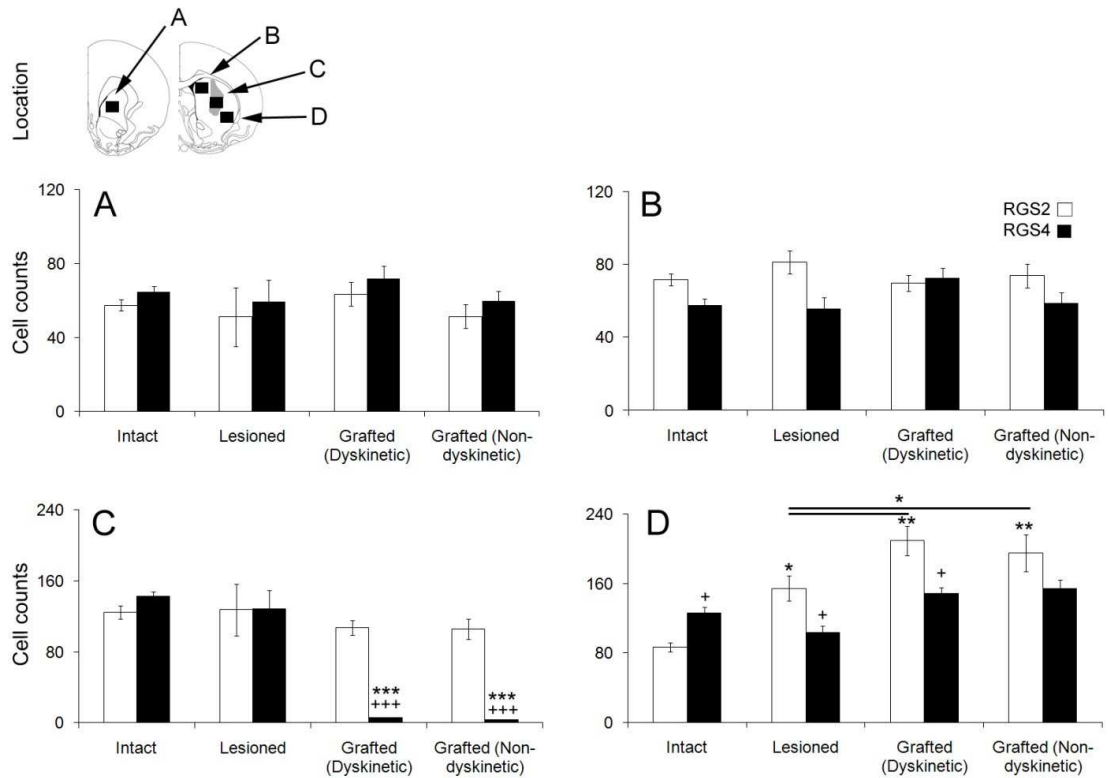


Fig. 7.5. *RGS2* and *RGS4* positive cell counts from *in situ* hybridisation were counted in an 1mm² area of the anterior medial striatum (A), dorsomedial striatum (B), medial striatum (C) and ventrolateral striatum (D) for intact, lesioned, and transplanted rats that either displayed AIMs above threshold level, in response to 2.5mg/kg of methamphetamine (Dyskinetic), or those that did not (Non-dyskinetic). Significant differences between intact striatal cell counts are annotated by $p < 0.05^*$, $p < 0.01^{**}$ and $p < 0.001^{***}$ and between levels of *RGS2* and *RGS4* positive cells within a group as $p < 0.05^+$ and $p < 0.001^{+++}$. Values are expressed as means \pm SEM.

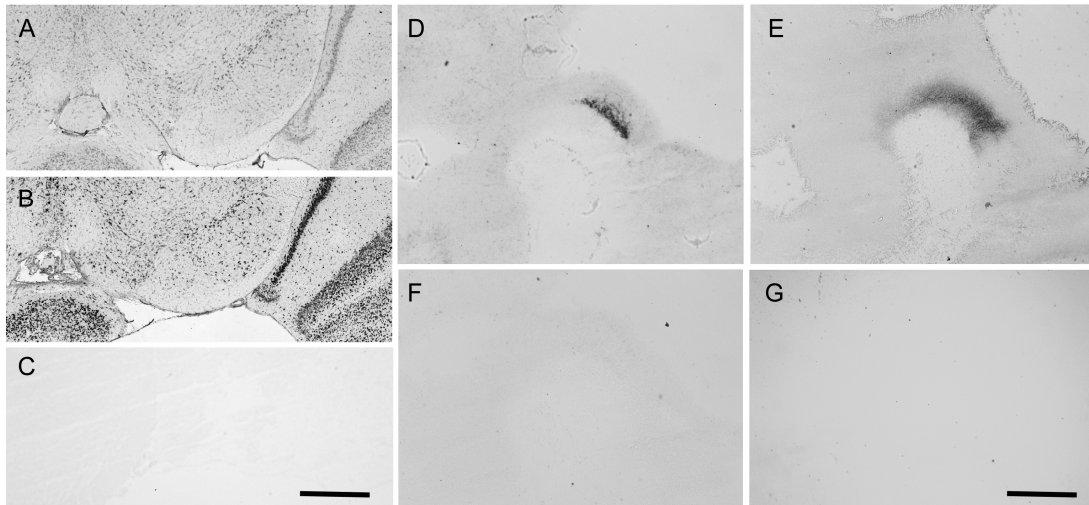


Fig. 7.6. Photomicrographs depicting the presence or absence of *RGS2* (A, D) and *RGS4* (B, F) positive cells in the adult (A-B) and developing midbrain of E14 embryos (D,F), by *in situ* hybridisation. The presence of TH at the E14 developmental stage is also shown (E) and antisense oligonucleotide probes for *RGS2* and *RGS4* were used as negative-controls throughout (C,G). Scale bar for A-C = 2mm and E-G = 1mm.

7.4. Discussion

7.4.1. Graft Correlates of GID

The proportion of 5-HT and TH positive cells within the transplant varied from 20 -90% between rats. Data presented here on total cell population analysis revealed that grafts had on average approximately double the amount of 5-HT neurones compared to TH, indicative of a wide dissection technique. Nevertheless, this 2:1 ratio was classified as within the normal range achieved by most investigators in a recent study (Garcia et al., 2011). There were positive correlations between the numbers of TH or 5-HT cells in the transplant and total integrated AIMs following methamphetamine, which is therefore reflective of previously reported graft size- AIM patterns first observed by (Lane et al., 2006b). Since the percentage of 5-HT cells in the transplanted tissue were not correlated to AIMs, significant 5-HT cell count-AIMs correlations are likely to be the result of graft size difference, as graft volumes are also correlated to 5-HT cell counts. Further, there was no difference between the numbers of TH or 5-HT cells present in the transplants of dyskinetic and non-dyskinetic groups, adding to the increasing body of evidence to suggest that AIM expression, both to L-DOPA and methamphetamine, is independent of grafted TH:5-HT cell ratios (Garcia et al., 2011, Lane et al., 2009a). Interestingly, TH:5-HT ratios in the 1:10 range are still sufficient to reduce LID

(Garcia et al., 2011), indicative of their negligible role in both amphetamine and L-DOPA driven AIMs. It is also clear that the weak positive correlations between AIMs and both the number of TH and 5-HT positive cells are likely to manifest by the rats which had small grafts in comparison to the total cohort, thereby skewing the outcome. Certainly this type of relationship exists (Lane et al., 2006) but has a ceiling effect. Once grafts reach a size in excess of approximately 2000 dopamine cells AIMs manifest highly in dyskinetic rats regardless.

Using autoradiography it can be shown for the first time that D₁ and D₂ receptor binding profiles were not correlated to AIM expression and binding density levels did not differ between dyskinetic and non-dyskinetic subtypes. This is unusual as D₂ receptors present on nigral cells are involved in pre-synaptic regulation of dopamine release to maintain the extracellular dopamine concentration (Cragg and Rice, 2004, Venton et al., 2003). Our findings may reflect the generally low levels of D₂ receptors present within the graft of either grafted group, therefore preventing any meaningful correlations. It cannot be ruled out however that DAT levels may have differed between dyskinetic and non-dyskinetic grafted groups resulting in changes to extracellular dopamine concentrations leading to dyskinesia, compared to non-dyskinetic rats receiving methamphetamine treatment, warranting further investigation. This theory however is unlikely, as the grafting of dissociated VM tissue from DAT KO mice does not lead to spontaneous AIMs and excessive extracellular dopamine, but rather a large compensatory reduction in pre-synaptic dopamine release (Jones et al., 1998).

It is unsurprising from the dopamine receptor analysis that the downstream target of the D₂ receptor *RGS4* was also of low abundance within the graft and the basal cell expression was not associated with methamphetamine driven dyskinesia. However the possibility that the *RGS4* gene failed to 'switch on' in the transplanted tissue cannot be ruled out, as it would in the normal development of the SNc neurones. Unlike TH and *RGS2*, these data show that in rat E14 embryos taken from the same litters as used for the transplant, *RGS4* is not yet present. This suggests that the maturation of the transplanted VM tissue in the adult denervated striatum, contributed to the absence of *RGS4*, as the result of the loss of appropriate developmental signals. In contrast low levels of the D₁ receptor were not matched by associated *RGS2* levels, where cell counts of the latter were very high and similar to the proportion of TH cells in the transplant. This can be explained however, since A9 dopamine cells express G-protein activated inwardly-rectifying potassium (GIRK) channels (Saenz del

Burgo et al., 2008) and these are regulated predominantly by RGS2 proteins (Lomazzi et al., 2008), in addition to their role in the regulation D₁ receptors. The equal number of TH and RGS2 positive cells in the graft and the positive correlation between their receptive cell counts may therefore exist because of the disproportionate presence of the A9 subtype in the grafted tissue. In agreement A9 neurones have been found to make up approximately 80% of all rat derived TH cells in the graft (*personal communication: Marija Fjodovova*). Co-labelling studies of cell type and RGS may be able to answer some of the questions generated by this research, however in the absence of viable RGS antibodies will prove difficult.

7.4.2. Efficiency of Graft to Normalise Lesion and L-DOPA Induced Changes

L-DOPA has been found to cause a long-lasting increase in dopamine receptor levels and in particular the sensitisation of the D₁-like receptors. The low levels of D₂ receptors within the graft are unlikely to be because of the average 2:1 ratio of 5-HT:TH neurones, as the D₂ receptor should also be localised on 5-HT neurones (Aman et al., 2007), but instead is reflective of the reinnervation of TH and 5-HT fibres into the denervated striatum. The presence of dopamine receptors on the TH and 5-HT fibres should therefore have caused an increase in receptor density post-transplantation in dorsomedial and lateral striatal areas, yet a decrease in receptor levels was observed in these regions, indicative of a renormalisation of post-synaptic receptor levels on MSNs. Similar D₁ and D₂ renormalisation from pre-graft levels was observed previously by use of E14- E15 derived tissue (Gagnon et al., 1991, Rioux et al., 1991), reiterating findings in this study. Up-regulations of D₁ receptors in the lesioned striatum were mild and did not reach statistical levels of significance, which may be due to the post-lesion latency, since D₁ binding increases were only found between 1-16 weeks post-lesion (Narang and Wamsley, 1995), a much shorter time period than used in this study. Up-regulations of D₂ receptors were higher in this study than that of Narang and Wamsley (1995), likely reflecting the continued trafficking of receptors to the plasma membrane longer than 16 weeks post-lesion. Therefore the time of transplantation post-lesion may affect the final outcome of dopamine receptor levels, and the graft induced changes may too take several weeks to manifest.

From previous data presented in this thesis (Chapter 5) it was found that 6-OHDA and L-DOPA treatment is insufficient to change the basal expression of RGS transcripts in mice. In accordance no changes in the number of RGS4 positive cells were found in rats following the same protocols, yet RGS2 cells were found to be moderately increased post-lesion. These data

show that after a graft the number of *RGS2* cells appears to increase further in the lateral regions that are likely innervated by transplanted cells. The ventrolateral region is of particular interest in relation to LID as it has been implicated in the upregulation of PDyn mRNA, a hallmark of dyskinesia (Carlsson et al., 2005, Cenci et al., 1998, Winkler et al., 2002b) and to orofacial stereotypes after direct injection of amphetamine into this location (Kelley et al., 1988), which indicate this area as a highly innervated, causing much intracellular signalling and behavioural changes once stimulated. Grafts in close proximity to the ventrolateral region have also been found to be involved in both the reduction of LID and the induction of methamphetamine induced AIMs (Carlsson et al., 2006b) and thus the upregulation of basal *RGS2* in the ventrolateral striatum could therefore be triggered by dopamine released from the graft and/ or synaptic connections. *RGS2* mRNA upregulation may represent a mechanism by which intracellular signalling is reduced, as *RGS2* is a negative modulator of G-protein signalling for D₁ receptors. Although basal levels of *RGS* were not correlated to amphetamine driven AIMs, it cannot be ruled out that under the presence of amphetamine this may have been the case.

7.4.3. Conclusions

The proportion of 5-HT cells, cell surface expression of D₁ and D₂ receptors, and quantities of *RGS2* and *RGS4* positive cells, present in the transplant and denervated striatum, did not differ between transplanted dyskinetic and non-dyskinetic cohorts and were not correlated to AIMs triggered by methamphetamine. In this study, the number of transplanted cells was the only determinant of the severity of amphetamine induced AIMs. We observed that the graft was able to normalise lesion-induced upregulations of D₁ and D₂ receptors by a large reduction of dopamine receptors in the vicinity of the graft and a moderate reduction in the lateral areas of the striatum. *RGS2* labelled cells were of high abundance in the graft due its role in A9 dopamine neurones and 5-HT neurones, whereas *RGS4* was of a significantly reduced expression either because of its down regulation below threshold levels of detection, or the absence of a developmental trigger ‘switching on’ the gene. In addition, basal *RGS2* expression was increased in the ventrolateral areas of the striatum as determined by the increased number of cells, perhaps reflecting a negative modulator role in D₁ expressing MSNs. It can therefore be suggested that D₁ and D₂ dopamine receptors and their respective RGS modulators, do not show potential to be used as new ‘biomarkers’ of GID. New

'biomarkers' may be found with the use of transgenic mice, however until research covered in this thesis (Chapter 8), there has not yet been a wild-type mouse model of GID.

8. A Mouse Model of GID

Summary

AIMs can be initiated by a single injection of methamphetamine (2.5mg/kg) in hemiparkinsonian rats. This study explores whether mice of C57/Bl6 and CD1 strains transplanted with primary VM derived tissue at day E12 of embryonic development also develop post-transplantation AIMs. Prior to grafting, mice were primed with L-DOPA for 21 days during which time AIMs and rotation were compared between strains. No significant differences were apparent between strains with regard to AIMs, however CD1 mice rotated less than C57/Bl6. Post-transplantation methamphetamine-induced AIMs were seen in approximately 65% of the cohort and all limb, trunk and orofacial dyskinetic components were observed and scored on a specific dyskinesia rating scale. At this stage there were no differences in AIMs and rotational asymmetry between C57/Bl6 and CD1 strains. Transplants were sufficient in size to cause a shift in rotation toward the contralateral direction in a number of animals and subsequent histological analysis of the transplanted tissue revealed surviving dopaminergic cells, with fibre outgrowth within the lateral motor regions of the striatum.

8.1. Introduction

A number of clinical trials have shown the survival of transplanted dopaminergic cells, their functional integration into the host neural tissue and the amelioration of the symptoms of PD (Freed et al., 2001, Lindvall et al., 1989, Madrazo et al., 1988, Olanow et al., 2003, Redmond, 2002, Redmond et al., 1993). The development of abnormal involuntary movements (AIMs) 6-12 months after the procedure was first noted by Freed et al. (2001) and was found to be unrelated to their anti-parkinsonian medication. Subsequently termed graft-induced dyskinesia (GID), this issue has been highly damaging to the progress of cell transplantation therapy. There has since been a drive to find out the mechanism of GID so that it may be prevented or managed whilst maintaining or improving the efficacy of the transplants. In particular there has been a search for appropriate animal models of GID for preclinical research into the condition.

Embryonic VM grafts transplanted into the denervated striatum of rats following unilateral 6-OHDA lesions of MFB provide the standard model used to assess the functional efficacy of cell replacement in PD (Bjorklund and Stenevi, 1979, Bjorklund et al., 1981, Dunnett et al., 1981). Quantifiable GID elicited in the absence of any treatment, like the spontaneous movements, found in patients, have not been observed in animal models of PD. In two studies, mild spontaneous dyskinesia in transplanted 6-OHDA lesioned rats were reported, although the behaviours were transient in expression, sporadic and mild in severity (Vinuela et al., 2008, Lane et al., 2006b), therefore lacking the consistency required to be used as a model of GID. Thus, post-transplantation AIMs are normally induced in the grafted hemiparkinsonian rat model using amphetamine, at a dose where no AIMs or stereotypy are seen in lesion-only control groups (Carlsson et al., 2006b, Lane et al., 2006b). Experimental GID is not the same as amphetamine-induced stereotypic behaviours and hence is not seen in amphetamine-treated lesion-only rats, as described in Chapters 6 and 7. AIMs in grafted rats vary in appearance, yet on the whole look phenotypically similar to LID, with dystonic hind limb positions, choreic forelimb, chewing and gnawing movements commonly observed, mirroring the human form.

Clinical trials have reported reductions in the duration and severity of LIDs in transplanted patients and a reduction in the 'off' phase (Lindvall et al., 1992). In experimental models, LID

is reduced by a graft (Lee et al., 2000) and studies have suggested that transplants may reduce the development of abnormal movements when L-DOPA is administered after the graft (Steece-Collier et al., 2009). Therefore, a greater understanding of how graft innervation changes both ‘on’ and ‘off’ dyskinesia following transplantation is much needed. Prior to transplantation, 6-OHDA lesioned rodents are usually primed with L-DOPA for 3- 4 weeks to elicit LID, as described by Winkler et al., (2002), thus causing the long term maladaptive changes in the denervated striatum associated with this aberrant behaviour (Cenci and Konradi, 2010, Cenci et al., 2009, Picconi et al., 2003, Winkler et al., 2002b, Lane et al., 2006b). There is a greater tendency for methamphetamine-induced AIMs in animals primed for LID, although a proportion of the primed experimental cohort will still not develop dyskinesia, termed ‘non-dyskinetic’ (Lane et al., 2009a). It is therefore important to consider L-DOPA priming in the creation of a mouse model of GID. Furthermore, L-DOPA priming is of fundamental importance to the clinical translation of the model, as the majority of PD patients that will undergo transplantation therapy are likely to be on L-DOPA treatment.

A mouse model of GID has not yet been evaluated, due to the lack of optimisation in appropriate behavioural tests, poor post-lesion survival rates and the insufficient characterisation of LID (addressed in Chapters 3 and 4). Although successful grafting and the rotational response to selective psychostimulants has previously been reported in the mouse (Thompson et al., 2009, Veng et al., 2002, Zhou et al., 1993, Shimizu et al., 1990, Brundin et al., 1989, Shimizu et al., 1988), appropriately sized grafts needed for the assessment of GID have been difficult to reproduce. It seems likely therefore that many of these now optimised factors needed for model development, can be combined to create a mouse model of GID, which should prove invaluable for combined use with transgenic mice and importantly for mouse derived cell line transplantation studies.

This chapter will compare LID and GID AIM development in two different mouse strains (C57/ Bl6 and CD1). Specifically, methamphetamine and L-DOPA-induced rotation will be assessed pre- and post-transplantation and AIMs scored simultaneously for both of these agents, over 3 hours post injection. A greater understanding of why only some patients develop GID may be gained by comparing dyskinetic and non-dyskinetic groups, therefore this study aims to split transplanted mice into these respective groups. Groups will be based on methamphetamine-mediated AIMs above and below the defined thresholds used for the rat

(Lane et al., 2006b), as recorded on the scoring system for LID in rats and mice (Cenci and Lundblad, 2007, Winkler et al., 2002b).

8.2. Experimental Design

30 adult male CD1 (Harlan) and 30 C57Bl6 (Charles River) mice weighing 25g or more at the time of arrival were lesioned with 6-OHDA at the MFB (previous studies in Chapter 4 showed this to be the most appropriate lesion site to precipitate LID following L-DOPA). Four weeks after the lesion, mice were tested for lesion extent using methamphetamine (2.5mg/kg) induced rotation. 26 CD1 and 20 C57/ Bl6 mice were chosen for the final study, based on rotation scores of greater than 5 per minute. All mice were then given daily injections of L-DOPA and benzerazide (10mg/kg each) for 21 days, where a stable AIM plateau was reached. L-DOPA-induced AIMs were compared between CD1 (n=15) and C57/ Bl6 (n=14) mice at day 21, further exclusions were made on the basis of illness of the animal or AIMs below a defined dyskinesia threshold (Cenci and Lundblad, 2007, Winkler et al., 2002b). Seven weeks post-lesion the average weight (after the recovery of weight loss in the first 2 weeks, described in Chapter 3) of both mouse strains was recorded. CD1 (n=9) and C57/ Bl6 (n=11) lesioned mice were then transplanted with E12 tissue from the developing VM of matched strains, the remaining mice served as lesioned and L-DOPA primed controls (CD1: n=6; C57/ Bl6: n=3). Prior to implantation, tissue was dissociated into crude single cell suspensions and 200,000 cells transplanted per μl , at two levels in the striatum, as detailed in Chapter 2. The grafts were left to mature for 16 weeks in the absence of any treatment.

Methamphetamine (2.5mg/kg) was used to induce turning and AIMs in mice, where they were sub divided into 'dyskinetic' (CD1: n=3; C57/ Bl6: n=6) and 'non-dyskinetic' (CD1: n=3; C57/ Bl6: n=3) groups. All mice were perfusion-fixed with 1.5% paraformaldehyde 72 h after the last methamphetamine injection, when AIMs were no longer present. Fixed brains were cut, stored and prepared for immunohistochemistry and the numbers of TH positive cells were quantified in the grafted tissue using stereological counting protocols. The remaining mice (CD1: n=3; C57/ Bl6: n=2) had failed grafts defined by (a) lack of rotational change in comparison to pre-graft levels and (b) by very few (<100) surviving cells seen in the graft post-mortem.

Amphetamine-induced rotation and weight between mouse strains was analysed by Student T-tests and 2-way ANOVAs with Dunnett's *post hoc* comparisons used to compare AIMs (L-DOPA and methamphetamine) and L-DOPA-induced rotation, between pre and post transplantation time points, for each strain. A further T-test was used to compare the numbers of transplanted TH cells between strains and a Pearson's test used to measure the cell number-AIM correlation.

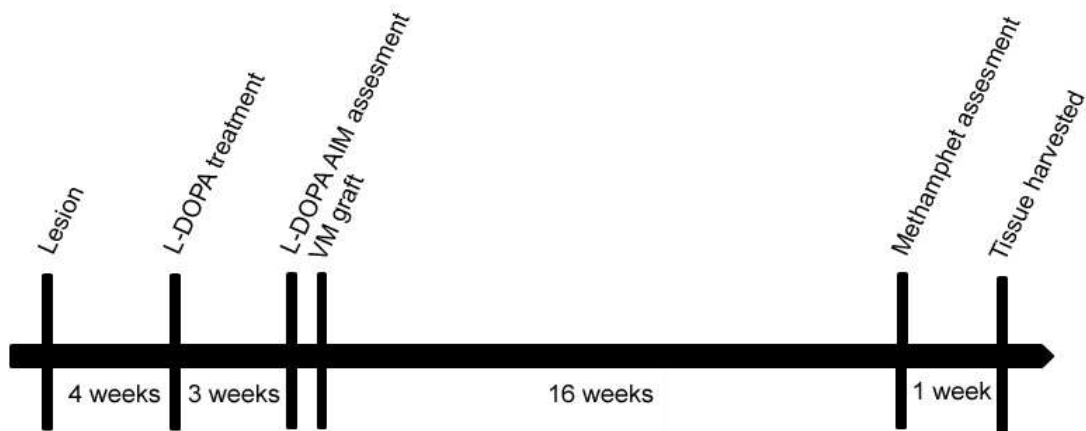


Fig. 8.1. Time line of experiments carried out for Chapter 8, to optimise a mouse model of amphetamine driven GID.

8.3. Results

8.3.1. Basal weight of CD1 and C57/Bl6 mice

The two strains of mice were generally different sizes, the C57/ Bl6 strain was approximately half the weight of the CD1 strain ($T= 27.91, p<0.001^{***}$).

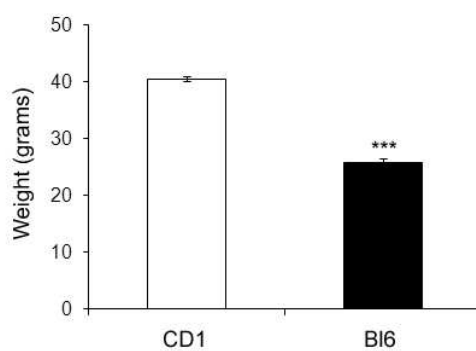


Fig. 8.2. The weight of CD1 and C57/ Bl6 mice. Significant differences between strains are annotated as $p<0.001^{***}$. Values are expressed as Mean \pm SEM.

8.3.2. Amphetamine Mediated Rotation in CD1 and C57/B16 mice

Methamphetamine-treated mice rotated ipsilaterally post-lesion (Fig. 8.3A). At this time point the C57/ B16 strain had a significantly higher total net rotation score than the CD1 strain ($T=3.21, p<0.05^*$). Post-graft rotations were predominantly contralateral in direction (Fig. 8.3B), however no difference was found between strains in the same test at 16 weeks after the transplant ($T=1.64, p=ns$).

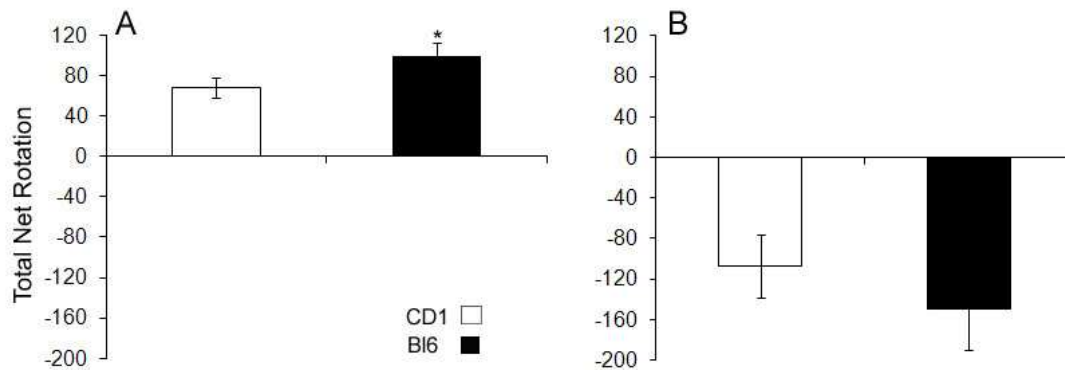


Fig. 8.3. Total net rotations in response to methamphetamine (2.5mg/kg) in CD1 and C57/ B16 mice 4 weeks after 6-OHDA lesion (A), and 16 weeks post-transplantation (B), scored over 60 minutes at peak rotation. Significant differences between strains are annotated as $p<0.05^*$. Values are expressed as Mean \pm SEM.

8.3.2. L-DOPA-induced rotation and AIMS in C57/Bl6 and CD1 strains

L-DOPA-induced rotations were significantly reduced by the presence of a graft (Fig. 8.3A; $F_{1,13}= 4.70, p<0.05$), where $p<0.05$ for both strains. CD1 mice had a lower rotational response to L-DOPA post-graft compared to the C57/Bl6 strain post-graft (Fig. 8.3A; $F_{1,13}= 4.98, p<0.05$), not seen at the pre-graft level. No difference between strains at either the pre-graft or post-graft time points, but in both groups total integrated AIMS were significantly reduced by the presence of a graft (Fig 8.3A: $F_{1,13}= 14.23, p<0.001$, *post hoc* $p<0.05$ for C57/ Bl6 and $p<0.001$ for CD1). LID was also reduced post-transplantation for each of the three AIM subtypes when considered separately (Fig. 8.3C-E: Hindlimb: $F_{1,13}= 10.12, p<0.01$; Forelimb: $F_{1,13}= 9.23, p<0.01$; Axial: $F_{1,13}= 18.67, p<0.001$), but not for the orolingual component (Fig. 8.3D: $F_{1,13}= 2.21, p= ns$), *post hoc* comparisons are indicated on Fig. 8.3. There were also no differences between strain for any of the L-DOPA-induced AIM components.

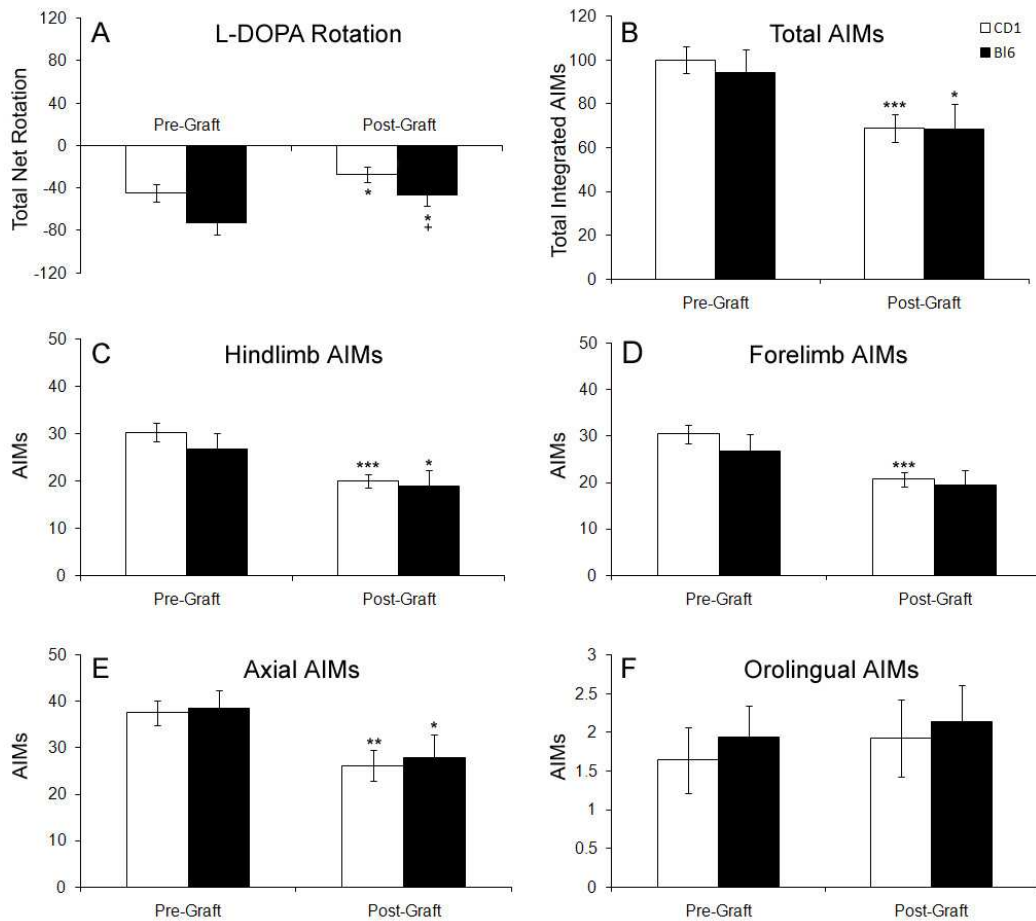


Fig. 8.3. LID and L-DOPA induced rotation in hemi-parkinsonian mice. Total net contralateral rotations in response to L-DOPA (10mg/kg) in CD1 and C57/ Bl6 mice 7 weeks after 6-OHDA lesion (Pre-graft) and 16 weeks post-transplantation (Post-graft) (A). Total integrated AIMs, scored on defined rating scales (Cenci and Lundblad, 2007, Winkler et al., 2002b), were also assessed after at pre-graft and post-graft time points (B). AIMs of each sub-component were also assessed for the hindlimb (C), forelimb (D), Axial (E) and orolingual (F) parameters. Significant differences by 2-way ANOVA and Dunnett's *post hoc* test between pre-graft and post-graft levels are annotated as $p < 0.05^*$, $p < 0.05^*$ and $p < 0.001^{***}$ and between strains as $p < 0.05^+$. Values are expressed as Mean \pm SEM.

8.3.2. Amphetamine-Induced AIMs in the Transplanted Mouse

Methamphetamine (2.5mg/kg)-induced AIMs were not observed in lesion-only control mice or those considered non-dyskinetic from either strain (Fig. 8.4). Methamphetamine induced AIMs in 66% of the grafted cohort in both CD1 and C57/ B16 strains. Furthermore, neither the time course of behaviours over the 3 h post-injection (Fig. 8.4A) or total integrated AIMs differed between strains (Fig. 8.4B: $F_{1,21} = 0.46$, $p=ns$). Mice which expressed AIMs in response to methamphetamine (dyskinetic mice) were significantly higher in comparison to lesion only and non-dyskinetic counterparts (defined as mice with no, or minimal AIMs) ($F_{2,21} = 9.11$, $p < 0.01$), where $p < 0.01$ for both strains (Fig. 8.4B). The expression of methamphetamine-induced AIMs for each component on the rating scale was also only present in the dyskinetic group (Table 8.1: axial: $F_{2,21} = 6.66$, $p < 0.01$; orolingual: $F_{2,21} = 4.31$, $p < 0.05$; forelimb: $F_{2,21} = 7.04$, $p < 0.01$; hindlimb: $F_{2,21} = 8.21$, $p < 0.01$). No difference found between strains for any of the AIM components or Time-point*Strain interactions. Fig. 8.5 is a pictorial representation AIM component seen in all dyskinetic mice.

Post-mortem analysis of the brains of dyskinetic animals revealed high numbers of TH positive cells in transplants within the denervated striatum (Fig. 8.6.), which were equivalent between CD1 and C57/ B16 strains ($F_{1,13} = 0.31$, $p=ns$) and between dyskinetic and non-dyskinetic groups ($F_{1,13} = 1.01$, $p=ns$). From the 400,000 cells transplanted approximately 3% of these were surviving dopaminergic neurones, based on calculations previously used for the approximate percentage of dopamine neurones per VM (Castilho et al., 2000). There was a moderate positive correlation between cell counts in the grafted tissue of dyskinetic mice and AIMs, however a statistical level of significance was not reached (Fig. 8.6D; $r = 0.52$, $p=ns$). In addition there were no correlations found between TH cell counts and either pre-graft LID ($r = 0.12$, $p=ns$) or post-graft LID ($r = 0.24$, $p=ns$) (data not shown). There were also no correlations found between pre- and post graft LID and methamphetamine-induced AIMs (data not shown).

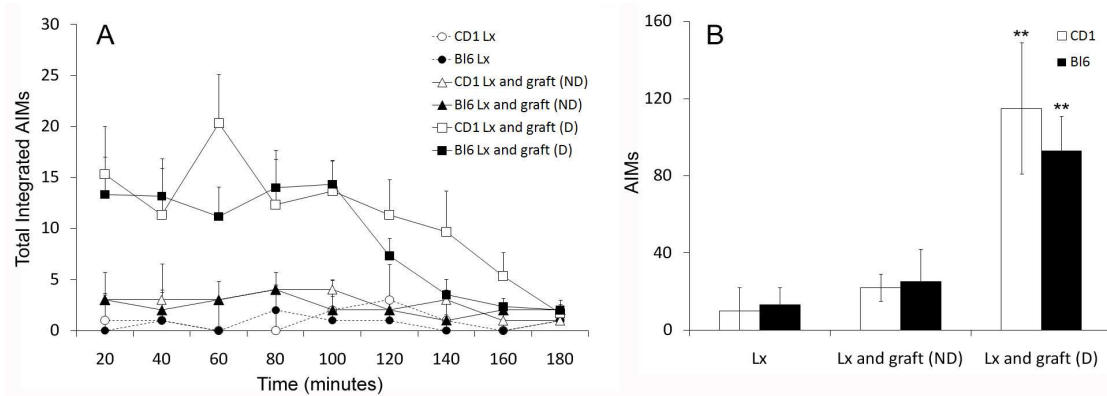


Fig. 8.4. AIMs triggered by 2.5mg/kg of methamphetamine in the unilateral 6-OHDA lesioned mouse, 16 weeks after the transplantation of E12 VM tissue. AIMs were observed over 180 minutes post injection (A) and total integrated AIMs (B) are shown for lesioned controls that have been L-DOPA primed (Lx) and transplanted CD1 and C57/ B16 mouse strains that were either non-dyskinetic (ND) or dyskinetic (D), based off the rating scale described by (Cenci and Lundblad, 2007, Winkler et al., 2002b). Significant differences are annotated as $p < 0.01^{**}$. Values are expressed as Mean \pm SEM.

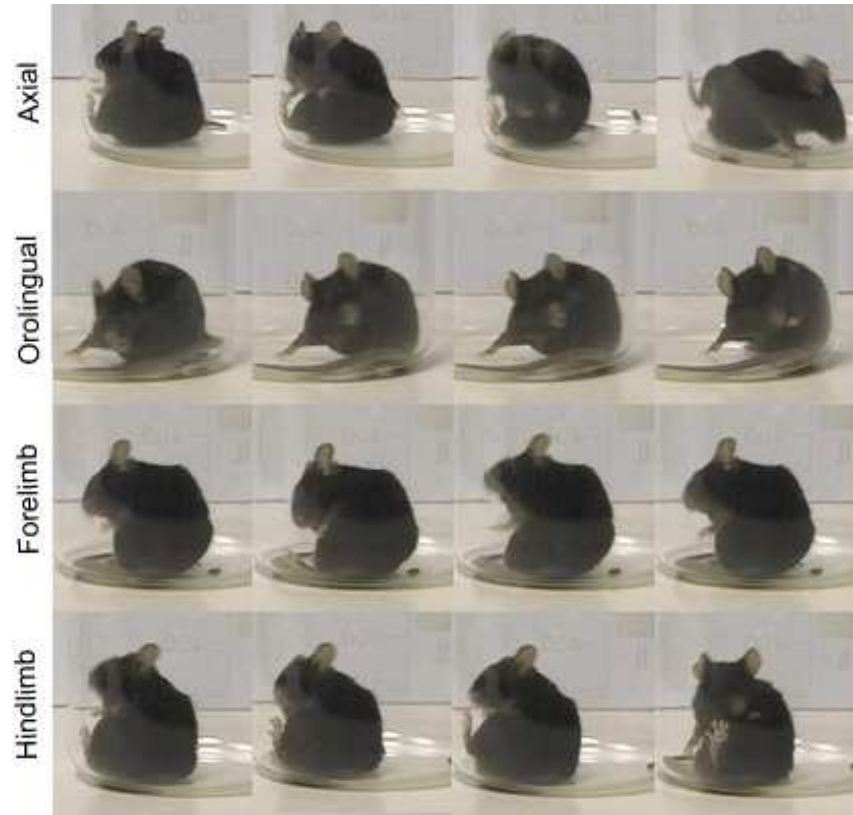


Fig. 8.5. AIMs induced by 2.5mg/kg of methamphetamine the unilateral 6-OHDA lesioned mouse, 16 weeks after the transplantation of E12 VM tissue. AIMs were observed for all four dyskinesia components (Axial, orolingual, forelimb and hindlimb) based an existing rating scale (Cenci and Lundblad, 2007, Winkler et al., 2002b).

	<i>Pre-transplantation</i>		<i>Post-transplantation (Non-Dyskinetic group)</i>		<i>Post-transplantation (Dyskinetic group)</i>	
	<i>CD1</i>	<i>C57/ Bl6</i>	<i>CD1</i>	<i>C57/ Bl6</i>	<i>CD1</i>	<i>C57/ Bl6</i>
<i>Axial</i>	4.89 ± 0.88	5.73 ± 0.26	6.89 ± 1.23	7.03 ± 2.21	45.33 ± 11.78**	32.31 ± 7.63**
<i>Orolingual</i>	0.11 ± 0.01	0.11 ± 0.01	2.11 ± 0.01 *	1.66 ± 2.15	2.33 ± 0.88*	3.17 ± 1.11*
<i>Forelimb</i>	2.12 ± 1.25	3.45 ± 1.78	6.40 ± 7.02	8.45 ± 3.78	35.00 ± 12.00***	28.00 ± 5.09**
<i>Hindlimb</i>	1.25 ± 0.31	1.04 ± 0.10	9.91 ± 6.76	5.04 ± 9.03	32.33 ± 10.73**	29.50 ± 5.84**

Table 8.1. Axial, orolingual, forelimb and hindlimb AIM components initiated by 2.5mg/kg of methamphetamine, based off the rating scale described by (Cenci and Lundblad, 2007, Winkler et al., 2002b). Significant differences are annotated as $p < 0.05^*$, $p < 0.01^{**}$ and $p < 0.001^{***}$. Values are expressed as Mean ± SEM.

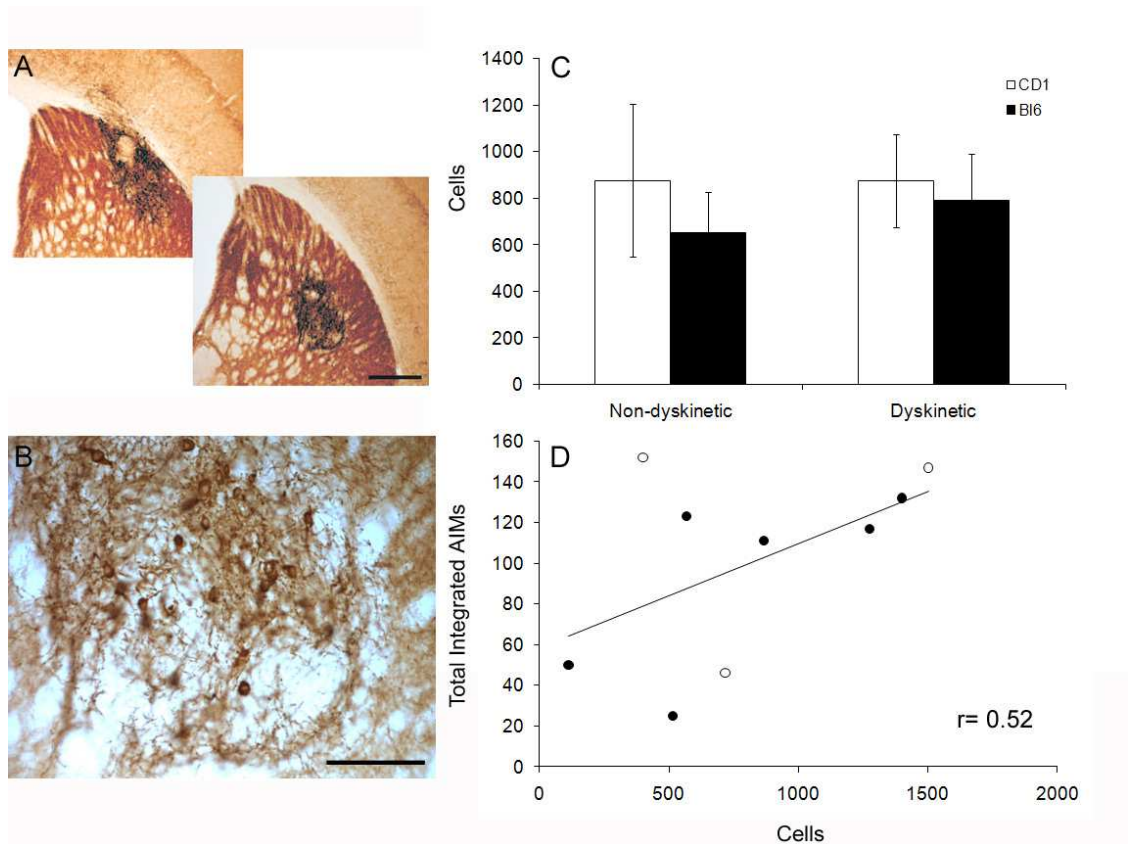


Fig. 8.6. Photomicrographs depicting representative dopaminergic grafts in mice (A-B), where the scale bar on the low magnification picture is 1mm and on high magnification image are 200 μ m. The total number of cells in the graft were quantified in CD1 and C57/ Bl6 strains, from dyskinetic and non-dyskinetic groups (C), and correlated to total integrated AIMs scored following 2.5mg/kg of methamphetamine (D). White circles = CD1 mice (n=3) and black circles = C57/ Bl6 mice (n=6). Values are expressed as Mean \pm SEM.

8.4. Discussion

8.4.1 *Optimisation of the Mouse GID model*

The optimisation of the GID mouse model is dependent on two factors, firstly the survival of a sufficient number of transplanted TH positive cells, and secondly the ability of the mouse to undertake all of the procedures necessary to generate the rat GID model i.e. survival, sufficient lesioning, L-DOPA priming and AIMS triggered by 2.5mg/kg of methamphetamine.

The experiments presented here provide evidence that TH cells from E12 VM tissue can be transplanted successfully into the striatum of the unilateral 6-OHDA lesioned mouse model, with approximately 3% of transplanted cells surviving and expressing TH. The percentage of dopaminergic cells that survive in most other mouse studies using this transplantation model has largely not been quantified/ estimated (Brundin et al., 1986, Low et al., 1987, Shimizu et al., 1988, Shimizu et al., 1990, Witt and Triarhou, 1995), with recent quantified transplantation studies using rat as the host even though donor tissue is derived from mice (Grealish et al., 2010a), therefore comparisons are difficult. A recent study has shown that mouse cells transplanted into the mouse SNc can survive and project to partially reinnervate the denervated striatum (Thompson et al., 2009). The TH cells transplanted in Thompson et al. were GFP labelled under the TH promoter and approximately 10% of TH/GFP-positive cells survived. As the GFP tag enabled a very fine and controlled dissection of the VM, few 5-HT neurones would be expected to be present. However the proportion of dopamine cells in the graft, generated by a normal dissection technique (as used in this study) is approximately 33-66%, with the remaining neurones largely made up of 5-HT neurones (Garcia et al., 2011). Thus in this experiment the total surviving neurones are likely more than the 3% dopamine cell component (as 5-HT neurones were not taken into account), making total cell comparisons to Thompson et al. (2009) inaccurate.

The number surviving dopaminergic neurons following rat-rat transplants varies hugely between reported studies (Abrous et al., 1993, Arbuthnott et al., 1985, Carlsson et al., 2009, Carlsson et al., 2006b, Dawson et al., 1991, Dunnett et al., 1983b, Ishida et al., 1990, Lane et al., 2008, Lane et al., 2009b, Lane et al., 2006b, Rioux et al., 1993, Steece-Collier et al., 2003, Torres and Dunnett, 2007). This may relate to simple experimental criteria such as the

number of cells transplanted or the dilution of cells in the transplantation media. The appropriate concentration of cells may be difficult to achieve, as dilution of the cells to a certain point is necessary for practical reasons, but too dilute and the loss of cell-cell contacts may have a detrimental effect on survival and functional recovery. The numbers of rat derived dopaminergic neurons in transplanted rats relate to the extent of functional recovery, with small grafts (Mean: 280 ± 63) that are unable to reduce ipsilateral turning and large grafts (Mean: $17,403 \pm 1229$) that cause robust contralateral turning (Lane et al., 2006b). In accordance, the numbers of grafted TH positive neurons in the C57/Bl6 and CD1 mice of this study (Mean: 976 ± 116) give rise to less pronounced contralateral turning, likely due to a lower cell number than those seen in defined large rat grafts. When comparing mouse and rat studies, it is also important to consider embryonic age as this can affect the levels of survival in the rat (Torres et al., 2008, Torres et al., 2007), where E12 is favoured over E14. Based on the Carnegie stage equivalence, E12 mouse is the same developmental stage as E13.5 rat, and is therefore relatively comparable to rat E14. This may offer another explanation as to why grafts were smaller than that seen in the rat.

The reduction in LID following a graft has also been reported previously in the rat (Carlsson et al., 2006b, Garcia et al., 2011, Lane et al., 2006b, Steece-Collier et al., 2009) and was found to be dependent on the number of cells transplanted and L-DOPA priming, rather than total numbers of dopamine neurones. There was an approximate 30% reduction in total integrated AIMs in this study, providing further evidence that transplanted cells are acting as a constant source of dopamine and either handling the dopamine derived from L-DOPA in a less pulsatile, more controlled manner and/or normalising the sensitivity of the post-synaptic receptors. The modest reduction in LID in the mice reported here and the lack of correlation between AIMs (pre or post-graft) with number of cells in the graft is likely the result of small graft sizes and the low numbers of mice used. These variables, may also explain why there was a lack of correlation between amphetamine-mediated AIMs and L-DOPA mediated AIMs (pre or post-graft), and why the former was so variable between mice. It has also been reported that novel L-DOPA driven stereotypic behaviours can develop following transplantation (Steece-Collier et al., 2003); possibly reflecting incomplete reinnervation of the striatum. These behaviours, forepaw tapping and forelimb facial stereotypies, were not seen in this study. It is unlikely that these moderate sized grafts were able to reinnervate the whole striatum, therefore these previous findings may be species specific, or may arise by different means.

The lesion technique and robust LID expression in mice at the pre-graft stage and a reduction of LID post-graft are critical characteristics in the development of an efficient model of GID. These factors have been addressed in this study and in Chapters 3 and 4. The present experiment shows that the final factor needed for the generation of the model, which is the trigger by 2.5mg/kg of amphetamine, was able to generate AIMs which are comparable to those described previously for the rat (Lane et al., 2006b). As with the rat, methamphetamine-induced AIMs, in this study, were generally less severe and more stereotyped compared to LID. In agreement with Lane et al., amphetamine-mediated AIMs in transplanted mice were positively correlated to the number of cells in the graft, yet in this study significance was not reached. Importantly, these data show the survival of dopaminergic cells and subsequent amphetamine triggered AIMs in the host striatum of both CD1 and C57/Bl6 strains, despite dramatically different weights and small discrepancies between amphetamine-mediated rotations at the pre-graft stage.

8.4.2 Future directions

The current data show that a mouse model of GID can be established and that AIMs can be correlated to graft size, however there are a number of avenues in which this model can be used to assess GID mechanisms and/ or reiterate other rat model findings. As with the rat, the influence on host and donor 5-HT innervations, graft placement, influence of previous L-DOPA treatment and other biochemical markers can be analysed to emphasis findings across species. In addition, this model may provide a useful tool for the analysis of GID in transgenic mice and for allografts of mouse derived cell lines, such as those with genetic cell type specific markers, without the need for immunosuppression. There is still some controversy over the distribution of dopaminergic neurons from different sources, ie A9 and A10 derived populations (reviewed in Stromberg et al., 2010). This may be resolved by the use of labelled cell populations derived from transgenic mice, which will be more easily identified and tracked. Given the limited survival and functionality of stem cells lines when transplanted, the use of embryonic VM is still critical to the study of transplantation, as a greater understanding on the precise roles of these cell populations may be key to the function of stem cell grafts, without inducing dyskinetic side effects.

8.4.3 Conclusions

Overall this study demonstrated that grafts in CD1 and C57/ B16 are sufficient in size to cause functional improvements on amphetamine and L-DOPA-induced rotation, and reduce LID from levels seen prior to transplantation. Methamphetamine is able to trigger AIMs that are not seen in lesion only mice, thus providing a mouse model of GID that can be used alongside the already established rat model. As with the rat, a proportion of grafted cohort does not develop amphetamine triggered dyskinesia and in animals where significant AIMs occur these were correlated to the number of TH positive cells within the graft. Furthermore, this model may have a number of applications in the future to study the mechanisms of GID, where either CD1 or C57/ B16 strains are needed.

9. General Discussion

9.1. Animal Models of LID and GID- Pre-Clinical Efficiency.

The major goal in the generation of models of L-DOPA or dopamine-rich graft-induced AIMs is a similarity to PD-related dyskinesia, both in terms of phenotype ('face validity') and underlying mechanism ('construct validity'). The ultimate test for models of dyskinesia is their ability to accurately permit the translation of any therapeutic effect of new treatments to the patient ('predictive validity'), and this may only be the case if the underlying mechanisms are the same. In the case of GID, once an underlying mechanism has been established, it will be important to identify the efficiency of anti-dyskinetic treatments in models, using a combination of behavioural assessments and biochemical markers or 'biomarkers'.

9.1.1 Dyskinetic Phenotype

In both models, AIMs are considered to be phenotypically similar to dyskinesia, showing all of the involuntary movement subcomponents seen in the patients. Although unilateral 6-OHDA lesioned mice are useful in practical and financial terms, MPTP treated primates can be lesioned bilaterally, show bilateral movements in response to L-DOPA, and off medication they have profound akinesia, more closely mimicking late stage PD (Jenner et al., 1984). However the use of unilateral 6-OHDA lesioned rodents, including the mice described in this thesis are beneficial because of lateralised impairments and hence are of great benefit to pre-clinical science. The unilateral nature of this model means that it does not give rise to debilitating akinesia, although milder motor impairments are present, which has led to a behavioural deficit baseline which is well defined in rats, less so in mice. The 6-OHDA mouse model is being continuously optimised and is likely, in the future, likely to come to be used as frequently as the 'gold standard' rat model, as highlighted in **Chapter 3**. A major advantage of using the unilateral 6-OHDA lesion rodent model is that rotational asymmetry can be assessed simultaneously to LID, providing a means of measuring general locomotion. Amphetamine-induced AIMs in the transplanted rat model are also phenotypically similar to the clinical form (reviewed in Lane and Smith, 2010). Further, in **Chapter 8** it was shown that GID can also be modelled in two different strains of mouse, to the same extent as previously reported the rat (Lane et al., 2006b), therefore providing a new and valuable tool

for pre-clinical investigation. The testing of a new treatment for LID often follows a hierarchical pre-clinical system: invertebrates > rodents > primates > humans. This hierarchical system however will not stand up for the testing of therapeutic approaches to GID, as spontaneous AIMs have not been reproduced in primates and therefore research may need to be fast tracked from rodents to phase I clinical trials. As a solution, amphetamine-mediated AIMs might be used to model GID in the primate, however the usefulness as a representation of spontaneous GIDs in patients would be disputed.

9.1.2 Underlying mechanisms of Dyskinesia

The mechanisms of LID in rodents share characteristics of LID seen in the human condition. This seems to be the case in all aspects of the condition, including electrophysiological changes of the direct and indirect signalling pathways and the post-synaptic intracellular signalling dysregulation of FosB (Picconi et al., 2003, Westin et al., 2001, Tekumalla et al., 2001, Morgante et al., 2006). FosB/ Δ FosB is now an established biomarker of dyskinesia in the rodent model having been shown to be expressed in patient samples also (Tekumalla et al., 2001) and hence it was used in **Chapter 4** to show that the upregulation of this IEG in the 6-OHDA mouse reflects a similar profile of change to that previously reported in the rat (Andersson et al., 1999), with the extent of expression dependent on the lesion location along the nigrostriatal path and correlated with extent of dyskinesia. The magnitude of AIMs was highest in the MFB group for all L-DOPA doses and FosB/ Δ FosB expression was 2-fold higher at 25mg/kg, allowing for a robust phenotype that could be easily scored by the investigator. Therefore despite the mouse model being one of the hardest to implement in terms of survival and success rate, it is extremely useful for the study of dyskinesia. In addition, the MFB lesion group was the only one of the three to show loss of the 5-HT terminals. Although 5-HT loss was likely the result of non-specific uptake of toxin and/or mechanical damage, this is not necessarily detrimental to the model, as 5-HT losses are also seen in patients (Kish et al., 2008). In **Chapter 4** it was shown that fibre innervation patterns are positively correlated to dyskinesia, not previously found in the mouse, supporting the notion of dysregulated dopamine release from 5-HT neurons may contribute to LID in humans as it is noted across species.

Although cell type analysis has proven to be an interesting avenue for GID research, it is of fundamental importance to test all possible causes of GID in the pre-clinical models, see Fig. 9.1.

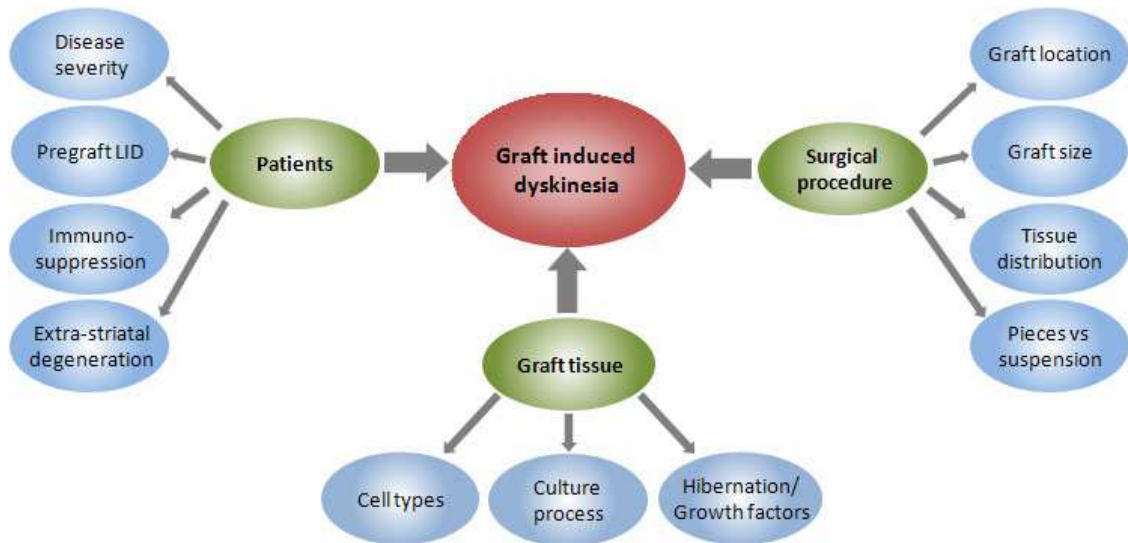


Figure 9.1. Factors of the transplantation process that may alter the outcome of GID. The same factors can also be considered for the functional integration of the transplant and can be broadly divided into three broad categories (Lane and Smith, 2010).

The pharmacological screen of compounds, known to reduced LID, in the transplanted rat model of amphetamine-induced dyskinesia (**Chapter 6**), has led to some unusual observations with regard to the glutamatergic system. Specifically that amantadine commonly used for the treatment of LID was ineffective at treating GID, and MK-801, a drug with similar mechanistic action, increased AIMS and reversed rotation. Research into this system however is limited and may represent a new avenue of investigation to uncover the mechanism of GID. The glutamatergic system is also linked to long-term electrophysiological changes and plasticity; these too have yet to be examined in either humans or animal models of GID, in contrast to LID where there is currently a major research focus. Importantly, rat models of LID also show the same long-term plasticity seen in the human, where an inability to reverse LTP is seen only when AIMS above threshold levels manifest (Morgante et al., 2006, Picconi

et al., 2003, Picconi et al., 2008). Such research is therefore overdue in amphetamine-driven transplanted rodent models of GID.

The wealth of preclinical investigation into LID suggests that rodent models of this debilitating side effect are closer to human form than models of GID are to the human form. However, there are a number of limitations of using LID models to investigate new treatments. The most profound is the translation of pharmacological agent co-treatments from rodents to humans. Many of the compounds targeting 5-HT, cannabinoid, adrenergic and glutamatergic systems that cause a significant decrease in L-DOPA induced AIMs in mouse and rat models (Dekundy et al., 2007, Lundblad et al., 2002, Lundblad et al., 2005, Fox et al., 2008b) have failed to do so when progressed to the stage of a clinical trial (Rascol et al., 1994, Wolf et al., 2010, Fox et al., 2008b, Manson et al., 2000, Carroll et al., 2004). It is unclear whether this was purely a failure of the model-patient translation, poor clinical trial design, or the result of a lower experimental number, resulting in statistical insignificance. Pre-clinical pharmacological treatment studies of amphetamine-initiated GID in rodent models, may be more effective for ruling out drugs prior to human testing, since the majority of compounds (used at the same doses as those for LID) were unable to alter AIMs (**Chapter 6**). Furthermore, other agents such as 5-HT_{1A} and 5-HT_{1B} agonists decrease AIMs in these animals and amantadine was insufficient to significantly reduce AIMs, all of which is consistent with findings in patient with GID, reported in (Lane et al., 2010).

9.1.3 Dyskinesia Biomarkers

In contrast to LID, biological markers of AIMs following an amphetamine injection in transplanted rodents have not been well established. An increase in c-fos and a decrease of FosB/ Δ FosB was found in the grafted model. However, correlations between these biomarkers and AIMs were not established (Lane et al., 2009b). Biological changes resulting from GID may be difficult to find in rodent models, since it is hard to distinguish between the positive effects of the graft, improved motor function and the negative effects of amphetamine-induced AIMs. One key issue is that there is no access to pathological specimens from patients with GID so understanding how and if these markers are relevant in GID has not been possible. 5-HT innervation of the graft and the denervated striatum is receiving much interest of late. In recent studies, the imaging of two patients with off medication GID showed 5-HT hyperinnervation and AIMs were subsequently suppressed by

pharmacological manipulation of 5-HT receptors (Politis et al., 2011b, Politis et al., 2010). Considering the data presented in **Chapter 7** and those from other studies (Garcia et al., 2011, Lane et al., 2009a) it seems unlikely that the proportions of 5-HT neurons within the graft and/or levels of striatal 5-HT innervation have a causative role in rodent models of GID or the alleviation of LID post-graft. The suitability of the model in this regard has proved to be accurate, as no GID was found in an ongoing foetal tissue clinical trial, despite variable numbers of 5-HT neurons in each of the 6 patients (Mendez et al., 2008). Nevertheless, 5-HT receptor agonism may provide a useful means to treat individuals, as shown by (Politis et al., 2010) and reiterated in the GID model, using compounds with greater specificity (**Chapter 6**). Further investigation is warranted, as 5-HT drugs currently licensed for patient use also have D₂ antagonistic properties, and may therefore lead to the suppression of GID by other means.

Some biochemical fingerprints of LID are recognised (sensitisation of D₁ receptors, the ERK pathway and IEG expression), yet the search for biochemical changes related to LID continues in order to better understand the mechanisms of dysregulation. Distinguishing between sensitised (chronic L-DOPA treatment) and non-sensitised (single L-DOPA injection) post synaptic mechanisms is one approach, as many animals are not 'primed' to develop AIMs with a single injection but may develop AIMs with chronic administration. In **Chapter 5** it was shown that *RGS2* mRNA transcripts were up-regulated in response to L-DOPA, but could not distinguish between long and short-term treatment. *RGS2* is therefore a biomarker for general L-DOPA action and does not permanently change basal levels within cells. Dysregulation of *RGS2* results from immediate D₁ receptor stimulation and may therefore be in part a compensatory mechanism, to hinder the priming response to L-DOPA by reducing the signalling transmission rate. Further basal levels of *RGS2* or *RGS4* did not differ between dyskinetic and non-dyskinetic transplanted rodents, thereby ruling these out as important basal biomarkers of GID. However, whether or not the change in RGS expression occurring after amphetamine injection would differ depending on AIM expression should not be overlooked at this stage. The search for hallmarks of GID thus far, including those presented in this thesis, are based on the screening of markers known in LID, yet it is unclear whether this is the best strategy. To some effect, the same sensitised post-synaptic response must be dysregulated in GID, as priming increases the severity of amphetamine triggered AIMs (Lane et al., 2009b), however IEG indicators of LID were not correlated to amphetamine driven AIMs (Lane et al., 2009b). Therefore further investigation of the differences between LID and GID, both in animal models and in the patients, will be invaluable to future of this research field. The

candidates for efficient biomarkers for use in rodent models of GID depend on data derived from clinical observations and the tissue of transplanted patients at post-mortem, of which there is little.

9.2. The Future of L-DOPA and Transplantation Strategies.

The future of both L-DOPA and transplantation strategies for the treatment of PD depends on their ability, separately or in combination, to treat or prevent major side effects (such as dyskinesia), their cost effectiveness, and their long-term efficacy relative to other treatments.

9.2.1 Dopamine Replacement

L-DOPA remains the single most important treatment for PD, readily accessible to a wide range of the population. Yet problems of dyskinesia, the drugs short half-life and non-motor symptoms are debilitating enough for the continued search for a new treatment (either for the prevention of PD or dyskinesia) and in an adjacent line of research, the possibility of a cure. Just as fundamental to the disease from a global perspective however is the availability of L-DOPA to all, where drug companies should be encouraged to reduce costs when selling to developing countries. L-DOPA therapy would be a viable long-term therapy if dyskinesia could be easily managed (although this would still not control non-motor symptoms). Novel pharmacological interventions for LID are much needed as most clinically available compounds do not sufficiently reduce AIMs and others only do so at doses that suppress overall locomotion in rodent models. The suppression of dyskinesia by modulation of the post-synaptic signalling cascade, using viral-mediated gene transfer of TH and co-factor synthesizing enzyme guanosine-5'-triphosphate cyclohydrolase-1, to increase dopamine synthesis may be an emerging alternative for delivering dopamine directly to the brain. The results of the phase I clinical trial have not yet been divulged, however the pre-clinical data is promising (Kirik et al., 2002). Another dopamine replacement strategy has been assessed in PD patients, where encapsulated retinal pigmented epithelial cells were implanted, for their hypothesised ability to produce L-DOPA. However, there were no differences in motor outcome compared to sham-operated controls (Gross et al., 2011). Thus, it would seem that 'in brain' dopamine delivery therapeutics are difficult to achieve, and are subject to factors including dopamine quantity, turnover and difficulty in reaching the whole of the target area.

Furthermore, these interventions do not detract from the requirement of invasive surgery and the comparative ease and availability of L-DOPA therapy.

Small molecule pharmacological interventions might represent a further emerging avenue for L-DOPA co-treatments. Novel small molecules may give the highly specific actions unattainable by current pharmacotherapy, as many standard compounds are derived or synthesised from natural derivatives. High throughput screening of randomly synthesised small molecules, or of ones that have been designed from specific pathways, has led to the discovery of modulators capable of interfering with specific protein-protein interactions (Blazer et al., 2011, Blazer et al., 2010, Fry, 2006). This approach may be advantageous either as a replacement for L-DOPA as a treatment in PD or in the screen for an L-DOPA co-treatment to control dyskinesia, as the current regulation of the sensitised ERK pathway by dopamine receptor modulation, or indirectly via the action of other receptors on the same membrane, has a global cell affect. Thus, problems arise from the balance of receptor occupancy and specificity to gain a therapeutic effect on LID, without suppressing general locomotion. For example RGS2 was found to be dysregulated by low dose L-DOPA (**Chapter 5**), which can be controlled by readily available dopamine and glutamate agonists/ antagonists (Taymans et al., 2005a, Taymans et al., 2004), however dopamine and glutamate antagonists only suppress AIMs at doses that suppress general movement. Therefore very specific targets at the site of the RGS-G α subunit interaction may provide a more powerful means of LID control. Recently, small molecules that interact with RGS4 at the G α binding site have been synthesised (Blazer et al., 2010, Blazer et al., 2011). One disadvantage of this approach is that they cause irreversible changes, however they often pass through the BBB and into cells readily (Chambers et al., 2011). Research of these compounds in PD models has so far only been looked at from a neuroprotection perspective (Chambers et al., 2011).

9.2.2. Cell Therapies

In the western world, reconstruction of the basal ganglia circuitry remains the ultimate goal in the treatment of PD and seems a realistic possibility in the future as only a few cell types are needed for reconstruction and with the procedure already proving beneficial in some patients (Freed et al., 1990, Freed et al., 2001, Freeman et al., 1995, Lindvall et al., 1992, Mendez et al., 1996, Olanow et al., 2003). Certainly the survival and function of transplanted dopamine neurons in PD patients after 14 years is possible (Mendez et al., 2008), and this would warrant

considering transplantation as a viable PD treatment if this level of function could be made more reliable and without risk or side effect. The forthcoming TransEUro trials will utilise lessons learnt from past transplantation studies and is testing the hypothesis that transplantation can be rendered more reliable, by utilising recent pre-clinical refinements, rigorous trial design, and the recruitment of younger patients. The future of cell therapies may be seen as under threat however after the observation of Lewy body pathology found within grafted cells (Kordower et al., 2008) and the emergence of GID in some patients (Freed et al., 2001). Other issues to be considered are the contribution of immune responses to transplant efficiency and patient welfare when under immunosuppression. Although successful treatment without any of these complications is the ultimate goal in transplantation, from an utilitarian perspective some of these issues may not hinder the momentum of this therapeutic strategy, by judgement of the cost-benefit ratio. A hitherto more important issue to be resolved is its unreliability.

The use of stem cell (SC) replacement in PD is dependent on the resolution of both scientific and political difficulties. Although primary tissue from surgical termination is generally regarded as safe, it is not standardised, not matched on allotype and will be extremely difficult to implement logistically for use as a mainstream therapy. Rather, findings from studies using primary fetal tissues, provide both the stimulus for, and are likely to pave the way for, new SC therapeutics. The primary cell strategy cannot be ruled out altogether, as more mainstream medical terminations that could be utilised, as tissue derived by this means is just as viable (Kelly et al., 2011). In addition, there are important issues that need to be resolved by pre-clinical investigation before the first SC clinical trial can be implemented, such as the prevention of graft overgrowth, improper localisation of transplanted cells by migration, development of GID and obtaining large enough yields of dopamine neurons to have a meaningful outcome. In the case of the former, this is likely to be overcome by new biotechnologies that will allow for the programmed suicide of tumorigenic and excessively proliferative cells (reviewed in Kiuru et al., 2009). It would be difficult however for governmental bodies to grant approval to genetically modified SCs. Resolution of the poor cell yield is likely to take longer and more pre-clinical research is needed. Furthermore the occurrence of GID may not be found until first trials. Further, preliminary work has also shown that SC grafts can be monitored *in vivo* by PET and MRI scans (Jackson et al., 2009), which have proved invaluable to primary cell transplantation trials clinical trials (Markham et al., 1994, Piccini et al., 2005). These key technical issues will influence the start date for the

first SC clinical trials, however the question of whether key issues have been explored enough lies within ethical committees.

In some regards, issues governing the initiation and patient selection for the first SC transplants at clinical trial should be considered independently to benchmarks previously established for primary tissue grafts. The International Society for Stem Cell Research (ISSCR) was set up for the translation of pre-clinical SC research to the clinic and incorporates expertise specific to each of its main foci, which include voluntary informed consent, patient monitoring, potential adverse events, medical intervention and social justice (Hyun et al., 2008), with much initial decision making from ethical committees (Hyun, 2010). There is a recent drive to answer the fundamental question of whether or not to start clinical trials with SCs using different ethical models, for example a utilitarian approach may disallow SC therapy on the grounds of safety and cost, however a more rights-based deontological argument would favour this treatment (Hug and Hermeren, 2011). If however, by using these tools, it is decided to be most appropriate to resolve all problems before conducting the first human trials, would we in fact be denying the basic human right of the patient to receive treatment after knowing all the risks. Moreover, if legitimate academic medicine restricts access to such options, desperate patients are likely to search elsewhere, often to less reputable commercially-driven sources, contributing to the growth of SC tourism?

9.3. Is there a Single Treatment for Parkinson's Disease?

There are now a variety of treatments available for PD, as well as some novel therapeutics discussed above that may be licensed in the forthcoming years. The viability of each as a PD treatment involves a combination of interacting factors, including cost and effectiveness.

The most important treatment strategies for most patients for quick diagnosis are formulated by scrupulous management of the motor symptoms by pharmacology, well-informed general practitioners and access to specialist PD nurses. There is still much work required to ensure patients get the best management of the disease and PD specialist nurses are currently scarce in the U.K. For example, in the Cardiff and Vale area there is currently only 1 nurse to every 850 patients (www.cardiffandvaleuhb.wales.nhs.uk). Using dopamine agonists and careful control of L-DOPA doses, it is possible to treat akinetic symptoms to delay the onset of dyskinesia development (Watts et al., 2010). Further research on small molecule

pharmacotherapy may alleviate parkinsonian symptoms or dyskinesia in the future, thus providing a cost effective and low risk strategy for many.

DBS is also currently available on the NHS, but access is restricted (the so called 'postcode lottery') since economic costs of this treatment are high and certain levels of expertise are needed both to perform the surgery and to monitor and maintain the implant devices. There is evidence that when comparing the predicted cost of PD patient care over a lifetime and in comparison to other diseases, a single DBS procedure costing £20,000 - £30,000 was approved by UK National Institute for Health and Clinical Excellence (NICE) (Shan et al., 2011), and subsequently this benefit-cost ratio is being calculated for the use of DBS in other countries. Since DBS is subject to the review of each patient and still does not treat non-motor symptoms, this will not be a strategy suitable for the majority of the PD population. Moreover, DBS is not without risk, and there have been several reports where DBS can induce dyskinesia as a side effect in patients, reported in a meta-analysis of clinical trials (Groiss et al., 2009) and also noted in the forelimb animal models that have received DBS (Quintana A, 2010).

Ultimately the reconstruction of the dopaminergic circuit is probably the preferred future strategy for the treatment of PD as this may be able to counteract some of the motor and non-motor pathological changes, without the need for further intervention. Transplantation strategies may only be rivalled by that of the protection of existing midbrain dopaminergic neurons, using neurotrophic factors or viral mediated gene transfer. Appropriate diffusion strategies for these agents have recently been optimised and treatments have been found to be safe in phase I trials (Gasmi et al., 2007, Herzog et al., 2007, Slevin et al., 2007). Although the support of diseased cells may be beneficial, the ultimate goal in neuroprotection is to stop disease progression. However, the major limitation of neuroprotective options at present is that viable targets for this strategy have not yet been identified, let alone clinically validated, even though there are number of early stage pre-clinical studies screening for intracellular pathway dysregulation. The recent modelling of PD in rodents through AAV-mediated over-expression of human mutant α -synuclein has highlighted pathological trafficking deficits that if prevented may be able stop denervation in the midbrain (Chung et al., 2009). Although pre-clinical neuroprotection studies are alluding to successful translation to patients, motor symptoms (and hence diagnosis) do not occur until a large proportion of dopamine neurons die. Intervention at this point would perhaps spare remaining cells and hinder disease progression, but would not lead to circuitry reconstruction that is possible with transplantation.

9.4. Final Summary

Research undertaken for this thesis has addressed some of the issues that need to be resolved in pre-clinical PD research: the continued optimisation of 6-OHDA lesion mouse models, their use to recapitulate LID, the search for new biomarkers of L-DOPA function, the screen for compounds that may suppress GID, the search for neuro-pathological correlates of GID and the creation of an amphetamine-driven mouse model of GID. Continued research into each of these aspects and others, will be needed to fully understand the mechanisms of LID, GID and graft integration and function, in the hope for an effective treatment for PD and/or its debilitating side effects. Although L-DOPA and transplantation are the focus of the experiments presented here, a ‘one size fits all’ approach to the treatment of PD may never be found, as symptomatic treatment depends on the specific patient problems and stringent observation by the clinician. Although findings using animal models are of fundamental importance to the translation of PD research to the clinic, we should always use lessons learnt from patient trials to feedback into pre-clinical science.

10. References

- ABERCROMBIE, M. 1946. Estimation of nuclear population from microtome sections. *The Anatomical record*, 94, 239-47.
- ABROUS, D. N., SHALTOT, A. R., TORRES, E. M. & DUNNETT, S. B. 1993. Dopamine-rich grafts in the neostriatum and/or nucleus accumbens: effects on drug-induced behaviours and skilled paw-reaching. *Neuroscience*, 53, 187-97.
- ADLER, C. H., SETHI, K. D., HAUSER, R. A., DAVIS, T. L., HAMMERSTAD, J. P., BERTONI, J., TAYLOR, R. L., SANCHEZ-RAMOS, J. & O'BRIEN, C. F. 1997. Ropinirole for the treatment of early Parkinson's disease. The Ropinirole Study Group. *Neurology*, 49, 393-9.
- ALBIN, R. L., YOUNG, A. B. & PENNEY, J. B. 1989. The functional anatomy of basal ganglia disorders. *Trends in neurosciences*, 12, 366-75.
- ALEXANDER, G. E., DELONG, M. R. & STRICK, P. L. 1986. Parallel organization of functionally segregated circuits linking basal ganglia and cortex. *Annual review of neuroscience*, 9, 357-81.
- ALLBUTT, H. N. & HENDERSON, J. M. 2007. Use of the narrow beam test in the rat, 6-hydroxydopamine model of Parkinson's disease. *J Neurosci Methods*, 159, 195-202.
- ALVAREZ-FISCHER, D., BLESSMANN, G., TROSOWSKI, C., BEHE, M., SCHURRAT, T., HARTMANN, A., BEHR, T. M., OERTEL, W. H., HOGLINGER, G. U. & HOFFKEN, H. 2007. Quantitative [(123)I]FP-CIT pinhole SPECT imaging predicts striatal dopamine levels, but not number of nigral neurons in different mouse models of Parkinson's disease. *NeuroImage*, 38, 5-12.
- ALVAREZ-FISCHER, D., HENZE, C., STRENZKE, C., WESTRICH, J., FERGER, B., HOGLINGER, G. U., OERTEL, W. H. & HARTMANN, A. 2008. Characterization of the striatal 6-OHDA model of Parkinson's disease in wild type and alpha-synuclein-deleted mice. *Experimental neurology*, 210, 182-93.
- AMAN, T. K., SHEN, R. Y. & HAJ-DAHMANE, S. 2007. D2-like dopamine receptors depolarize dorsal raphe serotonin neurons through the activation of nonselective cationic conductance. *The Journal of pharmacology and experimental therapeutics*, 320, 376-85.
- ANDERSON, G. R., SEMENOV, A., SONG, J. H. & MARTEMYANOV, K. A. 2007. The membrane anchor R7BP controls the proteolytic stability of the striatal specific RGS protein, RGS9-2. *The Journal of biological chemistry*, 282, 4772-81.
- ANDERSSON, M., HILBERTSON, A. & CENCI, M. A. 1999. Striatal fosB expression is causally linked with l-DOPA-induced abnormal involuntary movements and the associated upregulation of striatal prodynorphin mRNA in a rat model of Parkinson's disease. *Neurobiology of disease*, 6, 461-74.
- ANDERSSON, M., KONRADI, C. & CENCI, M. A. 2001. cAMP response element-binding protein is required for dopamine-dependent gene expression in the intact but not the dopamine-denervated striatum. *J Neurosci*, 21, 9930-43.
- ANDERSSON, M., WESTIN, J. E. & CENCI, M. A. 2003. Time course of striatal DeltaFosB-like immunoreactivity and prodynorphin mRNA levels after discontinuation of chronic dopaminomimetic treatment. *The European journal of neuroscience*, 17, 661-6.

- ANICHTCHIK, O. V., KASLIN, J., PEITSARO, N., SCHEININ, M. & PANULA, P. 2004. Neurochemical and behavioural changes in zebrafish *Danio rerio* after systemic administration of 6-hydroxydopamine and 1-methyl-4-phenyl-1,2,3,6-tetrahydropyridine. *Journal of neurochemistry*, 88, 443-53.
- ARAI, R., KARASAWA, N., GEFFARD, M. & NAGATSU, I. 1995. L-DOPA is converted to dopamine in serotonergic fibers of the striatum of the rat: a double-labeling immunofluorescence study. *Neuroscience letters*, 195, 195-8.
- ARBUTHNOTT, G., DUNNETT, S. & MACLEOD, N. 1985. Electrophysiological properties of single units in dopamine-rich mesencephalic transplants in rat brain. *Neurosci Lett*, 57, 205-10.
- BACKLUND, E. O., GRANBERG, P. O., HAMBERGER, B., KNUTSSON, E., MARTENSSON, A., SEDVALL, G., SEIGER, A. & OLSON, L. 1985. Transplantation of adrenal medullary tissue to striatum in parkinsonism. First clinical trials. *Journal of neurosurgery*, 62, 169-73.
- BAIRD, A. L., MELDRUM, A. & DUNNETT, S. B. 2001. The staircase test of skilled reaching in mice. *Brain Res Bull*, 54, 243-50.
- BARDINET, E., BHATTACHARJEE, M., DORMONT, D., PIDOUX, B., MALANDAIN, G., SCHUPBACH, M., AYACHE, N., CORNU, P., AGID, Y. & YELNIK, J. 2009. A three-dimensional histological atlas of the human basal ganglia. II. Atlas deformation strategy and evaluation in deep brain stimulation for Parkinson disease. *Journal of neurosurgery*, 110, 208-19.
- BARNEOUD, P., DESCOMBRIS, E., AUBIN, N. & ABROUS, D. N. 2000. Evaluation of simple and complex sensorimotor behaviours in rats with a partial lesion of the dopaminergic nigrostriatal system. *The European journal of neuroscience*, 12, 322-36.
- BARTUS, R. T., HERZOG, C. D., CHU, Y., WILSON, A., BROWN, L., SIFFERT, J., JOHNSON, E. M., JR., OLANOW, C. W., MUFSON, E. J. & KORDOWER, J. H. 2011. Bioactivity of AAV2-neurturin gene therapy (CERE-120): differences between Parkinson's disease and nonhuman primate brains. *Movement disorders : official journal of the Movement Disorder Society*, 26, 27-36.
- BEN-SHACHAR, D., ZUK, R. & GLINKA, Y. 1995. Dopamine neurotoxicity: inhibition of mitochondrial respiration. *J Neurochem*, 64, 718-23.
- BENABID, A. L., POLLAK, P., LOUVEAU, A., HENRY, S. & DE ROUGEMONT, J. 1987. Combined (thalamotomy and stimulation) stereotactic surgery of the VIM thalamic nucleus for bilateral Parkinson disease. *Applied neurophysiology*, 50, 344-6.
- BENSADOUN, J. C., DEGLON, N., TSENG, J. L., RIDET, J. L., ZURN, A. D. & AEBISCHER, P. 2000. Lentiviral vectors as a gene delivery system in the mouse midbrain: cellular and behavioral improvements in a 6-OHDA model of Parkinson's disease using GDNF. *Experimental neurology*, 164, 15-24.
- BERGER, A. 2000. Parkinson's disease linked with pesticide. *BMJ*, 321, 1175A.
- BERNHEIMER, H., BIRKMAYER, W., HORNYKIEWICZ, O., JELLINGER, K. & SEITELBERGER, F. 1973. Brain dopamine and the syndromes of Parkinson and Huntington. Clinical, morphological and neurochemical correlations. *Journal of the neurological sciences*, 20, 415-55.
- BERTON, O., GUIGONI, C., LI, Q., BIOULAC, B. H., AUBERT, I., GROSS, C. E., DILEONE, R. J., NESTLER, E. J. & BEZARD, E. 2009. Striatal overexpression of DeltaJunD resets L-DOPA-induced dyskinesia in a primate model of Parkinson disease. *Biol Psychiatry*, 66, 554-61.
- BETHLEM, J. & DEN HARTOG JAGER, W. A. 1960. The incidence and characteristics of Lewy bodies in idiopathic paralysis agitans (Parkinson's disease). *Journal of neurology, neurosurgery, and psychiatry*, 23, 74-80.

- BETHLEM, J. & DEN, H. J. W. 1960. [Study on the character of Lewy's corpuscles and their role in Parkinson's disease]. *Nederlands tijdschrift voor geneeskunde*, 104, 809-12.
- BEZARD, E., FERRY, S., MACH, U., STARK, H., LERICHE, L., BORAUD, T., GROSS, C. & SOKOLOFF, P. 2003. Attenuation of levodopa-induced dyskinesia by normalizing dopamine D3 receptor function. *Nature medicine*, 9, 762-7.
- BISHOP, C., KROLEWSKI, D. M., ESKOW, K. L., BARNUM, C. J., DUPRE, K. B., DEAK, T. & WALKER, P. D. 2009. Contribution of the striatum to the effects of 5-HT1A receptor stimulation in L-DOPA-treated hemiparkinsonian rats. *J Neurosci Res*, 87, 1645-58.
- BISHOP, G. B., CULLINAN, W. E., CURRAN, E. & GUTSTEIN, H. B. 2002. Abused drugs modulate RGS4 mRNA levels in rat brain: comparison between acute drug treatment and a drug challenge after chronic treatment. *Neurobiology of disease*, 10, 334-43.
- BJORKLUND, A., SCHMIDT, R. H. & STENEVI, U. 1980. Functional reinnervation of the neostriatum in the adult rat by use of intraparenchymal grafting of dissociated cell suspensions from the substantia nigra. *Cell and tissue research*, 212, 39-45.
- BJORKLUND, A. & STENEVI, U. 1979. Reconstruction of the nigrostriatal dopamine pathway by intracerebral nigral transplants. *Brain research*, 177, 555-60.
- BJORKLUND, A., STENEVI, U., DUNNETT, S. B. & IVERSEN, S. D. 1981. Functional reactivation of the deafferented neostriatum by nigral transplants. *Nature*, 289, 497-9.
- BJORKLUND, T., CARLSSON, T., CEDERFJALL, E. A., CARTA, M. & KIRIK, D. 2010. Optimized adeno-associated viral vector-mediated striatal DOPA delivery restores sensorimotor function and prevents dyskinesias in a model of advanced Parkinson's disease. *Brain : a journal of neurology*, 133, 496-511.
- BLANCHET, P. J., BOUCHER, R. & BEDARD, P. J. 1994. Excitotoxic lateral pallidotomy does not relieve L-dopa-induced dyskinesia in MPTP parkinsonian monkeys. *Brain research*, 650, 32-9.
- BLANCHET, P. J., GRONDIN, R., BEDARD, P. J., SHIOSAKI, K. & BRITTON, D. R. 1996. Dopamine D1 receptor desensitization profile in MPTP-lesioned primates. *European journal of pharmacology*, 309, 13-20.
- BLANDINI, F., LEVANDIS, G., BAZZINI, E., NAPPI, G. & ARMENTERO, M. T. 2007. Time-course of nigrostriatal damage, basal ganglia metabolic changes and behavioural alterations following intrastriatal injection of 6-hydroxydopamine in the rat: new clues from an old model. *The European journal of neuroscience*, 25, 397-405.
- BLAZER, L. L., ROMAN, D. L., CHUNG, A., LARSEN, M. J., GREEDY, B. M., HUSBANDS, S. M. & NEUBIG, R. R. 2010. Reversible, allosteric small-molecule inhibitors of regulator of G protein signaling proteins. *Molecular pharmacology*, 78, 524-33.
- BLAZER, L. L., ZHANG, H., CASEY, E. M., HUSBANDS, S. M. & NEUBIG, R. R. 2011. A nanomolar-potency small molecule inhibitor of regulator of G-protein signaling proteins. *Biochemistry*, 50, 3181-92.
- BLUME, S. R., CASS, D. K. & TSENG, K. Y. 2009. Stepping test in mice: a reliable approach in determining forelimb akinesia in MPTP-induced Parkinsonism. *Exp Neurol*, 219, 208-11.
- BLUNDELL, J., HOANG, C. V., POTTS, B., GOLD, S. J. & POWELL, C. M. 2008. Motor coordination deficits in mice lacking RGS9. *Brain research*, 1190, 78-85.
- BLUNT, S. B., JENNER, P. & MARSDEN, C. D. 1992. Autoradiographic study of striatal D1 and D2 dopamine receptors in 6-OHDA-lesioned rats receiving foetal ventral mesencephalic grafts and chronic treatment with L-dopa and carbidopa. *Brain research*, 582, 299-311.

- BOLDRY, R. C., PAPA, S. M., KASK, A. M. & CHASE, T. N. 1995. MK-801 reverses effects of chronic levodopa on D1 and D2 dopamine agonist-induced rotational behavior. *Brain research*, 692, 259-64.
- BONIFATI, V., FABRIZIO, E., CIPRIANI, R., VANACORE, N. & MECO, G. 1994. Buspirone in levodopa-induced dyskinesias. *Clinical neuropharmacology*, 17, 73-82.
- BORDET, R. & DESTEE, A. 1992. [From Parkinson's disease to Lewy body disease]. *Presse Med*, 21, 708-12.
- BOVE, J., PROU, D., PERIER, C. & PRZEDBORSKI, S. 2005. Toxin-induced models of Parkinson's disease. *NeuroRx : the journal of the American Society for Experimental NeuroTherapeutics*, 2, 484-94.
- BOYCE, S., KELLY, E., REAVILL, C., JENNER, P. & MARSDEN, C. D. 1984. Repeated administration of N-methyl-4-phenyl 1,2,5,6-tetrahydropyridine to rats is not toxic to striatal dopamine neurones. *Biochemical pharmacology*, 33, 1747-52.
- BRAAK, H. & BRAAK, E. 1990. Cognitive impairment in Parkinson's disease: amyloid plaques, neurofibrillary tangles, and neuropil threads in the cerebral cortex. *Journal of neural transmission. Parkinson's disease and dementia section*, 2, 45-57.
- BRAAK, H. & BRAAK, E. 2000. Pathoanatomy of Parkinson's disease. *Journal of neurology*, 247 Suppl 2, II3-10.
- BRAAK, H., DEL TREDICI, K., RUB, U., DE VOS, R. A., JANSEN STEUR, E. N. & BRAAK, E. 2003. Staging of brain pathology related to sporadic Parkinson's disease. *Neurobiol Aging*, 24, 197-211.
- BRAAK, H., RUB, U., SANDMANN-KEIL, D., GAI, W. P., DE VOS, R. A., JANSEN STEUR, E. N., ARAI, K. & BRAAK, E. 2000. Parkinson's disease: affection of brain stem nuclei controlling premotor and motor neurons of the somatomotor system. *Acta neuropathologica*, 99, 489-95.
- BRAUNGART, E., GERLACH, M., RIEDERER, P., BAUMEISTER, R. & HOENER, M. C. 2004. Caenorhabditis elegans MPP+ model of Parkinson's disease for high-throughput drug screenings. *Neuro-degenerative diseases*, 1, 175-83.
- BRENHOUSE, H. C. & STELLAR, J. R. 2006. c-Fos and deltaFosB expression are differentially altered in distinct subregions of the nucleus accumbens shell in cocaine-sensitized rats. *Neuroscience*, 137, 773-80.
- BRONSTEIN, J. M., TAGLIATI, M., ALTERMAN, R. L., LOZANO, A. M., VOLKMANN, J., STEFANI, A., HORAK, F. B., OKUN, M. S., FOOTE, K. D., KRACK, P., PAHWA, R., HENDERSON, J. M., HARIZ, M. I., BAKAY, R. A., REZAI, A., MARKS, W. J., JR., MORO, E., VITEK, J. L., WEAVER, F. M., GROSS, R. E. & DELONG, M. R. 2011. Deep brain stimulation for Parkinson disease: an expert consensus and review of key issues. *Archives of neurology*, 68, 165.
- BROOKS, D. J. & SAGAR, H. 2003. Entacapone is beneficial in both fluctuating and non-fluctuating patients with Parkinson's disease: a randomised, placebo controlled, double blind, six month study. *Journal of neurology, neurosurgery, and psychiatry*, 74, 1071-9.
- BROOKS, S. P. & DUNNETT, S. B. 2009. Tests to assess motor phenotype in mice: a user's guide. *Nature reviews. Neuroscience*, 10, 519-29.
- BROOKS, S. P., PASK, T., JONES, L. & DUNNETT, S. B. 2004. Behavioural profiles of inbred mouse strains used as transgenic backgrounds. I: motor tests. *Genes Brain Behav*, 3, 206-15.
- BROWN, L. L. & SHARP, F. R. 1995. Metabolic mapping of rat striatum: somatotopic organization of sensorimotor activity. *Brain research*, 686, 207-22.

- BRUNDIN, P., ISACSON, O., GAGE, F. H., PROCHIANTZ, A. & BJORKLUND, A. 1986. The rotating 6-hydroxydopamine-lesioned mouse as a model for assessing functional effects of neuronal grafting. *Brain research*, 366, 346-9.
- BRUNDIN, P., WIDNER, H., NILSSON, O. G., STRECKER, R. E. & BJORKLUND, A. 1989. Intracerebral xenografts of dopamine neurons: the role of immunosuppression and the blood-brain barrier. *Experimental brain research. Experimentelle Hirnforschung. Experimentation cerebrale*, 75, 195-207.
- BURBAUD, P., BONNET, B., GUEHL, D., LAGUENY, A. & BIOULAC, B. 1998. Movement disorders induced by gamma-aminobutyric agonist and antagonist injections into the internal globus pallidus and substantia nigra pars reticulata of the monkey. *Brain research*, 780, 102-7.
- BURCHETT, S. A., BANNON, M. J. & GRANNEMAN, J. G. 1999. RGS mRNA expression in rat striatum: modulation by dopamine receptors and effects of repeated amphetamine administration. *Journal of neurochemistry*, 72, 1529-33.
- BURCHETT, S. A., VOLK, M. L., BANNON, M. J. & GRANNEMAN, J. G. 1998. Regulators of G protein signaling: rapid changes in mRNA abundance in response to amphetamine. *Journal of neurochemistry*, 70, 2216-9.
- CALABRESI, P., GIACOMINI, P., CENTONZE, D. & BERNARDI, G. 2000a. Levodopa-induced dyskinesia: a pathological form of striatal synaptic plasticity? *Annals of neurology*, 47, S60-8; discussion S68-9.
- CALABRESI, P., GUBELLINI, P., CENTONZE, D., PICCONI, B., BERNARDI, G., CHERGUI, K., SVENNINGSSON, P., FIENBERG, A. A. & GREENGARD, P. 2000b. Dopamine and cAMP-regulated phosphoprotein 32 kDa controls both striatal long-term depression and long-term potentiation, opposing forms of synaptic plasticity. *The Journal of neuroscience : the official journal of the Society for Neuroscience*, 20, 8443-51.
- CALM-INVESTIGATORS 2009. Long-term effect of initiating pramipexole vs levodopa in early Parkinson disease. *Archives of neurology*, 66, 563-70.
- CALON, F., MORISSETTE, M., GHRIBI, O., GOULET, M., GRONDIN, R., BLANCHET, P. J., BEDARD, P. J. & DI PAOLO, T. 2002. Alteration of glutamate receptors in the striatum of dyskinetic 1-methyl-4-phenyl-1,2,3,6-tetrahydropyridine-treated monkeys following dopamine agonist treatment. *Progress in neuro-psychopharmacology & biological psychiatry*, 26, 127-38.
- CAO, X., YASUDA, T., UTHAYATHAS, S., WATTS, R. L., MOURADIAN, M. M., MOCHIZUKI, H. & PAPA, S. M. 2010. Striatal overexpression of DeltaFosB reproduces chronic levodopa-induced involuntary movements. *J Neurosci*, 30, 7335-43.
- CARLSSON, A. 1959. Detection and assay of dopamine. *Pharmacological reviews*, 11, 300-4.
- CARLSSON, A. & HILLARP, N. A. 1958. On the state of the catechol amines of the adrenal medullary granules. *Acta physiologica Scandinavica*, 44, 163-9.
- CARLSSON, A., LINDQVIST, M. & MAGNUSSON, T. 1957. 3,4-Dihydroxyphenylalanine and 5-hydroxytryptophan as reserpine antagonists. *Nature*, 180, 1200.
- CARLSSON, M., SVENSSON, A. & CARLSSON, A. 1991. Synergistic interactions between muscarinic antagonists, adrenergic agonists and NMDA antagonists with respect to locomotor stimulatory effects in monoamine-depleted mice. *Naunyn-Schmiedeberg's archives of pharmacology*, 343, 568-73.
- CARLSSON, T., CARTA, M., MUNOZ, A., MATTSSON, B., WINKLER, C., KIRIK, D. & BJORKLUND, A. 2008. Impact of grafted serotonin and dopamine neurons on

- development of L-DOPA-induced dyskinesias in parkinsonian rats is determined by the extent of dopamine neuron degeneration. *Brain*, 132, 319-35.
- CARLSSON, T., CARTA, M., WINKLER, C., BJORKLUND, A. & KIRIK, D. 2007. Serotonin neuron transplants exacerbate L-DOPA-induced dyskinesias in a rat model of Parkinson's disease. *The Journal of neuroscience : the official journal of the Society for Neuroscience*, 27, 8011-22.
- CARLSSON, T., WINKLER, C., BURGER, C., MUZYCZKA, N., MANDEL, R. J., CENCI, A., BJORKLUND, A. & KIRIK, D. 2005. Reversal of dyskinesias in an animal model of Parkinson's disease by continuous L-DOPA delivery using rAAV vectors. *Brain : a journal of neurology*, 128, 559-69.
- CARLSSON, T., WINKLER, C., LUNDBLAD, M., CENCI, M. A., BJORKLUND, A. & KIRIK, D. 2006. Graft placement and uneven pattern of reinnervation in the striatum is important for development of graft-induced dyskinesia. *Neurobiol Dis*, 21, 657-68.
- CARROLL, C. B., BAIN, P. G., TEARE, L., LIU, X., JOINT, C., WROATH, C., PARKIN, S. G., FOX, P., WRIGHT, D., HOBART, J. & ZAJICEK, J. P. 2004. Cannabis for dyskinesia in Parkinson disease: a randomized double-blind crossover study. *Neurology*, 63, 1245-50.
- CARTA, A. R., FRAU, L., PINNA, A., PONTIS, S., SIMOLA, N., SCHINTU, N. & MORELLI, M. 2008a. Behavioral and biochemical correlates of the dyskinesic potential of dopaminergic agonists in the 6-OHDA lesioned rat. *Synapse*, 62, 524-33.
- CARTA, A. R., FRAU, L., PONTIS, S., PINNA, A. & MORELLI, M. 2008b. Direct and indirect striatal efferent pathways are differentially influenced by low and high dyskinesic drugs: behavioural and biochemical evidence. *Parkinsonism Relat Disord*, 14 Suppl 2, S165-8.
- CARTA, M., CARLSSON, T., KIRIK, D. & BJORKLUND, A. 2007. Dopamine released from 5-HT terminals is the cause of L-DOPA-induced dyskinesia in parkinsonian rats. *Brain : a journal of neurology*, 130, 1819-33.
- CARTA, M., CARLSSON, T., MUNOZ, A., KIRIK, D. & BJORKLUND, A. 2008c. Involvement of the serotonin system in L-dopa-induced dyskinesias. *Parkinsonism & related disorders*, 14 Suppl 2, S154-8.
- CARTA, M., CARLSSON, T., MUNOZ, A., KIRIK, D. & BJORKLUND, A. 2008d. Serotonin-dopamine interaction in the induction and maintenance of L-DOPA-induced dyskinesias. *Progress in brain research*, 172, 465-78.
- CARTA, M., CARLSSON, T., MUNOZ, A., KIRIK, D. & BJORKLUND, A. 2010. Role of serotonin neurons in the induction of levodopa- and graft-induced dyskinesias in Parkinson's disease. *Movement disorders : official journal of the Movement Disorder Society*, 25 Suppl 1, S174-9.
- CARTER, R. J., LIONE, L. A., HUMBY, T., MANGIARINI, L., MAHAL, A., BATES, G. P., DUNNETT, S. B. & MORTON, A. J. 1999. Characterization of progressive motor deficits in mice transgenic for the human Huntington's disease mutation. *J Neurosci*, 19, 3248-57.
- CASTEELS, C., VANBILLOEN, B., VERCAMMEN, D., BOSIER, B., LAMBERT, D. M., BORMANS, G. & VAN LAERE, K. 2010. Influence of chronic bromocriptine and levodopa administration on cerebral type 1 cannabinoid receptor binding. *Synapse*, 64, 617-23.
- CASTILHO, R. F., HANSSON, O. & BRUNDIN, P. 2000. Improving the survival of grafted embryonic dopamine neurons in rodent models of Parkinson's disease. *Progress in brain research*, 127, 203-31.
- CENCI, M. A., CAMPBELL, K. & BJORKLUND, A. 1993. Neuropeptide messenger RNA expression in the 6-hydroxydopamine-lesioned rat striatum reinnervated by fetal

- dopaminergic transplants: differential effects of the grafts on preproenkephalin, preprotachykinin and prodynorphin messenger RNA levels. *Neuroscience*, 57, 275-96.
- CENCI, M. A. & KONRADI, C. 2010. Maladaptive striatal plasticity in L-DOPA-induced dyskinesia. *Progress in brain research*, 183, 209-33.
- CENCI, M. A., LEE, C. S. & BJORKLUND, A. 1998. L-DOPA-induced dyskinesia in the rat is associated with striatal overexpression of prodynorphin- and glutamic acid decarboxylase mRNA. *Eur J Neurosci*, 10, 2694-706.
- CENCI, M. A. & LUNDBLAD, M. 2007. Ratings of L-DOPA-induced dyskinesia in the unilateral 6-OHDA lesion model of Parkinson's disease in rats and mice. *Curr Protoc Neurosci*, Chapter 9, Unit 9 25.
- CENCI, M. A., OHLIN, K. E. & RYLANDER, D. 2009. Plastic effects of L-DOPA treatment in the basal ganglia and their relevance to the development of dyskinesia. *Parkinsonism & related disorders*, 15 Suppl 3, S59-63.
- CHAMBERS, J. W., PACHORI, A., HOWARD, S., GANNO, M., HANSEN, D., JR., KAMENECKA, T., SONG, X., DUCKETT, D., CHEN, W., LING, Y. Y., CHERRY, L., CAMERON, M. D., LIN, L., RUIZ, C. H. & LOGRASSO, P. 2011. Small Molecule c-jun-N-terminal Kinase (JNK) Inhibitors Protect Dopaminergic Neurons in a Model of Parkinson's Disease. *ACS chemical neuroscience*, 2, 198-206.
- CHEN, L., TOGASAKI, D. M., LANGSTON, J. W., DI MONTE, D. A. & QUIK, M. 2005. Enhanced striatal opioid receptor-mediated G-protein activation in L-DOPA-treated dyskinetic monkeys. *Neuroscience*, 132, 409-20.
- CHO, C., ALTERMAN, R., MIRAVITE, J., SHILS, J. & TAGLATI, M. 2005. Subthalamic DBS for the treatment of 'runaway' dyskinesias following embryonic or fetal tissue transplant. *Mov Disord*, 20, 1237.
- CHOI-LUNDBERG, D. L., LIN, Q., CHANG, Y. N., CHIANG, Y. L., HAY, C. M., MOHAJERI, H., DAVIDSON, B. L. & BOHN, M. C. 1997. Dopaminergic neurons protected from degeneration by GDNF gene therapy. *Science*, 275, 838-41.
- CHUNG, C. Y., KOPRICH, J. B., SIDDIQI, H. & ISACSON, O. 2009. Dynamic changes in presynaptic and axonal transport proteins combined with striatal neuroinflammation precede dopaminergic neuronal loss in a rat model of AAV alpha-synucleinopathy. *The Journal of neuroscience : the official journal of the Society for Neuroscience*, 29, 3365-73.
- COCHEN, V., RIBEIRO, M. J., NGUYEN, J. P., GURRUCHAGA, J. M., VILLAFANE, G., LOC'H, C., DEFER, G., SAMSON, Y., PESCHANSKI, M., HANTRAYE, P., CESARO, P. & REMY, P. 2003. Transplantation in Parkinson's disease: PET changes correlate with the amount of grafted tissue. *Movement disorders : official journal of the Movement Disorder Society*, 18, 928-32.
- CORASANITI, M. T., STRONGOLI, M. C., ROTIROTI, D., BAGETTA, G. & NISTICO, G. 1998. Paraquat: a useful tool for the in vivo study of mechanisms of neuronal cell death. *Pharmacology & toxicology*, 83, 1-7.
- COSTALL, B., FORTUNE, D. H. & NAYLOR, R. J. 1976a. Biphasic changes in motor behaviour following morphine injection into the nucleus accumbens [proceedings]. *Br J Pharmacol*, 57, 423P.
- COSTALL, B., MARSDEN, C. D., NAYLOR, R. J. & PYCOCK, C. J. 1976b. The relationship between striatal and mesolimbic dopamine dysfunction and the nature of circling responses following 6-hydroxydopamine and electrolytic lesions of the ascending dopamine systems of rat brain. *Brain Res*, 118, 87-113.
- COSTALL, B., NAYLOR, R. J. & PYCOCK, C. 1976c. Non-specific supersensitivity of striatal dopamine receptors after 6-hydroxydopamine lesion of the nigrostriatal pathway. *Eur J Pharmacol*, 35, 276-83.

- CRAGG, S. J. & RICE, M. E. 2004. DANCING past the DAT at a DA synapse. *Trends in neurosciences*, 27, 270-7.
- CROSSMAN, A. R. 1989. Neural mechanisms in disorders of movement. *Comparative biochemistry and physiology. A, Comparative physiology*, 93, 141-9.
- CUBO, E., GRACIES, J. M., BENABOU, R., OLANOW, C. W., RAMAN, R., LEURGANS, S. & GOETZ, C. G. 2001. Early morning off-medication dyskinesias, dystonia, and choreic subtypes. *Archives of neurology*, 58, 1379-82.
- DA SILVA-JUNIOR, F. P., BRAGA-NETO, P., SUELI MONTE, F. & DE BRUIN, V. M. 2005. Amantadine reduces the duration of levodopa-induced dyskinesia: a randomized, double-blind, placebo-controlled study. *Parkinsonism & related disorders*, 11, 449-52.
- DAMIER, P., HIRSCH, E. C., AGID, Y. & GRAYBIEL, A. M. 1999a. The substantia nigra of the human brain. I. Nigrosomes and the nigral matrix, a compartmental organization based on calbindin D(28K) immunohistochemistry. *Brain : a journal of neurology*, 122 (Pt 8), 1421-36.
- DAMIER, P., HIRSCH, E. C., AGID, Y. & GRAYBIEL, A. M. 1999b. The substantia nigra of the human brain. II. Patterns of loss of dopamine-containing neurons in Parkinson's disease. *Brain : a journal of neurology*, 122 (Pt 8), 1437-48.
- DARMOPIL, S., MUNETON-GOMEZ, V. C., DE CEBALLOS, M. L., BERNSON, M. & MORATALLA, R. 2008. Tyrosine hydroxylase cells appearing in the mouse striatum after dopamine denervation are likely to be projection neurones regulated by L-DOPA. *The European journal of neuroscience*, 27, 580-92.
- DAWSON, T. M., DAWSON, V. L., GAGE, F. H., FISHER, L. J., HUNT, M. A. & WAMSLEY, J. K. 1991. Functional recovery of supersensitive dopamine receptors after intrastriatal grafts of fetal substantia nigra. *Experimental neurology*, 111, 282-92.
- DAWSON, T. M., KO, H. S. & DAWSON, V. L. 2010. Genetic animal models of Parkinson's disease. *Neuron*, 66, 646-61.
- DE GORTARI, P. & MENGOD, G. 2010. Dopamine D1, D2 and mu-opioid receptors are co-expressed with adenylyl cyclase 5 and phosphodiesterase 7B mRNAs in striatal rat cells. *Brain research*, 1310, 37-45.
- DE MEDINACELI, L., FREED, W. J. & WYATT, R. J. 1982. An index of the functional condition of rat sciatic nerve based on measurements made from walking tracks. *Experimental neurology*, 77, 634-43.
- DEBEIR, T., GINESTET, L., FRANCOIS, C., LAURENS, S., MARTEL, J. C., CHOPIN, P., MARIEN, M., COLPAERT, F. & RAISMAN-VOZARI, R. 2005. Effect of intrastriatal 6-OHDA lesion on dopaminergic innervation of the rat cortex and globus pallidus. *Experimental neurology*, 193, 444-54.
- DEKUNDY, A., LUNDBLAD, M., DANYSZ, W. & CENCI, M. A. 2007. Modulation of L-DOPA-induced abnormal involuntary movements by clinically tested compounds: further validation of the rat dyskinesia model. *Behavioural brain research*, 179, 76-89.
- DEKUNDY, A., PIETRASZEK, M., SCHAEFER, D., CENCI, M. A. & DANYSZ, W. 2006. Effects of group I metabotropic glutamate receptors blockade in experimental models of Parkinson's disease. *Brain research bulletin*, 69, 318-26.
- DELONG, M. R., ALEXANDER, G. E., MITCHELL, S. J. & RICHARDSON, R. T. 1986. The contribution of basal ganglia to limb control. *Progress in brain research*, 64, 161-74.
- DEVOS, D. 2009. Patient profile, indications, efficacy and safety of duodenal levodopa infusion in advanced Parkinson's disease. *Movement disorders : official journal of the Movement Disorder Society*, 24, 993-1000.

- DEWAR, K. M. & READER, T. A. 1989. Distribution of dopamine D1 and D2 receptors in rabbit cortical areas, hippocampus, and neostriatum in relation to dopamine contents. *Synapse*, 4, 378-86.
- DEWAR, K. M., SOGHOMONIAN, J. J., BRUNO, J. P., DESCARRIES, L. & READER, T. A. 1990. Elevation of dopamine D2 but not D1 receptors in adult rat neostriatum after neonatal 6-hydroxydopamine denervation. *Brain research*, 536, 287-96.
- DIFIGLIA, M., PASIK, P. & PASIK, T. 1976. A Golgi study of neuronal types in the neostriatum of monkeys. *Brain research*, 114, 245-56.
- DOLPHIN, A. C. 1990. G protein modulation of calcium currents in neurons. *Annual review of physiology*, 52, 243-55.
- DOUCET, J. P., NAKABEPPU, Y., BEDARD, P. J., HOPE, B. T., NESTLER, E. J., JASMIN, B. J., CHEN, J. S., IADAROLA, M. J., ST-JEAN, M., WIGLE, N., BLANCHET, P., GRONDIN, R. & ROBERTSON, G. S. 1996. Chronic alterations in dopaminergic neurotransmission produce a persistent elevation of deltaFosB-like protein(s) in both the rodent and primate striatum. *Eur J Neurosci*, 8, 365-81.
- DOWD, E. & DUNNETT, S. B. 2004. Deficits in a lateralized associative learning task in dopamine-depleted rats with functional recovery by dopamine-rich transplants. *Eur J Neurosci*, 20, 1953-9.
- DOWD, E., MONVILLE, C., TORRES, E. M. & DUNNETT, S. B. 2005a. The Corridor Task: a simple test of lateralised response selection sensitive to unilateral dopamine deafferentation and graft-derived dopamine replacement in the striatum. *Brain Res Bull*, 68, 24-30.
- DOWD, E., MONVILLE, C., TORRES, E. M., WONG, L. F., AZZOUZ, M., MAZARAKIS, N. D. & DUNNETT, S. B. 2005b. Lentivector-mediated delivery of GDNF protects complex motor functions relevant to human Parkinsonism in a rat lesion model. *Eur J Neurosci*, 22, 2587-95.
- DUAN, C. L., SU, Y., ZHAO, C. L., LU, L. L., XU, Q. Y. & YANG, H. 2005. The assays of activities and function of TH, AADC, and GCH1 and their potential use in ex vivo gene therapy of PD. *Brain research. Brain research protocols*, 16, 37-43.
- DUNNETT, S. 2003. L-DOPA, dyskinesia and striatal plasticity. *Nature neuroscience*, 6, 437-8.
- DUNNETT, S. B., BJORKLUND, A. & LINDVALL, O. 2001. Cell therapy in Parkinson's disease - stop or go? *Nature reviews. Neuroscience*, 2, 365-9.
- DUNNETT, S. B., BJORKLUND, A., SCHMIDT, R. H., STENEVI, U. & IVERSEN, S. D. 1983a. Intracerebral grafting of neuronal cell suspensions. IV. Behavioural recovery in rats with unilateral 6-OHDA lesions following implantation of nigral cell suspensions in different forebrain sites. *Acta physiologica Scandinavica. Supplementum*, 522, 29-37.
- DUNNETT, S. B., BJORKLUND, A., SCHMIDT, R. H., STENEVI, U. & IVERSEN, S. D. 1983b. Intracerebral grafting of neuronal cell suspensions. V. Behavioural recovery in rats with bilateral 6-OHDA lesions following implantation of nigral cell suspensions. *Acta physiologica Scandinavica. Supplementum*, 522, 39-47.
- DUNNETT, S. B., BJORKLUND, A., STENEVI, U. & IVERSEN, S. D. 1981. Behavioural recovery following transplantation of substantia nigra in rats subjected to 6-OHDA lesions of the nigrostriatal pathway. I. Unilateral lesions. *Brain research*, 215, 147-61.
- DUNNETT, S. B., HERNANDEZ, T. D., SUMMERFIELD, A., JONES, G. H. & ARBUTHNOTT, G. 1988a. Graft-derived recovery from 6-OHDA lesions: specificity of ventral mesencephalic graft tissues. *Experimental brain research. Experimentelle Hirnforschung. Experimentation cerebrale*, 71, 411-24.

- DUNNETT, S. B., ISACSON, O., SIRINATHSINGHI, D. J., CLARKE, D. J. & BJORKLUND, A. 1988b. Striatal grafts in rats with unilateral neostriatal lesions--III. Recovery from dopamine-dependent motor asymmetry and deficits in skilled paw reaching. *Neuroscience*, 24, 813-20.
- DUNNETT, S. B., TORRES, E. M. & ANNETT, L. E. 1998. A lateralised grip strength test to evaluate unilateral nigrostriatal lesions in rats. *Neurosci Lett*, 246, 1-4.
- DUNNETT, S. B. A. B., A. 1992. *Neural transplantation - A Practical Approach*, Oxford, Oxford University Press.
- DUPRE, K. B., ESKOW, K. L., BARNUM, C. J. & BISHOP, C. 2008. Striatal 5-HT1A receptor stimulation reduces D1 receptor-induced dyskinesia and improves movement in the hemiparkinsonian rat. *Neuropharmacology*, 55, 1321-8.
- EL ATIFI-BOREL, M., BUGGIA-PREVOT, V., PLATET, N., BENABID, A. L., BERGER, F. & SGAMBATO-FAURE, V. 2009. De novo and long-term L-Dopa induce both common and distinct striatal gene profiles in the hemiparkinsonian rat. *Neurobiology of disease*, 34, 340-50.
- ENCARNACION, E. V. & HAUSER, R. A. 2008. Levodopa-induced dyskinesias in Parkinson's disease: etiology, impact on quality of life, and treatments. *European neurology*, 60, 57-66.
- ENGBER, T. M., PAPA, S. M., BOLDRY, R. C. & CHASE, T. N. 1994. NMDA receptor blockade reverses motor response alterations induced by levodopa. *Neuroreport*, 5, 2586-8.
- ERDFELDER, E., FAUL, F. & BUCHNER, A. 1996. GPOWER: A general power analysis program. *Behavior Research Methods, Instruments, & Computers*, 28, 1-11.
- ESKOW, K. L., DUPRE, K. B., BARNUM, C. J., DICKINSON, S. O., PARK, J. Y. & BISHOP, C. 2009. The role of the dorsal raphe nucleus in the development, expression, and treatment of L-dopa-induced dyskinesia in hemiparkinsonian rats. *Synapse*, 63, 610-20.
- ESLAMBOLI, A., ROMERO-RAMOS, M., BURGER, C., BJORKLUND, T., MUZYCZKA, N., MANDEL, R. J., BAKER, H., RIDLEY, R. M. & KIRIK, D. 2007. Long-term consequences of human alpha-synuclein overexpression in the primate ventral midbrain. *Brain : a journal of neurology*, 130, 799-815.
- ESPAY, A. J. 2010. Management of motor complications in Parkinson disease: current and emerging therapies. *Neurologic clinics*, 28, 913-25.
- FAHN, S., LIBSCH, L. R. & CUTLER, R. W. 1971. Monoamines in the human neostriatum: topographic distribution in normals and in Parkinson's disease and their role in akinesia, rigidity, chorea, and tremor. *Journal of the neurological sciences*, 14, 427-55.
- FAUCHEUX, B. A., BONNET, A. M., AGID, Y. & HIRSCH, E. C. 1999. Blood vessels change in the mesencephalon of patients with Parkinson's disease. *Lancet*, 353, 981-2.
- FENU, S., CARTA, A. & MORELLI, M. 1995. Intranigral injections of glutamate antagonists modulate dopamine D1-mediated turning behavior and striatal c-fos expression. *Journal of neural transmission. Supplementum*, 45, 75-81.
- FINDLEY, L. J., WOOD, E., LOWIN, J., ROEDER, C., BERGMAN, A. & SCHIFFLERS, M. 2011. The economic burden of advanced Parkinson's disease: an analysis of a UK patient dataset. *Journal of medical economics*.
- FINK, J. S. & SMITH, G. P. 1980. Mesolimbocortical dopamine terminal fields are necessary for normal locomotor and investigatory exploration in rats. *Brain Res*, 199, 359-84.
- FLECKENSTEIN, A. E., VOLZ, T. J., RIDDLE, E. L., GIBB, J. W. & HANSON, G. R. 2007. New insights into the mechanism of action of amphetamines. *Annual review of pharmacology and toxicology*, 47, 681-98.

- FOLLETT, K. A., WEAVER, F. M., STERN, M., HUR, K., HARRIS, C. L., LUO, P., MARKS, W. J., JR., ROTHLIND, J., SAGHER, O., MOY, C., PAHWA, R., BURCHIEL, K., HOGARTH, P., LAI, E. C., DUDA, J. E., HOLLOWAY, K., SAMII, A., HORN, S., BRONSTEIN, J. M., STONER, G., STARR, P. A., SIMPSON, R., BALTUCH, G., DE SALLES, A., HUANG, G. D. & REDA, D. J. 2010. Pallidal versus subthalamic deep-brain stimulation for Parkinson's disease. *The New England journal of medicine*, 362, 2077-91.
- FORNAGUERA, J. & SCHWARTING, R. K. 2002. Time course of deficits in open field behavior after unilateral neostriatal 6-hydroxydopamine lesions. *Neurotox Res*, 4, 41-9.
- FORNAI, F., LENZI, P., GESI, M., SOLDANI, P., FERRUCCI, M., LAZZERI, G., CAPOBIANCO, L., BATTAGLIA, G., DE BLASI, A., NICOLETTI, F. & PAPARELLI, A. 2004. Methamphetamine produces neuronal inclusions in the nigrostriatal system and in PC12 cells. *Journal of neurochemistry*, 88, 114-23.
- FORNAI, F., SCHLUTER, O. M., LENZI, P., GESI, M., RUFFOLI, R., FERRUCCI, M., LAZZERI, G., BUSCETI, C. L., PONTARELLI, F., BATTAGLIA, G., PELLEGRINI, A., NICOLETTI, F., RUGGIERI, S., PAPARELLI, A. & SUDHOF, T. C. 2005. Parkinson-like syndrome induced by continuous MPTP infusion: convergent roles of the ubiquitin-proteasome system and alpha-synuclein. *Proceedings of the National Academy of Sciences of the United States of America*, 102, 3413-8.
- FOX, S., SILVERDALE, M., KELLETT, M., DAVIES, R., STEIGER, M., FLETCHER, N., CROSSMAN, A. & BROTCHE, J. 2004. Non-subtype-selective opioid receptor antagonism in treatment of levodopa-induced motor complications in Parkinson's disease. *Movement disorders : official journal of the Movement Disorder Society*, 19, 554-60.
- FOX, S. H., BROTCHE, J. M. & LANG, A. E. 2008a. Non-dopaminergic treatments in development for Parkinson's disease. *Lancet neurology*, 7, 927-38.
- FOX, S. H., CHUANG, R. & BROTCHE, J. M. 2008b. Parkinson's disease--opportunities for novel therapeutics to reduce the problems of levodopa therapy. *Progress in brain research*, 172, 479-94.
- FRANCARDO, V., RECCHIA, A., POPOVIC, N., ANDERSSON, D., NISSBRANDT, H. & CENCI, M. A. 2011. Impact of the lesion procedure on the profiles of motor impairment and molecular responsiveness to L-DOPA in the 6-hydroxydopamine mouse model of Parkinson's disease. *Neurobiol Dis*.
- FREED, C. R., BREEZE, R. E., FAHN, S. & EIDELBERG, D. 2004. Preoperative response to levodopa is the best predictor of transplant outcome. *Annals of neurology*, 55, 896; author reply 896-7.
- FREED, C. R., BREEZE, R. E., ROSENBERG, N. L., SCHNECK, S. A., WELLS, T. H., BARRETT, J. N., GRAFTON, S. T., HUANG, S. C., EIDELBERG, D. & ROTTENBERG, D. A. 1990. Transplantation of human fetal dopamine cells for Parkinson's disease. Results at 1 year. *Archives of neurology*, 47, 505-12.
- FREED, C. R., BREEZE, R. E. & SCHNECK, S. A. 1995. Transplantation of fetal mesencephalic tissue in Parkinson's disease. *The New England journal of medicine*, 333, 730-1.
- FREED, C. R., GREENE, P. E., BREEZE, R. E., TSAI, W. Y., DUMOUCHEL, W., KAO, R., DILLON, S., WINFIELD, H., CULVER, S., TROJANOWSKI, J. Q., EIDELBERG, D. & FAHN, S. 2001. Transplantation of embryonic dopamine neurons for severe Parkinson's disease. *The New England journal of medicine*, 344, 710-9.
- FREED, C. R., LEEHEY, M. A., ZAWADA, M., BJUGSTAD, K., THOMPSON, L. & BREEZE, R. E. 2003. Do patients with Parkinson's disease benefit from embryonic dopamine cell transplantation? *Journal of neurology*, 250 Suppl 3, III44-6.

- FREED, W. J. 1983. Functional brain tissue transplantation: reversal of lesion-induced rotation by intraventricular substantia nigra and adrenal medulla grafts, with a note on intracranial retinal grafts. *Biological psychiatry*, 18, 1205-67.
- FREED, W. J. 2004. A perspective on transplantation therapy and stem cells for Parkinson's disease. *Cell transplantation*, 13, 319-27.
- FREED, W. J., KAROUM, F., SPOOR, H. E., MORIHISA, J. M., OLSON, L. & WYATT, R. J. 1983. Catecholamine content of intracerebral adrenal medulla grafts. *Brain research*, 269, 184-9.
- FREED, W. J., MORIHISA, J. M., SPOOR, E., HOFFER, B. J., OLSON, L., SEIGER, A. & WYATT, R. J. 1981. Transplanted adrenal chromaffin cells in rat brain reduce lesion-induced rotational behaviour. *Nature*, 292, 351-2.
- FREEMAN, T. B., OLANOW, C. W., HAUSER, R. A., NAUERT, G. M., SMITH, D. A., BORLONGAN, C. V., SANBERG, P. R., HOLT, D. A., KORDOWER, J. H., VINGERHOETS, F. J. & ET AL. 1995. Bilateral fetal nigral transplantation into the postcommissural putamen in Parkinson's disease. *Annals of neurology*, 38, 379-88.
- FRICKER, R. A., ANNETT, L. E., TORRES, E. M. & DUNNETT, S. B. 1996. The placement of a striatal ibotenic acid lesion affects skilled forelimb use and the direction of drug-induced rotation. *Brain Res Bull*, 41, 409-16.
- FRY, D. C. 2006. Protein-protein interactions as targets for small molecule drug discovery. *Biopolymers*, 84, 535-52.
- FULCERI, F., BIAGIONI, F., LENZI, P., FALLENI, A., GESI, M., RUGGIERI, S. & FORNAI, F. 2006. Nigrostriatal damage with 6-OHDA: validation of routinely applied procedures. *Annals of the New York Academy of Sciences*, 1074, 344-8.
- GAGNON, C., BEDARD, P. J., RIOUX, L., GAUDIN, D., MARTINOLI, M. G., PELLETIER, G. & DI PAOLO, T. 1991. Regional changes of striatal dopamine receptors following denervation by 6-hydroxydopamine and fetal mesencephalic grafts in the rat. *Brain research*, 558, 251-63.
- GALTREY, C. M. & FAWCETT, J. W. 2007. Characterization of tests of functional recovery after median and ulnar nerve injury and repair in the rat forelimb. *J Peripher Nerv Syst*, 12, 11-27.
- GARCIA, J., CARLSSON, T., DOBROSSY, M., NIKKHAH, G. & WINKLER, C. 2011. Impact of dopamine to serotonin cell ratio in transplants on behavioral recovery and L-DOPA-induced dyskinesia. *Neurobiol Dis*.
- GARDONI, F., PICCONI, B., GHIGLIERI, V., POLLI, F., BAGETTA, V., BERNARDI, G., CATTABENI, F., DI LUCA, M. & CALABRESI, P. 2006. A critical interaction between NR2B and MAGUK in L-DOPA induced dyskinesia. *The Journal of neuroscience : the official journal of the Society for Neuroscience*, 26, 2914-22.
- GARZON, J., RODRIGUEZ-MUNOZ, M. & SANCHEZ-BLAZQUEZ, P. 2005. Morphine alters the selective association between mu-opioid receptors and specific RGS proteins in mouse periaqueductal gray matter. *Neuropharmacology*, 48, 853-68.
- GASMI, M., BRANDON, E. P., HERZOG, C. D., WILSON, A., BISHOP, K. M., HOFER, E. K., CUNNINGHAM, J. J., PRINTZ, M. A., KORDOWER, J. H. & BARTUS, R. T. 2007. AAV2-mediated delivery of human neurturin to the rat nigrostriatal system: long-term efficacy and tolerability of CERE-120 for Parkinson's disease. *Neurobiology of disease*, 27, 67-76.
- GASPAR, P., FEBVRET, A. & COLOMBO, J. 1993. Serotonergic sprouting in primate MTP-induced hemiparkinsonism. *Exp Brain Res*, 96, 100-6.
- GERFEN, C. R. 1985. The neostriatal mosaic. I. Compartmental organization of projections from the striatum to the substantia nigra in the rat. *The Journal of comparative neurology*, 236, 454-76.

- GERFEN, C. R. 1989. The neostriatal mosaic: striatal patch-matrix organization is related to cortical lamination. *Science*, 246, 385-8.
- GERFEN, C. R. 1992. The neostriatal mosaic: multiple levels of compartmental organization. *Trends in neurosciences*, 15, 133-9.
- GERFEN, C. R., BAIMBRIDGE, K. G. & MILLER, J. J. 1985. The neostriatal mosaic: compartmental distribution of calcium-binding protein and parvalbumin in the basal ganglia of the rat and monkey. *Proceedings of the National Academy of Sciences of the United States of America*, 82, 8780-4.
- GERFEN, C. R. & SURMEIER, D. J. 2011. Modulation of striatal projection systems by dopamine. *Annual review of neuroscience*, 34, 441-66.
- GETHER, U., ASMAR, F., MEINILD, A. K. & RASMUSSEN, S. G. 2002. Structural basis for activation of G-protein-coupled receptors. *Pharmacology & toxicology*, 91, 304-12.
- GEURTS, M., HERMANS, E. & MALOTEAUX, J. M. 2002. Opposite modulation of regulators of G protein signalling-2 RGS2 and RGS4 expression by dopamine receptors in the rat striatum. *Neuroscience letters*, 333, 146-50.
- GEURTS, M., MALOTEAUX, J. M. & HERMANS, E. 2003. Altered expression of regulators of G-protein signaling (RGS) mRNAs in the striatum of rats undergoing dopamine depletion. *Biochemical pharmacology*, 66, 1163-70.
- GIL, S., PARK, C., LEE, J. & KOH, H. 2010. The roles of striatal serotonin and L: -amino-acid decarboxylase on L: -DOPA-induced Dyskinesia in a Hemiparkinsonian rat model. *Cell Mol Neurobiol*, 30, 817-25.
- GLINKA, Y. Y. & YODIM, M. B. 1995. Inhibition of mitochondrial complexes I and IV by 6-hydroxydopamine. *Eur J Pharmacol*, 292, 329-32.
- GODWIN-AUSTEN, R. B., FREARS, C. C., BERGMANN, S., PARKES, J. D. & KNILL-JONES, R. P. 1970. Combined treatment of parkinsonism with L-dopa and amantadine. *Lancet*, 2, 383-5.
- GOETZ, C. G., WUU, J., MCDERMOTT, M. P., ADLER, C. H., FAHN, S., FREED, C. R., HAUSER, R. A., OLANOW, W. C., SHOULSON, I., TANDON, P. K. & LEURGANS, S. 2008. Placebo response in Parkinson's disease: comparisons among 11 trials covering medical and surgical interventions. *Movement disorders : official journal of the Movement Disorder Society*, 23, 690-9.
- GOLD, S. J., HOANG, C. V., POTTS, B. W., PORRAS, G., PIOLI, E., KIM, K. W., NADJAR, A., QIN, C., LAHOSTE, G. J., LI, Q., BIOULAC, B. H., WAUGH, J. L., GUREVICH, E., NEVE, R. L. & BEZARD, E. 2007. RGS9-2 negatively modulates L-3,4-dihydroxyphenylalanine-induced dyskinesia in experimental Parkinson's disease. *The Journal of neuroscience : the official journal of the Society for Neuroscience*, 27, 14338-48.
- GOLD, S. J., NI, Y. G., DOHLMAN, H. G. & NESTLER, E. J. 1997. Regulators of G-protein signaling (RGS) proteins: region-specific expression of nine subtypes in rat brain. *The Journal of neuroscience : the official journal of the Society for Neuroscience*, 17, 8024-37.
- GRAFSTEIN-DUNN, E., YOUNG, K. H., COCKETT, M. I. & KHAWAJA, X. Z. 2001. Regional distribution of regulators of G-protein signaling (RGS) 1, 2, 13, 14, 16, and GAIP messenger ribonucleic acids by in situ hybridization in rat brain. *Brain research. Molecular brain research*, 88, 113-23.
- GREALISH, S., JONSSON, M. E., LI, M., KIRIK, D., BJORKLUND, A. & THOMPSON, L. H. 2010a. The A9 dopamine neuron component in grafts of ventral mesencephalon is an important determinant for recovery of motor function in a rat model of Parkinson's disease. *Brain : a journal of neurology*, 133, 482-95.

- GREALISH, S., MATTSSON, B., DRAXLER, P. & BJORKLUND, A. 2010b. Characterisation of behavioural and neurodegenerative changes induced by intranigral 6-hydroxydopamine lesions in a mouse model of Parkinson's disease. *Eur J Neurosci*, 31, 2266-78.
- GREALISH, S., XIE, L., KELLY, M. & DOWD, E. 2008. Unilateral axonal or terminal injection of 6-hydroxydopamine causes rapid-onset nigrostriatal degeneration and contralateral motor impairments in the rat. *Brain Res Bull*, 77, 312-9.
- GREENAMYRE, J. T., BETARBET, R. & SHERER, T. B. 2003. The rotenone model of Parkinson's disease: genes, environment and mitochondria. *Parkinsonism & related disorders*, 9 Suppl 2, S59-64.
- GRILLET, N., PATTYN, A., CONTET, C., KIEFFER, B. L., GORIDIS, C. & BRUNET, J. F. 2005. Generation and characterization of Rgs4 mutant mice. *Molecular and cellular biology*, 25, 4221-8.
- GROSS, S. J., WOJTECKI, L., SUDMEYER, M. & SCHNITZLER, A. 2009. Deep brain stimulation in Parkinson's disease. *Therapeutic advances in neurological disorders*, 2, 20-8.
- GROSS, R. E., WATTS, R. L., HAUSER, R. A., BAKAY, R. A., REICHMANN, H., VON KUMMER, R., ONDO, W. G., REISSIG, E., EISNER, W., STEINER-SCHULZE, H., SIEDENTOP, H., FICHTE, K., HONG, W., CORNFELDT, M., BEEBE, K. & SANDBRINK, R. 2011. Intra-striatal transplantation of microcarrier-bound human retinal pigment epithelial cells versus sham surgery in patients with advanced Parkinson's disease: a double-blind, randomised, controlled trial. *Lancet neurology*, 10, 509-19.
- GUO, S., TANG, W., SHI, Y., HUANG, K., XI, Z., XU, Y., FENG, G. & HE, L. 2006. RGS4 polymorphisms and risk of schizophrenia: an association study in Han Chinese plus meta-analysis. *Neuroscience letters*, 406, 122-7.
- HABER, S. N. & MCFARLAND, N. R. 1999. The concept of the ventral striatum in nonhuman primates. *Annals of the New York Academy of Sciences*, 877, 33-48.
- HAGELL, P., PICCINI, P., BJORKLUND, A., BRUNDIN, P., REHNCRONA, S., WIDNER, H., CRABB, L., PAVESE, N., OERTEL, W. H., QUINN, N., BROOKS, D. J. & LINDVALL, O. 2002. Dyskinesias following neural transplantation in Parkinson's disease. *Nature neuroscience*, 5, 627-8.
- HAGELL, P., SCHRAG, A., PICCINI, P., JAHANSHAHI, M., BROWN, R., REHNCRONA, S., WIDNER, H., BRUNDIN, P., ROTHWELL, J. C., ODIN, P., WENNING, G. K., MORRISH, P., GUSTAVII, B., BJORKLUND, A., BROOKS, D. J., MARSDEN, C. D., QUINN, N. P. & LINDVALL, O. 1999. Sequential bilateral transplantation in Parkinson's disease: effects of the second graft. *Brain : a journal of neurology*, 122 (Pt 6), 1121-32.
- HALLIDAY, G., HERRERO, M. T., MURPHY, K., MCCANN, H., ROS-BERNAL, F., BARCIA, C., MORI, H., BLESÁ, F. J. & OBESO, J. A. 2009. No Lewy pathology in monkeys with over 10 years of severe MPTP Parkinsonism. *Movement disorders : official journal of the Movement Disorder Society*, 24, 1519-23.
- HAMADA, I. & DELONG, M. R. 1992. Excitotoxic acid lesions of the primate subthalamic nucleus result in transient dyskinesias of the contralateral limbs. *Journal of neurophysiology*, 68, 1850-8.
- HAWKES, C. H., DEL TREDICI, K. & BRAAK, H. 2010. A timeline for Parkinson's disease. *Parkinsonism & related disorders*, 16, 79-84.
- HEFTI, F., MELAMED, E., SAHAKIAN, B. J. & WURTMAN, R. J. 1980. Circling behavior in rats with partial, unilateral nigro-striatal lesions: effect of amphetamine, apomorphine, and DOPA. *Pharmacology, biochemistry, and behavior*, 12, 185-8.

- HENRY, B., FOX, S. H., CROSSMAN, A. R. & BROTCHE, J. M. 2001. Mu- and delta-opioid receptor antagonists reduce levodopa-induced dyskinesia in the MPTP-lesioned primate model of Parkinson's disease. *Experimental neurology*, 171, 139-46.
- HERZOG, C. D., DASS, B., HOLDEN, J. E., STANSELL, J., 3RD, GASMI, M., TUSZYNSKI, M. H., BARTUS, R. T. & KORDOWER, J. H. 2007. Striatal delivery of CERE-120, an AAV2 vector encoding human neurturin, enhances activity of the dopaminergic nigrostriatal system in aged monkeys. *Movement disorders : official journal of the Movement Disorder Society*, 22, 1124-32.
- HERZOG, J., FIETZEK, U., HAMEL, W., MORSNOWSKI, A., STEIGERWALD, F., SCHRADER, B., WEINERT, D., PFISTER, G., MULLER, D., MEHDORN, H. M., DEUSCHL, G. & VOLKMANN, J. 2004. Most effective stimulation site in subthalamic deep brain stimulation for Parkinson's disease. *Movement disorders : official journal of the Movement Disorder Society*, 19, 1050-4.
- HERZOG, J., POGARELL, O., PINSKER, M. O., KUPSCH, A., OERTEL, W. H., LINDVALL, O., DEUSCHL, G. & VOLKMANN, J. 2008. Deep brain stimulation in Parkinson's disease following fetal nigral transplantation. *Movement disorders : official journal of the Movement Disorder Society*, 23, 1293-6.
- HOOKS, S. B., MARTEMYANOV, K. & ZACHARIOU, V. 2008. A role of RGS proteins in drug addiction. *Biochemical pharmacology*, 75, 76-84.
- HORNYKIEWICZ, O. 1982. Imbalance of brain monoamines and clinical disorders. *Progress in brain research*, 55, 419-29.
- HUG, K. & HERMEREN, G. 2011. Do we Still Need Human Embryonic Stem Cells for Stem Cell-Based Therapies? Epistemic and Ethical Aspects. *Stem cell reviews*.
- HUOT, P. & PARENT, A. 2007. Dopaminergic neurons intrinsic to the striatum. *Journal of neurochemistry*, 101, 1441-7.
- HYUN, I. 2010. The bioethics of stem cell research and therapy. *The Journal of clinical investigation*, 120, 71-5.
- HYUN, I., LINDVALL, O., AHRLUND-RICHTER, L., CATTANEO, E., CAVAZZANACALVO, M., COSSU, G., DE LUCA, M., FOX, I. J., GERSTLE, C., GOLDSTEIN, R. A., HERMEREN, G., HIGH, K. A., KIM, H. O., LEE, H. P., LEVY-LAHAD, E., LI, L., LO, B., MARSHAK, D. R., MCNAB, A., MUNSIE, M., NAKAUCHI, H., RAO, M., ROOKE, H. M., VALLES, C. S., SRIVASTAVA, A., SUGARMAN, J., TAYLOR, P. L., VEIGA, A., WONG, A. L., ZOLOTH, L. & DALEY, G. Q. 2008. New ISSCR guidelines underscore major principles for responsible translational stem cell research. *Cell stem cell*, 3, 607-9.
- IANCU, R., MOHAPEL, P., BRUNDIN, P. & PAUL, G. 2005. Behavioral characterization of a unilateral 6-OHDA-lesion model of Parkinson's disease in mice. *Behav Brain Res*, 162, 1-10.
- IKEDA, K., YOSHIKAWA, S., KUROKAWA, T., YUZAWA, N., NAKAO, K. & MOCHIZUKI, H. 2009. TRK-820, a selective kappa opioid receptor agonist, could effectively ameliorate L-DOPA-induced dyskinesia symptoms in a rat model of Parkinson's disease. *European journal of pharmacology*, 620, 42-8.
- IMPEY, S., OBRIETAN, K. & STORM, D. R. 1999. Making new connections: role of ERK/MAP kinase signaling in neuronal plasticity. *Neuron*, 23, 11-4.
- ISHIDA, Y., HASHITANI, T., KUMAZAKI, M., IKEDA, T. & NISHINO, H. 1990. Behavioral and biochemical effects of intra-accumbens dopaminergic grafts. *Brain research bulletin*, 24, 487-92.
- ISHIDA, Y., TODAKA, K., HASHIGUCHI, H., TAKEDA, R., MITSUYAMA, Y. & NISHIMORI, T. 2002. Morphological changes in immunopositive cells of ionotropic

- glutamate receptor subunits during the development of transplanted fetal ventral mesencephalic neurons. *Brain research*, 940, 79-85.
- ISHIHARA, L. S., CHEESBROUGH, A., BRAYNE, C. & SCHRAG, A. 2007. Estimated life expectancy of Parkinson's patients compared with the UK population. *Journal of neurology, neurosurgery, and psychiatry*, 78, 1304-9.
- JACKSON, J., CHAPON, C., JONES, W., HIRANI, E., QASSIM, A. & BHAKOO, K. 2009. In vivo multimodal imaging of stem cell transplantation in a rodent model of Parkinson's disease. *Journal of neuroscience methods*, 183, 141-8.
- JANKOVIC, J. 2008. Parkinson's disease: clinical features and diagnosis. *J Neurol Neurosurg Psychiatry*, 79, 368-76.
- JANKOVIC, J. & AGUILAR, L. G. 2008. Current approaches to the treatment of Parkinson's disease. *Neuropsychiatric disease and treatment*, 4, 743-57.
- JARVIS, M. F. & WAGNER, G. C. 1985. Neurochemical and functional consequences following 1-methyl-4-phenyl-1,2,5,6-tetrahydropyridine (MPTP) and methamphetamine. *Life sciences*, 36, 249-54.
- JAUNARAJ, K. L., DUPRE, K. B., STEINIGER, A., KLIQUEVA, A., MOORE, A., KELLY, C. & BISHOP, C. 2009. Serotonin 1B receptor stimulation reduces D1 receptor agonist-induced dyskinesia. *Neuroreport*, 20, 1265-9.
- JELLINGER, K. A. 1991. Pathology of Parkinson's disease. Changes other than the nigrostriatal pathway. *Molecular and chemical neuropathology / sponsored by the International Society for Neurochemistry and the World Federation of Neurology and research groups on neurochemistry and cerebrospinal fluid*, 14, 153-97.
- JENNER, P. 2003. The MPTP-treated primate as a model of motor complications in PD: primate model of motor complications. *Neurology*, 61, S4-11.
- JENNER, P. 2009. From the MPTP-treated primate to the treatment of motor complications in Parkinson's disease. *Parkinsonism & related disorders*, 15 Suppl 4, S18-23.
- JENNER, P., RUPNIAK, N. M., ROSE, S., KELLY, E., KILPATRICK, G., LEES, A. & MARSDEN, C. D. 1984. 1-Methyl-4-phenyl-1,2,3,6-tetrahydropyridine-induced parkinsonism in the common marmoset. *Neuroscience letters*, 50, 85-90.
- JESTE, D. V. & SMITH, G. P. 1980. Unilateral mesolimbocortical dopamine denervation decreases locomotion in the open field and after amphetamine. *Pharmacol Biochem Behav*, 12, 453-7.
- JOHNSTON, T. H., LEE, J., GOMEZ-RAMIREZ, J., FOX, S. H. & BROTHIE, J. M. 2005. A simple rodent assay for the in vivo identification of agents with potential to reduce levodopa-induced dyskinesia in Parkinson's disease. *Experimental neurology*, 191, 243-50.
- JOLKKONEN, J., JENNER, P. & MARSDEN, C. D. 1995. L-DOPA reverses altered gene expression of substance P but not enkephalin in the caudate-putamen of common marmosets treated with MPTP. *Brain research. Molecular brain research*, 32, 297-307.
- JOLLIVET, C., MONTERO-MENEI, C. N., VENIER-JULIENNE, M. C., SAPIN, A., BENOIT, J. P. & MENEI, P. 2004. Striatal tyrosine hydroxylase immunoreactive neurons are induced by L-dihydroxyphenylalanine and nerve growth factor treatment in 6-hydroxydopamine lesioned rats. *Neuroscience letters*, 362, 79-82.
- JONES, S. R., GAINETDINOV, R. R., JABER, M., GIROS, B., WIGHTMAN, R. M. & CARON, M. G. 1998. Profound neuronal plasticity in response to inactivation of the dopamine transporter. *Proceedings of the National Academy of Sciences of the United States of America*, 95, 4029-34.

- JUHASZ, J. R., HASBI, A., RASHID, A. J., SO, C. H., GEORGE, S. R. & O'DOWD, B. F. 2008. Mu-opioid receptor heterooligomer formation with the dopamine D1 receptor as directly visualized in living cells. *European journal of pharmacology*, 581, 235-43.
- KAARIAINEN, T. M., GARCIA-HORSMAN, J. A., PILTONEN, M. & MANNISTO, P. T. 2009. L-dopa-induced desensitization depends on 5-hydroxytryptamine imbalance in hemiparkinsonian rats. *Neuroreport*, 20, 313-8.
- KAPP, W. 1992. The history of drugs for the treatment of Parkinson's disease. *Journal of neural transmission. Supplementum*, 38, 1-6.
- KAWAGUCHI, Y. 1993. Physiological, morphological, and histochemical characterization of three classes of interneurons in rat neostriatum. *The Journal of neuroscience : the official journal of the Society for Neuroscience*, 13, 4908-23.
- KAWAGUCHI, Y., WILSON, C. J., AUGOOD, S. J. & EMSON, P. C. 1995. Striatal interneurons: chemical, physiological and morphological characterization. *Trends in neurosciences*, 18, 527-35.
- KATZENSCHLAGER, R., HUGHES, A., EVANS, A., MANSON, A. J., HOFFMAN, M., SWINN, L., WATT, H., BHATIA, K., QUINN, N. & LEES, A. J. 2005. Continuous subcutaneous apomorphine therapy improves dyskinesias in Parkinson's disease: a prospective study using single-dose challenges. *Movement Disorders*. 20(2):151-7.
- KELLEY, A. E., LANG, C. G. & GAUTHIER, A. M. 1988. Induction of oral stereotypy following amphetamine microinjection into a discrete subregion of the striatum. *Psychopharmacology*, 95, 556-9.
- KELLY, C. M., PRECIOUS, S. V., TORRES, E. M., HARRISON, A. W., WILLIAMS, D., SCHERF, C., WEYRAUCH, U. M., LANE, E. L., ALLEN, N. D., PENKETH, R., AMSO, N. N., KEMP, P. J., DUNNETT, S. B. & ROSSER, A. E. 2011. Medical terminations of pregnancy: a viable source of tissue for cell replacement therapy for neurodegenerative disorders. *Cell transplantation*.
- KIM, G., LEE, Y., JEONG, E. Y., JUNG, S., SON, H., LEE, D. H., ROH, G. S., KANG, S. S., CHO, G. J., CHOI, W. S. & KIM, H. J. 2010. Acute stress responsive RGS proteins in the mouse brain. *Molecules and cells*, 30, 161-5.
- KIRIK, D., ANNETT, L. E., BURGER, C., MUZYCZKA, N., MANDEL, R. J. & BJORKLUND, A. 2003. Nigrostriatal alpha-synucleinopathy induced by viral vector-mediated overexpression of human alpha-synuclein: a new primate model of Parkinson's disease. *Proceedings of the National Academy of Sciences of the United States of America*, 100, 2884-9.
- KIRIK, D., GEORGIEVSKA, B., BURGER, C., WINKLER, C., MUZYCZKA, N., MANDEL, R. J. & BJORKLUND, A. 2002. Reversal of motor impairments in parkinsonian rats by continuous intrastriatal delivery of L-dopa using rAAV-mediated gene transfer. *Proceedings of the National Academy of Sciences of the United States of America*, 99, 4708-13.
- KIRIK, D., ROSENBLAD, C. & BJORKLUND, A. 1998. Characterization of behavioral and neurodegenerative changes following partial lesions of the nigrostriatal dopamine system induced by intrastriatal 6-hydroxydopamine in the rat. *Exp Neurol*, 152, 259-77.
- KISH, S. J., TONG, J., HORNYKIEWICZ, O., RAJPUT, A., CHANG, L. J., GUTTMAN, M. & FURUKAWA, Y. 2008. Preferential loss of serotonin markers in caudate versus putamen in Parkinson's disease. *Brain : a journal of neurology*, 131, 120-31.
- KIURU, M., BOYER, J. L., O'CONNOR, T. P. & CRYSTAL, R. G. 2009. Genetic control of wayward pluripotent stem cells and their progeny after transplantation. *Cell stem cell*, 4, 289-300.

- KLEIN, A., METZ, G. A., PAPAZOGLU, A. & NIKKHAH, G. 2007. Differential effects on forelimb grasping behavior induced by fetal dopaminergic grafts in hemiparkinsonian rats. *Neurobiol Dis*, 27, 24-35.
- KLEIN, A., WESSOLLECK, J., PAPAZOGLU, A., METZ, G. A. & NIKKHAH, G. 2009. Walking pattern analysis after unilateral 6-OHDA lesion and transplantation of foetal dopaminergic progenitor cells in rats. *Behav Brain Res*, 199, 317-25.
- KNIFE, M. D., WICKREMARATCHI, M. M., WYATT-HAINES, E., MORRIS, H. R. & BEN-SHLOMO, Y. 2011. Quality of life in young- compared with late-onset Parkinson's disease. *Movement disorders : official journal of the Movement Disorder Society*, 26, 2011-8.
- KO, D. C., A.R. RAVENSCROFT, P. 2008. Changes in RGS Protein Expression in the Unilateral 6-OHDA-lesioned Rat Models of Parkinson's Disease and L-DOPA-induced Dyskinesia. *Parkinson's Disease U.K, York*, 3-4 of November.
- KOBYLECKI, C., CENCI, M. A., CROSSMAN, A. R. & RAVENSCROFT, P. 2010. Calcium-permeable AMPA receptors are involved in the induction and expression of L-DOPA-induced dyskinesia in Parkinson's disease. *Journal of neurochemistry*, 114, 499-511.
- KONITSIOTIS, S., BLANCHET, P. J., VERHAGEN, L., LAMERS, E. & CHASE, T. N. 2000. AMPA receptor blockade improves levodopa-induced dyskinesia in MPTP monkeys. *Neurology*, 54, 1589-95.
- KONRADI, C., WESTIN, J. E., CARTA, M., EATON, M. E., KUTER, K., DEKUNDY, A., LUNDBLAD, M. & CENCI, M. A. 2004. Transcriptome analysis in a rat model of L-DOPA-induced dyskinesia. *Neurobiology of disease*, 17, 219-36.
- KOOB, G. F., STINUS, L. & LE MOAL, M. 1981. Hyperactivity and hypoactivity produced by lesions to the mesolimbic dopamine system. *Behav Brain Res*, 3, 341-59.
- KORDOWER, J. H., CHU, Y., HAUSER, R. A., FREEMAN, T. B. & OLANOW, C. W. 2008. Lewy body-like pathology in long-term embryonic nigral transplants in Parkinson's disease. *Nature medicine*, 14, 504-6.
- KOVOOR, A., SEYFFARTH, P., EBERT, J., BARGHSHOON, S., CHEN, C. K., SCHWARZ, S., AXELROD, J. D., CHEYETTE, B. N., SIMON, M. I., LESTER, H. A. & SCHWARZ, J. 2005. D2 dopamine receptors colocalize regulator of G-protein signaling 9-2 (RGS9-2) via the RGS9 DEP domain, and RGS9 knock-out mice develop dyskinesias associated with dopamine pathways. *The Journal of neuroscience : the official journal of the Society for Neuroscience*, 25, 2157-65.
- KUAN, W. L., ZHAO, J. W. & BARKER, R. A. 2008. The role of anxiety in the development of levodopa-induced dyskinesias in an animal model of Parkinson's disease, and the effect of chronic treatment with the selective serotonin reuptake inhibitor citalopram. *Psychopharmacology*, 197, 279-93.
- KUMAR, R., LANG, A. E., RODRIGUEZ-OROZ, M. C., LOZANO, A. M., LIMOUSIN, P., POLLAK, P., BENABID, A. L., GURIDI, J., RAMOS, E., VAN DER LINDEN, C., VANDEWALLE, A., CAEMAERT, J., LANNOO, E., VAN DEN ABBEELE, D., VINGERHOETS, G., WOLTERS, M. & OBESO, J. A. 2000. Deep brain stimulation of the globus pallidus pars interna in advanced Parkinson's disease. *Neurology*, 55, S34-9.
- KUZUHARA, S., MORI, H., IZUMIYAMA, N., YOSHIMURA, M. & IHARA, Y. 1988. Lewy bodies are ubiquitinated. A light and electron microscopic immunocytochemical study. *Acta neuropathologica*, 75, 345-53.
- LANE, E. L., BJORKLUND, A., DUNNETT, S. B. & WINKLER, C. 2010. Neural grafting in Parkinson's disease unraveling the mechanisms underlying graft-induced dyskinesia. *Progress in brain research*, 184, 295-309.

- LANE, E. L., BRUNDIN, P. & CENCI, M. A. 2009a. Amphetamine-induced abnormal movements occur independently of both transplant- and host-derived serotonin innervation following neural grafting in a rat model of Parkinson's disease. *Neurobiology of disease*, 35, 42-51.
- LANE, E. L., DALY, C. S., SMITH, G. A. & DUNNETT, S. B. 2011. Context-driven changes in L-DOPA-induced behaviours in the 6-OHDA lesioned rat. *Neurobiology of disease*.
- LANE, E. L. & SMITH, G. A. 2010. Understanding graft-induced dyskinesia. *Regenerative medicine*, 5, 787-97.
- LANE, E. L., SOULET, D., VERCAMMEN, L., CENCI, M. A. & BRUNDIN, P. 2008. Neuroinflammation in the generation of post-transplantation dyskinesia in Parkinson's disease. *Neurobiology of disease*, 32, 220-8.
- LANE, E. L., VERCAMMEN, L., CENCI, M. A. & BRUNDIN, P. 2009b. Priming for L-DOPA-induced abnormal involuntary movements increases the severity of amphetamine-induced dyskinesia in grafted rats. *Exp Neurol*, 219, 355-8.
- LANE, E. L., WINKLER, C., BRUNDIN, P. & CENCI, M. A. 2006. The impact of graft size on the development of dyskinesia following intrastriatal grafting of embryonic dopamine neurons in the rat. *Neurobiology of disease*, 22, 334-45.
- LANGSTON, J. W. & BALLARD, P. A., JR. 1983. Parkinson's disease in a chemist working with 1-methyl-4-phenyl-1,2,5,6-tetrahydropyridine. *The New England journal of medicine*, 309, 310.
- LANGSTON, J. W. & PALFREMAN, J. 1995. *The Case of the Frozen Addicts* New York, Pantheon Books.
- LAVOIE, B., SMITH, Y. & PARENT, A. 1989. Dopaminergic innervation of the basal ganglia in the squirrel monkey as revealed by tyrosine hydroxylase immunohistochemistry. *The Journal of comparative neurology*, 289, 36-52.
- LEE, C. S., CENCI, M. A., SCHULZER, M. & BJORKLUND, A. 2000. Embryonic ventral mesencephalic grafts improve levodopa-induced dyskinesia in a rat model of Parkinson's disease. *Brain : a journal of neurology*, 123 (Pt 7), 1365-79.
- LEVY, R., VILA, M., HERRERO, M. T., FAUCHEUX, B., AGID, Y. & HIRSCH, E. C. 1995. Striatal expression of substance P and methionin-enkephalin in genes in patients with Parkinson's disease. *Neuroscience letters*, 199, 220-4.
- LEWITT, P. A., REZAI, A. R., LEEHEY, M. A., OJEMANN, S. G., FLAHERTY, A. W., ESKANDAR, E. N., KOSTYK, S. K., THOMAS, K., SARKAR, A., SIDDIQUI, M. S., TATTER, S. B., SCHWALB, J. M., POSTON, K. L., HENDERSON, J. M., KURLAN, R. M., RICHARD, I. H., VAN METER, L., SAPAN, C. V., DURING, M. J., KAPLITT, M. G. & FEIGIN, A. 2011. AAV2-GAD gene therapy for advanced Parkinson's disease: a double-blind, sham-surgery controlled, randomised trial. *Lancet neurology*, 10, 309-19.
- LI, X., PATEL, J. C., WANG, J., AVSHALUMOV, M. V., NICHOLSON, C., BUXBAUM, J. D., ELDER, G. A., RICE, M. E. & YUE, Z. 2010. Enhanced striatal dopamine transmission and motor performance with LRRK2 overexpression in mice is eliminated by familial Parkinson's disease mutation G2019S. *The Journal of neuroscience : the official journal of the Society for Neuroscience*, 30, 1788-97.
- LIANG, Q., SMITH, A. D., PAN, S., TYURIN, V. A., KAGAN, V. E., HASTINGS, T. G. & SCHOR, N. F. 2005. Neuroprotective effects of TEMPOL in central and peripheral nervous system models of Parkinson's disease. *Biochemical pharmacology*, 70, 1371-81.
- LICHTER, D. G., CORBETT, A. J., FITZGIBBON, G. M., DAVIDSON, O. R., HOPE, J. K., GODDARD, G. V., SHARPLES, K. J. & POLLOCK, M. 1988. Cognitive and motor

- dysfunction in Parkinson's disease. Clinical, performance, and computed tomographic correlations. *Archives of neurology*, 45, 854-60.
- LINDVALL, O., BARRY, D. I., KIKVADZE, I., BRUNDIN, P., BOLWIG, T. G. & BJORKLUND, A. 1988. Intracerebral grafting of fetal noradrenergic locus coeruleus neurons: evidence for seizure suppression in the kindling model of epilepsy. *Progress in brain research*, 78, 79-86.
- LINDVALL, O. & BJORKLUND, A. 2004. Cell therapy in Parkinson's disease. *NeuroRx : the journal of the American Society for Experimental NeuroTherapeutics*, 1, 382-93.
- LINDVALL, O., REHNCRONA, S., BRUNDIN, P., GUSTAVII, B., ASTEDT, B., WIDNER, H., LINDHOLM, T., BJORKLUND, A., LEENDERS, K. L., ROTHWELL, J. C., FRACKOWIAK, R., MARSDEN, D., JOHNELS, B., STEG, G., FREEDMAN, R., HOFFER, B. J., SEIGER, A., BYGDEMAN, M., STROMBERG, I. & OLSON, L. 1989. Human fetal dopamine neurons grafted into the striatum in two patients with severe Parkinson's disease. A detailed account of methodology and a 6-month follow-up. *Archives of neurology*, 46, 615-31.
- LINDVALL, O., WIDNER, H., REHNCRONA, S., BRUNDIN, P., ODIN, P., GUSTAVII, B., FRACKOWIAK, R., LEENDERS, K. L., SAWLE, G., ROTHWELL, J. C. & ET AL. 1992. Transplantation of fetal dopamine neurons in Parkinson's disease: one-year clinical and neurophysiological observations in two patients with putaminal implants. *Annals of neurology*, 31, 155-65.
- LIU, Y. J., CHEN, M. L., WANG, Y. C., CHEN, J. Y., LIAO, D. L., BAI, Y. M., LIN, C. C., CHEN, T. T., MO, G. H. & LAI, I. C. 2009. Analysis of genetic variations in the RGS9 gene and antipsychotic-induced tardive dyskinesia in schizophrenia. *American journal of medical genetics. Part B, Neuropsychiatric genetics : the official publication of the International Society of Psychiatric Genetics*, 150B, 239-42.
- LOMAZZI, M., SLESINGER, P. A. & LUSCHER, C. 2008. Addictive drugs modulate GIRK-channel signaling by regulating RGS proteins. *Trends in pharmacological sciences*, 29, 544-9.
- LOW, W. C., TRIARHOU, L. C., KASEDA, Y., NORTON, J. & GHETTI, B. 1987. Functional innervation of the striatum by ventral mesencephalic grafts in mice with inherited nigrostriatal dopamine deficiency. *Brain research*, 435, 315-21.
- LOZANO, A. M., LANG, A. E., LEVY, R., HUTCHISON, W. & DOSTROVSKY, J. 2000. Neuronal recordings in Parkinson's disease patients with dyskinesias induced by apomorphine. *Annals of neurology*, 47, S141-6.
- LU, S. Y., SHIPLEY, M. T., NORMAN, A. B. & SANBERG, P. R. 1991. Striatal, ventral mesencephalic and cortical transplants into the intact rat striatum: a neuroanatomical study. *Experimental neurology*, 113, 109-30.
- LUCHTMAN, D. W., SHAO, D. & SONG, C. 2009. Behavior, neurotransmitters and inflammation in three regimens of the MPTP mouse model of Parkinson's disease. *Physiology & behavior*, 98, 130-8.
- LUNDBLAD, M., ANDERSSON, M., WINKLER, C., KIRIK, D., WIERUP, N. & CENCI, M. A. 2002. Pharmacological validation of behavioural measures of akinesia and dyskinesia in a rat model of Parkinson's disease. *The European journal of neuroscience*, 15, 120-32.
- LUNDBLAD, M., PICCONI, B., LINDGREN, H. & CENCI, M. A. 2004. A model of L-DOPA-induced dyskinesia in 6-hydroxydopamine lesioned mice: relation to motor and cellular parameters of nigrostriatal function. *Neurobiology of disease*, 16, 110-23.
- LUNDBLAD, M., USIELLO, A., CARTA, M., HAKANSSON, K., FISONE, G. & CENCI, M. A. 2005. Pharmacological validation of a mouse model of L-DOPA-induced dyskinesia. *Experimental neurology*, 194, 66-75.

- MA, Y., FEIGIN, A., DHAWAN, V., FUKUDA, M., SHI, Q., GREENE, P., BREEZE, R., FAHN, S., FREED, C. & EIDELBERG, D. 2002. Dyskinesia after fetal cell transplantation for parkinsonism: a PET study. *Annals of neurology*, 52, 628-34.
- MADRAZO, I., LEON, V., TORRES, C., AGUILERA, M. C., VARELA, G., ALVAREZ, F., FRAGA, A., DRUCKER-COLIN, R., OSTROSKY, F., SKUROVICH, M. & ET AL. 1988. Transplantation of fetal substantia nigra and adrenal medulla to the caudate nucleus in two patients with Parkinson's disease. *The New England journal of medicine*, 318, 51.
- MAEDA, N., MATSUOKA, N. & YAMAGUCHI, I. 1994. Role of the dopaminergic, serotonergic and cholinergic link in the expression of penile erection in rats. *Jpn J Pharmacol*, 66, 59-66.
- MAEDA, T., KANNARI, K., SHEN, H., ARAI, A., TOMIYAMA, M., MATSUNAGA, M. & SUDA, T. 2003. Rapid induction of serotonergic hyperinnervation in the adult rat striatum with extensive dopaminergic denervation. *Neuroscience letters*, 343, 17-20.
- MANDEL, R. J., BRUNDIN, P. & BJORKLUND, A. 1990. The Importance of Graft Placement and Task Complexity for Transplant-Induced Recovery of Simple and Complex Sensorimotor Deficits in Dopamine Denervated Rats. *The European journal of neuroscience*, 2, 888-894.
- MANDEL, R. J. & RANDALL, P. K. 1985. Quantification of lesion-induced dopaminergic supersensitivity using the rotational model in the mouse. *Brain Res*, 330, 358-63.
- MANDEL, R. J. & RANDALL, P. K. 1990. Bromocriptine-induced rotation: characterization using a striatal efferent lesion in the mouse. *Brain research bulletin*, 24, 175-80.
- MANFREDSSON, F. P., OKUN, M. S. & MANDEL, R. J. 2009. Gene therapy for neurological disorders: challenges and future prospects for the use of growth factors for the treatment of Parkinson's disease. *Current gene therapy*, 9, 375-88.
- MANSON, A. J., IAKOVIDOU, E. & LEES, A. J. 2000. Idazoxan is ineffective for levodopa-induced dyskinesias in Parkinson's disease. *Movement disorders : official journal of the Movement Disorder Society*, 15, 336-7.
- MANSON, A. J., KATZENSCHLAGER, R., HOBART, J. & LEES, A. J. 2001. High dose naltrexone for dyskinesias induced by levodopa. *Journal of neurology, neurosurgery, and psychiatry*, 70, 554-6.
- MARIES, E., KORDOWER, J. H., CHU, Y., COLLIER, T. J., SORTWELL, C. E., OLARU, E., SHANNON, K. & STEECE-COLLIER, K. 2006. Focal not widespread grafts induce novel dyskinetic behavior in parkinsonian rats. *Neurobiology of disease*, 21, 165-80.
- MARIN, C., JIMENEZ, A., TOLOSA, E., BONASTRE, M. & BOVE, J. 2004. Bilateral subthalamic nucleus lesion reverses L-dopa-induced motor fluctuations and facilitates dyskinetic movements in hemiparkinsonian rats. *Synapse*, 51, 140-50.
- MARINOVA-MUTAFCHIEVA, L., SADEGHIAN, M., BROOM, L., DAVIS, J. B., MEDHURST, A. D. & DEXTER, D. T. 2009. Relationship between microglial activation and dopaminergic neuronal loss in the substantia nigra: a time course study in a 6-hydroxydopamine model of Parkinson's disease. *J Neurochem*, 110, 966-75.
- MARJAMA-LYONS, J. & KOLLER, W. 2000. Tremor-predominant Parkinson's disease. Approaches to treatment. *Drugs & aging*, 16, 273-8.
- MARKHAM, C. M., RAND, R. W., JACQUES, D. B., DIAMOND, S. G., KOPYOV, O. V. & SNOW, B. 1994. Transplantation of fetal mesencephalic tissue in Parkinson's patients. *Stereotactic and functional neurosurgery*, 62, 134-40.
- MARKS, W. J., JR., OSTREM, J. L., VERHAGEN, L., STARR, P. A., LARSON, P. S., BAKAY, R. A., TAYLOR, R., CAHN-WEINER, D. A., STOESSL, A. J., OLANOW, C. W. & BARTUS, R. T. 2008. Safety and tolerability of intraputaminal delivery of

- CERE-120 (adeno-associated virus serotype 2-neurturin) to patients with idiopathic Parkinson's disease: an open-label, phase I trial. *Lancet neurology*, 7, 400-8.
- MARSDEN, C. D. & OBESO, J. A. 1994. The functions of the basal ganglia and the paradox of stereotaxic surgery in Parkinson's disease. *Brain : a journal of neurology*, 117 (Pt 4), 877-97.
- MARVANOVA, M. & NICHOLS, C. D. 2007. Identification of neuroprotective compounds of caenorhabditis elegans dopaminergic neurons against 6-OHDA. *Journal of molecular neuroscience : MN*, 31, 127-37.
- MASLIAH, E., ROCKENSTEIN, E., VEINBERGS, I., MALLORY, M., HASHIMOTO, M., TAKEDA, A., SAGARA, Y., SISK, A. & MUCKE, L. 2000. Dopaminergic loss and inclusion body formation in alpha-synuclein mice: implications for neurodegenerative disorders. *Science*, 287, 1265-9.
- MATAMALES, M., BERTRAN-GONZALEZ, J., SALOMON, L., DEGOS, B., DENIAU, J. M., VALJENT, E., HERVE, D. & GIRAULT, J. A. 2009. Striatal medium-sized spiny neurons: identification by nuclear staining and study of neuronal subpopulations in BAC transgenic mice. *PLoS one*, 4, e4770.
- MATCHAM, J., MCDERMOTT, M. P. & LANG, A. E. 2007. GDNF in Parkinson's disease: the perils of post-hoc power. *Journal of neuroscience methods*, 163, 193-6.
- MAZLOOM, M. & SMITH, Y. 2006. Synaptic microcircuitry of tyrosine hydroxylase-containing neurons and terminals in the striatum of 1-methyl-4-phenyl-1,2,3,6-tetrahydropyridine-treated monkeys. *The Journal of comparative neurology*, 495, 453-69.
- MCGAUGHY, J., SANDSTROM, M., RULAND, S., BRUNO, J. P. & SARTER, M. 1997. Lack of effects of lesions of the dorsal noradrenergic bundle on behavioral vigilance. *Behavioral neuroscience*, 111, 646-52.
- MECO, G., STIRPE, P., EDITO, F., PURCARO, C., VALENTE, M., BERNARDI, S. & VANACORE, N. 2009. Aripiprazole in L-dopa-induced dyskinesias: a one-year open-label pilot study. *Journal of neural transmission*, 116, 881-4.
- MELA, F., MARTI, M., DEKUNDY, A., DANYSZ, W., MORARI, M. & CENCI, M. A. 2007. Antagonism of metabotropic glutamate receptor type 5 attenuates L-DOPA-induced dyskinesia and its molecular and neurochemical correlates in a rat model of Parkinson's disease. *Journal of neurochemistry*, 101, 483-97.
- MENDEZ, I., SADI, D. & HONG, M. 1996. Reconstruction of the nigrostriatal pathway by simultaneous intrastriatal and intranigral dopaminergic transplants. *The Journal of neuroscience : the official journal of the Society for Neuroscience*, 16, 7216-27.
- MENDEZ, I., VINUELA, A., ASTRADSSON, A., MUKHIDA, K., HALLETT, P., ROBERTSON, H., TIERNEY, T., HOLNESS, R., DAGHER, A., TROJANOWSKI, J. Q. & ISACSON, O. 2008. Dopamine neurons implanted into people with Parkinson's disease survive without pathology for 14 years. *Nature medicine*, 14, 507-9.
- METZ, G. A., TSE, A., BALLERMANN, M., SMITH, L. K. & FOUAD, K. 2005. The unilateral 6-OHDA rat model of Parkinson's disease revisited: an electromyographic and behavioural analysis. *Eur J Neurosci*, 22, 735-44.
- MEYERS, R. 1942. The modification of alternating tremors, rigidity and festination by surgery of basal ganglia. *Assoc Nerv Ment Dis proc*, 21, 602-655.
- MEYERS, R. 1951. Surgical experiments in the therapy of certain 'extrapyramidal' diseases: a current evaluation. *Acta psychiatrica et neurologica. Supplementum*, 67, 1-42.
- MEYERS, R., FRY, W. J., FRY, F. J., DREYER, L. L., SCHULTZ, D. F. & NOYES, R. F. 1959. Early experiences with ultrasonic irradiation of the pallidofugal and nigral complexes in hyperkinetic and hypertonic disorders. *Journal of neurosurgery*, 16, 32-54.

- MIKOS, A., ZAHODNE, L., OKUN, M. S., FOOTE, K. & BOWERS, D. 2010. Cognitive declines after unilateral deep brain stimulation surgery in Parkinson's disease: a controlled study using Reliable Change, part II. *The Clinical neuropsychologist*, 24, 235-45.
- MILESON, B. E., LEWIS, M. H. & MAILMAN, R. B. 1991. Dopamine receptor 'supersensitivity' occurring without receptor up-regulation. *Brain research*, 561, 1-10.
- MILLIGAN, G., MITCHELL, F. M., MULLANEY, I., MCCLUE, S. J. & MCKENZIE, F. R. 1990. The role and specificity of guanine nucleotide binding proteins in receptor-effector coupling. *Symposia of the Society for Experimental Biology*, 44, 157-72.
- MITCHELL, I. J., CLARKE, C. E., BOYCE, S., ROBERTSON, R. G., PEGGS, D., SAMBROOK, M. A. & CROSSMAN, A. R. 1989. Neural mechanisms underlying parkinsonian symptoms based upon regional uptake of 2-deoxyglucose in monkeys exposed to 1-methyl-4-phenyl-1,2,3,6-tetrahydropyridine. *Neuroscience*, 32, 213-26.
- MIYAZAKI, I., ASANUMA, M., HOZUMI, H., MIYOSHI, K. & SOGAWA, N. 2007. Protective effects of metallothionein against dopamine quinone-induced dopaminergic neurotoxicity. *FEBS letters*, 581, 5003-8.
- MONTOYA, C. P., ASTELL, S. & DUNNETT, S. B. 1990. Effects of nigral and striatal grafts on skilled forelimb use in the rat. *Prog Brain Res*, 82, 459-66.
- MONTOYA, C. P., CAMPBELL-HOPE, L. J., PEMBERTON, K. D. & DUNNETT, S. B. 1991. The "staircase test": a measure of independent forelimb reaching and grasping abilities in rats. *J Neurosci Methods*, 36, 219-28.
- MONVILLE, C., TORRES, E. M. & DUNNETT, S. B. 2005. Validation of the l-dopa-induced dyskinesia in the 6-OHDA model and evaluation of the effects of selective dopamine receptor agonists and antagonists. *Brain research bulletin*, 68, 16-23.
- MONVILLE, C., TORRES, E. M. & DUNNETT, S. B. 2006. Comparison of incremental and accelerating protocols of the rotarod test for the assessment of motor deficits in the 6-OHDA model. *J Neurosci Methods*, 158, 219-23.
- MOORE, A. E., CICCETTI, F., HENNEN, J. & ISACSON, O. 2001. Parkinsonian motor deficits are reflected by proportional A9/A10 dopamine neuron degeneration in the rat. *Experimental neurology*, 172, 363-76.
- MOORE, R. Y. & BLOOM, F. E. 1979. Central catecholamine neuron systems: anatomy and physiology of the norepinephrine and epinephrine systems. *Annual review of neuroscience*, 2, 113-68.
- MORGANTE, F., ESPAY, A. J., GUNRAJ, C., LANG, A. E. & CHEN, R. 2006. Motor cortex plasticity in Parkinson's disease and levodopa-induced dyskinesias. *Brain : a journal of neurology*, 129, 1059-69.
- MORGESE, M. G., CASSANO, T., CUOMO, V. & GIUFFRIDA, A. 2007. Anti-dyskinetic effects of cannabinoids in a rat model of Parkinson's disease: role of CB(1) and TRPV1 receptors. *Experimental neurology*, 208, 110-9.
- MORGESE, M. G., CASSANO, T., GAETANI, S., MACHEDA, T., LACONCA, L., DIPASQUALE, P., FERRARO, L., ANTONELLI, T., CUOMO, V. & GIUFFRIDA, A. 2009. Neurochemical changes in the striatum of dyskinetic rats after administration of the cannabinoid agonist WIN55,212-2. *Neurochemistry international*, 54, 56-64.
- MORIN, N., GREGOIRE, L., GOMEZ-MANCILLA, B., GASPARINI, F. & DI PAOLO, T. 2010. Effect of the metabotropic glutamate receptor type 5 antagonists MPEP and MTEP in parkinsonian monkeys. *Neuropharmacology*, 58, 981-6.
- MORRIS, H. R. 2005. Genetics of Parkinson's disease. *Annals of medicine*, 37, 86-96.
- MORRIS, H. R. 2007. Autosomal dominant Parkinson's disease and the route to new therapies. *Expert review of neurotherapeutics*, 7, 649-56.

- MUNOZ, A., CARLSSON, T., TRONCI, E., KIRIK, D., BJORKLUND, A. & CARTA, M. 2009. Serotonin neuron-dependent and -independent reduction of dyskinesia by 5-HT1A and 5-HT1B receptor agonists in the rat Parkinson model. *Experimental neurology*, 219, 298-307.
- MUNOZ, A., LI, Q., GARDONI, F., MARCELLO, E., QIN, C., CARLSSON, T., KIRIK, D., DI LUCA, M., BJORKLUND, A., BEZARD, E. & CARTA, M. 2008. Combined 5-HT1A and 5-HT1B receptor agonists for the treatment of L-DOPA-induced dyskinesia. *Brain*, 131, 3380-94.
- MURA, A., FELDON, J. & MINTZ, M. 2000. The expression of the calcium binding protein calretinin in the rat striatum: effects of dopamine depletion and L-DOPA treatment. *Experimental neurology*, 164, 322-32.
- NARABAYASHI, H., MAEDA, T. & YOKOCHI, F. 1987. Long-term follow-up study of nucleus ventralis intermedius and ventrolateralis thalamotomy using a microelectrode technique in parkinsonism. *Applied neurophysiology*, 50, 330-7.
- NARABAYASHI, H., MIYASHITA, N., HATTORI, Y., SAITO, K. & ENDO, K. 1997. Posteroventral pallidotomy: its effect on motor symptoms and scores of MMPI test in patients with Parkinson's disease. *Parkinsonism & related disorders*, 3, 7-20.
- NARANG, N. & WAMSLEY, J. K. 1995. Time dependent changes in DA uptake sites, D1 and D2 receptor binding and mRNA after 6-OHDA lesions of the medial forebrain bundle in the rat brain. *Journal of chemical neuroanatomy*, 9, 41-53.
- NASS, R., HALL, D. H., MILLER, D. M., 3RD & BLAKELY, R. D. 2002. Neurotoxin-induced degeneration of dopamine neurons in *Caenorhabditis elegans*. *Proceedings of the National Academy of Sciences of the United States of America*, 99, 3264-9.
- NASTUK, W. L., SU, P. & DOUBILET, P. 1976. Anticholinergic and membrane activities of amantadine in neuromuscular transmission. *Nature*, 264, 76-9.
- NICKLAS, W. J., VYAS, I. & HEIKKILA, R. E. 1985. Inhibition of NADH-linked oxidation in brain mitochondria by 1-methyl-4-phenyl-pyridine, a metabolite of the neurotoxin, 1-methyl-4-phenyl-1,2,5,6-tetrahydropyridine. *Life sciences*, 36, 2503-8.
- NISBET, A. P., FOSTER, O. J., KINGSBURY, A., EVE, D. J., DANIEL, S. E., MARSDEN, C. D. & LEES, A. J. 1995. Preproenkephalin and preprotachykinin messenger RNA expression in normal human basal ganglia and in Parkinson's disease. *Neuroscience*, 66, 361-76.
- NISSINEN, H., KUOPPAMAKI, M., LEINONEN, M. & SCHAPIRA, A. H. 2009. Early versus delayed initiation of entacapone in levodopa-treated patients with Parkinson's disease: a long-term, retrospective analysis. *European journal of neurology : the official journal of the European Federation of Neurological Societies*, 16, 1305-11.
- NOVA, I. C., PERRACINI, M. R. & FERRAZ, H. B. 2004. Levodopa effect upon functional balance of Parkinson's disease patients. *Parkinsonism & related disorders*, 10, 411-5.
- NUTT, J. G., WOODWARD, W. R., GANCHER, S. T. & MERRICK, D. 1987. 3-O-methyldopa and the response to levodopa in Parkinson's disease. *Annals of neurology*, 21, 584-8.
- OBESO, J. A., RODRIGUEZ-OROZ, M. C., RODRIGUEZ, M., DELONG, M. R. & OLANOW, C. W. 2000a. Pathophysiology of levodopa-induced dyskinesias in Parkinson's disease: problems with the current model. *Annals of neurology*, 47, S22-32; discussion S32-4.
- OBESO, J. A., RODRIGUEZ-OROZ, M. C., RODRIGUEZ, M., LANCIEGO, J. L., ARTIEDA, J., GONZALO, N. & OLANOW, C. W. 2000b. Pathophysiology of the basal ganglia in Parkinson's disease. *Trends in neurosciences*, 23, S8-19.
- ODIN, P., WOLTERS, E. & ANTONINI, A. 2008. Continuous dopaminergic stimulation achieved by duodenal levodopa infusion. *Neurological sciences : official journal of the*

Italian Neurological Society and of the Italian Society of Clinical Neurophysiology, 29 Suppl 5, S387-8.

- OGURA, T., OGATA, M., AKITA, H., JITSUKI, S., AKIBA, L., NODA, K., HOKA, S. & SAJI, M. 2005. Impaired acquisition of skilled behavior in rotarod task by moderate depletion of striatal dopamine in a pre-symptomatic stage model of Parkinson's disease. *Neurosci Res*, 51, 299-308.
- OLANOW, C. W., GOETZ, C. G., KORDOWER, J. H., STOESSL, A. J., SOSSI, V., BRIN, M. F., SHANNON, K. M., NAUERT, G. M., PERL, D. P., GODBOLD, J. & FREEMAN, T. B. 2003. A double-blind controlled trial of bilateral fetal nigral transplantation in Parkinson's disease. *Annals of neurology*, 54, 403-14.
- OLANOW, C. W., GRACIES, J. M., GOETZ, C. G., STOESSL, A. J., FREEMAN, T., KORDOWER, J. H., GODBOLD, J. & OBESO, J. A. 2009a. Clinical pattern and risk factors for dyskinesias following fetal nigral transplantation in Parkinson's disease: a double blind video-based analysis. *Movement disorders : official journal of the Movement Disorder Society*, 24, 336-43.
- OLANOW, C. W., KORDOWER, J. H., LANG, A. E. & OBESO, J. A. 2009b. Dopaminergic transplantation for Parkinson's disease: current status and future prospects. *Annals of neurology*, 66, 591-6.
- OLDS, M. E., JACQUES, D. B. & KOPYOV, O. 2006. Relation between rotation in the 6-OHDA lesioned rat and dopamine loss in striatal and substantia nigra subregions. *Synapse*, 59, 532-44.
- OLSSON, M., NIKKHAH, G., BENTLAGE, C. & BJORKLUND, A. 1995. Forelimb akinesia in the rat Parkinson model: differential effects of dopamine agonists and nigral transplants as assessed by a new stepping test. *J Neurosci*, 15, 3863-75.
- OUATTARA, B., BELKHIR, S., MORISSETTE, M., DRIDI, M., SAMADI, P., GREGOIRE, L., MELTZER, L. T. & DI PAOLO, T. 2009. Implication of NMDA receptors in the antidyskinetic activity of cabergoline, CI-1041, and Ro 61-8048 in MPTP monkeys with levodopa-induced dyskinesias. *Journal of molecular neuroscience : MN*, 38, 128-42.
- OUATTARA, B., HOYER, D., GREGOIRE, L., MORISSETTE, M., GASPARINI, F., GOMEZ-MANCILLA, B. & DI PAOLO, T. 2010. Changes of AMPA receptors in MPTP monkeys with levodopa-induced dyskinesias. *Neuroscience*, 167, 1160-7.
- PAGNUSSAT ADE, S., MICHAELSEN, S. M., ACHAVAL, M. & NETTO, C. A. 2009. Skilled forelimb reaching in Wistar rats: evaluation by means of Montoya staircase test. *J Neurosci Methods*, 177, 115-21.
- PAHAPILL, P. A. & LOZANO, A. M. 2000. The pedunculopontine nucleus and Parkinson's disease. *Brain : a journal of neurology*, 123 (Pt 9), 1767-83.
- PAILLE, V., BRACHET, P. & DAMIER, P. 2004. Role of nigral lesion in the genesis of dyskinesias in a rat model of Parkinson's disease. *Neuroreport*, 15, 561-4.
- PAILLE, V., HENRY, V., LESCAUDRON, L., BRACHET, P. & DAMIER, P. 2007. Rat model of Parkinson's disease with bilateral motor abnormalities, reversible with levodopa, and dyskinesias. *Movement disorders : official journal of the Movement Disorder Society*, 22, 533-9.
- PAILLE, V., PICCONI, B., BAGETTA, V., GHIGLIERI, V., SGOBIO, C., DI FILIPPO, M., VISCOMI, M. T., GIAMPA, C., FUSCO, F. R., GARDONI, F., BERNARDI, G., GREENGARD, P., DI LUCA, M. & CALABRESI, P. 2010. Distinct levels of dopamine denervation differentially alter striatal synaptic plasticity and NMDA receptor subunit composition. *The Journal of neuroscience : the official journal of the Society for Neuroscience*, 30, 14182-93.

- PAISAN-RUIZ, C., LANG, A. E., KAWARAI, T., SATO, C., SALEHI-RAD, S., FISMAN, G. K., AL-KHAIRALLAH, T., ST GEORGE-HYSLOP, P., SINGLETON, A. & ROGAEVA, E. 2005. LRRK2 gene in Parkinson disease: mutation analysis and case control association study. *Neurology*, 65, 696-700.
- PALCZEWSKI, K., KUMASAKA, T., HORI, T., BEHNKE, C. A., MOTOSHIMA, H., FOX, B. A., LE TRONG, I., TELLER, D. C., OKADA, T., STENKAMP, R. E., YAMAMOTO, M. & MIYANO, M. 2000. Crystal structure of rhodopsin: A G protein-coupled receptor. *Science*, 289, 739-45.
- PAPA, S. M., ENGBER, T. M., KASK, A. M. & CHASE, T. N. 1994. Motor fluctuations in levodopa treated parkinsonian rats: relation to lesion extent and treatment duration. *Brain Res*, 662, 69-74.
- PAPLA, I., FILIP, M. & PRZEGALINSKI, E. 2002. Effect of intra-tegmental microinjections of 5-HT1B receptor ligands on the amphetamine-induced locomotor hyperactivity in rats. *Polish journal of pharmacology*, 54, 351-7.
- PAQUETTE, M. A., ANDERSON, A. M., LEWIS, J. R., MESHUL, C. K., JOHNSON, S. W. & PAUL BERGER, S. 2010. MK-801 inhibits L-DOPA-induced abnormal involuntary movements only at doses that worsen parkinsonism. *Neuropharmacology*, 58, 1002-8.
- PAQUETTE, M. A., BRUDNEY, E. G., PUTTERMAN, D. B., MESHUL, C. K., JOHNSON, S. W. & BERGER, S. P. 2008. Sigma ligands, but not N-methyl-D-aspartate antagonists, reduce levodopa-induced dyskinesias. *Neuroreport*, 19, 111-5.
- PARISH, C. L., BELJAJEVA, A., ARENAS, E. & SIMON, A. 2007. Midbrain dopaminergic neurogenesis and behavioural recovery in a salamander lesion-induced regeneration model. *Development*, 134, 2881-7.
- PARKINSON, J. 1817. *An Essay on the Shaking Palsy*, Sherwood, Neely and Jones.
- PATTERSON, M. A., SZATMARI, E. M. & YASUDA, R. 2010. AMPA receptors are exocytosed in stimulated spines and adjacent dendrites in a Ras-ERK-dependent manner during long-term potentiation. *Proceedings of the National Academy of Sciences of the United States of America*, 107, 15951-6.
- PAVON, N., MARTIN, A. B., MENDIALDUA, A. & MORATALLA, R. 2006. ERK phosphorylation and FosB expression are associated with L-DOPA-induced dyskinesia in hemiparkinsonian mice. *Biological psychiatry*, 59, 64-74.
- PAXINOS, G., AND FRANKLIN, K.B.J. (ed.) 2001. *The Mouse Brain in Stereotaxic Coordinates*, London: Academic Press.
- PEARCE, R. K., JACKSON, M., SMITH, L., JENNER, P. & MARSDEN, C. D. 1995. Chronic L-DOPA administration induces dyskinesias in the 1-methyl-4-phenyl-1,2,3,6-tetrahydropyridine-treated common marmoset (*Callithrix jacchus*). *Movement disorders : official journal of the Movement Disorder Society*, 10, 731-40.
- PEELING, J., CORBETT, D., DEL BIGIO, M. R., HUDZIK, T. J., CAMPBELL, T. M. & PALMER, G. C. 2001. Rat middle cerebral artery occlusion: correlations between histopathology, T2-weighted magnetic resonance imaging, and behavioral indices. *J Stroke Cerebrovasc Dis*, 10, 166-77.
- PERESE, D. A., ULMAN, J., VIOLA, J., EWING, S. E. & BANKIEWICZ, K. S. 1989. A 6-hydroxydopamine-induced selective parkinsonian rat model. *Brain Res*, 494, 285-93.
- PEREZ-OTANO, I., HERRERO, M. T., OSET, C., DE CEBALLOS, M. L., LUQUIN, M. R., OBESO, J. A. & DEL RIO, J. 1991. Extensive loss of brain dopamine and serotonin induced by chronic administration of MPTP in the marmoset. *Brain research*, 567, 127-32.
- PERRY, E. K., KILFORD, L., LEES, A. J., BURN, D. J. & PERRY, R. H. 2003. Increased Alzheimer pathology in Parkinson's disease related to antimuscarinic drugs. *Annals of neurology*, 54, 235-8.

- PICCINI, P., LINDVALL, O., BJORKLUND, A., BRUNDIN, P., HAGELL, P., CERAVOLO, R., OERTEL, W., QUINN, N., SAMUEL, M., REHNCRONA, S., WIDNER, H. & BROOKS, D. J. 2000. Delayed recovery of movement-related cortical function in Parkinson's disease after striatal dopaminergic grafts. *Annals of neurology*, 48, 689-95.
- PICCINI, P., PAVESE, N., HAGELL, P., REIMER, J., BJORKLUND, A., OERTEL, W. H., QUINN, N. P., BROOKS, D. J. & LINDVALL, O. 2005. Factors affecting the clinical outcome after neural transplantation in Parkinson's disease. *Brain : a journal of neurology*, 128, 2977-86.
- PICCONI, B., CENTONZE, D., HAKANSSON, K., BERNARDI, G., GREENGARD, P., FISONE, G., CENCI, M. A. & CALABRESI, P. 2003. Loss of bidirectional striatal synaptic plasticity in L-DOPA-induced dyskinesia. *Nature neuroscience*, 6, 501-6.
- PICCONI, B., PAILLE, V., GHIGLIERI, V., BAGETTA, V., BARONE, I., LINDGREN, H. S., BERNARDI, G., ANGELA CENCI, M. & CALABRESI, P. 2008. L-DOPA dosage is critically involved in dyskinesia via loss of synaptic depotentiation. *Neurobiology of disease*, 29, 327-35.
- PIOLI, E. Y., MEISSNER, W., SOHR, R., GROSS, C. E., BEZARD, E. & BIOULAC, B. H. 2008. Differential behavioral effects of partial bilateral lesions of ventral tegmental area or substantia nigra pars compacta in rats. *Neuroscience*, 153, 1213-24.
- POEWE, W., ANTONINI, A., ZIJLMANS, J. C., BURKHARD, P. R. & VINGERHOETS, F. 2010. Levodopa in the treatment of Parkinson's disease: an old drug still going strong. *Clinical interventions in aging*, 5, 229-38.
- POLITIS, M., OERTEL, W. H., WU, K., QUINN, N. P., POGARELL, O., BROOKS, D. J., BJORKLUND, A., LINDVALL, O. & PICCINI, P. 2011. Graft-induced dyskinesias in Parkinson's disease: High striatal serotonin/dopamine transporter ratio. *Mov Disord*.
- POLITIS, M., WU, K., LOANE, C., QUINN, N. P., BROOKS, D. J., REHNCRONA, S., BJORKLUND, A., LINDVALL, O. & PICCINI, P. 2010. Serotonergic neurons mediate dyskinesia side effects in Parkinson's patients with neural transplants. *Science translational medicine*, 2, 38ra46.
- POLLACK, A. E. & STRAUSS, J. B. 1999. Time dependence and role of N-methyl-D-aspartate glutamate receptors in the priming of D2-mediated rotational behavior and striatal Fos expression in 6-hydroxydopamine lesioned rats. *Brain research*, 827, 160-8.
- POLYMERPOULOS, M. H., LAVEDAN, C., LEROY, E., IDE, S. E., DEHEJIA, A., DUTRA, A., PIKE, B., ROOT, H., RUBENSTEIN, J., BOYER, R., STENROOS, E. S., CHANDRASEKHARAPPA, S., ATHANASSIADOU, A., PAPAPETROPOULOS, T., JOHNSON, W. G., LAZZARINI, A. M., DUVOISIN, R. C., DI IORIO, G., GOLBE, L. I. & NUSSBAUM, R. L. 1997. Mutation in the alpha-synuclein gene identified in families with Parkinson's disease. *Science*, 276, 2045-7.
- PSIFOGEORGOU, K., PAKAKOSTA, P., RUSSO, S. J., NEVE, R. L., KARDASSIS, D., GOLD, S. J. & ZACHARIOU, V. 2007. RGS9-2 is a negative modulator of mu-opioid receptor function. *Journal of neurochemistry*, 103, 617-25.
- QUINTANA A, M. C., KERKERIAN-LE GOFF ET AL. 2010. *FENS Abstract*, 5, 107.27.
- RANDALL, P. K. 1984. Lesion-induced DA supersensitivity in aging C57BL/6J mice. *Brain research*, 308, 333-6.
- RASCOL, O., FABRE, N., BLIN, O., POULIK, J., SABATINI, U., SENARD, J. M., ANE, M., MONTASTRUC, J. L. & RASCOL, A. 1994. Naltrexone, an opiate antagonist, fails to modify motor symptoms in patients with Parkinson's disease. *Movement disorders : official journal of the Movement Disorder Society*, 9, 437-40.

- REDMOND, D. E., JR. 2002. Cellular replacement therapy for Parkinson's disease--where we are today? *The Neuroscientist : a review journal bringing neurobiology, neurology and psychiatry*, 8, 457-88.
- REDMOND, D. E., JR., ROBBINS, R. J., NAFTOLIN, F., MAREK, K. L., VOLLMER, T. L., LERANTH, C., ROTH, R. H., PRICE, L. H., GJEDDE, A., BUNNEY, B. S. & ET AL. 1993. Cellular replacement of dopamine deficit in Parkinson's disease using human fetal mesencephalic tissue: preliminary results in four patients. *Research publications - Association for Research in Nervous and Mental Disease*, 71, 325-59.
- RICHARDSON, J. R., QUAN, Y., SHERER, T. B., GREENAMYRE, J. T. & MILLER, G. W. 2005. Paraquat neurotoxicity is distinct from that of MPTP and rotenone. *Toxicological sciences : an official journal of the Society of Toxicology*, 88, 193-201.
- RICHTER, F., HAMANN, M. & RICHTER, A. 2008. Moderate degeneration of nigral neurons after repeated but not after single intrastriatal injections of low doses of 6-hydroxydopamine in mice. *Brain research*, 1188, 148-56.
- RIOUX, L., GAGNON, C., GAUDIN, D. P., DI PAOLO, T. & BEDARD, P. J. 1993. A fetal nigral graft prevents behavioral supersensitivity associated with repeated injections of L-dopa in 6-OHDA rats. Correlation with D1 and D2 receptors. *Neuroscience*, 56, 45-51.
- RIOUX, L., GAUDIN, D. P., GAGNON, C., DI PAOLO, T. & BEDARD, P. J. 1991. Decrease of behavioral and biochemical denervation supersensitivity of rat striatum by nigral transplants. *Neuroscience*, 44, 75-83.
- ROBINET, P. M. & BARDO, M. T. 2001. Dopamine D3 receptors are involved in amphetamine-induced contralateral rotation in 6-OHDA lesioned rats. *Pharmacology, biochemistry, and behavior*, 70, 43-54.
- RODRIGUEZ, J. J., GARCIA, D. R., NAKABEPPU, Y. & PICKEL, V. M. 2001. FosB in rat striatum: normal regional distribution and enhanced expression after 6-month haloperidol administration. *Synapse*, 39, 122-32.
- RODRIGUEZ, J. J., MONTARON, M. F., AUROUSSEAU, C., LE MOAL, M. & ABROUS, D. N. 1999. Effects of amphetamine and cocaine treatment on c-Fos, Jun-B, and Krox-24 expression in rats with intrastriatal dopaminergic grafts. *Experimental neurology*, 159, 139-52.
- ROZAS, G., LISTE, I., GUERRA, M. J. & LABANDEIRA-GARCIA, J. L. 1998. Sprouting of the serotonergic afferents into striatum after selective lesion of the dopaminergic system by MPTP in adult mice. *Neuroscience letters*, 245, 151-4.
- RYLANDER, D., IDERBERG, H., LI, Q., DEKUNDY, A., ZHANG, J., LI, H., BAISHEN, R., DANYSZ, W., BEZARD, E. & CENCI, M. A. 2010. A mGluR5 antagonist under clinical development improves L-DOPA-induced dyskinesia in parkinsonian rats and monkeys. *Neurobiology of disease*, 39, 352-61.
- RYLANDER, D., RECCHIA, A., MELA, F., DEKUNDY, A., DANYSZ, W. & CENCI, M. A. 2009. Pharmacological modulation of glutamate transmission in a rat model of L-DOPA-induced dyskinesia: effects on motor behavior and striatal nuclear signaling. *The Journal of pharmacology and experimental therapeutics*, 330, 227-35.
- SACKS, O. 1973. *Awakenings*, New York, Vintage Books.
- SAENZ DEL BURGO, L., CORTES, R., MENGOD, G., ZARATE, J., ECHEVARRIA, E. & SALLES, J. 2008. Distribution and neurochemical characterization of neurons expressing GIRK channels in the rat brain. *The Journal of comparative neurology*, 510, 581-606.
- SAKAI, K. & GASH, D. M. 1994. Effect of bilateral 6-OHDA lesions of the substantia nigra on locomotor activity in the rat. *Brain research*, 633, 144-50.

- SANTINI, E., VALJENT, E., USIELLO, A., CARTA, M., BORGKVIST, A., GIRAULT, J. A., HERVE, D., GREENGARD, P. & FISONE, G. 2007. Critical involvement of cAMP/DARPP-32 and extracellular signal-regulated protein kinase signaling in L-DOPA-induced dyskinesia. *The Journal of neuroscience : the official journal of the Society for Neuroscience*, 27, 6995-7005.
- SASAHARA, K., NITANAI, T., HABARA, T., KOJIMA, T., KAWAHARA, Y., MORIOKA, T. & NAKAJIMA, E. 1981. Dosage form design for improvement of bioavailability of levodopa IV: Possible causes of low bioavailability of oral levodopa in dogs. *Journal of pharmaceutical sciences*, 70, 730-3.
- SAVASTA, M., MENNICKEN, F., CHRITIN, M., ABROUS, D. N., FEUERSTEIN, C., LE MOAL, M. & HERMAN, J. P. 1992. Intrastriatal dopamine-rich implants reverse the changes in dopamine D2 receptor densities caused by 6-hydroxydopamine lesion of the nigrostriatal pathway in rats: an autoradiographic study. *Neuroscience*, 46, 729-38.
- SAWADA, H., OEDA, T., KUNO, S., NOMOTO, M., YAMAMOTO, K., YAMAMOTO, M., HISANAGA, K. & KAWAMURA, T. 2010. Amantadine for dyskinesias in Parkinson's disease: a randomized controlled trial. *PloS one*, 5, e15298.
- SCATTON, B., JAVOY-AGID, F., ROUQUIER, L., DUBOIS, B. & AGID, Y. 1983. Reduction of cortical dopamine, noradrenaline, serotonin and their metabolites in Parkinson's disease. *Brain research*, 275, 321-8.
- SCHALLERT, T., FLEMING, S. M., LEASURE, J. L., TILLERSON, J. L. & BLAND, S. T. 2000. CNS plasticity and assessment of forelimb sensorimotor outcome in unilateral rat models of stroke, cortical ablation, parkinsonism and spinal cord injury. *Neuropharmacology*, 39, 777-87.
- SCHALLERT, T., WHISHAW, I. Q., RAMIREZ, V. D. & TEITELBAUM, P. 1978. Compulsive, abnormal walking caused by anticholinergics in akinetic, 6-hydroxydopamine-treated rats. *Science*, 199, 1461-3.
- SCHAPIRA, A. H. 2010. Safinamide in the treatment of Parkinson's disease. *Expert opinion on pharmacotherapy*, 11, 2261-8.
- SCHAPIRA, A. H., EMRE, M., JENNER, P. & POEWE, W. 2009. Levodopa in the treatment of Parkinson's disease. *European journal of neurology : the official journal of the European Federation of Neurological Societies*, 16, 982-9.
- SCHMIDT, J. & WESTERMANN, K. H. 1980. Effects of preceding sensibilization by reserpine and haloperidol on toxicity of dopaminergic agonists. *Arch Toxicol Suppl*, 4, 479-81.
- SCHMIDT, R. H., BJORKLUND, A. & STENEVI, U. 1981. Intracerebral grafting of dissociated CNS tissue suspensions: a new approach for neuronal transplantation to deep brain sites. *Brain research*, 218, 347-56.
- SCHONEBERG, T., HOFREITER, M., SCHULZ, A. & ROMPLER, H. 2007. Learning from the past: evolution of GPCR functions. *Trends in pharmacological sciences*, 28, 117-21.
- SCHWARTING, R. K. & HUSTON, J. P. 1996. The unilateral 6-hydroxydopamine lesion model in behavioral brain research. Analysis of functional deficits, recovery and treatments. *Progress in neurobiology*, 50, 275-331.
- SCHWENDT, M., GOLD, S. J. & MCGINTY, J. F. 2006. Acute amphetamine down-regulates RGS4 mRNA and protein expression in rat forebrain: distinct roles of D1 and D2 dopamine receptors. *Journal of neurochemistry*, 96, 1606-15.
- SEALFON, S. C. & OLANOW, C. W. 2000. Dopamine receptors: from structure to behavior. *Trends in neurosciences*, 23, S34-40.
- SEEMAN, P., BZOWEJ, N. H., GUAN, H. C., BERGERON, C., REYNOLDS, G. P., BIRD, E. D., RIEDERER, P., JELLINGER, K. & TOURTELLOTTE, W. W. 1987. Human

- brain D1 and D2 dopamine receptors in schizophrenia, Alzheimer's, Parkinson's, and Huntington's diseases. *Neuropsychopharmacology : official publication of the American College of Neuropsychopharmacology*, 1, 5-15.
- SEEMAN, P., KO, F., JACK, E., GREENSTEIN, R. & DEAN, B. 2007. Consistent with dopamine supersensitivity, RGS9 expression is diminished in the amphetamine-treated animal model of schizophrenia and in postmortem schizophrenia brain. *Synapse*, 61, 303-9.
- SETSUIE, R., WANG, Y. L., MOCHIZUKI, H., OSAKA, H., HAYAKAWA, H., ICHIHARA, N., LI, H., FURUTA, A., SANO, Y., SUN, Y. J., KWON, J., KABUTA, T., YOSHIMI, K., AOKI, S., MIZUNO, Y., NODA, M. & WADA, K. 2007. Dopaminergic neuronal loss in transgenic mice expressing the Parkinson's disease-associated UCH-L1 I93M mutant. *Neurochemistry international*, 50, 119-29.
- SGAMBATO-FAURE, V., BUGGIA, V., GILBERT, F., LEVESQUE, D., BENABID, A. L. & BERGER, F. 2005. Coordinated and spatial upregulation of arc in striatonigral neurons correlates with L-dopa-induced behavioral sensitization in dyskinetic rats. *Journal of neuropathology and experimental neurology*, 64, 936-47.
- SHAN, D. E., WU, H. C., CHAN, L. Y. & LIU, K. D. 2011. Cost-utility analysis of Parkinson's disease. *Acta neurologica Taiwanica*, 20, 65-72.
- SHIBA, K., ARAI, T., SATO, S., KUBO, S., OHBA, Y., MIZUNO, Y. & HATTORI, N. 2009. Parkin stabilizes PINK1 through direct interaction. *Biochemical and biophysical research communications*, 383, 331-5.
- SHIMIZU, K., TSUDA, N., OKAMOTO, Y., MATSUI, Y., MIYAO, Y., TAMURA, K., YAMADA, M., NAKATANI, S., IKEDA, T. & MOGAMI, H. 1988. Transplant-induced recovery from 6-OHDA lesions of the nigrostriatal dopaminergic neurons in mice. *Acta neurochirurgica. Supplementum*, 43, 149-53.
- SHIMIZU, K., YAMADA, M., MATSUI, Y., TAMURA, K., MORIUCHI, S. & MOGAMI, H. 1990. Neural transplantation in mouse Parkinson's disease. *Stereotactic and functional neurosurgery*, 54-55, 353-7.
- SIERADZAN, K. A., FOX, S. H., HILL, M., DICK, J. P., CROSSMAN, A. R. & BROTCHE, J. M. 2001. Cannabinoids reduce levodopa-induced dyskinesia in Parkinson's disease: a pilot study. *Neurology*, 57, 2108-11.
- SILVERDALE, M. A., CROSSMAN, A. R. & BROTCHE, J. M. 2002. Striatal AMPA receptor binding is unaltered in the MPTP-lesioned macaque model of Parkinson's disease and dyskinesia. *Experimental neurology*, 174, 21-8.
- SIVAM, S. P. 1991. Dopamine dependent decrease in enkephalin and substance P levels in basal ganglia regions of postmortem parkinsonian brains. *Neuropeptides*, 18, 201-7.
- SIVAM, S. P., BREESE, G. R., NAPIER, T. C., MUELLER, R. A. & HONG, J. S. 1986a. Dopaminergic regulation of proenkephalin-A gene expression in the basal ganglia. *NIDA research monograph*, 75, 389-92.
- SIVAM, S. P., STRUNK, C., SMITH, D. R. & HONG, J. S. 1986b. Proenkephalin-A gene regulation in the rat striatum: influence of lithium and haloperidol. *Molecular pharmacology*, 30, 186-91.
- SLEVIN, J. T., GASH, D. M., SMITH, C. D., GERHARDT, G. A., KRYSCIO, R., CHEBROLU, H., WALTON, A., WAGNER, R. & YOUNG, A. B. 2006. Unilateral intraputamenal glial cell line-derived neurotrophic factor in patients with Parkinson disease: response to 1 year each of treatment and withdrawal. *Neurosurgical focus*, 20, E1.
- SLEVIN, J. T., GASH, D. M., SMITH, C. D., GERHARDT, G. A., KRYSCIO, R., CHEBROLU, H., WALTON, A., WAGNER, R. & YOUNG, A. B. 2007. Unilateral intraputamenal glial cell line-derived neurotrophic factor in patients with Parkinson

- disease: response to 1 year of treatment and 1 year of withdrawal. *Journal of neurosurgery*, 106, 614-20.
- SMITH G.A., MURPHY E., DUNNETT S.B. & E.L., L. 2011. *Ch 5. Induced Animal Models of Parkinson's Disease*, London, CRC Press.
- SMITH, G. A. & HEUER, A. 2011. 6-OHDA toxin models of PD in mice. Editors: Lane, EL and Dunnett, S.B. *Contemporary Animal Models with Movement Disorders*, Springer/Humana, U.K.
- SODERMAN, A. R. & UNTERWALD, E. M. 2008. Cocaine reward and hyperactivity in the rat: sites of mu opioid receptor modulation. *Neuroscience*, 154, 1506-16.
- SODERSTROM, K. E., MEREDITH, G., FREEMAN, T. B., MCGUIRE, S. O., COLLIER, T. J., SORTWELL, C. E., WU, Q. & STEECE-COLLIER, K. 2008. The synaptic impact of the host immune response in a parkinsonian allograft rat model: Influence on graft-derived aberrant behaviors. *Neurobiology of disease*, 32, 229-42.
- SONG, D. D. & HABER, S. N. 2000. Striatal responses to partial dopaminergic lesion: evidence for compensatory sprouting. *The Journal of neuroscience : the official journal of the Society for Neuroscience*, 20, 5102-14.
- SONSALLA, P. K., JOCHNOWITZ, N. D., ZEEVALK, G. D., OOSTVEEN, J. A. & HALL, E. D. 1996. Treatment of mice with methamphetamine produces cell loss in the substantia nigra. *Brain research*, 738, 172-5.
- SPILLANTINI, M. G., SCHMIDT, M. L., LEE, V. M., TROJANOWSKI, J. Q., JAKES, R. & GOEDERT, M. 1997. Alpha-synuclein in Lewy bodies. *Nature*, 388, 839-40.
- ST-PIERRE, J. A. & BEDARD, P. J. 1994. Intranigral but not intrastriatal microinjection of the NMDA antagonist MK-801 induces contralateral circling in the 6-OHDA rat model. *Brain research*, 660, 255-60.
- ST-PIERRE, J. A. & BEDARD, P. J. 1995. Systemic administration of the NMDA receptor antagonist MK-801 potentiates circling induced by intrastriatal microinjection of dopamine. *European journal of pharmacology*, 272, 123-9.
- STEECE-COLLIER, K., COLLIER, T. J., DANIELSON, P. D., KURLAN, R., YUREK, D. M. & SLADEK, J. R., JR. 2003. Embryonic mesencephalic grafts increase levodopa-induced forelimb hyperkinesia in parkinsonian rats. *Movement disorders : official journal of the Movement Disorder Society*, 18, 1442-54.
- STEECE-COLLIER, K., SODERSTROM, K. E., COLLIER, T. J., SORTWELL, C. E. & MARIES-LAD, E. 2009. Effect of levodopa priming on dopamine neuron transplant efficacy and induction of abnormal involuntary movements in parkinsonian rats. *The Journal of comparative neurology*, 515, 15-30.
- STEINER, J. A., ANGOT, E. & BRUNDIN, P. 2011. A deadly spread: cellular mechanisms of alpha-synuclein transfer. *Cell death and differentiation*.
- STENEVI, U., BJORKLUND, A. & SVENDGAARD, N. A. 1976. Transplantation of central and peripheral monoamine neurons to the adult rat brain: techniques and conditions for survival. *Brain research*, 114, 1-20.
- STOCCHI, F. 2006. The levodopa wearing-off phenomenon in Parkinson's disease: pharmacokinetic considerations. *Expert opinion on pharmacotherapy*, 7, 1399-407.
- STOCCHI, F., 2009. The therapeutic concept of continuous dopaminergic stimulation (CDS) in the treatment of Parkinson's disease. *Parkinsonian related Disorders*. 3:S68-71.
- STOCCHI, F., VACCA, L., DE PANDIS, M. F., BARBATO, L., VALENTE, M. & RUGGIERI, S. 2001. Subcutaneous continuous apomorphine infusion in fluctuating patients with Parkinson's disease: long-term results. *Neurological sciences : official journal of the Italian Neurological Society and of the Italian Society of Clinical Neurophysiology*, 22, 93-4.

- STROMBERG, I., BICKFORD, P. & GERHARDT, G. A. 2010. Grafted dopamine neurons: Morphology, neurochemistry, and electrophysiology. *Progress in neurobiology*, 90, 190-7.
- TAN, E. K. 2003. Dopamine agonists and their role in Parkinson's disease treatment. *Expert review of neurotherapeutics*, 3, 805-10.
- TANDE, D., HOGLINGER, G., DEBEIR, T., FREUNDLIEB, N., HIRSCH, E. C. & FRANCOIS, C. 2006. New striatal dopamine neurons in MPTP-treated macaques result from a phenotypic shift and not neurogenesis. *Brain : a journal of neurology*, 129, 1194-200.
- TAYMANS, J. M., CRUZ, C., LESAGE, A., LEYSEN, J. E. & LANGLOIS, X. 2005a. MK-801 alters RGS2 levels and adenylyl cyclase sensitivity in the rat striatum. *Neuroreport*, 16, 159-62.
- TAYMANS, J. M., KIA, H. K., CLAES, R., CRUZ, C., LEYSEN, J. & LANGLOIS, X. 2004. Dopamine receptor-mediated regulation of RGS2 and RGS4 mRNA differentially depends on ascending dopamine projections and time. *The European journal of neuroscience*, 19, 2249-60.
- TAYMANS, J. M., KIA, H. K., GROENEWEGEN, H. J., LEYSEN, J. E. & LANGLOIS, X. 2005b. Bilateral control of brain activity by dopamine D1 receptors: evidence from induction patterns of regulator of G protein signaling 2 and c-fos mRNA in D1-challenged hemiparkinsonian rats. *Neuroscience*, 134, 643-56.
- TAYMANS, J. M., LEYSEN, J. E. & LANGLOIS, X. 2003. Striatal gene expression of RGS2 and RGS4 is specifically mediated by dopamine D1 and D2 receptors: clues for RGS2 and RGS4 functions. *Journal of neurochemistry*, 84, 1118-27.
- TAYMANS, J. M., WINTMOLDERS, C., TE RIELE, P., JURZAK, M., GROENEWEGEN, H. J., LEYSEN, J. E. & LANGLOIS, X. 2002. Detailed localization of regulator of G protein signaling 2 messenger ribonucleic acid and protein in the rat brain. *Neuroscience*, 114, 39-53.
- TEKUMALLA, P. K., CALON, F., RAHMAN, Z., BIRDI, S., RAJPUT, A. H., HORNYKIEWICZ, O., DI PAOLO, T., BEDARD, P. J. & NESTLER, E. J. 2001. Elevated levels of DeltaFosB and RGS9 in striatum in Parkinson's disease. *Biological psychiatry*, 50, 813-6.
- TENOVOO, O., RINNE, U. K. & VILJANEN, M. K. 1984. Substance P immunoreactivity in the post-mortem parkinsonian brain. *Brain research*, 303, 113-6.
- TESTA, C. M., STANDAERT, D. G., YOUNG, A. B. & PENNEY, J. B., JR. 1994. Metabotropic glutamate receptor mRNA expression in the basal ganglia of the rat. *The Journal of neuroscience : the official journal of the Society for Neuroscience*, 14, 3005-18.
- THERMOS, K., WINKLER, J. D. & WEISS, B. 1987. Comparison of the effects of fluphenazine-N-mustard on dopamine binding sites and on behavior induced by apomorphine in supersensitive mice. *Neuropharmacology*, 26, 1473-80.
- THOMAS, G. M. & HUGANIR, R. L. 2004. MAPK cascade signalling and synaptic plasticity. *Nature reviews. Neuroscience*, 5, 173-83.
- THOMPSON, L. H., GREALISH, S., KIRIK, D. & BJORKLUND, A. 2009. Reconstruction of the nigrostriatal dopamine pathway in the adult mouse brain. *The European journal of neuroscience*, 30, 625-38.
- TOMIYAMA, M., KIMURA, T., MAEDA, T., KANNARI, K., MATSUNAGA, M. & BABA, M. 2005. A serotonin 5-HT1A receptor agonist prevents behavioral sensitization to L-DOPA in a rodent model of Parkinson's disease. *Neurosci Res*, 52, 185-94.

- TONG, Y. & SHEN, J. 2009. alpha-synuclein and LRRK2: partners in crime. *Neuron*, 64, 771-3.
- TORELLO, M. W., CZEKAJEWSKI, J., POTTER, E. A., KOBER, K. J. & FUNG, Y. K. 1983. An automated method for measurement of circling behavior in the mouse. *Pharmacology, biochemistry, and behavior*, 19, 13-7.
- TORRES, E. M., DOWD, E. & DUNNETT, S. B. 2008. Recovery of functional deficits following early donor age ventral mesencephalic grafts in a rat model of Parkinson's disease. *Neuroscience*, 154, 631-40.
- TORRES, E. M. & DUNNETT, S. B. 2007. Amphetamine induced rotation in the assessment of lesions and grafts in the unilateral rat model of Parkinson's disease. *European neuropsychopharmacology : the journal of the European College of Neuropsychopharmacology*, 17, 206-14.
- TORRES, E. M., LANE, E. L., HEUER, A., SMITH, G. A., MURPHY, E. & DUNNETT, S. B. 2011. Increased efficacy of the 6-hydroxydopamine lesion of the median forebrain bundle in small rats, by modification of the stereotaxic coordinates. *Journal of neuroscience methods*, 200, 29-35.
- TORRES, E. M., MONVILLE, C., GATES, M. A., BAGGA, V. & DUNNETT, S. B. 2007. Improved survival of young donor age dopamine grafts in a rat model of Parkinson's disease. *Neuroscience*, 146, 1606-17.
- TOYODA, H., ZHAO, M. G., ULZHOFFER, B., WU, L. J., XU, H., SEEBURG, P. H., SPRENGEL, R., KUNER, R. & ZHUO, M. 2009. Roles of the AMPA receptor subunit GluA1 but not GluA2 in synaptic potentiation and activation of ERK in the anterior cingulate cortex. *Molecular pain*, 5, 46.
- UNGERSTEDT, U. 1968. 6-Hydroxy-dopamine induced degeneration of central monoamine neurons. *Eur J Pharmacol*, 5, 107-10.
- UNGERSTEDT, U. 1971a. Postsynaptic supersensitivity after 6-hydroxy-dopamine induced degeneration of the nigro-striatal dopamine system. *Acta physiologica Scandinavica. Supplementum*, 367, 69-93.
- UNGERSTEDT, U. 1971b. Striatal dopamine release after amphetamine or nerve degeneration revealed by rotational behaviour. *Acta physiologica Scandinavica. Supplementum*, 367, 49-68.
- VALASTRO, B., ANDERSSON, M., LINDGREN, H. S. & CENCI, M. A. 2007. Expression pattern of JunD after acute or chronic L-DOPA treatment: comparison with deltaFosB. *Neuroscience*, 144, 198-207.
- VENG, L. M., BJUGSTAD, K. B., FREED, C. R., MARRACK, P., CLARKSON, E. D., BELL, K. P., HUTT, C. & ZAWADA, W. M. 2002. Xenografts of MHC-deficient mouse embryonic mesencephalon improve behavioral recovery in hemiparkinsonian rats. *Cell transplantation*, 11, 5-16.
- VENTON, B. J., ZHANG, H., GARRIS, P. A., PHILLIPS, P. E., SULZER, D. & WIGHTMAN, R. M. 2003. Real-time decoding of dopamine concentration changes in the caudate-putamen during tonic and phasic firing. *Journal of neurochemistry*, 87, 1284-95.
- VIARO, R., MORARI, M. & FRANCHI, G. 2011. Progressive motor cortex functional reorganization following 6-hydroxydopamine lesioning in rats. *The Journal of neuroscience : the official journal of the Society for Neuroscience*, 31, 4544-54.
- VINUELA, A., HALLETT, P. J., RESKE-NIELSEN, C., PATTERSON, M., SOTNIKOVA, T. D., CARON, M. G., GAINETDINOV, R. R. & ISACSON, O. 2008. Implanted reuptake-deficient or wild-type dopaminergic neurons improve ON L-dopa dyskinesias without OFF-dyskinesias in a rat model of Parkinson's disease. *Brain : a journal of neurology*, 131, 3361-79.

- VON CAMPENHAUSEN, S., BORNSCHEIN, B., WICK, R., BOTZEL, K., SAMPAIO, C., POEWE, W., OERTEL, W., SIEBERT, U., BERGER, K. & DODEL, R. 2005. Prevalence and incidence of Parkinson's disease in Europe. *European neuropsychopharmacology : the journal of the European College of Neuropsychopharmacology*, 15, 473-90.
- VON VOIGTLANDER, P. F. & MOORE, K. E. 1973. Turning behavior of mice with unilateral 6-hydroxydopamine lesions in the striatum: effects of apomorphine, L-DOPA, amantadine, amphetamine and other psychomotor stimulants. *Neuropharmacology*, 12, 451-62.
- WAKABAYASHI, K. 1989. [Parkinson's disease: the distribution of Lewy bodies in the peripheral autonomic nervous system]. *No to shinkei = Brain and nerve*, 41, 965-71.
- WAKABAYASHI, K., TAKAHASHI, H., OHAMA, E. & IKUTA, F. 1990. Parkinson's disease: an immunohistochemical study of Lewy body-containing neurons in the enteric nervous system. *Acta neuropathologica*, 79, 581-3.
- WALKER, A. E. 1952. Cerebral pedunculotomy for the relief of involuntary movements. II. Parkinsonian tremor. *The Journal of nervous and mental disease*, 116, 766-75.
- WALSH, S., FINN, D. P. & DOWD, E. 2011. Time-course of nigrostriatal neurodegeneration and neuroinflammation in the 6-hydroxydopamine-induced axonal and terminal lesion models of Parkinson's disease in the rat. *Neuroscience*, 175, 251-61.
- WALSH, S., MNICH, K., MACKIE, K., GORMAN, A. M., FINN, D. P. & DOWD, E. 2010. Loss of cannabinoid CB1 receptor expression in the 6-hydroxydopamine-induced nigrostriatal terminal lesion model of Parkinson's disease in the rat. *Brain research bulletin*, 81, 543-8.
- WANG, P., DHANASEKARAN, N. & LUTHIN, G. R. 1997. ERK activation and cellular proliferation in response to muscarinic acetylcholine receptor agonists. *Annals of the New York Academy of Sciences*, 812, 182-3.
- WATTS, R. L., LYONS, K. E., PAHWA, R., SETHI, K., STERN, M., HAUSER, R. A., OLANOW, W., GRAY, A. M., ADAMS, B. & EARL, N. L. 2010. Onset of dyskinesia with adjunct ropinirole prolonged-release or additional levodopa in early Parkinson's disease. *Movement disorders : official journal of the Movement Disorder Society*, 25, 858-66.
- WEDZONY, K. & CZYRAK, A. 1996. Competitive and non-competitive NMDA receptor antagonists induce c-Fos expression in the rat anterior, cingulate cortex. *Journal of physiology and pharmacology : an official journal of the Polish Physiological Society*, 47, 525-33.
- WEDZONY, K., CZYRAK, A., MACKOWIAK, M. & FIJAL, K. 1996. The impact of a competitive and a non-competitive NMDA receptor antagonist on dopaminergic neurotransmission in the rat ventral tegmental area and substantia nigra. *Naunyn-Schmiedeberg's archives of pharmacology*, 353, 517-27.
- WESTIN, J. E., ANDERSSON, M., LUNDBLAD, M. & CENCI, M. A. 2001. Persistent changes in striatal gene expression induced by long-term L-DOPA treatment in a rat model of Parkinson's disease. *Eur J Neurosci*, 14, 1171-6.
- WESTIN, J. E., LINDGREN, H. S., GARDI, J., NYENGAARD, J. R., BRUNDIN, P., MOHAPEL, P. & CENCI, M. A. 2006. Endothelial proliferation and increased blood-brain barrier permeability in the basal ganglia in a rat model of 3,4-dihydroxyphenyl-L-alanine-induced dyskinesia. *The Journal of neuroscience : the official journal of the Society for Neuroscience*, 26, 9448-61.
- WHONE, A. L., WATTS, R. L., STOESSL, A. J., DAVIS, M., RESKE, S., NAHMIAS, C., LANG, A. E., RASCOL, O., RIBEIRO, M. J., REMY, P., POEWE, W. H., HAUSER,

- R. A. & BROOKS, D. J. 2003. Slower progression of Parkinson's disease with ropinirole versus levodopa: The REAL-PET study. *Annals of neurology*, 54, 93-101.
- WICKREMARATCHI, M. M., KNIPE, M. D., SASTRY, B. S., MORGAN, E., JONES, A., SALMON, R., WEISER, R., MORAN, M., DAVIES, D., EBENEZER, L., RAHA, S., ROBERTSON, N. P., BUTLER, C. C., BEN-SHLOMO, Y. & MORRIS, H. R. 2011. The motor phenotype of Parkinson's disease in relation to age at onset. *Movement disorders : official journal of the Movement Disorder Society*, 26, 457-63.
- WINKLER, C., BENTLAGE, C., CENCI, M. A., NIKKHAH, G. & BJORKLUND, A. 2003. Regulation of neuropeptide mRNA expression in the basal ganglia by intrastriatal and intranigral transplants in the rat Parkinson model. *Neuroscience*, 118, 1063-77.
- WINKLER, C., KIRIK, D. & BJORKLUND, A. 2005. Cell transplantation in Parkinson's disease: how can we make it work? *Trends in neurosciences*, 28, 86-92.
- WINKLER, C., KIRIK, D., BJORKLUND, A. & CENCI, M. A. 2002a. L-DOPA-induced dyskinesia in the intrastriatal 6-hydroxydopamine model of parkinson's disease: relation to motor and cellular parameters of nigrostriatal function. *Neurobiol Dis*, 10, 165-86.
- WINKLER, C., KIRIK, D., BJORKLUND, A. & CENCI, M. A. 2002b. L-DOPA-induced dyskinesia in the intrastriatal 6-hydroxydopamine model of parkinson's disease: relation to motor and cellular parameters of nigrostriatal function. *Neurobiology of disease*, 10, 165-86.
- WITT, T. C. & TRIARHOU, L. C. 1995. Transplantation of mesencephalic cell suspensions from wild-type and heterozygous Weaver mice into the denervated striatum: assessing the role of graft-derived dopaminergic dendrites in the recovery of function. *Cell transplantation*, 4, 323-33.
- WOLF, E., SEPPI, K., KATZENSCHLAGER, R., HOCHSCHORNER, G., RANSMAYR, G., SCHWINGENSCHUH, P., OTT, E., KLOIBER, I., HAUBENBERGER, D., AUFF, E. & POEWE, W. 2010. Long-term antidyskinetic efficacy of amantadine in Parkinson's disease. *Movement disorders : official journal of the Movement Disorder Society*, 25, 1357-63.
- WOODLEE, M. T., ASSEO-GARCIA, A. M., ZHAO, X., LIU, S. J., JONES, T. A. & SCHALLERT, T. 2005. Testing forelimb placing "across the midline" reveals distinct, lesion-dependent patterns of recovery in rats. *Experimental neurology*, 191, 310-7.
- YAMAMOTO, N. & SOGHOMONIAN, J. J. 2009. Metabotropic glutamate mGluR5 receptor blockade opposes abnormal involuntary movements and the increases in glutamic acid decarboxylase mRNA levels induced by l-DOPA in striatal neurons of 6-hydroxydopamine-lesioned rats. *Neuroscience*, 163, 1171-80.
- YANAGISAWA, N., FUJIMOTO, S. & TAMARU, F. 1989. Bradykinesia in Parkinson's disease: disorders of onset and execution of fast movement. *European neurology*, 29 Suppl 1, 19-28.
- YASUDA, T., FUKUDA-TANI, M., NIHIRA, T., WADA, K., HATTORI, N., MIZUNO, Y. & MOCHIZUKI, H. 2007. Correlation between levels of pigment epithelium-derived factor and vascular endothelial growth factor in the striatum of patients with Parkinson's disease. *Experimental neurology*, 206, 308-17.
- YIN, L. L., CAO, Y. & XIE, K. Q. 2010. Decreased RGS9 protein level in the striatum of rodents undergoing MPTP or 6-OHDA neurotoxicity. *Neuroscience letters*, 479, 231-5.
- YOUNG, E. A., WALKER, J. M., LEWIS, M. E., HOUGHTEN, R. A., WOODS, J. H. & AKIL, H. 1986. [3H]dynorphin A binding and kappa selectivity of prodynorphin peptides in rat, guinea-pig and monkey brain. *European journal of pharmacology*, 121, 355-65.

- ZAHODNE, L. B., OKUN, M. S., FOOTE, K. D., FERNANDEZ, H. H., RODRIGUEZ, R. L., KIRSCH-DARROW, L. & BOWERS, D. 2009a. Cognitive declines one year after unilateral deep brain stimulation surgery in Parkinson's disease: a controlled study using reliable change. *The Clinical neuropsychologist*, 23, 385-405.
- ZAHODNE, L. B., OKUN, M. S., FOOTE, K. D., FERNANDEZ, H. H., RODRIGUEZ, R. L., WU, S. S., KIRSCH-DARROW, L., JACOBSON, C. E. T., ROSADO, C. & BOWERS, D. 2009b. Greater improvement in quality of life following unilateral deep brain stimulation surgery in the globus pallidus as compared to the subthalamic nucleus. *Journal of neurology*, 256, 1321-9.
- ZENG, B. Y., IRAVANI, M. M., JACKSON, M. J., ROSE, S., PARENT, A. & JENNER, P. 2010. Morphological changes in serotonergic neurites in the striatum and globus pallidus in levodopa primed MPTP treated common marmosets with dyskinesia. *Neurobiology of disease*, 40, 599-607.
- ZESIEWICZ, T. A. & HAUSER, R. A. 2001. Neurosurgery for Parkinson's disease. *Seminars in neurology*, 21, 91-101.
- ZHOU, F. C., BLEDSOE, S. & MURPHY, J. 1991. Serotonergic sprouting is induced by dopamine-lesion in substantia nigra of adult rat brain. *Brain Res*, 556, 108-16.
- ZHOU, H., FALKENBURGER, B. H., SCHULZ, J. B., TIEU, K., XU, Z. & XIA, X. G. 2007. Silencing of the Pink1 gene expression by conditional RNAi does not induce dopaminergic neuron death in mice. *International journal of biological sciences*, 3, 242-50.
- ZHOU, J., DATE, I., SAKAI, K., YOSHIMOTO, Y., FURUTA, T., ASARI, S. & OHMOTO, T. 1993. Xenogeneic dopaminergic grafts reverse behavioral deficits induced by 6-OHDA in rodents: effect of 15-deoxyspergualin treatment. *Neuroscience letters*, 163, 81-4.
- ZIGMOND, M. J. & STRICKER, E. M. 1989. Animal models of parkinsonism using selective neurotoxins: clinical and basic implications. *International review of neurobiology*, 31, 1-79.

11. Supplementary Data

Drug	Dose (mg/kg)	Duration	H<i>Li</i>	<i>Li</i>	<i>Ax</i>	<i>OL</i>
mAmphet SCH23390	2.5	51.27 ± 5.09	23.90 ± 3.09	25.72 ± 3.47	31.36 ± 6.17	2.18 ± 0.33
	0.05	31.72 ± 3.76*	16.72 ± 3.59*	18.00 ± 3.97*	22.73 ± 5.32	1.09 ± 0.62
	0.2	15.63 ± 2.39***	5.54 ± 2.14**	6.00 ± 1.83**	13.18 ± 2.01**	2.36 ± 0.86
Raclopride	0.5	33.45 ± 3.55*	18.18 ± 2.53*	18.27 ± 3.10*	21.63 ± 3.51	0.45 ± 0.20*
	2	32.00 ± 2.08**	14.81 ± 1.89*	14.09 ± 1.56**	18.90 ± 2.20**	0.72 ± 0.23*
Nafadotride	0.6	36.45 ± 1.84	24.63 ± 3.24	24.18 ± 2.66	35.81 ± 2.76	0.81 ± 0.22
	1	35.63 ± 1.47	16.63 ± 1.72*	18.18 ± 1.83*	23.36 ± 1.58	1.45 ± 0.31
Naloxone	4	48.45 ± 3.65	27.36 ± 5.14	27.54 ± 4.83	32.27 ± 2.58	3.30 ± 0.70
	8	44.72 ± 3.77	29.18 ± 3.44	27.63 ± 3.02	35.90 ± 7.23	2.50 ± 1.00
WIN55, 212-2	1	48.73 ± 3.32	31.36 ± 3.02	30.27 ± 3.01	31.90 ± 4.72	1.45 ± 0.67
	2.5	41.82 ± 3.91	31.27 ± 4.04	29.55 ± 3.65	32.00 ± 4.21	1.72 ± 0.58
CP94253	1.5	43.63 ± 3.11	26.45 ± 2.93	25.00 ± 2.54	24.81 ± 2.32	3.36 ± 0.81
	3	49.27 ± 3.97	20.90 ± 3.13	20.73 ± 2.90	7.45 ± 1.76***	7.00 ± 1.97**
8-OH-DPAT	0.05	50.45 ± 4.74	19.54 ± 3.32	19.00 ± 3.25	12.45 ± 2.01**	5.81 ± 1.63*
	0.1	33.09 ± 4.03**	11.54 ± 2.75**	11.45 ± 2.45**	13.27 ± 1.78**	0.45 ± 0.15*
Amantadine	20	53.18 ± 4.13	25.27 ± 3.00	25.00 ± 2.97	26.54 ± 5.32	1.54 ± 0.47
	40	41.27 ± 2.29	19.18 ± 2.67	19.45 ± 2.12	25.81 ± 2.53	0.63 ± 0.20
MTEP	1.25	48.45 ± 4.91	23.36 ± 2.13	22.18 ± 2.25	22.00 ± 2.89	3.09 ± 0.91
	6.25	43.63 ± 3.04	28.45 ± 2.57	27.90 ± 2.21	25.27 ± 4.57	1.45 ± 0.54
IEM1460	1	61.36 ± 5.18	34.45 ± 4.29	32.54 ± 4.00	32.90 ± 4.26	3.27 ± 1.38
	3	48.73 ± 2.91	27.72 ± 2.62	26.45 ± 2.10	30.09 ± 5.23	4.18 ± 2.00

Table 1. Breakdown of AIMs caused by 2.5mg/kg of methamphetamine, in grafted hemi-Parkinsonian rats treated with various pharmacological agents, into dyskinetic sub-components. Abbreviations: Hindlimb (H*Li*), Forelimb (*Li*), Axial (*Ax*) and Orolingual (*OL*). Stars indicate a significant differences between the combination treatments and methamphetamine alone, where $p < 0.05^*$, $p < 0.01^{**}$, $p < 0.001^{***}$. Values are expressed as means ± SEM.

Drug	Dose (mg/kg)	Dyskinesia	Rotation
L-DOPA	12 (15) ^a	127.86 ± 9.65	2349.20 ± 269.73
SCH23390	0.2	69.29 ± 5.27**	1234.48 ± 277.03**
Raclopride	2	90.86 ± 7.31**	1781.38 ± 234.12*
Amantadine	40	95.86 ± 10.21**	3078.14 ± 375.56*
L-DOPA	12 (15) ^a	134.46 ± 5.04	2106.80 ± 322.88
MTEP	6.25	108.40 ± 6.76**	1436.55 ± 218.77**
Naloxone	8	115.00 ± 7.11*	1902.63 ± 339.02*
L-DOPA	12 (15) ^a	138.12 ± 4.80	1978.43 ± 246.57
8-OH-DPAT	0.1	101.87 ± 3.44**	1905.31 ± 225.90*
CP94253	3	107.12 ± 7.57**	2519.70 ± 314.06*

Table 2. Total integrated AIMs and total net rotation caused by L-DOPA alone and co-administration with anti-dyskinetic agents. Data was taken in a latin square design by PhD student Ludivine Breger (BRG and Welsh School of Pharmacy). Stars indicate a significant differences between the combination treatments and L-DOPA alone, where $p < 0.05^*$, $p < 0.01^{**}$. Values are expressed as means ± SEM.

^a Brackets indicate dose of benzerazide.

12. Appendix

Appendix (I) – Primer Design

A) Insitu hybridisation primers

- Optimised for: -

- Primer length 20b +/- 2
- Primer Tm 60oC +/- 5
- Primer GC% 50 +/- 5
- Product length 300-800b
- Specificity: Mus musculus and Rattus norvegicus

1) RGS2

Left primer 5' –ATGCTACATGAGACAGGGAGACC– 3'
Right primer 3' –AACGGACACTGGTTCTACAGCAC– 5'
PRODUCT SIZE: 451bp

2) RGS4

Left primer 5' –TCCTTAAAGGGTGTCAGGTGAGC– 3'
Right primer 3' –TCTCAAACATCCATCTCCAGACC– 5'
PRODUCT SIZE: 443bp

3) RGS8

Left primer 5' –CCTTCCCTGGATCTTCAGCTACC– 3'
Right primer 3' –TCAGGAAGGATGGCTGTGAAGTC– 5'
PRODUCT SIZE: 599bp

4) RGS9

Left primer 5' –CCACAG TGAAGTCTTCGGTGTCC– 3'
Right primer 3' –ATGTCCACGGTGTGGCTGCTTC– 5'
PRODUCT SIZE: 674bp

B) Mus musculus QPCR primers

- Optimised for: -

- Primer length 20b +/- 2
- Primer Tm 60oC +/- 0.5
- Primer GC% 50 +/- 5
- Product length 75-125b

1) RGS2

Left primer 5' -ACGAAAACCCCAAGTTTCCT- 3'
Right primer 3' -CCTGCATTTAGTGCAAGCAA- 5'
PRODUCT SIZE: 110bp

2) RGS4

Left primer 5' -ACTGCTTAGGTGAGGGCAGA- 3'
Right primer 3' -TGACATTCTTGAGGGGAAGG- 5'
PRODUCT SIZE: 93bp

3) RGS8

Left primer 5' -TTCGAAAGGACGCCAATATC- 3'
Right primer 3' -GTCAAGGCTCTGGAAACAGC- 5'
PRODUCT SIZE: 122bp

4) RGS9

Left primer 5' -ACAGACCCACAAACCTCCTG- 3'
Right primer 3' -GTCATGTGGCTTGTCACCAC- 5'
PRODUCT SIZE: 125bp

5) GAPDH

Left primer 5' -TCTCCACACCTATGGTGCAA- 3'
RIGHT PRIMER 3' -CAAGAAACAGGGGAGCTGAG- 5'
PRODUCT SIZE: 106bp

Appendix (II) – Suppliers

Company	Location (Headquarters in U.K)
Ambion	Cambridge
Animal Care Limited	York
Bioehringer	Berkshire
Bioline	London
Bio-Rad	Bath
Bright	Cambridge
Chemicon	U.S.A
Charles River	Wilmington
Chapion photochemistry	U.S.A
Dako	Cambridge
Difco	Surrey
Fisher Scientific	Leicestershire
Harlan	Loughborough
Immunostar Inc	U.S.A
Invitrogen	Paisley
KOPF	U.S.A
Promerga	Southampton
QIAGEN	Crawley
Roche	Welwyn
Sandon Scientific	Middlesex
Santa Cruz	U.S.A
Sero-Wel	Birmingham
Sigma	Poole, Dorset
Thermoscientific	Leicester
Med Associates	St Albans
New England Biolabs	Herts
U.V.P	Cambridge
Vector Laboratories	Peterborough
VWR	Sussex
Xograph	Gloucester

Appendix (III) - Solutions

TRIS buffered Saline (stock)

48g TRIS base (Sigma)
36g Sodium Chloride (Sigma)
1000mls Distilled Water
pH 7.4

TRIS buffered Saline (working solution)

1:4 dilution of stock with distilled water
TWEEN (0.2%) (Sigma)
pH 7.4

Phosphate buffered saline

90g di-sodium hydrogen orthophosphate (Bhd)
45g Sodium Chloride (Sigma)
5000mls Distilled water
pH 7.3

Paraformaldehyde solution (20%)

90g Di-Sodium hydrogen phosphate (Bhd)
45g Sodium Chloride (Sigma)
Paraformaldehyde (20%)
3300mls Distilled water
pH 7.3

Sucrose solution (25%)

25g sucrose (Fisher Scientific)
100mls phosphate buffered saline (Sigma)

10x AP buffer (stock)

121.1g Tris-base (Sigma)
58.4g Sodium Chloride (Sigma)
8000mls Distilled Water
pH 9.5

1x AP buffer (working solution)

1:10 dilution with distilled (DEPC treated) water

Magnesium chloride

203.3g MgCl₂ x 6H₂O (Fisher Scientific)
10000mls Distilled Water

10x TE (stock)

12.1g Tris-base (Sigma)

3.27g EDTA (Sigma)
10000mls Distilled water

1x TE (working solution)

1:10 dilution in distilled (DEPC treated) water

20x PBS (stock)

160g Sodium Chloride (Sigma)
4g Potassium Chloride (Sigma)
28.84g Na₂HPO₄ x 2H₂O (Sigma)
4.1.4g KH₂PO₄ x H₂O (Sigma)
10000mls Distilled water
pH 7.4
1ml DEPC (Sigma)

1x PBS (working solution)

1:20 dilution in distilled (DEPC treated) water

1x T-PBS (working solution)

1:20 dilution in distilled water
TWEEN (0.2%) (Sigma)

20x SSC (stock)

175g Sodium Chloride (Sigma)
88.3g Tri-sodium citrate dehydrate (Sigma)
10000mls Distilled water
pH 7
1ml DEPC

5x SSC (working solution)

1:4 dilution in distilled (DEPC treated) water

2x SSC (working solution)

1:10 dilution in distilled (DEPC treated) water

0.2x SSC (working solution)

1:100 dilution in distilled (DEPC treated) water

50x Denhart Solution

1g Ficoll (Sigma)
1g Bovine serum albumin (non acetylated) (Sigma)
1g Polyvinylpyrrolidone (Sigma)
100mls Distilled water
Heated 50oC

10x TBS-T

100mls Tris-HCl (Sigma)
87.7g Sodium Chloride (Sigma)
100mls TWEEN (Sigma)

10000mls Distilled water

Prehybridisation/hybridisation buffer

5mls Formamide (50%) (Cal Biochem)
2.5mls 5x SSC
1ml Denhardt's
250u l Total yeast RNA (250u/ml) (Roche)
500ul herring Sperm (500u/ml) (Roche)

5x TBE (Running buffer)

54g Tris- base (Sigma)
27.5g Boric acid (Fisher)
20mls EDTA (0.5m) (Sigma)

TXTBS

250ml 1xTBS
500ul Triton X-100 (Sigma)
pH 7.4

ABC solution

5ul A (DAKO)
5ul B (DAKO)
1ml 1% serum in 1xTBS

Quench

10ml Methanol (Fisher Scientific)
10ml Hydrogen peroxide (VWR Prolabo BHD)
80ml Distilled water

TNS

6g Trisma base (Sigma)
1000ml Distilled water
pH 7.4

2x LB Laemmli loading buffer with 2-mercaptoethanol

5 ml (1M) or 4 ml (1.25 M) Tris-HCl
10ml Glycerol
20ml SDS
1ml Bromophenol blue (0.2 %)
100µl per 7 ml 2-mercaptoethanol (200 mM)
pH 6.8

10x Transfer Buffer (stock solution)

30.3g Tris base (250 mM)
117.5g Glycine (1.5 M)
1000ml Distilled water
pH 8.5

1x Transfer Buffer (working solution)

1:10 dilution in distilled (DEPC treated) water

Stacking Gel

1.0ml Acrylamide/BisAcylamide solution
620 μ l Tris-Base (1.25M)
50 μ l SDS
50 μ l APS
3.3ml Distilled water
pH 6.8

Resolving Gel

5.33ml Acrylamide/BisAcylamide solution
2.5ml Tris-Base (1.25M)
100 μ l SDS
100 μ l APS
1.97ml Distilled water
pH 8.8

Radio-Ligand Binding Buffer 1

6.075g Tris-HCl (50mM)
7.012g NaCl (120mM)
0.373g KCl (5mM)
0.36g CaCl₂ (2.5mM)
0.230g MgCl₂ (1mM)
pH 7.4

Radio-Ligand Binding Buffer 2

6.075 g Tris-HCl (50mM)
7.012 g NaCl (120mM)
1000ml Distilled water
pH 7.4